

p53 Regulation of Mitochondrial Biogenesis in Skeletal Muscle

Kaitlyn Beyfuss

A Thesis Submitted to the Faculty of Graduate Studies in Partial Fulfillment of the Requirements
for the Degree of

MASTER OF SCIENCE

Graduate Program in Kinesiology and Health Science

York University

Toronto, ON

May 2018

© **Kaitlyn Beyfuss, 2018**

Abstract

Mitochondria are dynamic organelles that produce energy for the cell. In skeletal muscle, mitochondria adapt as a result of regular exercise by increasing their content and improving their function, resulting in better muscle energy production. p53 is a protein that maintains basal mitochondria function in muscle. However, it is unknown whether it is required for skeletal muscle adaptations with exercise. We thus subjected normal, wild-type mice, as well as those with a specific p53 deletion within muscle, to a 6-week endurance training program. Our results confirm that p53 is required for mitochondrial maintenance in muscle under basal conditions, but that it is not required for the adaptive responses in mitochondrial content and function observed with training. This suggests that exercise can activate viable alternative compensatory pathways to maintain muscle health in the absence of p53.

Acknowledgements

My experience in the Master's of Science program at York University has deepened my passion for science and research and has truly shaped my mind to constantly question, reason analytically, and approach problems in a creative way. This has been a life changing experience and I will forever take with me the lessons I have learned and the friendships I have developed. Therefore, from the bottom of my heart, I would like to thank all of those that have assisted me throughout this journey.

First and foremost, I would like to express my deepest gratitude to my thesis advisor and mentor Dr. David Hood. You have always commended me on my organization and hard work in the lab, however it was truly you I have to thank for pushing me to reach the stars. Thank you for your knowledgeable guidance, your support, and most of all, the wonderful attitude you project to your students. You have helped me apply my previous experience in clinical research to advance my wet lab skills in basic science research. You have opened my eyes to the joys of developing a research project, using experimental skills to solve the question at hand, and to then modify the project to answer new questions that continually arise. I can honestly say that you have helped me to understand the importance of constantly asking new questions to advance research, and for that I will always be thankful. It has truly been an unbelievable pleasure working with you.

Part of this amazing environment created in Dr. Hood's lab is a result of the brilliant, passionate, and truly wonderful people that have dedicated their lives to science and research. An extremely special thank you to Avi and Ashley, the two who took me under their wings when I started, and who were always available for any question I had. Through the late hours at the lab, the long conferences, and the early mornings in class, we have developed a friendship that will last a lifetime. You are not only my mentors, but my confidants. Thank you for the support and love you have shown me over the past couple of years! To the rest of the lab members, especially Matt and Jon, who created an amazing and welcoming lab environment, you provided guidance, support and comic relief at just the right times. The family we have created at the lab has made this experience more special and treasured to me than any experience before.

I would lastly like to thank my family. The patience, support, understanding, and the time you have taken to understand my thesis has been more important than words can describe. You have always pushed me in the direction that I am passionate about, even if it differs from your personal interests, and as such I have developed my love for scientific research. Thank you for providing me with the strength to achieve my goals.

And finally, to my better half Martin, you have been right alongside me through the ups and downs of this winding process. I am speechless, something uncommon for me, in my appreciation for the strength, encouragement, and support that you have provided me. I am forever grateful for your push to follow my dreams, I couldn't have asked for a better person to accompany me along this journey.

Thank you to all for this amazing experience that I will cherish forever.

Table of Contents

Abstract.....	ii
Acknowledgements.....	iii
Table of Contents.....	iv
List of Tables.....	vi
List of Figures.....	x
List of Abbreviations.....	xii

Review of Literature **1**

1.0. Skeletal Muscle Function and Maintenance	2
1.1. Introduction: Importance of Muscle Health.....	2
1.2. Physiology of Skeletal Muscle.....	3
1.2.1. Structural Physiology.....	3
1.2.2. Cellular Structure.....	5
1.2.2.1. Mitochondrial Structure and Function.....	5
1.2.2.1a. Signaling Pathways Regulating Mitochondrial Health.....	9
2.0. Skeletal Muscle Adaptations to Exercise	11
2.1. Exercise: Its Pleiotropic Benefits.....	11
2.1.1. Acute versus Chronic Training: Teasing out the Differences.....	12
2.2. Aerobic Exercise-Mediating Signaling Pathway Regulation	14
2.2.1. Kinase Activation and Downstream Pathways	14
2.2.2. Intracellular Communication and Crosstalk	15
3.0. p53 Transcription Factor	16
3.1. Introduction to the Tumor Suppressor p53	16
3.1.1. Cellular Localization Dictates Function	17
3.2. p53 Signaling Pathways	20
3.2.1. Organelle Turnover and Destruction: Autophagy/Apoptosis	20
3.2.2. Cellular Maintenance of Stress: Cell Cycle Arrest/Senescence/Antioxidants.....	24
3.2.3. Improvements to Cellular Health: Mitochondrial Biogenesis, Metabolism	26
3.2.4. Does a Crosstalk Exist Between Pathways?	31
3.3. p53- Mediated Skeletal Muscle Adaptations with Exercise	33

3.3.1. Systematic Review of Literature: p53 and Acute vs Chronic Exercise	33
3.3.2. Regulatory Signaling Pathways with Endurance Exercise	36
3.3.3. Applicable Models to Study p53 Function	38
3.3.4. Systemic Benefits: Neurological Maintenance	42
3.4. Directions for Future Research	43
Research Objectives	45
Hypotheses	46
References	47
Manuscript	60
<hr/>	
The Role of p53 in Determining Mitochondrial Adaptations to Endurance Training in Skeletal Muscle	61
Abstract	62
Introduction	63
Methods	65
Results	75
Discussion	98
References	103
Acknowledgements	107
Author Contributions	107
Future Work	108
Appendices	109
<hr/>	
Appendix A: Manuscript Data and Statistical Analysis	110
Appendix B: Supplementary and Additional Data	170
Appendix C: Data and Statistical Analysis for Supplementary	188
Appendix D: Laboratory Methods and Protocols	227
Genotyping – p53 Whole Body Mice and Muscle-Specific Mice	227
Mitochondrial Isolations from Skeletal Muscle	233
Mitochondrial Respiration	237

Mitochondrial Reactive Oxygen Species (ROS) Emission	241
Western Blotting	247
COX Enzyme Activity Assay	259
Muscle Extraction Procedure – Protein Extracts	264
Mitochondrial Protein Release Assay for Cytochrome C and AIF.....	266
Nuclear and Cytosolic Fractionation	268
RNA Isolation	270
Reverse Transcription	273
Oligonucleotide Primer Design.....	275
Polymerase Chain Reaction (qPCR).....	277
Other Contributions to Literature	284
Peer-Reviewed publications.....	284
Published abstracts and conference proceedings	284
Oral presentations	284

List of Tables

Review of Literature	1
Table 1- p53 and exercise regimens.....	34
Manuscript	60
Table 1- List of primary antibodies used	71
Table 2- List of primer sequences used in qPCR analysis	74
Table 3- Phenotype, exercise capacity and mitochondria	81
Appendix A: Manuscript Data and Statistical Analysis	110
Table 3 – Phenotype, exercise capacity and mitochondrial parameters.....	110
A- Pre-training body mass and distance to exhaustion.....	110
B- Post-training phenotype	111
C- Mitochondrial yield and RCR.....	117
Table 2 – p53 protein and localization.....	121
B- Whole muscle total p53 protein	121
C- Whole muscle phosphorylated p53 (Ser ¹⁵) protein.....	121
E- Total p53 protein in nucleus and cytosol	122

F- Phosphorylated p53 (Ser ¹⁵) protein in nucleus and cytosol	123
H- Total p53 protein in IMF mitochondria.....	124
I- Total p53 protein in SS mitochondria.....	124
J- Phosphorylated p53 (Ser15) protein in IMF mitochondria	125
K- Phosphorylated p53 (Ser15) protein in SS mitochondria.....	125
Table (Fig) 3 – Physiological and mitochondrial adaptations to training.....	126
C- Performance test distance to exhaustion.....	126
D- Final lactate after acute exercise.....	127
E- COX enzyme activity.....	128
G- Whole muscle PGC-1 α protein.....	129
H- Whole muscle Tfam protein	130
Table 4 – Mitochondrial respiration.....	131
A- State 4 SS mitochondrial respiration	131
B- State 4 IMF mitochondrial respiration.....	132
C- State 3 SS mitochondrial respiration	133
D- State 3 IMF mitochondrial respiration.....	134
Table 5 – Mitochondrial ROS emission.....	135
A- State 4 SS mitochondrial ROS.....	135
B- State 4 IMF mitochondrial ROS	136
C- State 3 SS mitochondrial ROS.....	137
D- State 3 IMF mitochondrial ROS.....	138
Table 6 – mRNA transcripts complete data	139
A- mRNA fold change in WT mice with training	144
B- mRNA fold change in mKO mice and the effect of training.....	144
Table 7 – Regulators of p53 protein and its localization.....	145
A- Whole muscle Mdm2 protein	145
B- Whole muscle CHCHD4 protein	146
Table 8 – Mitochondrially-regulated apoptosis	147
A- Cytochrome c protein release from SS mitochondria, basally	147
B- Cytochrome c protein release from IMF mitochondria, basally.....	148
C- Cytochrome c protein release from SS mitochondria, H ₂ O ₂	149

D- Cytochrome c protein release from IMF mitochondria, H ₂ O ₂	150
E- Whole muscle Bax protein.....	151
F- Whole muscle Bcl-2 protein.....	152
G- Whole muscle p21 protein.....	153
Table 9 – Autophagy pathway with training.....	154
A- Whole muscle LC3 II/LC3 I protein ratio	154
B- Whole muscle p62 protein	155
C- Whole muscle Parkin protein.....	156
D- Whole muscle Beclin-1 protein	157
Table 10 - Physiological and mitochondrial comparison between untrained MS and WB mice.....	158
A- COX enzyme activity	158
B- PGC-1 α mRNA	159
C- Whole muscle PGC-1 α protein	160
D- State 3 SS mitochondrial respiration	161
E- State 3 SS mitochondrial ROS emission	162
F- Cytochrome c protein release from SS mitochondria, basal.....	163
Table 11 – Autophagy comparison between untrained MS and WB mice	164
B- Whole muscle LC3 II/ LC3 I protein ratio.....	164
C- Whole muscle p62 protein	165
D- Whole muscle Parkin protein.....	166
Table 12 –Training on physiological and mitochondrial adaptations in WB and MS mice.....	167
A- Post-training performance, distance to exhaustion.....	167
B- COX enzyme activity.....	168
C- Whole muscle PGC-1 α protein.....	169
Appendix B: Supplementary and Additional Data	170
Table 1- Complete antibody list.....	170
Table 2- Phenotype, exercise capacity and mitochondrial function comparison between MS and WB mice.....	171
Table 3- mRNA and protein fold change comparison	172

Table 4- Structural protein comparison to p53.....	173
Appendix C: Data and Statistical Analysis for Supplementary	188
Table 2- Physiological and mitochondrial parameters in WB and MS mice.....	188
A- Baseline exercise capacity, distance to exhaustion.....	188
B- Post-training phenotypic comparisons	190
C- Mitochondrial parameters (yield and RCR)	196
Table 3 – mRNA and protein fold change comparison.....	200
Table (Fig) 2B – Pre-training initial and final lactate	201
Table (Fig) 3 – Cage hanging test performance.....	202
A- Hanging time	202
B- Holding impulse.....	202
Table 4 – Neurological testing for cerebral function in WB KO mice	203
A- Balance beam test, time to cross.....	203
B- Balance beam test, number of paw slips.....	203
C- Vertical pole test, time	204
D- Cylinder escape test, time	204
Table 5 – DNA fragmentation.....	205
Table 6 – AIF mitochondrial protein release	206
A- AIF protein release in MS mice, basal.....	206
B- AIF protein release in WB mice, basal	207
C- AIF protein release in MS mice, H ₂ O ₂	208
D- AIF protein release in WB mice, H ₂ O ₂	209
Table 7 – Respiration in permeabilized fibres	210
A- state 3 and 4 respiration	210
B- state 3 and 4 respiration, fold change.....	211
C- state 3 and 4 respiration corrected for mitochondrial content	212
D- state 3 and 4 respiration corrected for mitochondrial content, fold change.....	213
Table 8 – ROS emission in permeabilized fibres	214
A- state 3 and 4 ROS	214
B- state 3 and 4 ROS, fold change.....	215
C- state 3 and 4 ROS corrected for mitochondrial content.....	216

D- state 3 and 4 ROS corrected for mitochondrial content, fold change.....	217
Table 9 - Antioxidant protein changes with training.....	218
A- Whole muscle Nrf2 protein	218
B- Whole muscle KEAP1 protein.....	219
Table 10 – Protein expression and comparison between WB and MS mice.....	220
A- p53 mRNA, MS WT.....	220
B- Whole muscle COX IV protein.....	220
D- Whole muscle Bax protein, untrained MS and WB	221
E- Whole muscle Bcl-2 protein, untrained MS and WB	222
F- Whole muscle p21 protein, untrained MS and WB	223
Table 11- IMF mitochondrial comparison between WB and MS mice	224
A- State 3 respiration	224
B- State 4 respiration	225
C- Cytochrome c protein release, basal	226

List of Figures

Review of Literature	1
Fig 1- Electron Transport Chain	7
Fig 2- p53 Protein Domain Structure.....	18
Fig 3- p53 Regulation of Autophagy and Apoptosis	21
Fig. 4- p53 Regulation of Mitochondrial Biogenesis	29
Fig. 5- Rodent Genetic Models.....	40
Manuscript.....	60
Fig. 1- Exercise Program	67
Fig. 2- p53 Protein and Cellular Distribution with Training	76
Fig. 3- Mitochondrial Content and Physiological Adaptations with Training	80
Fig. 4- Mitochondrial Respiration	82
Fig. 5- Mitochondrial Reactive Oxygen Species (ROS) Emission.....	83
Fig. 6- mRNA Transcripts of p53-Regulated Targets	85
Fig. 7- Regulators of p53 Expression and Localization	87
Fig 8- Training and Apoptosis.....	89

Fig. 9- Autophagic Protein Response to Training	91
Fig. 10- Mitochondrial Signaling Comparison between Untrained WB and MS Mice .	93
Fig. 11- Autophagy Protein Comparison between Untrained WB and MS Mice	95
Fig. 12- Mitochondrial Response to Training Comparison between WB and MS Mice	96
Appendix B: Supplementary and Additional Data	170
Fig. 1- Detailed Exercise Training Program.....	175
Fig. 2- Baseline Exercise Performance Test Comparison between WB and MS Mice	177
Fig. 3- Cage Hanging Performance Test	178
Fig. 4- Neurological Testing for Cerebral Function in WB KO Mice.....	179
Fig. 5- DNA Fragmentation.....	180
Fig. 6- AIF Mitochondrial Protein Release	181
Fig. 7- Respiration in Permeabilized Fibres	182
Fig. 8- ROS Emission in Permeabilized Fibres	183
Fig. 9- Antioxidant Protein Changes with Training	184
Fig. 10- Protein Expression and Comparison between Untrained WB and MS Mice .	185
Fig. 11- IMF Mitochondrial Comparison between Untrained WB and MS Mice.....	187

List of Abbreviations

14-3-3-σ	Negative regulator of cyclin-dependent kinases
16S rRNA	16 S ribosomal ribonucleic acid
20S proteasome	20 S (Svedberg sedimentation coefficient) proteasome
26 S proteasome	26 S (Svedberg sedimentation coefficient) proteasome
α-tub	Alpha tubulin
AA	Amino acids
ABTS	2,2'-azino-bis(3-ethylbenzthiazoline-6-sulfonic acid)
ADP	Adenosine diphosphate
AIF	Apoptosis inducing factor
Akt	Protein kinase B, serine/threonine-specific protein kinase
AMBRA1	Autophagy and beclin 1 regulator 1
AMPK	5' adenosine monophosphate-activated protein kinase
ANC	Adenine nucleotide carrier
ANT-I	Anti-inner mitochondrial membrane 1
anti-DNA-POD	Antibody binds to ss- and dsDNA
APAF-1	Apoptotic protease activating factor 1
ARE	Antioxidant response element
ATG	Autophagy-related genes
ATM	Ataxia-telangiectasiamutated
ATP	Adenosine triphosphate
ATR	ATM and rad 3-related
B2M	Beta-2-microglobulin
Bax	BCL2 associated X protein
Bcl-2	B-cell lymphoma 2
Bid	BH3 interacting-domain death agonist
Bim	Bcl-2-like protein 11
BNIP3	BCL2 interacting protein 3
BSA	Bis(trimethylsilyl)acetamide
CaMKII	Ca ²⁺ /calmodulin-dependent protein kinase II
CAT	Chloramphenicol acetyl transferase
CD	Cathepsin D, soluble lysosomal aspartic endopeptidase
CBP	cAMP response element binding protein (CREB) -binding protein
cDNA	Complementary DNA
CHCHD4	Coiled-coil-helix domain-containing protein
CHK1/2	Checkpoint kinase 1 or 2
CHO	Carbohydrate
ChREBP	Carbohydrate-responsive element-binding protein
Cop1	Caspase recruitment domain family member 1
COX I, II, IV	Cytochrome C oxidase isoform 1, 2, 4
Cre	Cyclization recombinase, tyrosine recombinase enzyme
CT	Threshold cycle
CUL3	Cullin3 E3 ubiquitin ligase
DBD	DNA binding region
DEC1	Deleted in esophageal cancer 1

DNA	Deoxyribonucleic acid
Drp1	Dynamamin related protein 1
E2F	DNA-binding transcription factors
ECL	Enhanced chemiluminescence
EDL	Extensor digitorum longus
ELISA	Enzyme-linked immunosorbent assay
EndoG	Endonuclease G
ERK	Extracellular signal-regulated kinase-1
ETC	Electron transport chain
FADH₂	Dihydroflavine-adenine dinucleotide
FAO	Fatty acid oxidation
FdxR	Ferredoxin reductase
FIP200	Focal adhesion kinase (FAK) family interacting protein of 200 kD
Fis1	Mitochondrial fission 1 protein
G1 phase	Gap 1 phase – interphase, preparation for mitosis
G1/S checkpoint	Gap 1/Synthesis checkpoint, transition of G1 to S phase
G2 phase	Gap 2 phase, growth phase
G2/M checkpoint	Gap 2/Mitosis checkpoint, ensures DNA repair before mitosis
GADD45a	Growth arrest and DNA-damage-inducible protein
G6PD	Glucose-6-phosphate dehydrogenase
GAPDH	Glyceraldehyde 3-phosphate dehydrogenase
GLS2	Glutaminase 2
GLUT 1/4	Glucose transporter 1 (different tissues) or 4 (muscle)
GPX1	Glutathione peroxidase 1
GSH	Glutathione
GTPase	Guanosine triphosphate hydrolases
H2DCF-DA	Dichlorodihydro-fluorescein diacetate
H₂O₂	Hydrogen peroxide
HCl	Hydrochloric acid
HDAC	Histone deacetylases
IGFBP-3	Insulin-like growth factor-binding protein 3
IMF	Intermyofibrillar mitochondria
IR	Irradiation
JNK	Jun n-amino-terminal kinases
K₂HPO₄	Dipotassium hydrogen phosphate
KCl	Potassium chloride
KEAP1	Kelch-like ECH-associated protein 1
KO	Knockout
LAMP 1/2	Lysosomal-associated membrane protein 1 or 2
LC3 I / II	Light chain 3B I or II (lipidated)
LoxP	Locus of X (cross)-over in P1, targeted by Cre recombinase
MAPK	Mitogen-activated protein kinase
MCK	Muscle creatine kinase
Mdm2	Mouse double minute 2 homolog
Mfn2	Mitofusin-2
MHC	Major histocompatibility complex

MHCIIa	Myosin heavy chain isoforms in type IIa
MHCIIx	Myosin heavy chain isoforms in type IIx
MHCIIβ	Myosin heavy chain isoforms in type I beta
MnSOD	Manganese-dependent superoxide dismutase, Superoxide dismutase 2 (SOD2)
MOMP	Mitochondrial outer membrane permeabilization
MOPS	3-(N-morpholino)propanesulfonic acid
mRNA	Messenger RNA
MS	Muscle specific mice
mtDNA	Mitochondrial DNA
mTORC1	Mammalian target of rapamycin complex 1
MyoD	Myogenic differentiation protein
NADH	Nicotinamide adenine dinucleotide
NEDD8	Neural precursor cell expressed developmentally downregulated protein 8
NER	Nuclear extraction reagent
NF-kB	Nuclear factor-kappa beta
Nix	Bcl2/E1B 19 kDa-interacting protein 3-like protein
NoxA	NADPH oxidase activator, pro-apoptotic member
NQO1	NAD(P)H:quinone oxidoreductase 1
NRF 1/2	Nuclear respiratory factor 1 or 2
Nrf2	Nuclear factor E2-related factor 2
NUGEMPs	Nuclear genes encoding mitochondrial proteins
Opa1	Optic atrophy protein 1
p21	Protein 21, cyclin-dependent kinase inhibitor (CKI)
p300	Protein 300, histone acetyltransferase
p53	Protein 53, tumor suppressor protein
p53R2	p53 inducible ribonucleotide reductase
p62	Nucleoporin p62, aka sequestosome 1 (SQSTM1)
p63	Transformation-related protein 63, p53 tumor suppressor protein family
p66Shc	Protein p63 Shc (Src homologous- collagen homologue) adaptor
p73	Protein 73, p53 tumor suppressor protein family
PAI-1	Plasminogen activator inhibitor-1
PCAF	P300/CBP-associated factor
PCNA	Proliferating cell nuclear antigen
PCR	Polymerase chain reaction
PFK1	Phosphofructokinase-1
PGC-1α	Peroxisome proliferator-activated receptor gamma coactivator 1-alpha
PGM	Phosphoglycerate mutase
PI3K	Phosphatidylinositol-3 kinase
PIAS-1	Protein inhibitor of activated STAT 1
PIG 3/6	p53-inducible gene 3 or 6
PIM	Protein import machinery
PINK1	PTEN-induced putative kinase 1
Pirh2	p53-induced RING domain E3 ubiquitin protein ligase
PML-IV	Promyelocytic leukemia protein 4
Polg1	Polymerase gamma 1
PP2A	Protein phosphatase 2

PPP	Pentose phosphate pathway
PRD	Phosphoenolpyruvate-dependent sugar phosphotransferase system regulation domain
PTEN	Phosphatase and tensin homolog
Puma	p53 upregulated modulator of apoptosis
Rb protein	Retinoblastoma protein
REG	Regenerating protein
RNA	Ribonucleic acid
RNS	Reactive nitrogen species
ROS	Reactive oxygen species
S phase	Synthesis phase, DNA replication phase
SCO2	Cytochrome c oxidase assembly protein 2
SDS-PAGE	Sodium dodecyl sulfate polyacrylamide gel through electrophoresis
Set9	Su(var)3-9, Enhancer-of-zeste and Trithorax (SET) protein domain 9
SIRT-1	Silent mating type information regulation 2 homolog) 1
SS	Subsarcolemmal mitochondria
SV40	Simian vacuolating virus 40
TA	Tibialis anterior
TAD 1/2	2-N-terminal transcriptional activating domains 1 and 2
TBST	Tris-buffered-saline-tween
TET	Ten-eleven translocation domain
Tfam	Mitochondrial transcription factor A
TIGAR	TP53-inducible glycolysis and apoptosis regulator
Topors	Topoisomerase I (TOP 1) binding arginine/serine rich protein
TRP53	Transformation related protein 53
TSC 1/2	Tuberous sclerosis 1 or 2
Ub	Ubiquitin
Ubc9	Ubiquitin carrier protein 9
UbcH5B/C	Ubiquitin conjugating enzymes
ULK1	Unc-51 like autophagy activating kinase
UPR	Unfolded protein response
UQ	Ubiquinone
VDAC	Voltage-dependent anion channel
VO2	Maximum rate of oxygen consumption
WB	Whole body mice
Wks	Weeks
WT	Wildtype
Ψ	Membrane potential

REVIEW OF LITERATURE

1.0. Skeletal Muscle Function and Maintenance

1.1. Introduction: Importance of Muscle Health

Skeletal muscle is a dynamic tissue that coordinates movement, posture, and homeostasis through multiple signaling pathways including metabolism, thermogenesis, and mitochondrial biogenesis (67, 127). Though it is one of three major muscle types, the others being cardiac and smooth muscle, it comprises 40-50% of the total body mass of a healthy individual (64). Its dominant presence throughout the body allows it to serve as an energy reservoir and metabolic regulator of interorgan crosstalk (9).

Energy metabolism is a critical function of skeletal muscle. Its role in glucose uptake and storage for the conversion of chemical energy to mechanical energy is required both for movement and optimal organ function. Energy derived for work is primarily through ATP production which requires rapid re-synthesis for continued availability. The second source of readily available energy is creatine phosphate which is a reservoir of high energy phosphate bonds vital to rebuild ATP (110). Carbohydrates (CHO) are the only macronutrient that can generate ATP aerobically and anaerobically. Anaerobically, glucose/glycogen utilization in the cytosol generates low levels of ATP and builds lactic acid which can impede muscle contractions over time (110, 177). The aerobic pathway on the other hand provides 18 times more ATP due to pyruvate entry into the Krebs' cycle within the mitochondria. ATP can additionally be provided by metabolizing fats and proteins. Triglycerides can be hydrolyzed to generate fatty acids which undergo β -oxidation in the mitochondria producing high energy yields per each acetyl-coA unit. However, this process requires greater oxygen levels than CHO oxidation (110). The requirement for amino acid substrate utilization for fuel is increased when other substrates are unavailable. During prolonged exercise with normal substrate availability, protein oxidation

accounts for only 5% of the energy requirements (108, 110). Therefore, the major requirements are CHO oxidation, which increases with exercise intensity, and fat oxidation, which increases from low to moderate exercise duration, but decreases from moderate to high exercise intensities.

Numerous conditions and diseases lead to an imbalance in the metabolic demands placed on muscle. This can outweigh the protein synthesis occurring with dietary intake and eventually can lead to muscle atrophy and a loss of appropriate metabolic functioning. The specific conditions that lower dietary intake, such as malnutrition and starvation, and those that alter the metabolic load on muscle, such as cancer, immune disorders and muscular dystrophies, can have serious consequences (9, 169). Most of these conditions are associated with variable degrees of inflammation which activate proinflammatory cytokines to accelerate muscle catabolism (111). Ultimately, the loss of muscle mass, function, and strength can lead to longer recovery times, selective fiber type transitions, slower wound healing, physical disability, and greater health care costs (3, 60, 109, 136). To combat these adverse outcomes, controlled nutrition and exercise programs can be implemented for muscle recovery to promote overall health (5, 9, 82, 175).

1.2. Physiology of Skeletal Muscle

1.2.1. Structural Physiology

Skeletal muscle consists of bundles of single large cells, termed myocytes, which develop from myoblast fusion in a process known as myogenesis (35). Its architecture originates through several distinct phases: 1) embryonic phase, wherein mesoderm-derived structures generate template muscle fibers, 2) perinatal phase, whereby myogenic progenitors proliferate and myofibrillar protein synthesis peaks and plateaus, 3) mature phase, wherein progenitors enter into quiescence and reside in muscle as satellite cells, and 4) regenerative phase, whereby satellite cells in the fiber sarcolemma expand mitotically and differentiate into new fibers when

damaged (7, 14). Each muscle fiber contains multiple myofibrils, composed of cylindrical bundles of thick myosin and thin actin filaments, each of which are organized to form repeating sarcomere units.

Muscle fibers are delineated based on their myosin profiles. Myosin is a hexameric protein consisting of four light chains which modulate interactions between myosin and actin, and two heavy chains (fast and slow) which are differentiated into nine isoforms to dictate appropriate fiber composition (128). With an influx of calcium into the sarcoplasmic reticulum, rapid repetition of myosin, working in conjunction with actin to form a cross-bridge, initiates a power stroke that allows for contraction (35). Differences in muscle types are a result of metabolic properties, histochemical features, and most importantly, structural protein composition based primarily on the myosin heavy chain (MHC) protein, which dictates the velocity of contraction (9, 128). There are three pure fiber types containing a single MHC isoform. Slow twitch red type I fibers with the MHC β isoform function as oxidative and fatigue resistant fibers. Fast twitch red type IIa fibers with the MHCIIa isoform contain intermediate metabolic properties for fast oxidative capacity. Lastly, fast twitch white type IIx fibers with the MHCIIx isoform for high glycolytic energy production, result in high force output but consequentially have a high fatigue rate (126, 138, 148). Fast twitch white type IIb fibers with the MHCIIb isoform are analogous to the type IIx fibers, but are found in humans and not mammals. Hybrid fibers types are further created through the mix of major isoforms and include type I/IIA (IC), IIA/I (IIC), IIAD, IIDA, and IIBD (126). The dynamic property of muscle is a result of fiber type transitions. This is associated with gradual changes in energy costs as a result of different muscle usage patterns that dictate sequential and reversible transitions of slow-to-fast

and fast-to-slow transformations following the paradigm MHCII β \leftrightarrow MHCIIa \leftrightarrow MHCIIx \leftrightarrow MHCIIb (126).

1.2.2. Cellular Structure

To interpret how muscle adapts to incoming stimuli in order to provide energy for cellular and mechanical functions, a thorough understanding of the components and properties of the myocyte is required. Myocytes are similar in organelle structure to other eukaryotic cells, however the addition of myofibrils allows for its contractile ability. Under apt conditions, the cell functions to meet energy and signaling demands, however under conditions such as starvation or organelle dysfunction, other pathways are induced to maintain cellular integrity. Though all organelles are essential, skeletal muscle plasticity is attributed to mitochondria.

1.2.2.1. Mitochondrial Structure and Function

The endosymbiotic theory postulates that the rise of mitochondria within cells, approximately 1.45 billion years ago, occurred through eukaryotic engulfment to provide its anaerobic host with aerobic capacity (105). As the symbiosis matured, the mitochondrial organelle transferred a portion of its bacterial plasmid to the nucleus, thereby losing its ability to survive as a free-living organism. The current 16.5 kb mitochondrial plasmid now possesses 37 genes coding for two ribosomal RNAs (12S and 16S rRNA), 22 tRNAs, and 13 electron transport chain genes for energy generation (64, 170, 176). The remaining gene products from the original mitochondrial genome (~1200) are now encoded within chromosomal DNA. These proteins are imported into the mitochondria via protein import machinery (PIM) (170).

Mitochondria are elliptically shaped double phospholipid membraned organelles with multiple folds in the inner membrane called cristae (64, 76). The matrix of the mitochondria

contains the mtDNA. Outside of the inner membrane is the intermembrane space which is enclosed by the outer membrane. The inner membrane contains the subunits of the electron transport chain (ETC) which is made up of five complexes (Figure 1). Ubiquinone and cytochrome c proteins shuttle electrons between complexes I \rightarrow III and II \rightarrow III, and complexes III \rightarrow IV respectively. As the electrons are shuttled across the complexes, proton pumping is facilitated out of complexes I, III, and IV and into the intermembrane space (27, 99). This creates an electrochemical potential gradient that facilitates proton re-entry into the matrix through complex V (ATP synthase), thus generating ATP energy for cellular utilization (27, 99). This is known as the chemiosmotic theory for energy generation (113). It is important to note that reactive oxygen species (ROS) and heat are by-products of energy metabolism that likely activate/regulate downstream signaling mechanisms (115). The production of superoxides and radical formation at the NADH dehydrogenase complex I and cytochrome bc1 complex III, as a result of substrate unavailability and/or electron slippage through the buildup of the electrochemical gradient, can lead to detrimental outcomes such as peroxidized lipids, oxidized proteins and damaged DNA, if not removed (66, 112, 116, 135). On the other hand, mitochondrial-derived ROS can exert beneficial effects, when maintained at a certain threshold, by acting as signaling mechanism for mitochondrial biogenesis (22, 66, 72). Therefore, it seems that there is a specific threshold tolerance of the cell to ROS production levels.

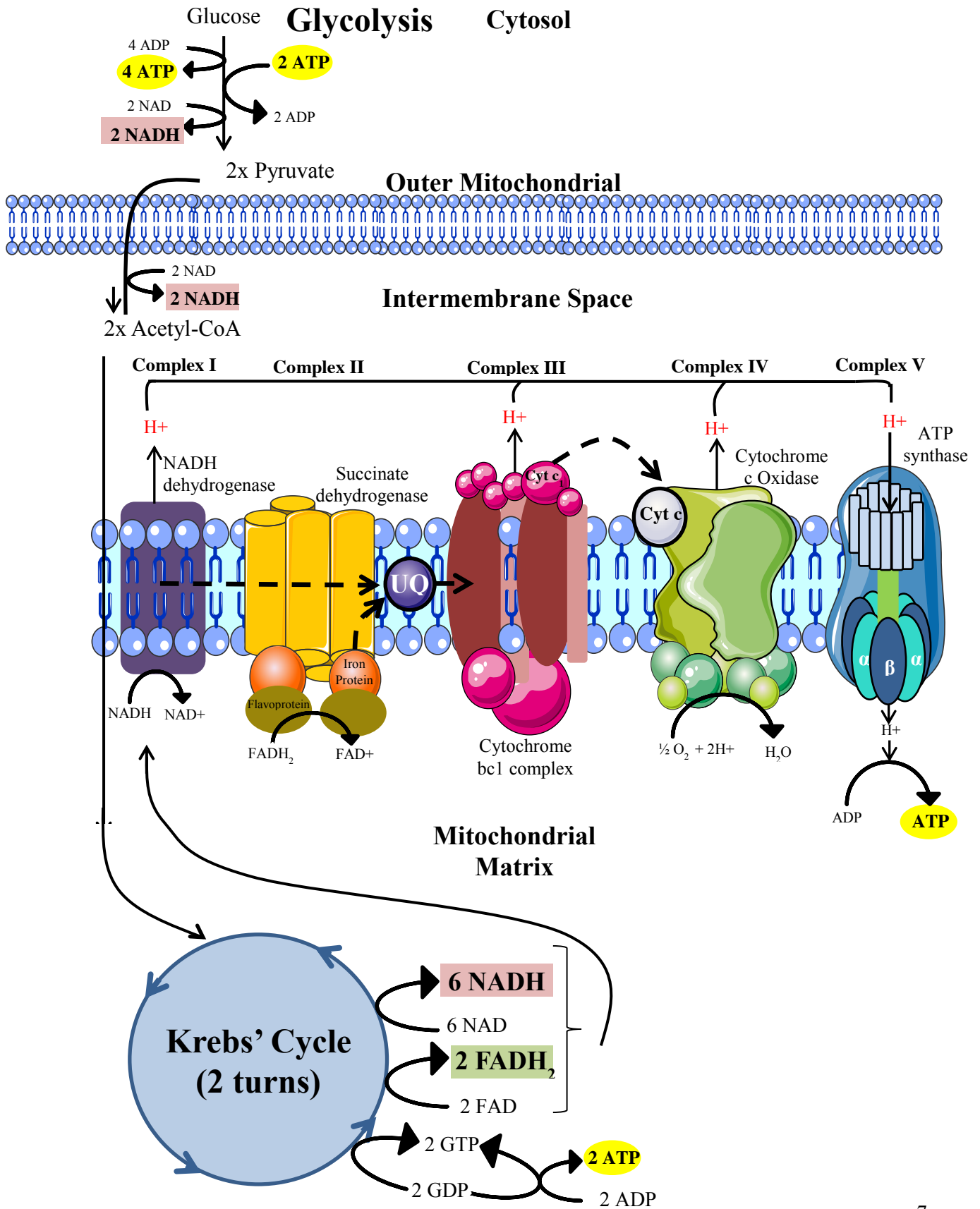


Figure 1. Substrate utilization and schematic representation of the electron transport chain. Large carbohydrates are broken down into glucose molecules that can enter into glycolysis within the cytosol, which is then further broken down into two pyruvate molecules in a process that yields 4 ATP. Pyruvate diffuses into the intermembrane space where it is converted to acetyl-CoA through a transition reaction yielding NADH. Acetyl-CoA, two per glucose molecule, can then enter into the Krebs' cycle. Lipids are broken down to acetyl-coA units through beta-oxidation, yielding large amounts of ATP depending on the size of the fatty acid molecule. Proteins are the last energy source to be catabolized, and are broken down to amino acids through deamination to then enter into the Krebs' cycle. Once substrates diffuse into the mitochondrial matrix, acetyl-coA enters the aerobic Krebs' cycle yielding 3 NADH, 1 FADH₂ and 1 ATP per acetyl-coA, or a total of 6 NADH, 2 1 FADH₂, and 2 ATP per glucose molecule. The NADH and FADH₂ substrates, generated from both anaerobic and aerobic processes, can then be utilized by the electron transport chain (ETC) to generate ATP energy. NADH and FADH₂ are oxidized by complexes I (NADH dehydrogenase) and II (succinate dehydrogenase) respectively. The electrons donated from these processes are passed through subsequent complexes including complex III (cytochrome bc1) through reduction of the mobile electron carrier ubiquinone (UQ), and complex IV (cytochrome c oxidase) by cytochrome c reduction to generate energy required to pump protons into the intermembrane space. This transfer process through the ETC can result in the escape of electrons through complexes I and III prematurely which reduces oxygen and generates H₂O₂, also known as reactive oxygen species (ROS). The final electron acceptor is oxygen to produce H₂O. This electron transfer throughout the ETC contributes to the buildup of H⁺ ions in the intermembrane space, creating a proton gradient which is utilized by complex V (ATP synthase) to convert ADP to ATP in a process known as chemiosmosis. This entire process produces an ATP yield of approximately 36 ATP.

Mitochondria function to regulate cellular signaling processes. The dynamic property of mitochondria are a result of its existence as a functional reticulum, maintained through fission and fusion events (28, 70). This interconnected network ultimately facilitates oxygen diffusion and allows for mitochondrial quality control (28, 115). Interestingly, the presence of a reticulum conflicts with the well-known existence of mitochondrial sub-populations which form within their own networks in discrete subcellular locations. The rise of separate populations with distinct biochemical differences is presumed to be a result of the different energy requirements of specific locations within the myofiber. The subsarcolemmal (SS) mitochondria are located beneath the sarcolemmal membrane in close proximity to myonuclei, therefore permitting greater adaptations to stimuli (5, 34, 85). These mitochondria provide ATP energy for nuclear and membrane functions, exhibit higher membrane potentials, and produce greater amounts of ROS (34, 123). The intermyofibrillar (IMF) mitochondria coalesce within the myofibrils and comprise 80-85% of the total mitochondrial volume (5, 34). They have a greater rate of oxygen consumption, ~2.5-fold greater than SS populations, and consequentially generate higher ATP levels to supply myosin and actin with energy for muscular contractions (4, 5). Furthermore, this population has higher rates of protein import and synthesis, and a greater capacity for fatty acid oxidation (115, 159). As these populations differ in their structure and function, and possibly in the signaling pathways that may exist to facilitate these differences, they do share similar mechanisms to regulate metabolic demands.

1.2.2.1a. Signaling Pathways Regulating Mitochondrial Health

There are many important signaling mechanisms that are employed by the cell to maintain optimal skeletal muscle function. The primary mechanism of mitochondrial biogenesis ensures regulation of energy sensitive pathways including calcium homeostasis, ROS production

and signaling, and apoptosis. As a result, a healthy mitochondrial pool is required, with its dynamics tightly regulated by opposing fission and fusion processes. Fusion, through Opa1 and Mfn-2 proteins, coincides with signals that induce mitochondrial biogenesis, such as endurance training, leading to the intermixing of mitochondrial material and expansion of the reticulum (70, 83). Fission on the other hand, facilitated by Fis-1 and Drp-1 proteins, promotes the division of organelles leading to a reduction of the reticulum.

Additional signals that regulate the health of the mitochondrial pool includes the antioxidant production pathway whereby primary enzyme antioxidants, non-enzymatic antioxidants, and dietary antioxidants function to maintain redox balance (112, 132). In response to changes in the cellular environment, optimal mitochondrial functioning may be disrupted through increased ROS/RNS leading to DNA, protein, and lipid damage. This induces either the cell death or mitophagy pathways. Mitophagy, a component of autophagy, utilizes numerous mechanisms to signal the binding of damaged mitochondria to the phagophore causing the organelle to be engulfed within the autophagosome and directed to the lysosome for degradation (140). With greater genotoxic stress levels due to DNA damage, hypoxia, and oxidative stress, the mitochondria can a source of cellular death through permeabilization of the outer mitochondrial membrane (MOMP) (87). Ultimately, maintenance of a healthy mitochondrial reticulum is required for optimal skeletal muscle function, which can be regulated by the tight coordination of numerous signaling mechanisms.

2.0. Skeletal Muscle Adaptations to Exercise

2.1. Exercise: Its Pleiotropic Benefits

Exercise is a beneficial signal, not only for skeletal muscle cellular health and maintenance, but for whole body health and fitness as well. The exercise regimen, based on type of exercise as well as its parameters including duration, frequency, intensity and length, can induce a variety of molecular and phenotypic adaptations. Furthermore, the application of a recovery period following exercise allows for a sufficient interval in which transient changes in gene expression can induce adaptations. Therefore, depending on the type of exercise regimen and its parameters, one can optimize and maximize the desired results.

Skeletal muscle is a major recipient for the advantageous effects of exercise. Increased fiber contractility with aerobic exercise can lead to elevated myoglobin, increased capillarization, and enhanced mitochondrial content to ultimately improve the oxidative capacity of muscle (65, 77, 117). Interestingly, growth of the capillary network, through a process known as angiogenesis, is thought to precede adaptations in skeletal muscle. Aerobic exercise preferentially utilizes lipid energy metabolism which reduces the formation of lactic acid and the use of high energy phosphate, and attenuates the loss of glycogen to reduce the rate at which muscle fatigues (64). With other types of exercise, such as with resistance exercise, hypertrophy is a consequence due to fiber enlargement according to the myonuclear domain theory (125, 152). Whole body health can further be improved with prolonged exercise regimens as observed through cardiovascular benefits, greater endurance and work capacity, enhanced nutrient delivery and uptake, and even enriched mood and cognition (6, 64, 68, 78, 164). As a result of its pleiotropic effects in skeletal muscle and throughout the body, exercise can be utilized as an intervention to promote a healthier phenotype, and reduce and even reverse symptoms associated

with aging, muscle atrophy, and mitochondrial disease (66). However, due to the immense variety of signals that regulate adaptations to exercise including fiber type composition, intercellular crosstalk, nutrient requirements and mitochondrial content and function, the different exercise parameters will result in unique effects in muscle (119).

2.1.1. Acute versus Chronic Training: Teasing out the Differences

Exercise can be grouped into two major categories: Resistance and Aerobic exercise. Aerobic exercise in particular is further subcategorized into acute exercise and prolonged exercise, for which each category results in an umbrella of distinct molecular and morphological effects.

Aerobic exercise provides numerous beneficial results to skeletal muscle, as a result of its ability to induce mitochondrial biogenesis to a greater extent than with resistance exercise. Depending on the level of training prior to undergoing a single bout of exhaustive exercise, it can produce significant adaptations. An acute bout is sufficient enough to increase signaling kinases such as p38 MAPK (0.5-fold), AMPK (2.5-fold), and CaMKII (2.5-fold) which further remain elevated after 3 hours of recovery (143, 166). These kinases activate numerous transcription factors such as the mitochondrial transcription factors NRF-1 and 2, antioxidant transcription factor Nrf2, and the guardian of the genome p53, facilitating enhanced nuclear localization and activation. Additionally, the major mitochondrial coactivator PGC-1- α , can also be phosphorylated by these signaling kinases, allowing for its subcellular localization. Once in the nucleus, PGC-1 α can assist in the transcription of Nuclear Genes Encoding Mitochondrial Proteins (NUGEMPs) such as COX IV (60%), Tfam (50%) and NRF-1 (200%), which can be further increased during a recovery period (143, 166). The antioxidant pathway is notably

activated with acute exercise leading to Nrf2-mediated transcription of GSH and MnSOD antioxidants at a threshold of above 90 minutes of acute exercise (171). Furthermore, autophagy has also been shown to increase following an acute bout of endurance exercise. Increased LC3-II and reduced p62 levels are indicative markers of autophagy activation (166). DNA fragmentation, a marker of cell death caused by an increase in the Bax/Bcl-2 ratio and caspase 3 activation, has been noted following eccentric resistance exercise and acute strenuous treadmill exercise programs; chronic aerobic exercise training can relieve these effects (84, 156, 157). Further mechanisms induced with acute exercise include increased muscle protein turnover, activation of the UPR, and transient changes in myogenic and metabolic genes (20, 81, 88, 178).

With endurance training on the other hand, mitochondrial content can increase from 30-100% within a time frame of 4 to 6 weeks (66). As such, greater adaptations will be apparent in the low oxidative fibers, where the greatest percentage of mitochondrial content is found. Improvements associated with endurance capacity are a result of mitochondrial biogenesis and its improved reticular formation. Increased NUCLEAR ENCAPSULATED PROTEIN transcription factors such as p53, and the coactivator PGC-1 α , enhance mitochondrial content and facilitates a reduction in glycolytic activation (lowered lactic acid production, attenuated glycogen utilization, reduced phosphocreatine usage) to prevent an acidotic state, and increases fatty acid fuel oxidation (62, 64). Other adaptive signals include accelerated mRNA turnover for rapid phenotypic plasticity, reduced ROS activation, attenuated apoptotic signaling, and increased autophagy to maintain a healthy organelle pool (42, 61, 66, 89, 165). These improvements over time assist in the transition to a greater oxidative fiber phenotype and improve capillary density to enhance respiratory capacity and increase contractile capability (45, 46). Various models of exercise training exist, including constant and progressive treadmill training, electrical stimulation, and

voluntary wheel running. Manipulations in these parameters can alter signaling mechanisms to lead to the aforementioned effects to enhance muscular endurance.

2.2 Aerobic Exercise-Mediating Signaling Pathway Regulation

2.2.1. Kinase Activation and Downstream Pathways

With cross bridge cycling during contractile activity, there is an increase in specific signaling pathways that collectively activate transcription factors within the nucleus and mitochondria to alter gene expression. These signals include a) a reduced ATP/free ADP ratio, b) changes in intracellular calcium levels following release from the sarcoplasmic reticulum, and c) an increase in oxygen consumption and consequentially its by-product reactive oxygen species, which cooperatively leads to the activation of intracellular protein kinases such as AMPK, CaMKII, Akt, and MAPKs to trigger post-translational protein modifications (63, 66, 77). Phosphorylation of transcription factor p53 and transcriptional coactivator PGC-1 α , the master regulators of cellular homeostasis and mitochondrial biogenesis respectively, allows for their nuclear localization and activation of NUGEMPs such as NRF-1/2 and Tfam (119). Once these genes are transcribed, they proceed through the central dogma of protein formation, forming their respective mRNAs which then exit the nucleus and are translated to functional proteins in the cytosol. Tfam, once folded, can be imported into the mitochondria through the TIM and TOM complexes to regulate mtDNA transcription and replication (68, 147). Other proteins imported into the mitochondria, such as those regulated by p53, including cytochrome c oxidase assembly (SCO2) and apoptosis inducing factor (AIF) proteins, as well as other metabolic enzymes, function to assist in the formation of the multi-subunit ETC complexes to increase muscle aerobic capacity (68). Furthermore, enhanced transcription of mitochondrial DNA by Poly increases COX I and II gene expression to improve mitochondrial respiration with aerobic

exercise. Ultimately these signals lead to the activation of mitochondrial biogenesis and expansion of the reticulum with exercise which can feedback to other signaling mechanisms such as the antioxidant and mitophagy pathways to maintain optimal cellular homeostasis.

2.2.2. Intracellular Communication and Crosstalk

Intercellular and intracellular crosstalk is the process of exchanging molecular messages and material between and within cells respectively, to maintain optimal physiological activity and coordinate homeostasis, adaptation, and survival (130). This ability for cell-cell communication is mediated by numerous mechanisms including ligand-receptor signaling, secretion/uptake of the exosome transmitting system, intercellular structures (synapses, gap junctions), organelles, and trafficking signaling molecules (130, 183). Thus, in order to maintain optimal cellular homeostasis for ideal tissue health, communication is required between signaling mechanisms regulating cellular proliferation, maintenance, and degradation.

With varying stress loads, dependent on the type, duration and intensity, cellular degradation pathways may be activated to prevent aberrant proliferation and signaling. Prior to this however, certain signaling mechanisms are employed under to maintain cellular integrity. Antioxidant enzyme defenses are regulated by the major transcription factor Nrf2 to produce enzymes such as SOD2, catalase, glutathione peroxidase, and reductase to neutralize ROS/RNS (129). Furthermore cell cycle arrest and autophagy pathways can be activated to allow for genomic repair and dysfunctional organelle removal, respectively. However, when ROS production exceeds the antioxidant capacity, apoptosis can be triggered (66). Thus cellular maintenance, whilst under the influence of exercise, is required through signaling cross-talk to maintain optimal mitochondrial biogenesis to suffice workload requirements, without generating above threshold ROS levels that induce cell death pathways.

3.0. p53 Transcription Factor

3.1. Introduction to the Tumor Suppressor p53

The tumor suppressor protein p53 is a rapid-response transcriptional regulator of diverse signaling pathways involved in maintaining cellular homeostasis. Thus, it is affectionately termed the “Guardian of the Genome” for its master regulatory role. Immense progress has since been made from its initial and monumental discovery in 1979 by David Lane and Lionel Crawford. The p53 protein was an unexpected finding during an immunoprecipitation experiment for the T tumour antigen of the Simian Virus 40, whereby a protein with a molecular weight of 53 kDa accompanied the antigen (90). Due to the presence of p53 in numerous cancer cell lines and the SV40 cell line, it became persistently characterized as an oncogene. It took a decade of elaborate investigations before its true role as a tumor suppressor was revealed. This spurred research into the role of p53 in cancer biology for the reason that approximately 50% of malignancies carry a p53 mutation/inactivation (24, 56, 69). Within the last forty years, and ~78,000 publications later, research on p53 has exploded to define its numerous applications in cancer and other diseases.

New discoveries on the pleiotropic effects of p53 on signaling mechanisms that maintain cellular and genomic integrity are continuously being made. With varying levels of stress, specific modifications to the p53 protein, activate or impair downstream signaling pathways that regulate cell cycle arrest and senescence, pro- and anti-oxidant function, apoptosis, DNA repair, metabolism, differentiation, and angiogenesis (93). Though its many roles in the cell are known, research on the communication that occurs between these pathways to maintain cellular homeostasis are still being pursued, with the goal to elucidate how p53 leads to cooperative interactions depending on the level of cellular stress.

3.1.1. Cellular Localization Dictates Function

The p53 gene, also termed TP53 in humans or TRP53 in rodents, contains a large core-DNA binding domain (DBD) that is preceded by two N-terminal transactivation regions with a proline rich domain for protein-protein interactions, and is additionally followed by a tetramerisation (TET)/oligomerization motif and C-terminal regulatory region (101, 122). Interestingly, the DBD is the region that undergoes heavy mutagenesis during tumour formation, with >90% of the mutations occurring within this section (122). Following post-transcriptional modifications, the p53 gene codes for eleven exons with two translational start sites in exons 2 and 4, that when translated, create the 393 amino acid that homodimerizes to form the functional p53 protein structure (122). Post-translational modifications can occur in all of these domains leading to high variability in the stability and function of p53 (Figure 2). The p53 pathway is divided into distinct sections: 1) input signals that trigger cellular biochemical changes, 2) detection of signals by upstream mediators that initiate alterations to the p53 protein, 3) activation/inhibition of p53 and its subcellular localization, 4) p53 downstream signaling activation by transcriptional regulation or sequence specific protein-protein interactions, and 5) cellular outputs of these signaling pathways (93). Intrinsic and extrinsic stress signals induce post-translational modifications to the p53 protein through mediators such as kinases (ATM, ATR, Chk1 and 2, JNK, p38, AMPK), phosphatases (PP2A), sumoylases (PIAS-1, Ubc9, Topors, SUMO1), deacetylases (HDAC, SIRT-1), neddyases (NEDD8), methylases (Set9), acetyltransferases (p300, CBP, PCAF), and ubiquitin enzymes (UbcH5B/C, Mdm2, Pirh2) (92, 93). Phosphorylation is the dominant covalent modification as it occurs on ten different residues within the 100 amino acid N-terminal region and within the C-terminus, and as such can be targeted by numerous kinases (92). This modification can destabilize the interaction between

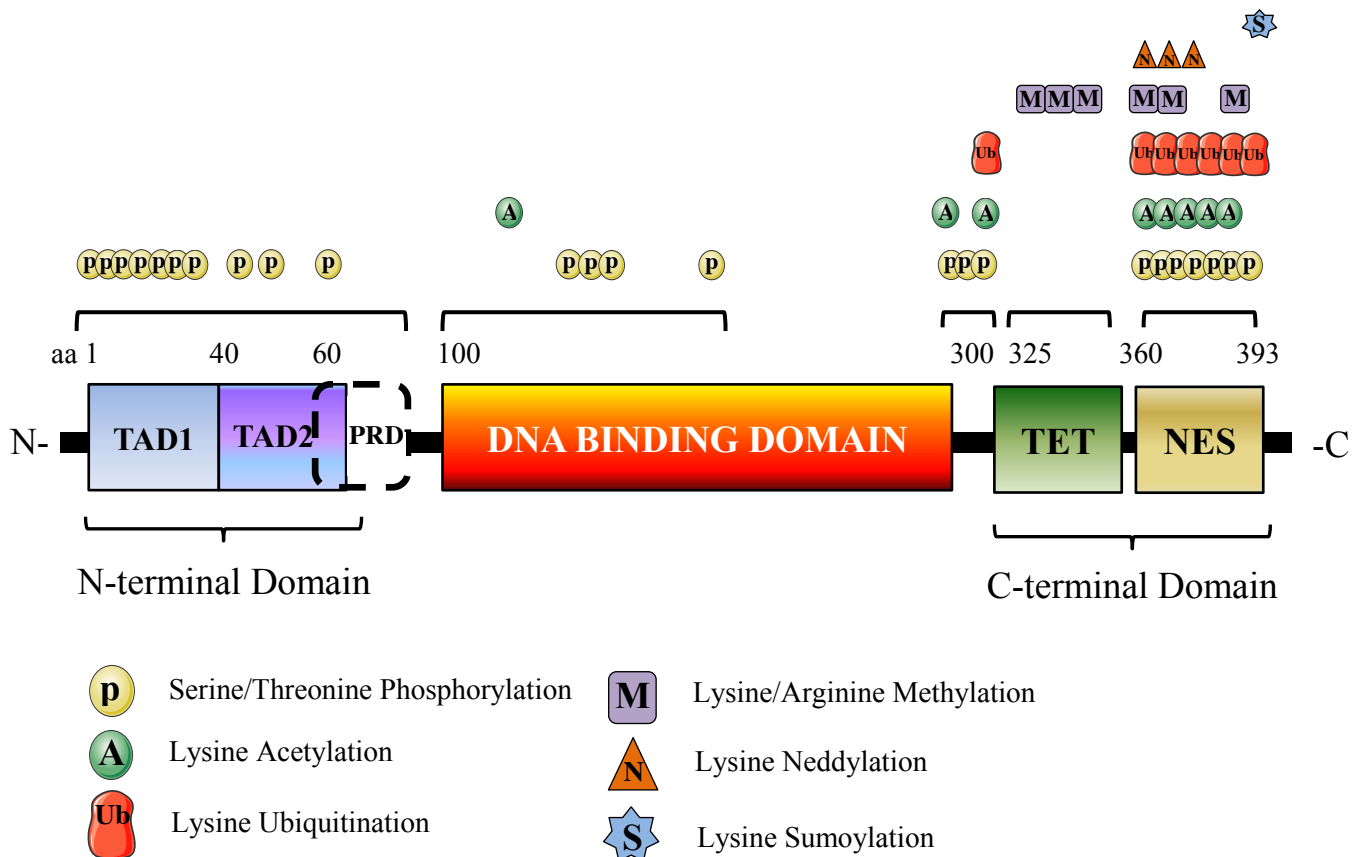


Figure 2. p53 protein domain structure and post-translational modifications. Schematic representation of the 393 amino acid domain structure of the p53 protein indicating the important sites where numerous post-translational modifications occur such as phosphorylation, acetylation, methylation, sumoylation, ubiquitination, and neddylaton. There are numerous phosphorylation sites within TAD1 (Serine 6, 9, 15, 20, 33, 37 and Threonine 18), TAD2 (Serine 46 and Threonine 55, 81), DBD (Serine 149, 215 and Threonine 150, 155), before the TET (Serine 313-315), and within the REG (Serine 366, 371, 376, 378, 392 and Threonine 377, 387). Acetylation sites are present within the DBD (Lysine 120), before the TET (Lysine 305, 320), and within the REG (Lysine 370, 372, 373, 381, 382). Methylation sites are found within the TET (Arginine 333, 335, 337) and within the REG (Lysine 370, 372, 382). Ubiquitination for targeted degradation specifically occurs before the TET (Arginine 320) and within the REG (Arginine 370, 372, 37, 381, 382, 386). Neddylaton and sumoylation are less frequent, occurring within the REG at Arginine 370, 372, 373 and Arginine 386 respectively. Abbreviations: N-terminal transactivation domain (TAD), proline-rich domain (PRD), tetramerisation domain (TET), C-terminal regulatory domain (REG), nuclear export signal (NES), amino acids (aa). Figure adapted from (101).

p53 and its negative regulators (Mdm2, Pirh2, Cop1) to prevent ubiquitination and proteasomal degradation in the cytosol (92).

In response to stress, phosphorylated p53, most commonly found on Ser15, Thr18 and Ser20, is stabilized and accumulates in the cytosol (30, 144). It can then localize to varying subcellular compartments, such as the nucleus or mitochondria, to regulate genomic integrity. Upon exposure of its nuclear localization motif in the C-terminal region, p53 enters the nucleus to bind to p53-response elements identified by RRRCWWGYYY (R=purine, W=A or T, Y=pyrimidine) consensus sequences (93). A p53 response element comprises two of these 10 base-paired sequences, often located in the first or second intron or within the 5' region, interspersed by 0-13 base pairs (93). Approximately 13,774 genes have p53 response elements within their promoters and can therefore be transcriptionally regulated by p53 (161). Hence, due to the high volume of p53- consensus sequences, p53 can transcribe and regulate genes in numerous pathways including those within apoptosis, autophagy, metabolism, cell cycle arrest/senescence, and mitochondrial biogenesis.

Though nuclear localization can occur with a host of intrinsic and extrinsic signals that expose the nuclear localization motif on p53, p53 does not contain a mitochondrial targeting sequence and therefore mitochondrial localization has been shown to occur with specific signals including high cellular stress (signals that induce apoptosis), and more recently exercise. The localization of p53 either to the mitochondrial membrane or to the matrix dictates the signaling response. With apoptotic stress signals, p53 localizes to the mitochondrial membrane to interact with multi-domain members of the anti- and pro-apoptotic Bcl-2 family to inhibit/activate respectively, leading to robust MOMP induction (168). This process is facilitated by Bax/Bak oligomerization on the outer membrane to initiate pore formation as well as opening of the

mitochondrial permeability transition pore (mtPTP) that simultaneously releases lethal proteins to activate enzymatic caspase machinery for chromatin degradation, and increases mitochondrial swelling through cytosolic influx (168). On the other hand, with exercise stimuli, p53 can localize to the mitochondrial matrix to regulate mtDNA integrity for maintenance and proliferation of the mitochondrial pool.

3.2. p53 Signaling Pathways

Within the last decade, the mechanisms by which p53 regulates homeostasis are becoming apparent and may be distinguished based on the intensity of oxidative stress. Exquisite sensitivity of the p53 pathway is essential, as highlighted by studies assessing cellular function when p53 is overexpressed, reduced, or completely removed (69). Though the well-known molecular functions of p53 have been determined through knockout models, overexpression models cause an imbalance in normal p53 isoform ratios leading to a premature aging phenotype (69, 103, 163). Though numerous studies have attempted to fully understand p53 regulation of signaling pathways, the debate still ensues on how cellular stress signals induce its activation.

3.2.1. Organelle Turnover and Destruction: Autophagy/Apoptosis

To maintain a healthy organelle pool and optimal cellular function, selective signaling processes, such as autophagy, are induced in response to stress to catabolize accumulated misfolded/aggregated proteins, dysfunctional organelles, and intracellular pathogens (49). When cellular dysfunction reaches a critical level, apoptosis is induced. Autophagy and apoptosis are processes that involve overlapping kinase and transcriptional regulators, but they differ in their activation depending on the level of genotoxic intensity. p53 is an upstream transcriptional regulator of both pathways (Figure 3).

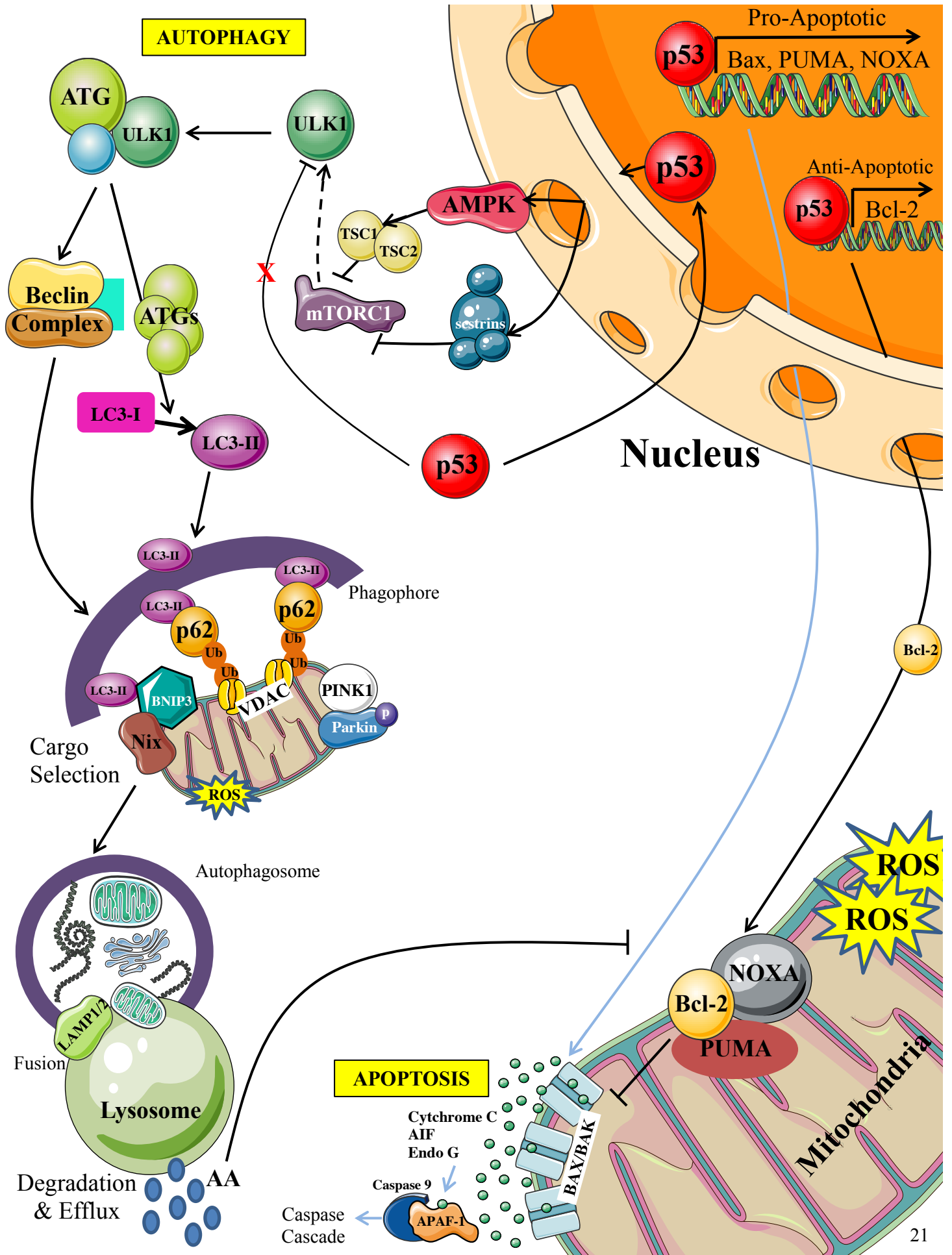


Figure 3. p53 maintenance of cellular homeostasis and survival through regulation of the autophagy/mitophagy and apoptosis pathways. Autophagy and apoptosis are similar processes that involve overlapping kinase and transcriptional regulators to maintain cellular homeostasis through degradation of dysfunctional organelles and cells, respectively. However, they differ in their activation depending on the level of genotoxic intensity imposed on the cell. p53 is interestingly an upstream transcriptional regulator of both pathways. p53 can upregulate the autophagy pathway through the transcriptional activation of AMPK, TSC1 and 2 (Tuberous Sclerosis Complex 1 and 2), and sestrins 1 and 2 to ultimately inhibit mTORC1 (mammalian target of rapamycin complex 1), a transcription factor that dephosphorylates the serine threonine kinase ULK1 (Unc-51 Like Autophagy Activating Kinase 1), a central regulator of autophagy induction. Cytoplasmic p53 levels inhibit autophagy by blocking the activation of ULK1. With mTORC1 inhibition, ULK1 can form a complex with ATG13 (autophagy related gene 13) and FIP200 (FAK family kinase-interacting protein) allowing for Beclin-1 complex activation with PI3K (phosphoinositide 3-kinase) and AMBRA1 (activating molecule in Beclin-1-regulated autophagy) for subsequent initiation of phagophore formation. Additionally, ATGs (ATG3, ATG 4, ATG5, ATG7, ATG10, ATG12, ATG16) allow for LC3-I to LC3-II (Microtubule-associated protein 1A/1B-light chain 3) lipidation which can then surround the phagophore and direct it to tagged mitochondrial membrane proteins (ubiquitinated VDAC (Voltage-dependent anion-selective channel 1) and associated adaptor protein p62). This process is initiated through increased mitochondrial ROS levels and decreased membrane potential leading to PINK1 (PTEN-induced putative kinase 1) phosphorylation of Parkin. Additional membrane proteins like Nix and BNIP3 assist in phagophore binding and surrounding of the dysfunctional organelle. The damaged mitochondria is then engulfed in the autophagosome and directed to the lysosome where it can then fuse with the assistance of LAMP 1 and 2 (Lysosome-associated membrane proteins 1 and 2) and be degraded into functional amino acid (AA) components. p53 has been shown to additionally transcriptionally regulate LAMP 2 and cathepsin D lysosomal proteins, and therefore plays a role in autophagic substrate clearance. With exercise, there may be a shift favouring autophagy to regulate cellular homeostasis, whereby degraded amino acid components may inhibit activation of apoptosis. In the nucleus, p53 can further transcribe proteins to maintain cellular homeostasis such as through p21, a cellular senescent protein, and Bcl-2, a protein preventing Bax/Bak membrane integration and oligomerization and subsequent MOMP (mitochondrial outer-membrane permeabilization) (indicated by the black line in apoptosis). MOMP is a process of intrinsic apoptosis in which p53-transcribed apoptotic markers localize to the mitochondria and BH3-only proteins (BID or BIM) can induce the oligomerization of Bax leading to cytochrome c release, among other proteins, which can then bind APAF-1 to caspase 9 to initiate the caspase cascade and subsequent apoptosome formation for completion of the apoptotic process (indicated by blue line in apoptosis).

p53 can act as either an endogenous repressor or activator of autophagy depending on its localization with stress intensities. Under basal non-stressful conditions, cytosolic p53 represses autophagy by interacting with the FIP200 protein of the upstream ULK1-ATG13-ATG101-FIP200 complex thus blocking the formation of autophagosomes and inhibiting autophagy (104, 160, 182). However, upon cellular stress, p53 localizes to the nucleus to transcriptionally regulate activators of the pathway like AMPK and TSC 1 and 2, core-machinery components including numerous ATG's, autophagy initiator ULK1, and lysosomal protein-encoding genes such as cathepsin D and LAMP 2 (80). Nuclear p53 therefore upregulates autophagy through the activation of AMPK, TSC1 and 2, and sestrin1 and 2 which inhibit MTORC1, thus leading to the activation of ULK1. ULK1 complex initiation can then activate the Beclin-1 complex concomitant with PI3K and AMBRA1 for phagophore formation, which is assisted by ATGs that lipidate LC3-I to LC3-II to surround the phagophore and direct targeted organelles/dysfunctional proteins to the autophagosome (114). Autophagosomes travel along microtubules to fuse with the lysosome for degradation into functional amino acids. Interestingly, p53 can also localize to the mitochondria to interact with cyclophilin D which promotes an association with ANT-I in the inner mitochondrial membrane to open the mitochondrial transition pore (31, 104). This process stimulates autophagic removal of dysfunctional mitochondria detected by the dissipated proton gradient (104). However, the opening of this pore beyond a critical threshold can lead to MOMP and cell death. Thus a fine line in the crosstalk between these two pathways is required.

There are numerous ways in which cell death can be induced: extrinsic apoptosis, intrinsic apoptosis, regulated necrosis, autophagic cell death, and mitotic catastrophe (104). p53 is primarily involved in regulating the intrinsic apoptosis pathway. Upon high levels of genotoxic stress, p53 nuclear localization allows for its transcriptional regulation of numerous pro-

apoptotic genes such as Bax, Puma, and Bid (34). Furthermore, p53 has an extra-nuclear function where it can bind and inactivate Bcl-2 while activating multi-domain Bcl-2 family proteins (Bak and Bax), or it can itself localize to the mitochondria to interact with cyclophilin D; both processes induce MOMP (34). MOMP is a process of intrinsic apoptosis in which p53-transcribed proteins localize to the mitochondria, and with the assistance of BH3-only proteins (BID, BIM, PUMA, NOXA), to induce the oligomerization of the Bax/Bak heterodimer on the outer mitochondrial membrane (104). This leads to an opening in the mitochondrial transition pore (mtPTP). This pore structure is composed of a hexokinase on the cytosolic surface, VDAC on the outer mitochondrial membrane, creatine kinase and nucleoside diphosphate kinase within the intermembrane space, and ANC on the inner mitochondrial membrane (15). Thus, the increased release of cytochrome c, among other proteins like AIF and EndoG, initiates APAF-1 association with caspase 9 to induce the caspase cascade and subsequent apoptosome formation for completion of the apoptotic process (104).

3.2.2. Cellular Maintenance of Stress: Cell Cycle Arrest/Senescence/Antioxidants

Upon exposure of low to moderate levels of cellular stress, the cell manages these perturbations through regulatory pathways including antioxidant enzyme production and cell cycle arrest and senescence, as a safeguard mechanism against cell death or mutation. Redox signaling, through the generation of ROS and its by-products hydrogen peroxide, alkoxyl/peroxyl radicals and peroxynitrite, can either lead to detrimental cellular oxidative stress when produced in large quantities, or they can act as a second messenger system under low to moderate stress levels (97). Upstream kinases regulated by ROS include p38 MAPK, ATM, and ERK which can phosphorylate p53 on cysteine residues 124, 135, 141, 182 and 277, as these contain redox-sensitive thiol groups (97). Under non-toxic ROS conditions, p53 sustains

antioxidant gene expression by regulating the levels of MnSOD, catalase, SCO2, and GPX1 (97). MnSOD converts oxygen radicals to H₂O₂, and GPX and catalase converts H₂O₂ to H₂O. Furthermore, an interesting cross-talk exists between p53-mediated antioxidant transcription and the major antioxidant Nrf2-KEAP1-ARE signaling pathway. Nrf2 levels are maintained by its negative regulator KEAP1, which directs Nrf2 to the CUL3 E3 ubiquitin ligase for proteasomal degradation (37). Interestingly, the p53-target gene p21 can stabilize Nrf2 by binding KEAP1 and preventing its degradation (32, 137). The Nrf2 pathway reciprocates by transcribing NQO1 which interacts with p53, thus blocking its degradation by the 20S proteasome (10, 137). Though the existence of this beneficial cross-talk yields new roles for p53 in mediating oxidative stress, there are discrepancies wherein the Nrf2 pathway can increase p53 degradation by Mdm2, and p53 can reduce Nrf2 binding to the ARE through competitive inhibition (43, 137, 181). With greater ROS levels, p53 can switch to trans-activate pro-oxidant ROS-generating enzymes like NQO1, PIG3/6 and FDXR, and apoptotic genes including Bax, Puma, and p66Shc to uncouple mitochondrial electron transport, leading to MOMP (97, 121). Hence, a fine balance between antioxidant production and incoming oxidants is required; if the balance tips, oxidative stress ensues and cell cycle arrest/senescence, autophagy, and apoptosis pathways become activated.

Cell cycle arrest is the initial step of cellular senescence, whereby cells sustaining limited DNA damage can initiate arrest at the G1 and G2 phase during checkpoints G1/S and G2/M, respectively to afford the opportunity to repair DNA damage (80). G1 arrest prevents replication of damaged/mutated DNA, while G2 arrest prevents improper chromosomal segregation (185). It is important to note that skeletal muscle cells cannot undergo cell cycle arrest and senescence as they are post-mitotic; mitotic stem cells, or satellite cells, can undergo this process. p53 is an upstream transcriptional regulator of numerous cell cycle arrest genes, the most prominent being

p21, a cyclin/cyclin-dependent kinase inhibitor (1, 134). p21 functions to induce G1 arrest following DNA damage by inhibiting kinase phosphorylation and activation of pRb, or by binding to E2F and PCNA (1, 134). The p21-PCNA complex blocks PCNA's role as a polymerase processivity factor in DNA replication, but not its DNA repair function (94). The Rb protein induces senescence rather than cell cycle arrest by repressing gene transcription and progression into the S phase (48). The G2/M checkpoint is additionally proposed to be regulated by p53 to prevent premature entry into the S phase (94). Gadd45a and 14-3-3- σ are genes transcriptionally regulated by p53 to stimulate G2 arrest. .

In response to cumulative increases in stress levels causing DNA damage, such as by IR or oxidative stress, the p53 pathway is activated resulting in cellular senescence (134). Senescent cells lack proliferative markers, have an enlarged flattened morphology, and express the lysosomal enzyme β -galactosidase (26). p53 is activated by upstream signals including ATR-ATM (phosphorylates p53 at Ser15), Chk2 (phosphorylates p53 at Ser20), PCAF (acetylates p53 at K320), and PML-IV (acetylates p53 at Lys382 and phosphorylates at Ser15 and Ser46), allowing for its dissociation from Mdm2 and its nuclear localization and transcription of senescent genes (134). p53 transcribes senescent genes p21, DEC1, and PAI-1 which inhibits a protease that promotes the G1/S transition (134). Conserved sequence identity in the DBD regions of p53-regulated genes allows for p53 family members p63 and p73 to activate p21 and DEC1, thus allowing for redundancy (134).

3.2.3. Improvements to Cellular Health: Mitochondrial Biogenesis, Metabolism

p53 promotes cell viability by enhancing the activation of catabolic pathways to maintain energy production during periods of low nutrient availability (102). These metabolic signaling pathways include fatty acid oxidation (FAO), mitochondrial respiration, and glucose metabolism.

Within the glucose energy pathway, p53 limits glycolytic flux directly at the transcriptional level through repression of glucose transporter genes GLUT1 and GLUT4, or indirectly through inhibition of NF- κ B (79, 102, 150). p53 can additionally suppress the insulin receptor promoter, thereby further reducing cellular glucose uptake (102, 173). p53 also binds PGM to inhibit enzyme catalysis of 1,3-bisphosphoglycerate to 1,2-bisphosphoglycerate, suppresses ChREBP to stimulate lipid and nucleotide biogenesis, and regulates G6PD to catalyze the rate limiting step in the pentose phosphate pathway (PPP) (102, 160). p53 further transcriptionally upregulates TIGAR which inhibits fructose-2,6-bisphosphate, thus impairing glycolysis progression and diverting glycolytic intermediates into the PPP (13). Though overwhelming evidence indicates that p53 negatively regulates glycolysis, depending on the energy requirements of the cell, p53 can switch to facilitate glycolysis by transcriptionally regulating hexokinase II levels which catalyzes the first step in glycolysis (106). A fine balance in glycolytic energy production is therefore required. The Warburg effect, a shift towards a high glycolytic rate for rapid ATP synthesis caused by mutated p53, can lead to increased cellular proliferation (121). FAO is another energy pathway regulated by p53. Nutrient deprivation is one mechanism which mediates AMPK-dependent activation of β -oxidation to initiate p53 activation of fatty acid uptake and mitochondrial oxidation proteins (86). Inhibition of p53 on the other hand reduces mitochondrial biogenesis and decreases oxygen consumption, facilitating a more anaerobic environment and thus changing the ATP production ratio of glycolysis versus oxidative phosphorylation from 3:1 rather than the normal 1:3 ratio (121). Mitochondrial respiration is regulated by p53 through its promotion of oxidative phosphorylation genes such as the SCO2 regulator of complex IV composition of the ETC, AIF which is an essential subunit of complex I

of the ETC, PGC-1 α -mediated activation of NUGEMPs such as COX-IV, and post-transcriptional regulation of COX-II by p53R2 on mtDNA (19, 102, 107, 153).

Proper mitochondrial function, indicated by appropriate respiration and ROS output, allows for these organelles to exist as part of a dynamic network regulated by fusion and fission events. Knockout (KO) studies on p53 have revealed reduced fission events due to the ability of p53 to transcriptionally regulate Drp1, an adaptor protein that serves as a mitochondrial targeting sequence, and Fis1 a recruiter of mediator fission proteins (18, 95, 145). p53 also regulates fusion by transcriptionally activating Mfn2, a GTPase that signals for accelerated mitochondrial fusion events (118, 172). No evidence has yet concluded the vital necessity for p53 maintenance of the mitochondrial network due to the presence of redundant signaling. However, mitochondrial morphological detriments have been observed using p53 KO models. A deficit in the volume of SS (61%) and IMF (70%) mitochondrial subfractions was observed in the absence of p53, with further structural deficits in IMF mitochondria evidence by reduced reticular network and in the SS mitochondria which displayed cristae deformities (141). These resulting morphological differences are a result of a lack in p53 expression in the nuclear and mitochondrial compartments. In the nucleus, p53 transcribes its own NUGEMPS such as COX IV, SCO2, AIF and Tfam, or it can transcribe PGC-1 α which co-transcriptionally regulates NRF-1 and 2 to enhance the expression of Tfam, cytochrome c, ETC proteins, and import machinery proteins (64, 75, 141). Within the mitochondria, p53 displays an intrinsic 3' \rightarrow 5' exonuclease activity for base excision repair, interacts with Poly and mtDNA to increase replication, facilitates Tfam binding to mtDNA to regulate copy number and transcriptional activity, and transcribes vital COX subunits such as COX I and II (Figure 4) (2, 141). As such COX activity, a

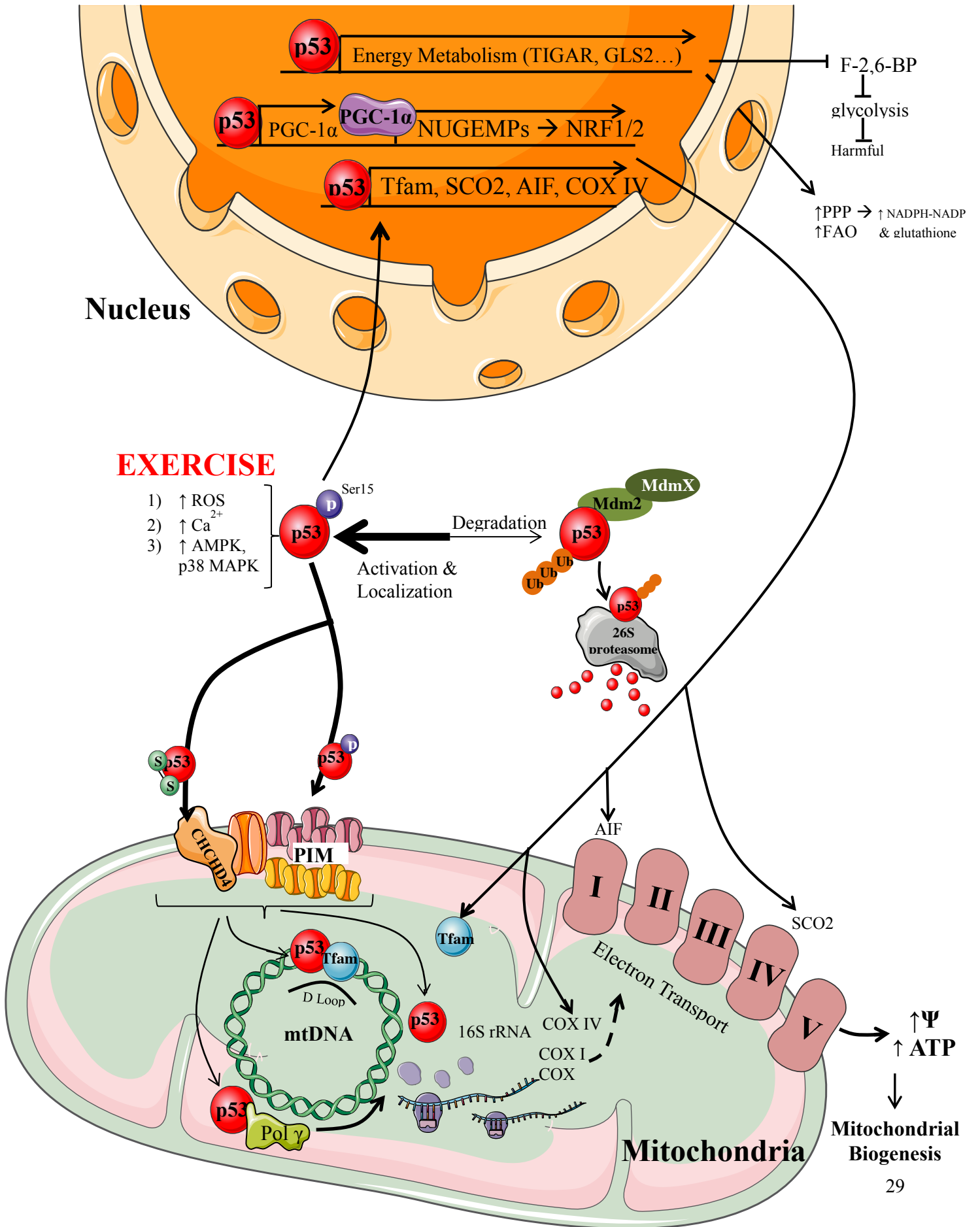


Figure 4. p53 regulation of mitochondrial biogenesis with exercise. Muscular contractions induce the activation of numerous signals, such as kinase phosphorylation, increased ROS production, enhanced calcium production through action potential generation, and an increased AMP: ATP ratio, which collectively leads to p53 phosphorylation of its Serine15 residue to enhance its stability and activation. Once activated, p53 cellular localization to the mitochondria through PIM (protein import machinery), rather than to the nucleus, is increased and assisted by CHCHD4 (coiled-coil-helix-coiled-coil-helix domain containing 4) import machinery by cysteine-135 residue modification of p53. As shown in previous studies, once in the mitochondria, p53 has numerous roles including assisting Tfam, a nuclear p53-regulated gene, in binding to the D loop region (regulatory sequences that contain the only three promoters of mtDNA) where it can regulate mitochondrial replication and transcription. Additionally, p53 can bind polymerase gamma to the mtDNA, the only polymerase to regulate the mitochondrial plasmid, and can also increase 16S rRNA production to facilitate improved translation. Ultimately, once in the mitochondria, p53 can increase mitochondrial biogenesis through enhanced production of ATP by improving the efficiency of the electron transport chain. Though there may be greater mitochondrial relative to nuclear p53 localization, nuclear p53 levels are still required to bind to the regulatory sequence regions of NUGEMP promoters. This is accomplished both through p53's direct transcription of mitochondrial biogenesis proteins such as Tfam, COX IV (Cytochrome c oxidase subunit 4), SCO2 (Cytochrome C Oxidase Assembly Protein), and AIF (Apoptosis Inducing Factor) as well as its regulation of PGC-1 α at multiple E-Boxes to enhance NUGEMP transcription. p53 additionally regulates glycolysis through the regulation of enzymes, such as TIGAR (TP53-inducible glycolysis and apoptosis regulator), which impairs fructose-2,6-bisphosphate in the glycolytic pathway (4). Through glycolysis inhibition, there is a greater reliance on the pentose phosphate pathway (PPP) and fatty acid oxidation (FAO) to increase oxidative phosphorylation and energy production. It is predicted that with training, there will be an increased drive for p53 cellular localization, rather than remaining in the cytoplasm where it can be degraded by the Mdm2 – MdmX (Mouse double minute 2 homolog) complex which functions as an E3 ubiquitin ligase to direct p53 to the 26S proteasome for degradation to maintain a low pool of this protein. Interestingly, Mdm2 can signal for p53 mono-ubiquitination within the nucleus, thus exposing its nuclear export signal to allow for cytoplasmic accumulation and poly-ubiquitination to increase degradation. Abbreviations: Ψ = membrane potential.

marker of mitochondrial biogenesis, was reduced by 26% in p53 whole body KO mice (141). This complex, essential for its role in aerobic respiration, is made up of 13 subunits, both nuclear and mtDNA-encoded, and primarily catalyzes electron transfer from reduced cytochrome c to molecular oxygen. p53 KO models indicate impaired respiration, evident by a 40% reduction in state 3 IMF respiration, and increased ROS production observed by 1.5-3 fold increases in state 4 and state 3 levels in IMF mitochondria (141). The greater deficits observed in the IMF subfraction pose significant repercussions as this population comprises 80-85% of the total mitochondrial volume (67). These results allude to the vital requirement of p53 in the regulation of proper mitochondrial morphology and adaptability towards incoming stimuli.

3.2.4. Does a Crosstalk Exist Between Pathways?

p53 has been dubbed the “molecular policeman” for its role in lowering ROS levels and repairing DNA to promote survival (good cop); with high stress intensity it initiates cellular senescence and cell death (bad cop) (50). Therefore, coordinated communication is required, i.e. “cross-talk”, between the signaling mechanisms regulated by p53.

In pre-mitotic satellite stem cells, temporary cell cycle arrest is initiated in response to exogenous or endogenous sources of oxidative stress. When stress accumulates and the repair mechanisms are overwhelmed, p53 downregulates the proliferative potential by inducing cellular senescence (16). The p53 target p21 is the major rheostat of this pathway. This is confirmed by one study whereby at day 1 cell cycle arrest is induced, and when p21 is switched off they can revert back to their proliferative state, but by day 3 cells acquire a senescent morphology (17, 29).

On the other hand, in post-mitotic differentiated skeletal muscle cells, two major pathways are employed to limit the damage induced by oxidative stress, in order to enhance cell survival. The antioxidant enzyme production system is evolutionarily conserved to protect and preserve cellular components, and is thus the first responder to cellular oxidative stress. Redox imbalance plays a pivotal role in driving cellular deterioration. p53-dependent processes that enhance antioxidant production can be accomplished by either p21-mediated activation of Nrf2 transcription at the ARE region, or p53 specific binding to the ARE (32). Additionally, p53 can transcriptionally activate upstream autophagy regulators such as AMPK and sestrins, as well as additional regulatory proteins including *Ulk1* and *Atg's* (36, 41, 80, 174). Prolonged stress induces mitochondrial depolarization and fragmentation to further assist in mitophagic removal (44). Failure to restore homeostasis through the aforementioned signaling pathways, can lead to the transcription of cell death proteins towards apoptosis, rather than autophagy (120, 160).

Essential crosstalk is required for mechanisms facilitating antioxidant enzyme production, metabolism, and mitochondrial biogenesis. p53 promotes a shift away from glycolysis under exercise stimuli, navigating away from the well-known cancerous Warburg pathway (184). Mitochondrial integrity and oxidative capacity is maintained by antioxidant systems through both p53-dependent and independent mechanisms, with a fine coordination occurring between the upstream regulators Nrf2, p53, and PGC-1 α . With mitochondrial biogenesis, increased respiration and ROS by-products are released, requiring a larger volume response by antioxidants regulators. If ROS production increases to a substantial level, inhibition of mitochondrial biogenesis may occur to allow antioxidant removal of ROS before continuing the mitochondrial proliferation processes (16).

The literature available on the regulation of numerous signaling mechanisms by p53 is astounding. However, researchers are at the point of amalgamating primary research to create mechanistic models of p53 to determine how these different pathways exhibit a fine crosstalk with various oxidative stressors, such as exercise, to maintain cellular homeostasis.

3.3. p53- Mediated Skeletal Muscle Adaptations with Exercise

3.3.1. Systematic Review of Literature: p53 and Acute vs Chronic Exercise

Acute and chronic contractile activity triggers a plethora of signals that induce beneficial metabolic and biochemical adaptations to enhance muscle health and performance. For example, the moderate increases in ROS produced by exercise are able to repair and strengthen the oxidative capacity of the cell by increasing mitochondrial content and fuel oxidation (96, 133, 154). To date, a total of seven exercise studies in animal models have assessed the role of p53 regulatory pathways with exercise (Table 1).

One bout of acute exercise is sufficient to initiate transcriptional signaling towards mitochondrial biogenesis (33, 142). A host of upstream signals, such as ROS production and calcium signaling, enhances AMPK and p38 MAPK kinase expression leading to Ser¹⁵ phosphorylation of p53 to facilitate both nuclear and mitochondrial localization (66, 142–144). In the nucleus, p53 binds to response elements within the PGC-1 α promoter, specifically at site -2317 in mouse or -1237 in humans, to enhance the expression of NUGEMPs such as Tfam, COX IV, SCO2, and AIF (38, 98, 107, 124, 143). With an acute exercise bout, a recovery period of ~3 hours further improves signaling events (i.e. nuclear p53 localization and transcriptional regulation) to further enhance mitochondrial biogenesis proteins in both rodent and human models (52, 144, 158). p53 localizes to mitochondria where it acts as an exonuclease on mtDNA,

Publication Information	Research Model	Age at Start (wks)	Stress Intensity	Length of Stress	p53 expression	p53 cellular localization	Regulation of Signaling Pathways with Stress	
							mRNA	Protein
Acute Exercise Programs								
Saleem & Hood, J Physiol, 2013	(C57BL/6J p53 KO & WT mice n=6)	12	15 m/min for 90 min (± 3hr recovery)	90 min	↓ p53 mRNA (w/ acute and acute + recovery)	↑ p-p53 @ ser ¹⁵ in SS & IMF mito ↓ p53 in nucleus	↑ PGC-1α, ↑Tfam, ↑NRF-1 ↑COX-IV, ↑CS, ↑COX-I greater with 3 hr recovery	n/a
Saleem et al., Am J Physiol Cell Physiol, 2014	C57BL/6J p53 KO & WT mice n=6	8	15 m/min for 90 min (± 3hr recovery)	90 min	n/a	n/a	↑ PGC-1α, ↑Tfam, ↑NRF-1, ↑COX-IV greater with 3 hr recovery	↑ p-p38 MAPK @ tyr ¹⁸⁰ , ↑p-AMPK @ tyr ¹⁷² , ↑p-CaMKII @ tyr ²⁸⁶ , ↑LC3-II (mito)
Chronic Exercise Programs								
Qi et al., Free Radic Biol Med, 2011	Goto-Kakizaki rats n=7	10-12	progressive: 20m/min @ 30min → 1 hr	8 wk (6days/wk)	↓ p53 protein	n/a	↓TIGAR, ↑ mtDNA (ATPase + CytB)	↓ TIGAR, ↑ COX II, ↑ GSH, ↑ GSH:GSSG
Safdar et al., Skelet Muscle, 2016	C57BL/6J PolG WT & KO, p53 MSKO & PolG-p53-MSKO mice n=4-6	12	15 m/min @ 45 min	26 wk (3days/wk)	no change	↓ nuclear p53 ↑mito p53 (↑ p53-polG-tfam @ Cox II + cyto)	↑ mtDNA copy number	↑ SOD2, ↑ catalase, ↑ Tfam, ↑ ERRα
Park et al., Circ Res, 2009	C57BL/6J p53 KO & WT & HT mice n=5	8-12	progressive: 10m/min @ 40 min → 14 m/min @ 90 min	5 wk (5 days /wk)	n/a	n/a	↑ Tfam, ↑ mtDNA copy number	↑ SDH
Saleem et al., Physiol Genomics, 2009	C57BL/6J p53 KO & WT mice n=7-8	9-12	Voluntary Wheel Running Program; Acute In Situ Stimulation (1& 3 TPS)	6-8 wk	↑ p-p53 @ ser ¹⁵ (acute)	n/a	n/a	↑ COX (chronic), ↑ p-AMPK @ tyr ¹⁷² + ↑ p-p38 @ tyr ¹⁸⁰ (acute)
Siu & Always, J Appl Physiol, 2005	(Japanese Coturnix quails n=8)	8 and 208	Stretch-overload model (12% body weight over the left humeral-ulnar joint for joint extension)	7 and 21 days	n/a	↑ nuclear p53	n/a	↑ Id2 (nuclear) (7 days in PAT; 7 & 21 days in ALD)

Table 1: Literature compiled on p53 and exercise regimens. Literature (7 studies) was grouped by acute (2 studies) or chronic (5 studies) exercise. Arrows indicate whether markers regulated by this form of stress increased (↑) or decreased (↓) in expression and/or activation. If a WT vs KO model is employed, only the results from the WT group are indicated. A caveat to this is the study published by Safdar et al., *Skelet Muscle*, 2016 which examines exercise in Polg1 MSKO models only. Various time measurements are indicated for the length of imposed stress. This table has been adapted from Beyfuss & Hood (2018). **Abbreviations:** WT (wildtype), KO (knockout), HT (heterozygous), MSKO (muscle specific KO), mito (mitochondria), SS (sub-sarcolemmal), IMF (intermyofibrillar), PAT (patagialis), ADL (anterior latissimus dorsi).

and increases the expression and binding of Tfam and Polg1 to mtDNA to maintain genomic integrity, and enhance SS and IMF mitochondrial biogenesis (2, 11, 144, 180).

In contrast to acute bout of exercise, training is classified as repeated bouts of endurance exercise interspersed with recovery sessions over a period of time. The result of chronic exercise is a heightened adaptive state in which signaling responses to each exercise bout is attenuated, including ROS production (98). This adaptation is modulated by p53 signaling which is one of the major upstream regulators that confers increased mitochondrial content and improved mtDNA integrity, decreased cellular senescent and apoptotic signaling, less emphasis on glycolytic energy utilization and more on oxidative phosphorylation, reduced lactate production, and ultimately improved VO₂ max and skeletal muscle performance (124, 139, 141). Though it is true that a 5-fold reduction in the exercise ability of p53 whole body KO mice is observed during an 8-week voluntary wheel running program, and that the subcellular localization of p53 seems indispensable for exercise-mediated mtDNA repair (initiator of Tfam-Polg1 complexes) and mitochondrial biogenesis and respiration (transcription of NUGEMPs, TIGAR, SCO2, p53R2), the absence of p53 does not seem to necessarily hinder the ability to adapt with exercise (124, 139, 141). One study showed a similar increase in mitochondrial content compared to wildtype (WT) mice in response to exercise, indicating that exercise provokes the overlap of redundant signals to induce normal adaptations in mitochondria (141). An interesting divergence in the signaling patterns in humans arises in response to exercise, whereby short interval training, more than continuous exercise in humans, increases p53 Ser¹⁵ phosphorylation and PGC-1 α nuclear localization for enhanced mitochondrial biogenesis and respiration (51, 52). However, another study reported no differences in signaling or gene expression when high and lower intensity exercise regimens were performed, when matched for workload (12). Therefore, further

examination into the variable parameters associated with exercise, including sex, age, exercise protocol and muscle type, is required.

3.3.2. Regulatory Signaling Pathways with Endurance Exercise

Though mitochondrial biogenesis is the well-known adaptation that enhances muscle plasticity with exercise, as described above, there are numerous additional signaling mechanisms regulated by p53 under the influence of aerobic exercise to improve skeletal muscle health (16).

Antioxidant production is one of the first signaling pathways activated in response to increased oxidative stress, i.e. ROS generation, with acute and chronic exercise. In skeletal muscle, antioxidants are produced in an intensity-dependent manner and commonly include MnSOD, GPX, CAT, and NQO1 (39, 59, 91, 131). Nrf2, the major upstream regulator of these antioxidant enzymes, is increased by 1.5-fold in response to exercise training (37). p53 also transcriptionally regulates many of these enzymes including MnSOD, GPX1, and GLS2 to maintain cellular integrity (23). The metabolic shift in energy substrate utilization is another early response mechanism to improve mitochondrial handling of exercise. p53 directly transcribes glycolysis regulators (i.e. TIGAR) to switch substrate utilization towards oxidative phosphorylation and away from glycolytic energy usage, thereby reducing lactate production.

Exercise, though a beneficial form of induced “oxidative stress” due to signaling ROS-mediated cascades, is still an oxidative stressor that can activate various pathways. In response to exercise, satellite cells play a pivotal role in regeneration and are activated, proliferate, undergo self-renewal, and differentiate into mature muscle cells (86, 179). The cell cycle arrest pathway is activated with moderate endurance exercise and is transcriptionally regulated by p53. This is confirmed by Yu et al. (2016), whereby mice trained for 10 weeks expressed elevated levels of

p21 (29%), PTEN (12%), and IGFBP-3 (25%) compared to sedentary controls. Greater intensities of oxidative stress, such as telomere erosion, DNA lesions and high ROS levels, induces cellular senescence and can be a precipitating cause for sarcopenia, the degenerative loss in skeletal muscle mass with age (21, 53). This pathway is not commonly activated with exercise as exercise is often used a treatment to reverse sarcopenia or pathological muscle degeneration.

Autophagy is known to be activated with acute endurance exercise, however whether it is mediated by p53 is ambiguous (54, 57, 58, 164). One study by He et al. (2012) showed increased lipidated LC3II and degraded p62 with acute exercise, while Saleem et al. (2014) found no differences in these proteins in WT mice following an exhaustive exercise bout. However, an increase in ubiquitination (Ub), a tag for the removal of cellular debris, was found in p53 KO mice indicating p53-independent targeting of dysfunctional organelles for degradation (143). This discrepancy may be due to a lack of intensity or duration of the exercise protocol. Perhaps a greater intensity is required, as indicated by one study whereby an upregulation of autophagy proteins was found after an ultraendurance bout of exercise lasting 24 hours in humans (74). Mitophagy, on the other hand, is upregulated with acute exercise as indicated by increased mitochondrial LC3II, p62 and Ub expression, which can also function independently of p53 (143). Maintenance of the mitochondrial reticulum is further maintained through fission and fusion events whereby chronic contractile activity increases the reticulum through increased (53%) Mfn2 protein, known to have a p53-response element within its promoter, and Opa1 (71). Should the mitochondria become dysfunctional in response to exercise, p53-regulated fission proteins such as Drp1 can be activated to shuttle damaged mitochondria towards mitophagy. Further research is warranted to determine the p53-regulated maintenance of the mitochondrial

reticulum through fusion and fission events with exercise, and once fission is underway, the process by which both mitophagy and autophagy are induced in skeletal muscle.

With strenuous bouts of exercise, high ROS levels can destabilize the mitochondrial membrane to induce apoptosis, as evidenced by increased DNA fragmentation and reduced Bcl-2 levels (146, 151). However, it has been shown that an 8 week exercise training protocol, reduced apoptosis by increasing Bcl-2 and reducing APAF-1 and Bax transcript levels; signals all dependent on p53 activation (151). Furthermore, another study revealed with chronic contractile activity an increase in mitochondrial biogenesis and a simultaneous decrease in apoptotic susceptibility indicated by reduced IMF ROS production and diminished cytochrome c and AIF protein release (4). As apoptosis is the last resort to maintaining cellular integrity, earlier signaling pathways in response to exercise are activated in an intensity-dependent manner.

3.3.3. Applicable Models to Study p53 Function

Live animal work (i.e. *in vivo* experimentation), is the typical stage following *in vitro* cell work, and before detailed human analysis. The benefits of utilizing rodent models, which share a 99% genomic similarity to humans, allows for further genetic engineering to determine the morphological and molecular regulation by specific genes (167). Various models have been utilized including transgenic, tissue specific deletions/knockdowns, and whole body gene deletions/knockdowns.

Whole body genetic deletions of the p53 gene have been utilized for decades in cancer research and are now expanding their use to understand other p53-mediated pathways. To create this model, a neomycin cassette is used to replace approximately 40% of the coding sequences in the TRP53 locus extending from exons 2 to 6, which contains the translation start codon, of the

total 11 exon structure (73). The average age for spontaneous tumour development in these mice is approximately 6 months of age, after which they die by 10 months of age (40). Though phenotypically there are no observed differences, deficits in exercise capacity have been noted to be a result of reduced gait synchronization (25, 141). Campana et al. (2003), demonstrated differences in fiber type distribution whereby in the EDL, p53 KO mice displayed significantly fewer fast fibers (Type IIA) and more hybrid fibers (IC) than their WT counterparts, while in the oxidative soleus muscle p53 KO muscle contained a greater percentage of IIA than IA fibers. As it is unknown whether the discrepancies in skeletal muscle function are a result of p53 deletion in the muscle, or p53 deletion in neural networks, further investigations are necessary. Work previously described on understanding the phenotypic characteristics, morphological differences, skeletal muscle function, and signaling pathways mediated by p53 has been widely published using this whole body knockout model (107, 124, 141, 143–145).

Though a wealth of evidence is present confirming the essential role that p53 plays in regulating whole body metabolism and skeletal muscle mitochondrial function, the importance of p53 in regulating skeletal muscle health cannot be established from whole body p53 deletion. Thus, a muscle specific p53 knockout model, one that has been recently developed, allows for greater analysis into p53 regulatory signaling pathways solely in skeletal muscle (47). This model is created by breeding two mouse strains. The first strain is a transgenic mouse expressing the Cre recombinase gene driven by the muscle creatine kinase (MCK) promoter found in skeletal muscle (47). The second strain is a homozygous mouse with a floxed p53 allele, whereby LoxP restriction sites are located at exons 2 and 10 (47). Once these two strains breed, their progeny will have the functional part of the p53 gene, flanked at exons 2 and 10, excised by Cre recombinase to create a muscle specific knockout (Figure 5). Efficiency of the knockout

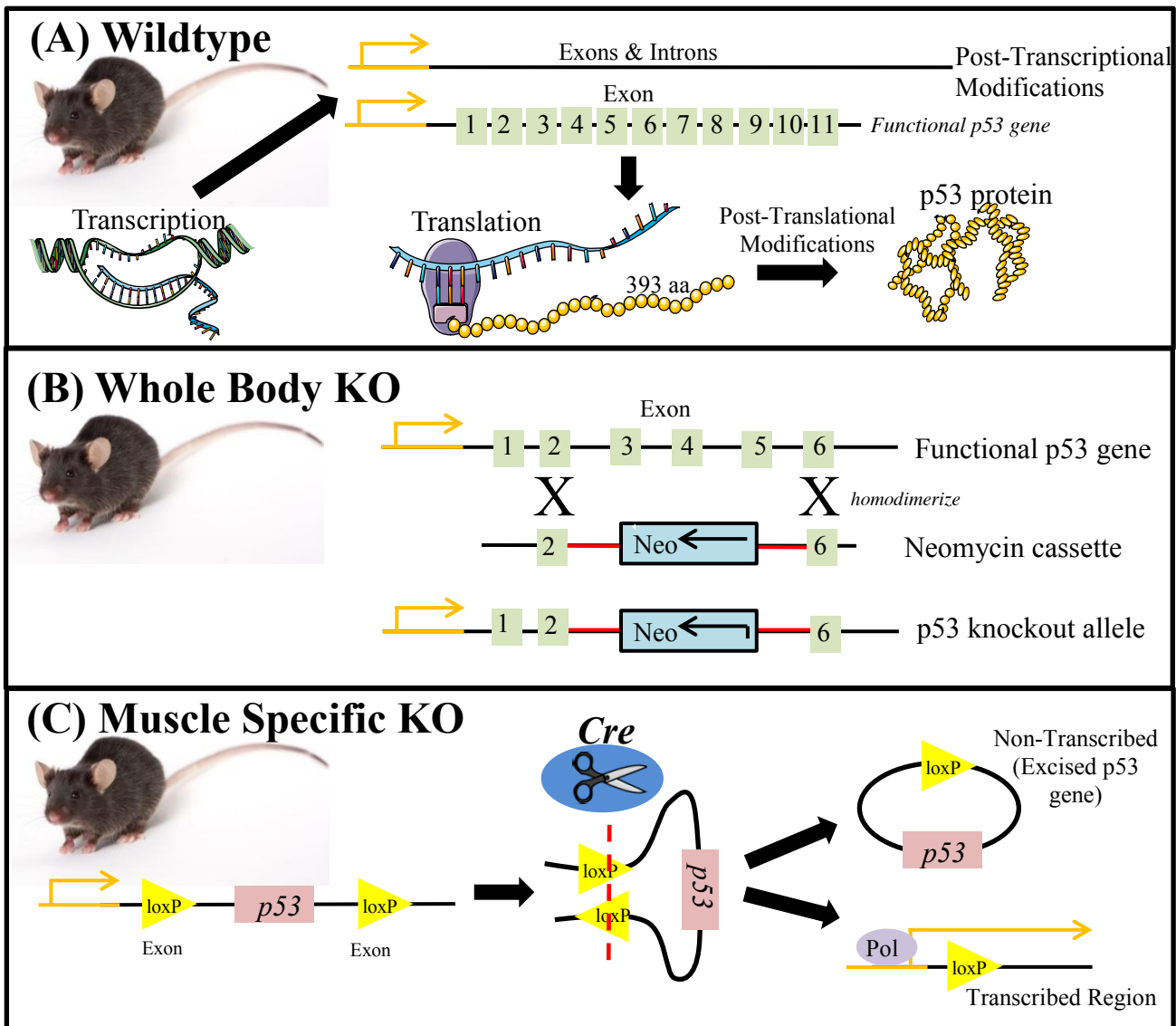


Figure 5. Rodent Genetic Models. (A) Wildtype (WT) mice contained regular gene expression and optimal ability for transcription and translation; (B) Whole Body (WB) knockout (KO) mice were created using a neomycin (NEO) cassette to replace 40% of the p53 coding region by homodimerizing with exons 2 and 6 thus replacing this region so that it cannot be translated; (C) Muscle Specific KO (mKO) mice were created using a Cre-lox recombinase system. In one mouse, exons 2 and 10 are flanked by loxP sites. These mice are bred with mice that contain a cre recombinase gene under the control of a promoter of interest, i.e. the MCK promoter for skeletal muscle. The progeny will have the loxP sites cleaved leading to removal of the p53 allele and ablation of its expression solely in skeletal muscle.

was confirmed by measuring p53 mRNA and protein expression which revealed a 70% and 60% reduction respectively, indicating that this the Cre-lox recombination system does not completely remove functional p53 protein from skeletal muscle, as it does in the whole body KO mice (155). One theory is that the observed p53 protein reflects the expression of protein from non-muscle fibre cells within skeletal muscle tissue, however further analysis is required to determine whether the present protein is functional (155). According to observations following these mice across 15 months of age, no overt differences in total body weight, skeletal muscle mass, muscle histology, grip strength, or organ/tissue (heart, liver, kidney, fat pad) masses were observed (47). Further analysis into signaling mechanisms was performed indicating no difference in mitochondrial content, evidenced by similar electron transport chain protein expression and citrate synthase enzyme activity (155). Furthermore, mitochondrial biogenesis proteins were comparable between genotypes, while mitochondrial dynamics was analogous with comparable fission and fusion protein expression (155). Lastly, fatty acid transport and carbohydrate metabolism were similar between groups (155). Therefore, p53 in fully-differentiated skeletal muscle may not be required for maintenance into adulthood, as its absence does not induce any overt phenotype nor does it affect any significant signaling pathways (47, 155).

To elucidate whether the alterations in exercise capacity observed with training are the result of p53 loss in skeletal muscle and not the result of the systemic deletion of p53, both mouse models are useful to employ. One theory on the observed differences that may exist between the neomycin cassette insertion (WB) and Cre-lox recombination-mediated p53 deletion (mKO), may indeed be a result of the timing of p53 deletion. In mKO mice, p53 would be deleted at approximately 13 days into embryonic development, whereas in the germline WB mice, p53 is absent throughout the entirety of embryonic development (100, 149). As p53 plays a significant

role in the differentiation phase of myogenesis, greater mitochondrial deficits may be observed in the WB mice as a result of its loss during this developmental period (155). Furthermore, it is posited that the impairments observed in mitochondrial content and function in WB KO mice is a secondary consequence of the loss of p53 in alternative tissues, rather than loss of p53 in skeletal muscle fibres. Previously, these WB mice have been observed to experience lower spontaneous activity, which could be a result of p53 KO loss in skeletal muscle, however it could also be a result of the loss of p53 in neural networks. Therefore, further research is warranted to determine the role p53 plays neurologically.

3.3.4. Systemic Benefits: Neurological Maintenance

Consistent endurance aerobic exercise provides many systemic benefits that extend life expectancy and reduce morbidity by improving cardiovascular function, shifting substrate requirement towards lipid utilization, and ameliorating contractile and metabolic dysfunction due to disease states and aging (66). The role of p53 in skeletal muscle with exercise is more well-known compared to its systemic effects, especially in neurological functioning with exercise.

Regular engagement in aerobic exercise is associated with superior brain structure and integrity, neural connectivity, and greater circulation of cerebral blood flow and neurotrophin release to ultimately improve strategic executive functions (working memory, volitional inhibition, selective/sustained attention) (55). When neural networks are dysfunctional as a result of p53 deletion and inhibition of its apoptotic function, exacerbation of neural deficits in response to adverse stimuli, like exercise, can reduce the activation of motor synchronization structures and networks (8, 25). Motor synchronization is primarily controlled by the olivocerebellar system connected by axons of the olivary cells to Purkinje cells in the cerebellum (25). During coordinated movements such as running, groups of Purkinje cells fire synchronously in

response to olivary input allowing for movement. Though no differences were found in exercise capacity under an acute bout of exercise, when a rotarod test was performed, the WB p53 KO mice displayed significantly reduced walking times (10%), which was more pronounced at higher rotation speeds (30%) (25). Interestingly, all other neurological responses and reflexes (clasping movement of paws, horizontal/vertical rearing, evidence of ataxia, anxiety dispositions, and gait) were similar between the KO and WT mice (25). Another study by Amson et al. (2000), observed that during the an open field test and Morris water maze test, p53 KO mice displayed reduced thigmotaxis (wall-seeking tendency), and reduced central activity, spatial learning, and memory capacity. Therefore, advanced analysis into the role of p53 in the maintenance of neural structure and connectivity for optimal exercise performance is required through further analysis of neurological function between WB p53 KO and WT models.

3.4. Directions for Future Research

Regular exercise, either through acute bouts of exercise or endurance training programs, can induce a plethora of adaptive outcomes leading to numerous physical and mental health benefits. Though p53 is a relatively new player in this field, it is established as a major transcriptional regulator of signaling mechanisms facilitating these beneficial adaptations. However, further understanding of the p53-mediated coordination of signaling pathways with varying intensities, durations, and types of exercise/oxidative stress is still required. This can be accomplished by determining an optimal exercise protocol to elicit the specific activation of beneficial downstream signaling pathways like antioxidant and metabolic events. Fine tuning of this protocol will depend on the intensity (low versus high; progressive versus consistent), the duration (2, 4, 6, 8 weeks; every day versus certain days/week), and the type of exercise (aerobic versus anaerobic versus resistance). Greater analysis into the subcellular compartmentalization of

p53 can assist in determining the activation of specific signaling pathways, concomitant with microarrays or co-immunoprecipitation assays to determine the upregulation of specific markers by p53 within each signaling pathway. Then exposing the model to some form of stress will allow for an understanding in the coordinated upregulation of pathways that maintain cellular homeostasis. Furthermore, understanding model differences that occur between whole body deletion and muscle specific deletion will yield new findings on the essential requirement of p53 in skeletal muscle. The integration of p53 in the regulatory networks governing specific adaptations is astounding and further work in this field will contribute to fitting the pieces of the signaling puzzle together to provide a picture of the cellular cooperation that occurs in response to exercise.

Research Objectives

To understand the role of p53 in directly regulating skeletal muscle mitochondrial signaling basally and under the influence of exercise training, we must first assess p53 regulation in WT mice. p53 transcriptional regulation will be determined through mRNA analysis and by understanding p53 subcellular localization. p53 translational regulation will be determined through protein and post-translational modification analysis. Once an understanding of p53 in skeletal muscle at the transcriptional and translational level is understood, both basally and under the influence of exercise, the next objective will be to understand whether the 6-week progressive training program has been piloted correctly, i.e. is of sufficient intensity and duration to increase mitochondrial biogenesis adaptations in skeletal muscle. Once it is understood that the training program induces the appropriate adaptations, we will observe the signaling pathways of mitochondrial biogenesis, antioxidant production, cell cycle arrest, autophagy and apoptosis, in both WT and p53 KO mice, basally and under the influence of exercise. This will be required to understand whether these signaling pathways are regulated by p53 basally and whether exercise induced adaptation are dependent on p53. Furthermore, if these pathways are regulated by p53 basally, we will investigate whether exercise-training is sufficient to attenuate the deficit induced by the basal absence of p53. Lastly, we are interested in investigating the neurological role of p53 in regulating exercise ability, and will thus employ a whole body p53 deletion model in addition to a skeletal muscle p53 deletion model. This will delineate whether p53 deletion in alternative tissues impacts skeletal muscle signaling.

Hypotheses

We hypothesize that:

1. The 6-week training protocol will lead to sufficient increases in mitochondrial biogenesis in skeletal muscle, with a notable reduction in the training adaptation of the KO mice;
2. Training will activate p53 through post-translational serine phosphorylation, increase its mRNA and protein content, and lead to enhanced nuclear and mitochondrial localization;
3. In response to an endurance training program, p53 will be required to upregulate cell cycle arrest, autophagy, mitochondrial biogenesis and antioxidant enzyme production signaling pathways, and will downregulate cellular senescent and apoptosis;
4. p53 whole body KO will have greater deficits in exercise capacity and mitochondrial biogenesis rather than the muscle specific mKO model, as a result of the influence of possible neurological lesions on walking synchronization.

References

1. **Abbas T, Dutta A.** p21 in cancer: intricate networks and multiple activities. *Nat Rev Cancer* 9: 400–414, 2009.
2. **Achanta G, Sasaki R, Feng L, Carew JS, Lu W, Pelicano H, Keating MJ, Huang P.** Novel role of p53 in maintaining mitochondrial genetic stability through interaction with DNA Pol γ . *EMBO J* 24: 3482–3492, 2005.
3. **Adams GR, Hather BM, Baldwin KM, Dudley G.** Skeletal Muscle Myosin Heavy Chain Composition and Resistance Training. *J Appl Physiol* 74: 911–915, 1993..
4. **Adhihetty PJ, Ljubicic V, Hood DA.** Effect of chronic contractile activity on SS and IMF mitochondrial apoptotic susceptibility in skeletal muscle. *Am J Physiol Endocrinol Metab* 292: E748-55, 2007.
5. **Adhihetty PJ, Irrcher I, Joseph A, Ljubicic V, Hood DA.** Plasticity of skeletal muscle mitochondria in response to contractile activity . *Experimental Physiol* 88:99-107, 2003.
6. **Agudelo LZ, Femenia T, Orhan F, Porsmyr-Palmertz M, Goiny M, Martinez-Redondo V, Correia JC, Izadi M, Bhat M, Schuppe-Koistinen I, Pettersson A, Ferreira DMS, Krook A, Barres R, Zierath JR, Erhardt S, Lindskog M, Ruas JL.** Skeletal muscle PGC-1 α 1 modulates kynurenine metabolism and mediates resilience to stress-induced depression. *Cell* 159: 33–45, 2014.
7. **Allbrook D.** Skeletal Muscle Regeneration. *Muscle Nerve* 4: 234–245, 1981.
8. **Amson R, Lassalle JM, Halley H, Prieur S, Lethrosne F, Roperch JP, Israeli D, Gendron MC, Duyckaerts C, Checler F, Dausset J, Cohen D, Oren M, Telerman A.** Behavioral alterations associated with apoptosis and down-regulation of presenilin 1 in the brains of p53-deficient mice. *PNAS* 97: 5346–5350, 2000.
9. **Argilés JM, Campos N, Lopez-Pedrosa JM, Rueda R, Rodriguez-Mañas L.** Skeletal muscle regulates metabolism via interorgan crosstalk: roles in health and disease. *JAMDA* 17: 789–796, 2016.
10. **Asher G, Lotem J, Sachs L, Kahana C, Shaul Y.** Mdm-2 and ubiquitin independent p53 proteasomal degradation by NQO1. *PNAS* 99: 13125–13130, 2002.
11. **Bakhanashvili M, Grinberg S, Bonda E, Rahav G.** Excision of nucleoside analogs in mitochondria by p53 protein. *AIDS* 23: 779–88, 2009.
12. **Bartlett JD, Louhelainen J, Iqbal Z, Cochran AJ, Gibala MJ, Gregson W, Close GL, Drust B, Morton J.** Reduced carbohydrate availability enhances exercise-induced p53 signaling in human skeletal muscle: implications for mitochondrial biogenesis. *AJP Regul Integr Comp Physiol* 304: R450–R458, 2013.
13. **Bensaad K, Tsuruta A, Selak MA, Vidal MNC, Nakano K, Bartrons R, Gottlieb E, Vousden K.** TIGAR, a p53-inducible regulator of glycolysis and apoptosis. *Cell* 126:

- 107–120, 2006.
14. **Bentzinger CF, Wang YX, Rudnicki M.** Building muscle: molecular regulation of myogenesis. *Cold Spring Harb Perspect Biol* 4: a008342, 2012.
 15. **Bernardi P, Di Lisa F.** The mitochondrial permeability transition pore: molecular nature and role as a target in cardioprotection. *J Mol Cell Cardiol* 78: 100–106, 2015.
 16. **Beyfuss K, Hood DA.** A systematic review of p53 regulation of oxidative stress in skeletal muscle. *Redox Rep* 23: 100–117, 2018.
 17. **Blagosklonny M.** Cell cycle arrest is not yet senescence , which is not just cell cycle arrest : terminology for TOR - driven aging. *Aging (Albany NY)* 4: 159–165, 2012.
 18. **van der Blik AM, Shen Q, Kawajiri S.** Mechanisms of mitochondrial fission and fusion. *Cold Spring Harb Perspect Biol* 5: a011072–a011072, 2013.
 19. **Bourdon A, Minai L, Serre V, Jais JP, Sarzi E, Aubert S, Chrétien D, de Lonlay P, Paquis-Flucklinger V, Arakawa H, Nakamura Y, Munnich A, Rötig A.** Mutation of RRM2B, encoding p53-controlled ribonucleotide reductase (p53R2), causes severe mitochondrial DNA depletion. *Nat Genet* 39: 776–780, 2007.
 20. **Brestoff JR, Clippinger B, Spinella T, von Duvillard SP, Nindl BC, Arciero P.** An acute bout of endurance exercise but not sprint interval exercise enhances insulin sensitivity. *Appl Physiol Nutr Metab* 34: 25–32, 2009.
 21. **Brioché T, Lemoine-Morel S.** Oxidative stress, sarcopenia, antioxidant strategies and exercise: molecular aspects. *Curr Pharm Des* 22: 2264–78, 2016.
 22. **Brookes PS, Yoong Y, Robotham JM, Anders MW, Sheu S.** Calcium, ATP, and ROS: a mitochondrial love-hate triangle. *AJP Cell Physiol* 287: C817–C833, 2004.
 23. **Budanov A.** The role of tumor suppressor p53 in the antioxidant defence and metabolism. *Subcell Biochem* 85: 337–358, 2014.
 24. **Bykov VJN, Wiman K.** Novel cancer therapy by reactivation of the p53 apoptosis pathway. *Ann Med* 35: 458–465, 2003.
 25. **Campana ALM, Rondi-Reig L, Tobin C, Lohof AM, Picquet F, Falempin M, Weitzman JB, Mariani J.** p53 inactivation leads to impaired motor synchronization in mice. *Eur J Neurosci* 17: 2135–2146, 2003.
 26. **Campisi J.** Aging, cellular senescence, and cancer. *Annu Rev Physiol* 75: 685–705, 2013.
 27. **Chaban Y, Boekema EJ, Dudkina N.** Structures of mitochondrial oxidative phosphorylation supercomplexes and mechanisms for their stabilisation. *Biochim Biophys Acta* 1837: 418–426, 2014.
 28. **Chan DC.** Fusion and fission: interlinked processes critical for mitochondrial health. *Annu Rev Genet* 46: 265–287, 2012.

29. **Chang BD, Broude EV, Fang J, Kalinichenko TV, Abdryashitov R, Poole JC, Roninson I.** p21Waf1/Cip1/Sdi1-induced growth arrest is associated with depletion of mitosis-control proteins and leads to abnormal mitosis and endoreduplication in recovering cells. *Oncogene* 19: 2165–2170, 2000.
30. **Chehab NH, Malikzay A, Stavridi ES, Halazonetis T.** Phosphorylation of Ser-20 mediates stabilization of human p53 in response to DNA damage. *PNAS* 96: 13777–13782, 1999.
31. **Chen B, Xu M, Zhang H, Wang JX, Zheng P, Gong L, Wu GJ, Dai T.** Cisplatin-induced non-apoptotic death of pancreatic cancer cells requires mitochondrial cyclophilin-D-p53 signaling. *Biochem Biophys Res Commun* 437: 526–531, 2013.
32. **Chen W, Sun Z, Wang XJ, Jiang T, Huang Z, Fang D, Zhang D.** Direct interaction between Nrf2 and p21Cip1/WAF1 upregulates the Nrf2-mediated antioxidant response. *Mol Cell* 34: 663–673, 2009.
33. **Chen YW, Nader GA, Baar K, Fedele MJ, Hoffman EP, Esser K.** Response of rat muscle to acute resistance exercise defined by transcriptional and translational profiling. *J Physiol* 545: 27–41, 2002.
34. **Cogswell AM, Stevens RJ, Hood DA.** Properties of skeletal muscle mitochondria isolated from subsarcolemmal and intermyofibrillar regions. *Am J Physiol* 264: C383-9, 1993.
35. **Cooper G.** *The cell: A molecular approach*. 2nd ed. Sunderland: Sinauer Associates, 2000.
36. **Crighton D, Wilkinson S, O’Prey J, Syed N, Smith P, Harrison PR, Gasco M, Garrone O, Crook T, Ryan K.** DRAM, a p53-induced modulator of autophagy, is critical for apoptosis. *Cell* 126: 121–134, 2006.
37. **Crilly MJ, Tryon LD, Erlich A, Hood DA.** The role of Nrf2 in skeletal muscle contractile and mitochondrial function. *J Appl Physiol* 121: 730–740, 2016.
38. **Donahue RJ, Razmara M, Hoek JB, Knudsen T.** Direct influence of the p53 tumor suppressor on mitochondrial biogenesis and function. *FASEB J* 15: 635–44, 2001.
39. **Done AJ, Traustadóttir T.** Nrf2 mediates redox adaptations to exercise. *Redox Biol* 10: 191–199, 2016.
40. **Donehower L.** The p53-deficient mouse: a model for basic and applied cancer studies. *Semin Cancer Biol* 7: 269–278, 1996.
41. **Eby KG, Rosenbluth JM, Mays DJ, Marshall CB, Barton CE, Sinha S, Johnson KN, Tang L, Pietenpol J.** ISG20L1 is a p53 family target gene that modulates genotoxic stress-induced autophagy. *Mol Cancer* 9: 95, 2010.
42. **Erlich AT, Tryon LD, Crilly MJ, Memme JM, Moosavi ZSM, Oliveira AN, Beyfuss K, Hood DA.** Function of specialized regulatory proteins and signaling pathways in

- exercise-induced muscle mitochondrial biogenesis. *Integr Med Res* 5: 187–197, 2016.
43. **Faraonio R, Vergara P, Di Marzo D, Pierantoni MG, Napolitano M, Russo T, Cimino F.** p53 suppresses the Nrf2-dependent transcription of antioxidant response genes. *J Biol Chem* 281: 39776–39784, 2006.
 44. **Filomeni G, De Zio D, Cecconi F.** Oxidative stress and autophagy: the clash between damage and metabolic needs. *Cell Death Differ* 22: 377–388, 2015.
 45. **Fluck M, Hoppeler H.** Molecular basis of skeletal muscle plasticity – from gene to form and function. *Rev Physiol Biochem Pharmacol* 146: 159–216, 2003.
 46. **Fluck M.** Functional, structural and molecular plasticity of mammalian skeletal muscle in response to exercise stimuli. *J Exp Biol* 209: 2239–2248, 2006.
 47. **Fox DK, Ebert SM, Bongers KS, Dyle MC, Bullard SA, Dierdorff JM, Kunkel SD, Adams C.** p53 and ATF4 mediate distinct and additive pathways to skeletal muscle atrophy during limb immobilization. *AJP Endocrinol Metab* 307: E245–E261, 2014.
 48. **Giacinti C, Giordano A.** RB and cell cycle progression. *Oncogene* 25: 5220–5227, 2006.
 49. **Glick D, Barth S, Macleod K.** Autophagy: cellular and molecular mechanisms. *J Pathol* 221: 3–12, 2010.
 50. **Gottlieb E, Vousden K.** p53 regulation of metabolic pathways. *Cold Spring Harb Perspect Biol* 2: a001040, 2009.
 51. **Granata C, Oliveira RSF, Little JP, Renner K, Bishop D.** Mitochondrial adaptations to high-volume exercise training are rapidly reversed after a reduction in training volume in human skeletal muscle. *FASEB J* 30: 3413–3423, 2016.
 52. **Granata C, Oliveira RSF, Little JP, Renner K, Bishop D.** Sprint-interval but not continuous exercise increases PGC-1 α protein content and p53 phosphorylation in nuclear fractions of human skeletal muscle. *Sci Rep* 7: 44227, 2017.
 53. **Grounds M.** Age-associated changes in the response of skeletal muscle cells to exercise and regeneration. *Ann NY Acad Sci* 854: 78–91, 1998.
 54. **Grumati P, Coletto L, Schiavinato A, Castagnaro S, Bertaggia E, Sandri M, Bonaldo P.** Physical exercise stimulates autophagy in normal skeletal muscles but is detrimental for collagen VI-deficient muscles. *Autophagy* 7: 1415–1423, 2011.
 55. **Guiney H, Machado L.** Benefits of regular aerobic exercise for executive functioning in healthy populations. *Psychon Bull Rev* 20: 73–86, 2013.
 56. **Hainut P, Hollstein M.** p53 and human cancer: the first ten thousand mutations. *Adv Cancer Res* 77: 81–137, 2000.
 57. **He C, Bassik MC, Moresi V, Sun K, Wei Y, Zou Z, An Z, Loh J, Fisher J, Sun Q, Korsmeyer S, Packer M, May HI, Virgin HW, Gilpin C, Xiao G, Bassel-Duby R, Scherer PE, Levine B.** Exercise-induced BCL2-regulated autophagy is required for

- muscle glucose homeostasis. *Nature* 481: 511–515, 2012.
58. **He C, Sumpter RJ, Levine B.** Exercise induces autophagy in peripheral tissues and in the brain. *Autophagy* 8: 1548–1551, 2012.
 59. **Higuchi M, Cartier LJ, Chen M, Holloszy J.** Superoxide dismutase and catalase in skeletal muscle: adaptive response to exercise. *J Gerontol* 40: 281–286, 1985.
 60. **Hirani V, Blyth F, Naganathan V, Le Couteur DG, Seibel MJ, Waite LM, Handelsman DJ, Cumming R.** Sarcopenia is associated with incident disability, institutionalization, and mortality in community-dwelling older men: the concord health and ageing in men project. *JAMDA*, 2015.
 61. **Holloszy JO, Booth F.** Biochemical adaptations to endurance exercise in muscle. *Annu Rev Physiol* 38: 273–291, 1976.
 62. **Holloszy JO, Oscai LB, Don I, Molé P.** Mitochondrial citric acid cycle and related enzymes: adaptive response to exercise. *Biochem Biophys Res Commun* 40: 1368–1373, 1970.
 63. **Hood DA, Adhietty PJ, Colavecchia M, Gordon JW, Irrcher I, Joseph AM, Lowe ST, Rungi A.** Mitochondrial biogenesis and the role of the protein import pathway. *Med Sci Sports Exerc* 35: 86–94, 2003.
 64. **Hood DA, Irrcher I, Ljubicic V, Joseph A.** Coordination of metabolic plasticity in skeletal muscle. *J Exp Biol* 209: 2265–2275, 2006.
 65. **Hood DA, Saleem A.** Exercise-induced mitochondrial biogenesis in skeletal muscle. *Nutr Metab Cardiovasc Dis* 17: 332–337, 2007.
 66. **Hood DA, Ugucioni G, Vainshtein A, D'souza D.** Mechanisms of exercise-induced mitochondrial biogenesis in skeletal muscle: implications for health and disease. *Compr Physiol* 1: 1119–1134, 2011.
 67. **Hood DA.** Contractile activity-induced mitochondrial biogenesis in skeletal muscle. *J Appl Physiol* 90: 1137–1157, 2001.
 68. **Hood DA.** Mechanisms of exercise-induced mitochondrial biogenesis in skeletal muscle. *Appl Physiol Nutr Metab* 34: 465–472, 2009.
 69. **Horn HF, Vousden K.** Coping with stress: multiple ways to activate p53. *Oncogene* 26: 1306–1316, 2007.
 70. **Iqbal S, Hood DA.** The role of mitochondrial fusion and fission in skeletal muscle function and dysfunction. *Front Biosci* 1: 157–172, 2015.
 71. **Iqbal S, Ostojic O, Singh K, Joseph AM, Hood DA.** Expression of mitochondrial fission and fusion regulatory proteins in skeletal muscle during chronic use and disuse. *Muscle Nerve* 48: 963–970, 2013.
 72. **Irrcher I, Ljubicic V, Hood DA.** Interactions between ROS and AMP kinase activity in

- the regulation of PGC-1alpha transcription in skeletal muscle cells. *Am J Physiol Cell Physiol* 296: C116-23, 2009.
73. **Jacks T, Remington L, Williams BO, Schmitt EM, Halachmi S, Bronson RT, Weinberg R.** Tumor spectrum analysis in p53-mutant mice. *Curr Biol* 4: 1–7, 1994.
 74. **Jamart C, Francaux M, Millet GY, Deldicque L, Frère D, Féasson L.** Modulation of autophagy and ubiquitin-proteasome pathways during ultra-endurance running. *J Appl Physiol* 112: 1529–1537, 2012.
 75. **Jornayvaz FR, Shulman G.** Regulation of mitochondrial biogenesis. *Essays Biochem* 47: 69–84, 2010.
 76. **Joseph AM, Hood DA.** Plasticity of TOM complex assembly in skeletal muscle mitochondria in response to chronic contractile activity. *Mitochondrion* 12: 305–312, 2012.
 77. **Joseph AM, Pilegaard H, Litvintsev A, Leick L, Hood DA.** Control of gene expression and mitochondrial biogenesis in the muscular adaptation to endurance exercise. *Essays Biochem* 42: 13–29, 2006.
 78. **Kavazis AN, McClung JM, Hood DA, Powers S.** Exercise induces a cardiac mitochondrial phenotype that resists apoptotic stimuli. *Am J Physiol Hear Circ Physiol* 294: H928–H935, 2008.
 79. **Kawauchi K, Araki K, Tobiume K, Tanaka N.** Activated p53 induces NF-kB DNA binding but suppresses its transcriptional activation. *Biochem Biophys Res Commun* 372: 137–141, 2008.
 80. **Kenzelmann Broz D, Mello SS, Biegging KT, Jiang D, Dusek RL, Brady CA, Sidow A, Attardi L.** Global genomic profiling reveals an extensive p53-regulated autophagy program contributing to key p53 responses. *Genes Dev* 27: 1016–1031, 2013.
 81. **Kim K, Kim YH, Lee SH, Jeon MJ, Park SY, Doh K.** Effect of exercise intensity on unfolded protein response in skeletal muscle of rat. *Korean J Physiol Pharmacol* 18: 211–216, 2014.
 82. **Kimball SR, Jefferson L.** Signaling pathways and molecular mechanisms through which branched-chain amino acids mediate translational control of protein synthesis. *J Nutr* 136: 227S–231S, 2006.
 83. **Kirkwood SP, Packer L, Brooks G.** Effects of endurance training on a mitochondrial reticulum in limb skeletal muscle. *Arch Biochem Biophys* 255: 80–88, 1987.
 84. **Koçtürk S, Kayatekin BM, Resmi H, Açıkgöz O, Kaynak C, Özer E.** The apoptotic response to strenuous exercise of the gastrocnemius and soleus muscle fibers in rats. *Eur J Appl Physiol* 102: 515–524, 2008.
 85. **Krieger DA, Tate CA, McMillin-Wood J, Booth F.** Populations of rat skeletal muscle mitochondria after exercise and immobilization. *J Appl Physiol* 48: 23–28, 1980.

86. **Kuang S, Rudnicki M.** The emerging biology of satellite cells and their therapeutic potential. *Trends Mol Med* 14: 82–91, 2008.
87. **Kubli DA, Gustafsson A.** Mitochondria and mitophagy: the yin and yang of cell death control. *Circ Res* 111: 1208–1221, 2012.
88. **Laguens RP, Lozada BB, Gomez Dumm CL, Beramendi A.** Effect of acute and exhaustive exercise upon the fine structure of heart mitochondria. *Experimentia* 22: 244–246, 1966.
89. **Lai RYJ, Ljubicic V, D'souza D, Hood DA.** Effect of chronic contractile activity on mRNA stability in skeletal muscle. *Am J Physiol Cell Physiol* 299: C155–163, 2010.
90. **Lane D, Crawford L.** T antigen is bound to a host protein in SV40-transformed cells. *Nature* 278: 261–263, 1979.
91. **Laughlin MH, Simpson T, Brown R, Smith JK, Korthuis R.** Skeletal muscle oxidative capacity, antioxidant enzymes, and exercise training. *J Appl Physiol* 68: 2337–2343, 1990.
92. **Lavin MF, Gueven N.** The complexity of p53 stabilization and activation. *Cell Death Differ* 13: 941–950, 2006.
93. **Levine AJ, Hu W, Feng Z.** The p53 pathway: what questions remain to be explored? *Cell Death Differ* 13: 1027–1036, 2006.
94. **Levine A.** p53, the cellular gatekeeper for growth and division. *Cell* 88: 323–331, 1997.
95. **Li J, Donath S, Li Y, Qin D, Prebhakar BS, Li P.** miR-30 regulates mitochondrial fission through targeting p53 and the dynamin-related protein-1 pathway. *PLoS Genet* 6: e1000795, 2010.
96. **Li X, Fang P, Mai J, Choi ET, Wang H, Yang X.** Targeting mitochondrial reactive oxygen species as novel therapy for inflammatory diseases and cancers. *J Hematol Oncol* 6: 19, 2013.
97. **Liu B, Chen Y, Clair D.** ROS and p53: versatile partnership. *Free Rad Bio Med* 44: 1529–1535, 2008.
98. **Ljubicic V, Joseph AM, Saleem A, Ugucioni G, Collu-Marchese M, Lai RYJ, Nguyen LMD, Hood DA.** Transcriptional and post-transcriptional regulation of mitochondrial biogenesis in skeletal muscle: effects of exercise and aging. *Biochim Biophys Acta* 1800: 223–234, 2010.
99. **Lowell BB, Spiegelman BM.** Towards a molecular understanding of adaptive thermogenesis. *Nature* 404: 652–660, 2000.
100. **Lyons GE, Muhlebach S, Moser A, Masood R, Paterson BM, Buckingham ME, Perriard J.** Developmental regulation of creatine-kinase gene-expression by myogenic factors in embryonic mouse and chick skeletal-muscle. *Development* 113: 1017–1029, 1991.

101. **Maclaine NJ, Hupp T.** The regulation of p53 by phosphorylation: a model for how distinct signals integrate into the p53 pathway. *Aging (Albany NY)* 1: 490–502, 2009.
102. **Maddocks ODK, Vousden K.** Metabolic regulation by p53. *J Mol Med* 89: 237–245, 2011.
103. **Maier B, Gluba W, Bernier B, Turner T, Mohammad K, Guise T, Sutherland A, Thorner M, Scrabble H.** Modulation of mammalian life span by the short isoform of p53. *Genes Dev* 18: 306–319, 2004.
104. **Marino G, Niso-Santano M, Baehrecke EH, Kroemer G.** Self-consumption: the interplay of autophagy and apoptosis. *Nat Rev Mol Cell Biol* 15: 81–94, 2014.
105. **Martin WF, Mentel M.** The Origin of Mitochondria. *Nat Educ* 3: 58, 2010.
106. **Mathupala SP, Ko YH, Pedersen P.** Hexokinase II: Cancer’s double-edged sword acting as both facilitator and gatekeeper of malignancy when bound to mitochondria. *Oncogene* 25: 4777–4786, 2006.
107. **Matoba S, Kang JG, Patino WD, Wragg A, Boehm M, Gravrilova O, Hurley PJ, Bunz F, Hwang P.** p53 regulates mitochondrial respiration. *Science (80)* 312: 1650–1653, 2006.
108. **McArdle WD, Katch FI, Katch V.** *Essentials of Exercise Physiology*. 2nd ed. Lippincott Williams & Wilkins, 2000.
109. **McLeod M, Breen L, Hamilton D, Lee P.** Live strong and prosper: the importance of skeletal muscle strength for healthy ageing. *Biogerontology* 17: 497–510, 2016.
110. **Melzer K.** Carbohydrate and fat utilization during rest and physical activity. *e-SPEN* 6: e45–e52, 2011.
111. **Michaud M, Balardy L, Moulis G, Gaudin C, Peyrot C, Vellas B, Cesari M, Nourhashemi F.** Proinflammatory cytokines, aging, and age-related diseases. *JAMDA* 14: 877–882, 2013.
112. **Min K, Smuder AJ, Kwon OS, Kavazis AN, Szeto HH, Powers S.** Mitochondrial-targeted antioxidants protect skeletal muscle against immobilization-induced muscle atrophy. *J Appl Physiol* 111: 1459–1466, 2011.
113. **Mitchell P.** Coupling of phosphorylation to electron and hydrogen transfer by a chemi-osmotic type of mechanism. *Nature* 191: 144–148, 1961.
114. **Mizushima N.** Autophagy : process and function. *Genes Dev* 21: 2861–2873, 2007.
115. **Moyes CD, Hood DA.** Origins and consequences of mitochondrial variation in vertebrate muscle. *Annu Rev Physiol* 65: 177–201, 2003.
116. **Muller FL, Liu Y, Van Remmen H.** Complex III releases superoxide to both sides of the inner mitochondrial membrane. *J Biol Chem* 279: 49064–49073, 2004.

117. **Nader GA, Esser K.** Intracellular signaling specificity in skeletal muscle in response to different modes of exercise. *J Appl Physiol* 90: 1936–1942, 2001.
118. **Neuspiel M, Zunino R, Gangaraju S, Rippstein P, McBride H.** Activated mitofusin 2 signals mitochondrial fusion, interferes with Bax activation, and reduces susceptibility to radical induced depolarization. *J Biol Chem* 280: 25060–25070, 2005.
119. **Nguyen LMD, Hood DA.** Contractile activity-induced gene expression in fast- and slow-twitch muscle. *Appl Physiol Nutr Metab* 36: 233–241, 2011.
120. **Nikoletopoulou V, Markaki M, Palikaras K, Tavernarakis N.** Crosstalk between apoptosis, necrosis and autophagy. *Biochim Biophys Acta* 1833: 3448–3459, 2013.
121. **Olovnikov IA, Kravchenko JE, Chumakov P.** Homeostatic functions of the p53 tumor suppressor: regulation of energy metabolism and antioxidant defense. *Semin Cancer Biol* 19: 32–41, 2008.
122. **Olsson A, Manzl C, Strasser A, Villunger A.** How important are post-translational modifications in p53 for selectivity in target-gene transcription and tumour suppression? *Cell Death Differ* 14: 1561–1575, 2007.
123. **Palmer JW, Tandler B, Hoppel C.** Biochemical properties of subsarcolemmal and interfibrillar mitochondrial isolated from rat cardiac muscle. *J Biol Chem* 252: 8731–8739, 1977.
124. **Park JY, Wang PY, Matsumoto T, Sung HJ, Choi JW, Anderson SA, Leary SC, Balaban RS, Hwang P.** p53 improves aerobic exercise capacity and augments skeletal muscle mitochondrial DNA content. *Circ Res* 105: 705–712, 2009.
125. **Petrella JK, Kim JS, Mayhew DL, Cross JM, Bamman M.** Potent myofiber hypertrophy during resistance training in humans is associated with satellite cell-mediated myonuclear addition: a cluster analysis. *J Appl Physiol* 104: 1736–1742, 2008.
126. **Pette D, Vrbová G.** The contribution of neuromuscular stimulation in elucidating muscle plasticity revisited. *Eur J Transl Myol* 27: 33–39, 2017.
127. **Pette D, Staron RS.** Transitions of muscle fiber phenotypic profiles. *Histochem Cell Biol* 115: 359–372, 2001.
128. **Pette D.** Myosin isoform, muscle fiber types and transition. *Microsc Res Tech* 50: 500–509, 2000.
129. **Pham-Huy LA, He H, Pham-Huy C.** Free radicals, antioxidants in disease and health. *Int J Biomed Sci* 4: 89–96, 2008.
130. **Plotnikov EY, Silachev DN, Popkov VA, Zorova LD, Pevzner IB, Zorov SD, Jankauskas SS, Babenko V, Sukhikh GT, Zorov D.** Intercellular signalling cross-talk: to kill, to heal and to rejuvenate. *Hear Lung Circ* 26: 648–659, 2017.
131. **Powers SK, Criswell D, Lawler J, Ji LL, Martin D, Herb RA, Dudley G.** Influence of

- exercise and fiber type on antioxidant enzyme activity in rat skeletal muscle. *Am J Physiol* 35: R375-80, 1994.
132. **Powers SK, Duarte J, Kavazis AN, Talbert E.** Reactive oxygen species are signalling molecules for skeletal muscle adaptation. *Exp Physiol* 95: 1–9, 2009.
 133. **Qi Z, He J, Zhang Y, Shao Y, Ding S.** Exercise training attenuates oxidative stress and decreases p53 protein content in skeletal muscle of type 2 diabetic Goto-Kakizaki rats. *Free Radic Biol Med* 50: 794–800, 2011.
 134. **Qian Y, Chen X.** Tumor suppression by p53: making cells senescent. *Histol Histopathol* 25: 515–526, 2010.
 135. **Quinlan CL, Treberg JR, Perevoshchikova IV, Orr A, Martin D.** Native rates of superoxide production from multiple sites in isolated mitochondria measured using endogenous reporters. *Free Radic Biol Med* 53: 1807–1817, 2012.
 136. **Rizzoli R, Reginster JY, Arnal JF, Bautmans I, Beaudart C, Bischoff-Ferrari H, Biver E, Boonen S, Brandi ML, Chines A, Cooper C, Epstein S, Fielding RA, Goodpaster B, Kanis Kaufman JM, Laslop A, Malafarina V, Manas LR, Mitlak BH, Oreffo O.** Quality of life in sarcopenia and frailty. *Calcif Tissue Int* 93: 101–120, 2013.
 137. **Rotblat B, Melino G, Knight R.** NRF2 and p53: januses in cancer? *Oncotarget* 3: 1272–83, 2012.
 138. **Roy RR, Monke SR, Allen D, Edgerton V.** Modulation of myonuclear number in functionally overloaded and exercised rat plantaris fibers. *J Appl Physiol* 87: 634–642, 1999.
 139. **Safdar A, Khrapko K, Flynn JM, Saleem A, De Lisio M, Johnston APW, Kratysberg Y, Samjoo IA, Kitaoka Y, Ogborn DI, Little JP, Raha S, Parise G, Akhtar M, Hettinga BP, Rowe G, Arany Z, Prolla TA, Tarnopolsky MA.** Exercise-induced mitochondrial p53 repairs mtDNA mutations in mutator mice. *Skelet Muscle* 6: 7, 2016.
 140. **Saito T, Sadoshima J.** The molecular mechanisms of mitochondrial autophagy/mitophagy in the heart. *Circ Res* 116: 1477–1490, 2015.
 141. **Saleem A, Adhietty PJ, Hood DA.** Role of p53 in mitochondrial biogenesis and apoptosis in skeletal muscle. *Physiol Genomics* 37: 58–66, 2009.
 142. **Saleem A, Carter H, Iqbal S, Hood DA.** Role of p53 within the regulatory network controlling muscle mitochondrial biogenesis. *Exerc Sport Sci Rev* 39: 199–205, 2011.
 143. **Saleem A, Carter HN, Hood DA.** p53 is necessary for the adaptive changes in cellular milieu subsequent to an acute bout of endurance exercise. *AJP Cell Physiol* 306: C241–C249, 2014.
 144. **Saleem A, Hood DA.** Acute exercise induces tumour suppressor protein p53 translocation to the mitochondria and promotes a p53-Tfam-mitochondrial DNA complex in skeletal muscle. *J Physiol* 591: 3625–3636, 2013.

145. **Saleem A, Iqbal S, Zhang Y, Hood DA.** Effect of p53 on mitochondrial morphology, import, and assembly in skeletal muscle. *Am J Physiol - Cell Physiol* 308: C319–C329, 2015.
146. **Sandri M, Carraro U, Podhorska-Okolov M, Rizzi C, Arslan P, Monti D, Franceschi C.** Apoptosis, DNA damage and ubiquitin expression in normal and mdx muscle fibers after exercise. *FEBS Lett* 373: 291–295, 1995.
147. **Scarpulla R.** Nuclear control of respiratory gene expression in mammalian cells. *J Cell Biochem* 97: 673–683, 2006.
148. **Schiaffino S, Reggiani C.** Fiber types in mammalian skeletal muscles. *Physiol Rev* 91: 1447–1531, 2011.
149. **Schmid P, Lorenz A, Hameister H, Montenarh M.** Expression of p53 during mouse embryogenesis. *Development* 113: 857–865, 1991.
150. **Schwartzberg-Bar-Yoseph F, Armoni M, Karnieli E.** The tumor suppressor p53 down-regulates glucose transporters GLUT1 and GLUT4 gene expression. *Cancer Res* 64: 2627–2633, 2004.
151. **Siu PM, Bryner RW, Martyn JK, Alway S.** Apoptotic adaptations from exercise training in skeletal and cardiac muscles. *FASEB J* 18: 1150–1152, 2004.
152. **Snijders T, Smeets JSJ, van Kranenburg J, Kies AK, van Loon LJC, Verdijk L.** Changes in myonuclear domain size do not precede muscle hypertrophy during prolonged resistance-type exercise training. *Acta Physiol* 216: 231–239, 2016.
153. **Stambolsky P, Weisz L, Shats I, Klein Y, Goldfinger N, Oren M, Rotter V.** Regulation of AIF expression by p53. *Cell Death Differ* 13: 2140–2149, 2006.
154. **Steinbacher P, Eckl P.** Impact of oxidative stress on exercising skeletal muscle. *Biomolecules* 5: 356–377, 2015.
155. **Stocks B, Dent JR, Joanisse S, McCurdy CE, Philp A.** Skeletal muscle fibre-specific knockout of p53 does not reduce mitochondrial content or enzyme activity. *Front Physiol* 8: 1–10, 2017.
156. **Sudo M, Kano Y.** Myofiber apoptosis occurs in the inflammation and regeneration phase following eccentric contractions in rats. *J Physiol Sci* 59: 405–412, 2009.
157. **Sun Y, Cui D, Zhang Z, Zhang T, Shi J, Jin H, Ge Z, Ji L, Ding S.** Attenuated oxidative stress following acute exhaustive swimming exercise was accompanied with modified gene expression profiles of apoptosis in the skeletal muscle of mice. *Oxid Med Cell Longev* 2016, 2016.
158. **Tachtsis B, Smiles WJ, Lane SC, Hawley JA, Camera D.** Acute endurance exercise induces nuclear p53 abundance in human skeletal muscle. *Front Physiol* 7: 144, 2016.
159. **Takahashi M, Hood DA.** Protein import into subsarcolemmal and intermyofibrillar

- skeletal muscle. *J Biol Chem* 271: 27285–27291, 1996.
160. **Tasdemir E, Maiuri MC, Galluzzi L, Vitale I, Djavaheri-mergny M, Amelio MD, Criollo A, Morselli E, Zhu C, Harper F, Nannmark U, Samara C, Pinton P, Vicencio JM, Carnuccio R, Moll UM, Madeo F, Paterlini-Brechot P, Rizzuto R, Szabadkai G, Pierron G, Blomgren K, Tavernarakis N, Codogno P, Cecconi F, Kroemer G.** Regulation of autophagy by cytoplasmic p53. *Nat Cell Biol* 10: 676–687, 2008.
 161. **Tebaldi T, Zaccara S, Alessandrini F, Bisio A, Ciribilli Y, Inga A.** Whole-genome cartography of p53 response elements ranked on transactivation potential. *BMC Genomics* 16: 464, 2015.
 162. **Tong X, Zhao F, Mancuso A, Gruber JJ, Thompson C.** The glucose-responsive transcription factor ChREBP contributes to glucose-dependent anabolic synthesis and cell proliferation. *PNAS* 106: 21660–21665, 2009.
 163. **Tyner SD, Venkatachalam S, Choi J, Jones S, Ghebranious N, Igelmann H, Lu X, Soron G, Cooper B, Brayton C, Hee Park S, Thompson T, Karsenty G, Bradley A, Donehower L.** p53 mutant mice that display early ageing-associated phenotypes. *Nature* 415: 45–53, 2002.
 164. **Vainshtein A, Hood DA.** The regulation of autophagy during exercise in skeletal muscle. *J Appl Physiol* 120: 664–673, 2016.
 165. **Vainshtein A, Kazak L, Hood DA.** Effects of endurance training on apoptotic susceptibility in striated muscle. *J Appl Physiol* 110: 1638–1645, 2011.
 166. **Vainshtein A, Tryon LD, Pauly M, Hood DA.** Role of PGC-1 α during acute exercise-induced autophagy and mitophagy in skeletal muscle. *Am J Physiol - Cell Physiol* 308: C710–C719, 2015.
 167. **Vandamme T.** Use of rodents as models of human diseases. *J Pharm Bioallied Sci* 6: 2–9, 2014.
 168. **Vaseva AV, Moll U.** The mitochondrial p53 pathway. *Biochim Biophys Acta* 1787: 414–420, 2009.
 169. **Ventadour S, Attaix D.** Mechanisms of skeletal muscle atrophy. *Curr Opin Rheumatol* 18: 631–635, 2006.
 170. **Wallace D.** A mitochondrial paradigm of metabolic and degenerative diseases, aging, and cancer: a dawn for evolutionary medicine. *Annu Rev Genet* 39: 359, 2005.
 171. **Wang P, Li CG, Qi Z, Cui D, Ding S.** Acute exercise stress promotes Ref1/Nrf2 signalling and increases mitochondrial antioxidant activity in skeletal muscle. *Exp Physiol* 101: 410–420, 2016.
 172. **Wang W, Cheng X, Lu J, Wei J, Fu G, Zhu F, Jia C, Zhou L, Xie H, Zheng S.** Mitofusin-2 is a novel direct target of p53. *Biochem Biophys Res Commun* 400: 587–592, 2010.

173. **Webster NJG, Resnik JL, Reichart DB, Strauss B, Haas M, Seely B.** Repression of the insulin receptor promoter by the tumor suppressor gene product p53 : a possible mechanism for receptor overexpression in breast cancer. *Cancer Res* 56: 2781–2788, 1996.
174. **White E.** Autophagy and p53. *Cold Spring Harb Perspect Med* 6: a026120, 2017.
175. **Wilkinson DJ, Hossain T, Hill DS, Phillips BE, Crossland H, Williams J, Loughna P, Churchward-Venne TA, Breen L, Phillips SM, Etheridge T, Rathmacher JA, Smith K, Szewczyk NJ, Atherton P.** Effects of leucine and its metabolite β -hydroxy- β -methylbutyrate on human skeletal muscle protein metabolism. *J Physiol* 591: 2911–2923, 2013.
176. **Williams R.** Mitochondrial gene expression in mammalian striated muscle. *J Biol Chem* 261: 12390–12394, 1986.
177. **Wilmore JH.** *Human Kinetics*. 3rd ed. 2004.
178. **Yang Y, Creer A, Jemiolo B, Trappe S.** Time course of myogenic and metabolic gene expression in response to acute exercise in human skeletal muscle. *J Appl Physiol* 98: 1745–1752, 2005.
179. **Yin H, Price F, Rudnicki M.** Satellite cells and the muscle stem cell niche. *Physiol Rev* 93: 23–67, 2013.
180. **Yoshida Y, Izumi H, Torigoe T, Ishiguchi H, Itoh H, Kang D.** p53 physically interacts with mitochondrial transcription factor A and differentially regulates binding to damaged DNA. *Cancer Res* 63: 3729–3734, 2003.
181. **You A, Nam CW, Wakabayashi N, Yamamoto M, Kensler TW, Kwak M.** Transcription factor Nrf2 maintains the basal expression of Mdm2: An implication of the regulation of p53 signaling by Nrf2. *Arch Biochem Biophys* 507: 356–364, 2011.
182. **Yu X, Munoz-Alarcon A, Ajayi A, Webling K, Steinhof A, Langel U, Strom A.** Inhibition of autophagy via p53-mediated disruption of ULK1 in a SCA7 polyglutamine disease model. *J Mol Neurosci* 50: 586–599, 2013.
183. **Zhang N, Bing T, Shen L, Song R, Wang L, Liu X, Liu M, Li J, Tan W, Shangguan D.** Intercellular connections related to cell-cell crosstalk specifically recognized by an aptamer. *Angew Chemie - Int Ed* 55: 3914–3918, 2016.
184. **Zheng J.** Energy metabolism of cancer: glycolysis versus oxidative phosphorylation (review). *Oncol Lett* 4: 1151–1157, 2012.
185. **Zuckerman V, Wolyniec K, Sionov RV, Haupt S, Haupt Y.** Tumour suppression by p53: the importance of apoptosis and cellular senescence. *J Pathol* 219: 3–15, 2009.

Manuscript

The Role of p53 in Determining Mitochondrial Adaptations to Endurance Training in Skeletal Muscle

Kaitlyn Beyfuss, Avigail T. Erlich, Matthew Triolo, David A. Hood

Muscle Health Research Centre, School of Kinesiology and Health Science, York University,
Toronto, Ontario, M3J 1P3, Canada

To whom correspondence should be addressed:

David A. Hood
School of Kinesiology
York University, Toronto, ON
M3J 1P3, Canada
Tel: (416) 736-2100 ext. 66640
Fax: (416) 736-5698
Email: dhood@yorku.ca

Abstract

p53 plays an important role in regulating mitochondrial homeostasis. However, it is unknown whether p53 is required for the physiological and mitochondrial adaptations with exercise training. Furthermore, it is also unknown whether impairments in the absence of p53 are a result of its loss in skeletal muscle, or a secondary effect due to its deletion in alternative tissues. Thus, we investigated the role of p53 in regulating mitochondria both basally, and under the influence of exercise, by subjecting C57Bl/6J whole-body (WB) and muscle-specific p53 knockout (mKO) mice to a 6-week training program. Our results confirm that p53 is important for regulating mitochondrial content and function, as well as proteins within the autophagy and apoptosis pathways. Despite an increased proportion of phosphorylated p53 (Ser¹⁵) in the mitochondria, p53 is not required for training-induced adaptations in exercise capacity or mitochondrial content and function. In comparing mouse models, similar directional alterations were observed in basal and exercise-induced signaling modifications in WB and mKO mice, however the magnitude of change was less pronounced in the mKO mice. Our data suggest that p53 is required for basal mitochondrial maintenance in skeletal muscle, but is not required for the adaptive responses to exercise training.

Introduction

The tumor suppressor protein p53 is a rapid-response transcriptional regulator of numerous pathways involved in maintaining cellular homeostasis. Though extensively researched in the context of cancer and its role in the Warburg effect, few studies have examined the role of p53 in skeletal muscle, an organ that comprises 40% of total body mass (19, 23). Skeletal muscle is an exceptionally malleable tissue that can adapt to multiple physiological stimuli (2, 19), and mitochondria are the organelles that display plasticity within muscle.

Recently, the role of p53 has been examined in mitochondrial biogenesis within skeletal muscle. Exercise enhances p53 activation through kinase activation (AMPK, p38 MAPK) leading to the phosphorylation of specific p53 residues to increase its mitochondrial and nuclear localization (35, 37, 38). Once in mitochondria, p53 functions to enhance biogenesis through its interaction with Tfam, and its requirement for the expression of mtDNA gene products in response to exercise (1, 36, 48). Acute exercise has specifically been shown to increase p53 serine15 phosphorylation and subsequent localization to subsarcolemmal (SS) and intermyofibrillar (IMF) mitochondria, with concomitant increases in mtDNA copy number and elevated COX-I protein (37, 38). p53 additionally localizes to the nucleus where it can bind to the promoters of PGC-1 α and nuclear genes encoding mitochondrial proteins (NuGEMPs) such as Tfam, COX IV, and SCO2, to upregulate transcription (26, 33, 38). p53 mitochondrial localization with acute exercise seems to be preferred over nuclear accumulation (38), however it has yet to be established whether exercise training modifies this distribution and further, and whether p53 is required within the mitochondria for adaptation purposes.

p53 is also known to play a role in regulating additional mitochondrial-dependent signaling pathways, including autophagy/mitophagy and apoptosis. Within the cytosol, p53 acts

as an upstream endogenous repressor of autophagy, through its interaction with the ULK1 complex (31, 45). When nuclear localized, p53 can regulate autophagy through transcription of upstream activators AMPK and TSC2 (14), as well as lysosomal genes (13, 21, 37). Furthermore, p53 monitors ubiquitination and regulates autophagy flux through LC3 and p62 modulation (21, 37, 40). Although autophagic flux and lysosomal activation in response to acute exercise does not depend on p53, it is required for the regulation of ubiquitination (37). However, it has not been established how the autophagy pathway is regulated by p53 with exercise training. p53 is also well-known for its role in regulating apoptosis, since it can transcriptionally regulate numerous pro-apoptotic genes including Bax and Bid to induce DNA fragmentation (16, 35, 47). Furthermore p53 itself can localize to the mitochondrial surface where it can regulate permeability transition pore kinetics (30, 47). Chronic exercise has been previously shown to reduce the Bax:Bcl-2 ratio (42, 46) concomitant with reductions in cytochrome c and AIF protein release (3), indicative of anti-apoptotic adaptations in mitochondria. However, the role of p53 in mediating these exercise training effects on the apoptotic pathway is still unknown. Furthermore, literature published on the role of p53 in regulating autophagy, apoptosis, mitochondrial biogenesis and metabolism, have been established largely through the use of a whole body p53 knockout model. Though this research has elucidated novel roles for p53, recently published work utilizing a muscle-specific p53 knockout model did not observe any reductions in mitochondrial content or the expression of nuclear genes encoding mitochondrial proteins (15, 43). Thus, the purpose of this study was to elucidate the role of p53 in regulating skeletal muscle adaptations to endurance training, particularly related to the mitochondrial biogenesis, autophagy, and apoptosis pathways. To accomplish this, we utilized a muscle-specific p53 deficient mouse and when relevant, compared

this model to traditionally employed p53 whole body knockout animals under identical endurance training stimuli.

Methods

Animal Breeding. The C57Bl/6J whole body (WB) p53 wildtype (WT) and knockout (KO) mouse groups originated from two companies, one from Taconic labs (New York, USA) and one from the Jackson Laboratory (California, USA). The C57Bl/6J muscle specific (MS) p53 WT and KO mice were generously provided by Dr. Christopher M. Adams (Iowa, USA). Mice were bred and treated experimentally in accordance with principles of the York University Animal Care Committee in accordance with the Canadian Council on Animal Care. Progeny of breeding pairs were genotyped using ear clippings obtained from each mouse for crude DNA extraction. Extracts were then added to a polymerase chain reaction (PCR) tube containing DNA Taq polymerase (Sigma Jumpstart REDtaq Ready Mix PCR Reaction Mix). Forward and reverse primers for the WT and KO *p53* gene were added to test the genotype of the whole body mice, whereas for the muscle-specific mice, a forward and reverse primer for the *Cre* gene was added. Genomic differences were detected using PCR amplification and the reaction products were separated on 2% agarose gels at 120 V for ~one hour and visualized with the ethidium bromide.

Experimental Design. At approximately 12-14 weeks of age, male C57Bl/6J WT and KO mice in the WB and MS mouse models were matched for sex and body weight. All mice were acclimatized to the treadmill for two days prior to the first graded exercise performance test. Animals commenced at 5m/min for 5 min, followed by 10 m/min for 10 min, then increasing from 15 m/min to 20 to 25 m/min for 5 min each before beginning the exhaustive portion of increased the speed by 1 m/min every 3 min until exhaustion. Exhaustion was defined as the

point whereby mice remained on an electric shock pad for 10 seconds despite prodding with air currents. Lactate measurements were obtained following removal from the treadmill to ensure that exhaustion was reached. Mice in both models were then randomized to a sedentary or training group. The sedentary group involved no treadmill exercise for 6 weeks, while the training group participated in a 6-week training protocol exercising 5 days/week and beginning at 5 m/min for 20 min and progressing to 26 m/min for 90 min. Following the 6 weeks, both the sedentary and training groups underwent a second exercise performance test following the same parameters as the first. Approximately 48 hours later, all mice underwent an acute bout of treadmill exercise at 15 m/min for 90 min. Full details are in Figure 1. All mice were sacrificed by cervical dislocation immediately following the acute bout for instantaneous tissue removal.

Tissue Extraction and Experimental Organization. All mice underwent the same tissue extraction protocol. One gastrocnemius (~ 170 mg) and one tibialis anterior (TA) (~50 mg) were extracted and immediately snap frozen and stored at -80°C for mRNA analysis, whole muscle western blotting, and COX enzyme activity. Part of one TA (~ 30 mg) was placed in buffer and utilized for nuclear/cytosolic fractionation. The rest of the skeletal muscle (one gastrocnemius, two quadriceps femoris, two triceps) (~ 1000 mg) was utilized for mitochondrial fractionation and subsequent functional testing. The heart and epididymal fat were removed, weighed, and frozen in liquid nitrogen for later use. Frozen skeletal muscle samples were pulverized into a powder with a stainless steel mortar cooled to the temperature of liquid nitrogen and stored in liquid nitrogen for subsequent analysis.

Fig. 1

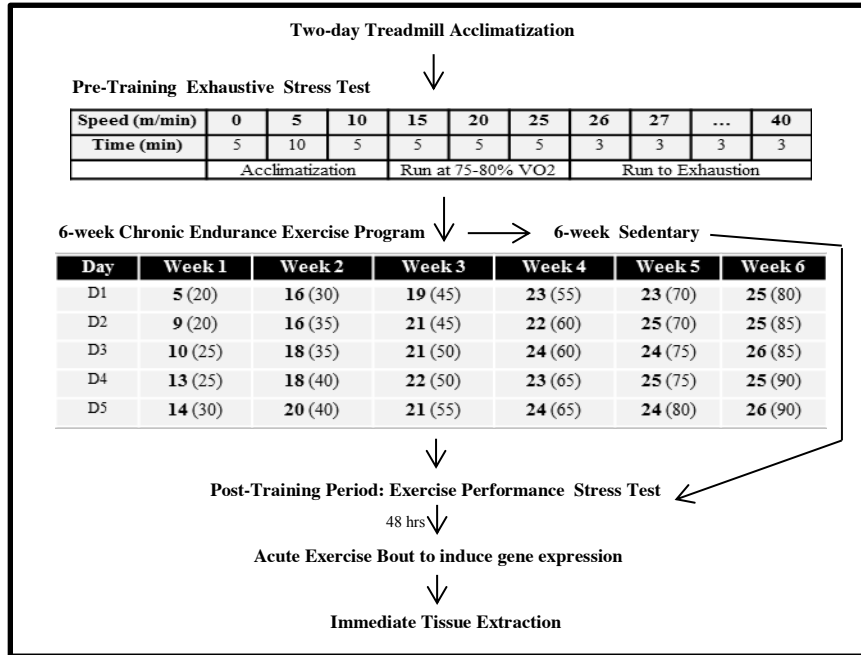


Figure 1. Exercise training protocol. Muscle specific (MS) WT and p53 mKO mice and whole body (WB) WT and p53 KO mice underwent a two-day acclimatization program to the treadmill followed by an exhaustive performance test to measure baseline differences between mouse model and genotype. Mice were randomized to a training and sedentary arm. Mice in the training group underwent a 6-week progressive training program. Speed was expressed in m/min and (time) was measured in minutes. Once individual programs were completed, all mice underwent a second exhaustive performance test to measure training adaptations. Following 48 hours, animals were subjected to an acute bout of exercise to upregulate transcriptional signaling, followed by immediate extraction of the skeletal muscles, heart, and epididymal fat.

Protein Extraction. Tissue powders were diluted 5X with an extraction buffer containing protease and phosphatase inhibitors. Diluted samples were rotated end-over-end at 4°C for one hour, followed by sonication at 3x3 at 30% of maximum power. Samples were then centrifuged at 4°C for 10 minutes at 16,000g and the supernate was stored at -80°C until required.

Protein Concentration. The Bradford protein assay was used to determine the protein concentration of samples, as previously described (6). Briefly, to standardize for concentration, bovine serum albumin (2mg/ml) was combined with double distilled water and Sakamoto extraction buffer in eppendorf tubes. Protein extracts were mixed with double- distilled water and analyzed in comparison with the standard curve using a Bio-Tek Synergy HT micro plate reader.

Mitochondrial Fractionation. Briefly, approximately 1000 mg of fresh skeletal muscle was minced, homogenized, and subjected to differential centrifugation to yield the SS and IMF subfractions (11). The mitochondria were re-suspended in a small volume of resuspension buffer (100 mM KCl, 10 mM MOPS, and 0.2% BSA at pH=7.4). All centrifugation steps were carried out at 4°C. Mitochondrial homogenates were analyzed for protein content using the Bradford assay, and used immediately for mitochondrial respiration, ROS analysis, and the protein release assay before being frozen at -80°C for later biochemical analysis by immunoblotting.

Mitochondrial Respiration. Isolated SS and IMF mitochondria (50 µl) were incubated with 250 µl of $\dot{V}O_2$ buffer (in mM: 250 sucrose, 50 KCl, 25 Tris·HCl, 10 K₂HPO₄, pH=7.4), at 30°C in a water-jacketed respiratory chamber with continuous stirring. Respiration rates (nanomoles O₂·min⁻¹·mg⁻¹) were evaluated in the presence of 10 mM glutamate (state 4 or passive

respiration) and 0.44 mM ADP (state 3 or active respiration) with the use of a Clark oxygen electrode.

Mitochondrial Reactive Oxygen Species (ROS) Production. SS and IMF mitochondria (50 µg) were incubated with 50 µM dichlorodihydro-fluorescein diacetate (H₂DCF-DA) and $\dot{V}O_2$ buffer at 37°C for 30 min in a polystyrene 96-well plate. The fluorescence emission (between 485 and 528 nm) is directly proportional to ROS production and was measured with a Synergy HT microplate reader. ROS production was assessed during state 4 and state 3 respiration by the addition of 10 mM glutamate and 0.44 mM ADP respectively, to isolated mitochondria immediately before the addition of H₂DCF-DA.

Nuclear and Cytosolic Fractionation. Nuclear and cytosolic fractions were prepared from freshly isolated skeletal muscle using a commercially available nuclear extraction kit (Pierce NE-PER, Rockford, IL, USA). Approximately 50 mg of skeletal muscle was minced and homogenized in CER-I buffer containing protease inhibitor cocktail Complete, EDTA free (Roche Applied Sciences, Mannheim, Germany). After a series of wash steps, nuclear proteins were extracted in high salt NER buffer supplemented with protease-inhibitors. The cytosolic fraction was spun at 100,000 x g at 4°C for 60 min to obtain pure cytosolic fraction.

Cytochrome c Oxidase (COX) Enzyme Activity. Mitochondrial extracts from skeletal muscle were added to a test solution containing fully reduced cytochrome c. Enzyme activity was determined as the maximal rate of oxidation of fully reduced cytochrome c measured by the change in absorbance at 550 nm in a Synergy HT microplate reader at 30°C. Full protocol is previously described elsewhere (12).

Protein Release Assay. Isolated SS and IMF mitochondrial fractions (150 μ g) were incubated in resuspension medium for 60 min at 30°C as described previously (3). Reaction mixtures were subsequently centrifuged at 14,000 g (4°C) to pellet mitochondria, and the supernate was analyzed for cytochrome *c* and AIF release from the mitochondria by Western blot analysis.

Immunoblotting. Whole muscle and isolated subfractions including mitochondrial, nuclear, and cytosolic protein extracts were separated on a 10% - 15% sodium dodecyl sulfate polyacrylamide gel through electrophoresis (SDS-PAGE) at 120V for ~90 minutes. Proteins were then transferred onto a nitrocellulose membrane. The membrane was stained with Ponceau Red, cut at the appropriate molecular weights, and blocked in 5% skim milk for one hour to prevent non-specific binding. The membrane strips were immunoblotted overnight at 4°C with a primary antibody, as detailed in Table 1. Membranes were washed three times (5 min each) with tris-buffered-saline-tween-20 (TBST) solution containing 25 mM Tris-HCL (pH=7.5), 1 mM NaCl and 0.1% Tween 20. Membranes were incubated with the appropriate secondary antibody coupled to horseradish peroxidase at room temperature for one hour. Loading controls were utilized for specific extracts. GAPDH was utilized for whole muscle extracts, VDAC for mitochondrial subfractions, and histone 2B and α -tubulin were utilized for nuclear and cytosolic fractions, respectively. Following incubation, membranes were washed three times again in TBST, developed using an enhanced chemiluminescence (ECL) kit and Imager technology, and quantified via densitometric analysis based on signal intensity using the Sigma Scan Pro Version 5 software (Jandel Scientific, San Rafael, CA).

Table 1. List of primary and secondary antibodies for immunoblotting.

Antibody	Product Number	Company
Upstream Regulators of p53		
Mdm2	n/a	Provided by Dr. Olivier Birot
CHCHD4	Sc-98628	Santa Cruz Biotechnology
Phospho-p53 (ser15)	9284S	Cell Signaling
Total-p53	PAB 421	Provided by Dr. Samuel Benchimol
Autophagy Markers		
LC3 A/B	4108 S	Cell Signaling
p62	Ab56416	Abcam
Parkin	4211 S	Cell Signaling
Beclin 1	3738 S	Cell Signaling
Antioxidant Markers		
KEAP1	10503-2-AP	Proteintech
Nrf2	Sc-722	Santa Cruz Biotechnology
Mitochondrial Biogenesis Markers		
PGC-1 α	ab3242	EMD Millipore
Tfam	n/a	Antibody made in house
COX IV	ab14744	Abcam
Cellular Senescent and Apoptosis Markers		
p21	Sc-397	Santa Cruz Biotechnology
Bcl-2	Sc-7382	Santa Cruz Biotechnology
Bax	Sc-493	Santa Cruz Biotechnology
Cytochrome C	556433	BD Pharmingen
Loading Controls		
GAPDH	Ab8245	Abcam
α -Tubulin	CP06-100ug	Calbiochem
VDAC	ab14734	Abcam
H2B	2934 S	Cell Signaling

RNA Isolation. Total RNA was isolated from approximately 70 - 80mg of frozen powdered muscle tissue according to the manufacturer's instructions. Briefly, tissue was added to TRIzol[®] reagent, homogenized, and mixed with chloroform. Samples were centrifuged at 4°C at 16,000g for 15 min and the aqueous supernate was transferred to a new tube with the addition of isopropanol and left overnight at -20°C to precipitate. Samples were again centrifuged at 16,000 g for 10 min and the resultant supernate was discarded. The pellet was resuspended in 10-20 µl of sterile H₂O. RNA concentration and quality were measured using the Nanodrop 2000 (Thermo Scientific, Wilmington, DE, USA). SuperScript[®] III reverse transcriptase (Invitrogen, Carlsbad, CA, USA) was used to reverse transcribe 1.5 µg of total RNA into cDNA.

mRNA Expression Analyses. The mRNA expression of *SCO2*, *TIGAR*, *Mdm2*, *p62*, *LC3*, *p52*, *p21*, *Bax*, *PGC-1α*, and *Tfam* were quantified using the 7500 Real-Time PCR system (Applied Biosystems Inc., Foster City, CA, USA) and SYBR[®] Green chemistry (PerfeC₁a SYBR[®] Green Supermix, ROX, Quanta BioSciences, Gaithersburg, MD, USA). First-strand cDNA synthesis from 2µg of total RNA was performed with primers using Superscript III transcriptase (Invitrogen) according to the manufacturer's directions. Forward and reverse primers (Table 2) for the aforementioned genes were designed based on sequences available in GenBank (<http://www.ncbi.nlm.nih.gov/entrez/query.fcgi>) using the MIT Primer 3 designer software (http://wi.mit.edu/cgi-bin/primer3/primer3_www.cgi), and were confirmed for specificity using the basic local alignment search tool (www.ncbi.nlm.nih.gov/BLAST/). *B2M* and *GAPDH* were used as housekeeping genes, the expression of which did not change between conditions, genotype and rodent model. Each well within a 96-well plate contained: SYBR[®] Green SuperMix, forward and reverse primers (20 µM), sterile H₂O and 10 ng of cDNA, for a final reaction volume of 25 µl. All samples were run in duplicate simultaneously with negative

controls that contained no cDNA. The PCR program consisted of an initial holding stage (95°C for 10 min), an amplification phase (40 cycles at 60°C for 1 min, 95°C for 15 sec), and melting stage (95°C for 15 sec, 60°C for 1 min, 95°C for 25 sec). Melting point dissociation curves generated by the instrument were used to confirm the specificity of the amplified product. Primer efficiency curves were generated for each set to ensure $100 \pm 2\%$ efficiency. For quantification, the threshold cycle (CT) number of endogenous reference genes was subtracted from the CT number of the target gene [$\Delta\text{CT} = \text{CT}(\text{target}) - \text{CT}(\text{reference})$]. The ΔCT value of the control tissue was subtracted from the ΔCT value of the experimental tissue [$\Delta\Delta\text{CT} = \Delta\text{CT}(\text{experimental}) - \Delta\text{CT}(\text{control})$]. Results were reported as fold-changes using the $\Delta\Delta\text{CT}$, calculated as $2^{-\Delta\Delta\text{CT}}$.

Statistical Analysis. Data were analyzed using the Graph Pad Prism 7.0 software and values are reported as means \pm SEM. All data was analyzed using a two-way ANOVA and Bonferroni post-tests unless otherwise indicated. Significance levels were set at $p \leq 0.05$.

Table 2. List of primer oligonucleotide sequences used in real-time qPCR analysis for *Mus Musculus*.

Gene	Forward Primer (5' → 3')	Reverse Primer (5' → 3')
<i>PGC-1a</i>	TTCCACCAAGAGCAAGTAT	CGCTGTCCCATGAGGTATT
<i>Tfam</i>	GAAGGGAATGGGAAAGGTAGA	AACAGGACATGGAAAGCAGAT
<i>p53</i>	CCGACCTATCCTTACCATCATC	TTCTTCTGTACGGCGGTCTC
<i>Mdm2</i>	TCAGACAGGAGAAAGCGATACA	CACGAAGGGTCCAGCATCTT
<i>SCO2</i>	TCCCTTCACCCTTCGCTGAAC	CAGTAGCATCGTGGACCTGAA
<i>TIGAR</i>	CATTCAAGGACAAGGCGTAGAT	TGGAGAAGGCGTGGGTAAA
<i>p21</i>	CACCACCAAGCCATTCCATA	ACTGCCAATCACCACACTAT
<i>p62</i>	TGTGGTGGGAACCTCGCTATAA	CAGCGGCTATGAGAGAAGCTA
<i>LC3</i>	GCTTGCAGCTCAATGCTAAC	CCTGCGAGGCATAAACCATGT
<i>GAPDH</i>	AACACTGAGCATCTCCCTCA	GTGGGTGCAGCGAACTTTAT
<i>b2 microglobulin</i>	GGTCTTTCTGGTGCTTGTCT	TATGTTCCGGCTTCCCATTCT

PGC-1 α , peroxisome proliferator-activated receptor- γ coactivator-1 α ; Tfam, mitochondrial transcription factor; Mdm2, Mouse double minute 2 homolog; SCO2, synthesis of cytochrome-c oxidase 2; TIGAR, TP53-inducible glycolysis and apoptosis regulator; LC3, light chain 3; GAPDH, Glyceraldehyde 3-phosphate dehydrogenase; *b2 microglobulin*, *beta-2 microglobulin*.

Results

Exercise-induced p53 localization to the nucleus is reduced with training and increases to the mitochondria. p53 protein expression in whole muscle, nuclear and cytosolic fractions, as well as mitochondrial subfractions was examined following the final acute exercise test in both trained and untrained WT mice. Total p53 protein was reduced by 2.6-fold with exercise training (Fig. 2A, B). However, the proportion of activated p53, measured by p53-Ser¹⁵ phosphorylation, was increased by 2.5-fold following exercise in the trained state (Fig. 2A, C).

p53 was largely localized to the cytosolic fraction in both trained and untrained muscle (Fig. 2D, E). However, the distribution of phosphorylated p53 (Ser¹⁵) differed. In untrained muscle p-p53 was largely (70%) nuclear-localized, whereas trained muscle exhibited only 40% of p-p53 in the nucleus (Fig. 2D, F). Exercise training also reduced total p53 levels within SS and IMF mitochondria by 2.1-2.6-fold. However, activated p53 localization increased in both IMF and SS mitochondrial subfractions by ~2.3-fold following acute exercise in trained muscle (Fig. 2, G-K).

Confirmation of muscle specific mouse model. The muscle-specific genotype was confirmed through the Cre recombinase transcript (Fig. 3A). When the Cre recombinase gene is expressed, it targets the LoxP restriction sites at exons 2 and 10 of the p53 transcript, allowing for targeted excision and deletion of p53 solely within skeletal muscle to create the mKO model. In agreement with previous literature (15, 43), this abolished p53 protein expression (Fig. 3B).

Exercise training induces a leaner phenotype and increases cardiac hypertrophy regardless of genotype. The phenotypic characteristics of the p53 WT and mKO mice are described in Table 3. No difference in baseline parameters including body mass or exercise capacity were observed

Fig. 2

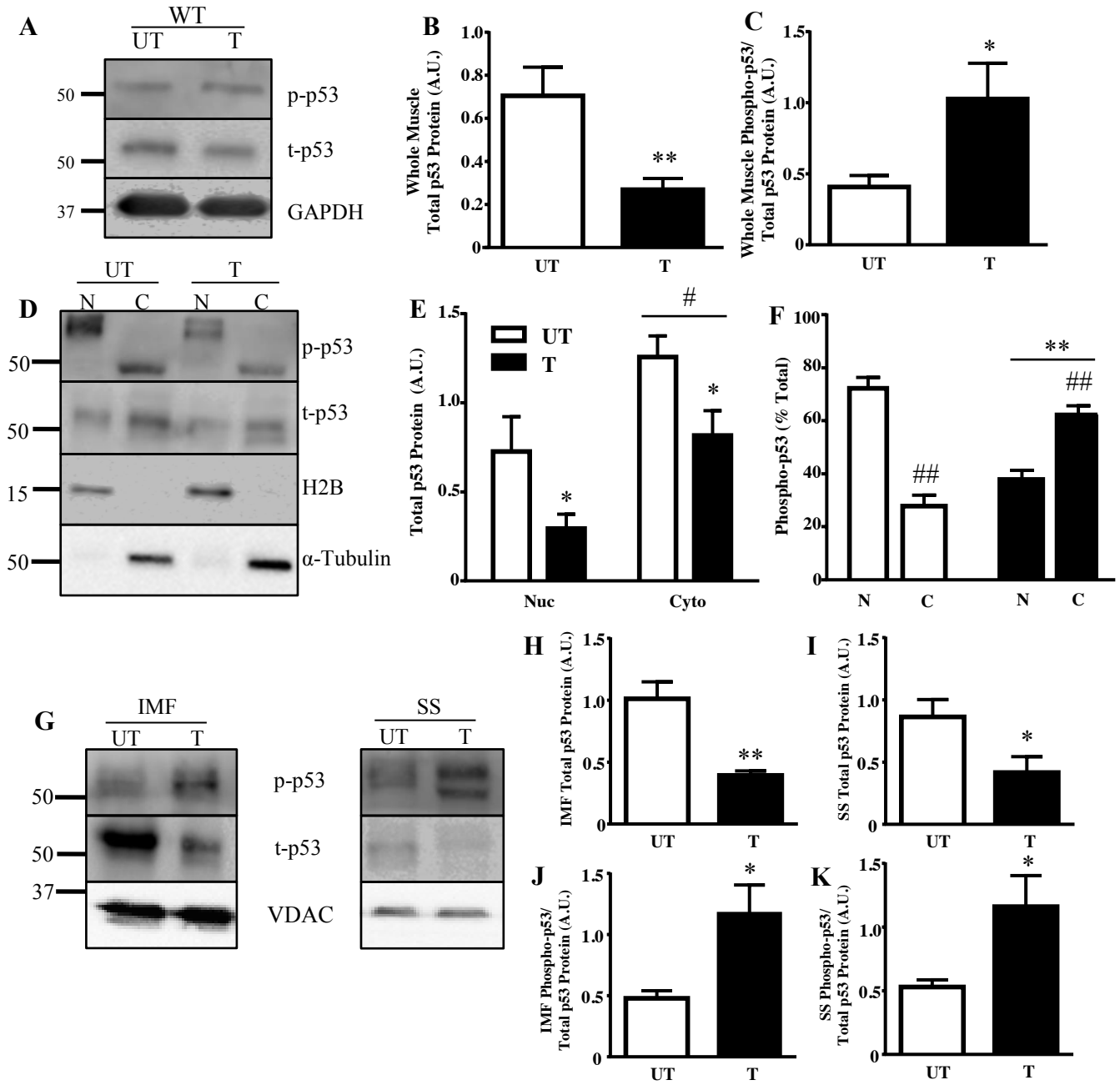


Figure 2. p53 subcellular localization with training. **A)** Whole muscle **B)** total p53 protein and **C)** phosphorylated p53-Ser¹⁵ protein was measured in WT mice. GAPDH was utilized as the loading control for all immunoblotting in whole muscle (n=6-7/group); *p<0.05, **p<0.01, UT vs. T, Student's t-test. **D)** p53 protein was measured in nuclear and cytosolic fractions in WT mice. H2B was used as a nuclear loading control and α -tubulin was used as a cytosolic loading control. Basally and with training, nuclear and cytosolic **E)** total p53 protein, and **F)** percent total of phosphorylated p53-Ser¹⁵ protein was measured (n=4-5/group); *p<0.05, UT vs. T; #p<0.05, Nuclear vs. Cytosolic (n=4-5/group), Student's t-test, 2-way ANOVA. A main effect of training was observed. **G)** Mitochondrial p53 protein was examined in SS and IMF mitochondrial subfractions. VDAC was utilized as a mitochondrial loading control. Total p53 protein in **H)** IMF, and **I)** SS mitochondria was measured (n=4-5/group); *p<0.05, **p<0.01, UT vs. T, Student's t-test. Activated p53, corrected for total, was additionally measured in **J)** IMF, and **K)** SS mitochondria (n=4-5/group); *p<0.05, UT vs. T, Student's t-test. Data are presented as mean \pm SEM.

between genotypes (Table 3A). Training induced a leaner phenotype in both WT and mKO mice compared to their untrained counterparts, exemplified by 28% and 56% reduction in epididymal fat mass in WT and mKO mice, respectively (Table 3B). No effect of training was observed on quadriceps or gastrocnemius skeletal muscle mass (Table 3B). Cardiac hypertrophy (7-21%), a typical consequence of training, was also evident (Table 3B).

p53 is not required for exercise capacity adaptations to a long term training program. A post-training exercise performance test was employed to examine whether p53 is required for whole body performance improvements with training. Both WT and mKO trained mice significantly improved their exercise capacity by ~2.3-fold relative to untrained mice (Fig. 3C). Blood lactate levels were markedly elevated (>10 mM) in all WT and mKO animals following the exercise test, with a 12-27% reduction observed in the trained animals, an expected adaptation to training (Fig. 3D). There was no difference in final lactate production levels between genotypes under basal conditions.

p53 is required to maintain basal mitochondrial content and function, but not for exercise training-induced adaptations. Untrained mKO mice exhibited a 17% reduction in mitochondrial content, as measured by COX activity, compared to the untrained WT mice (Fig. 3E). In addition, PGC-1 α protein was reduced by 36%, accompanied by a 28% reduction in Tfam levels (Fig. 3, F-H). In response to training, both WT and mKO mice increased their mitochondrial content by 1.3- and 1.7-fold respectively, relative to untrained counterparts (Fig. 3E). SS and IMF mitochondrial yield increased with training by ~31% and ~22% respectively, with no reduction observed in the mKO mice under basal conditions (Table 3C). The respiratory control ratio measured in mitochondrial subfractions was not significantly affected by training (Table 3C). Training increased PGC-1 α protein levels by 1.8-2.6-fold, regardless of genotype ($p < 0.05$;

Fig. 3*F, G*). Tfam protein levels also increased in the mKO mice with training by 2.1-fold, while only a modest increase was observed in the WT mice (Fig. 3*F, H*). Therefore mitochondrial biogenesis markers increase with exercise training, even in the absence of p53.

Mitochondrial function was assessed by measuring respiration and reactive oxygen species production (ROS) in both SS and IMF subfractions. No baseline differences in SS or IMF state 4 mitochondrial respiration were observed in the absence of p53 (Fig. 4*A, B*). However, state 3 respiration in SS mitochondria was 2-fold higher in the mKO mice, but was 22% lower in the IMF subfraction, indicating a differential dependency on p53 (Fig. 4*C, D*). With exercise training, state 4 respiration increased similarly in both genotypes, by ~2.2-fold in SS mitochondria and by 1.4-1.7-fold in IMF mitochondria ($p < 0.05$; Fig. 4*A, B*). State 3 respiration in SS mitochondria improved by 4.8-fold in the WT mice with training, but only increased by 1.7-fold in the mKO mice (Fig. 4*C*). IMF state 3 respiration did not improve in the WT mice with training, but training did attenuate the deficit observed in the mKO mice, such that state 3 respiration was similar to control values (Fig. 4*D*). Therefore, SS mitochondria appear to adapt more readily to training stimuli compared to the IMF mitochondria, with only a minor dependency on p53.

In the absence of p53, state 3 and 4 ROS levels were elevated under basal conditions in both the SS and IMF subfractions (Fig. 5*A, B, D*). Exercise training attenuated state 3 and 4 SS ROS levels by 23-58% in WT mice and normalized ROS production in both SS and IMF subfractions under state 3 and state 4 conditions in mKO mice ($p < 0.05$; Fig. 5, *A-D*). Thus, although the absence of p53 led to increase ROS levels under basal conditions, p53 is not required for the adaptive decreases in mitochondrial ROS production with training.

Fig. 3

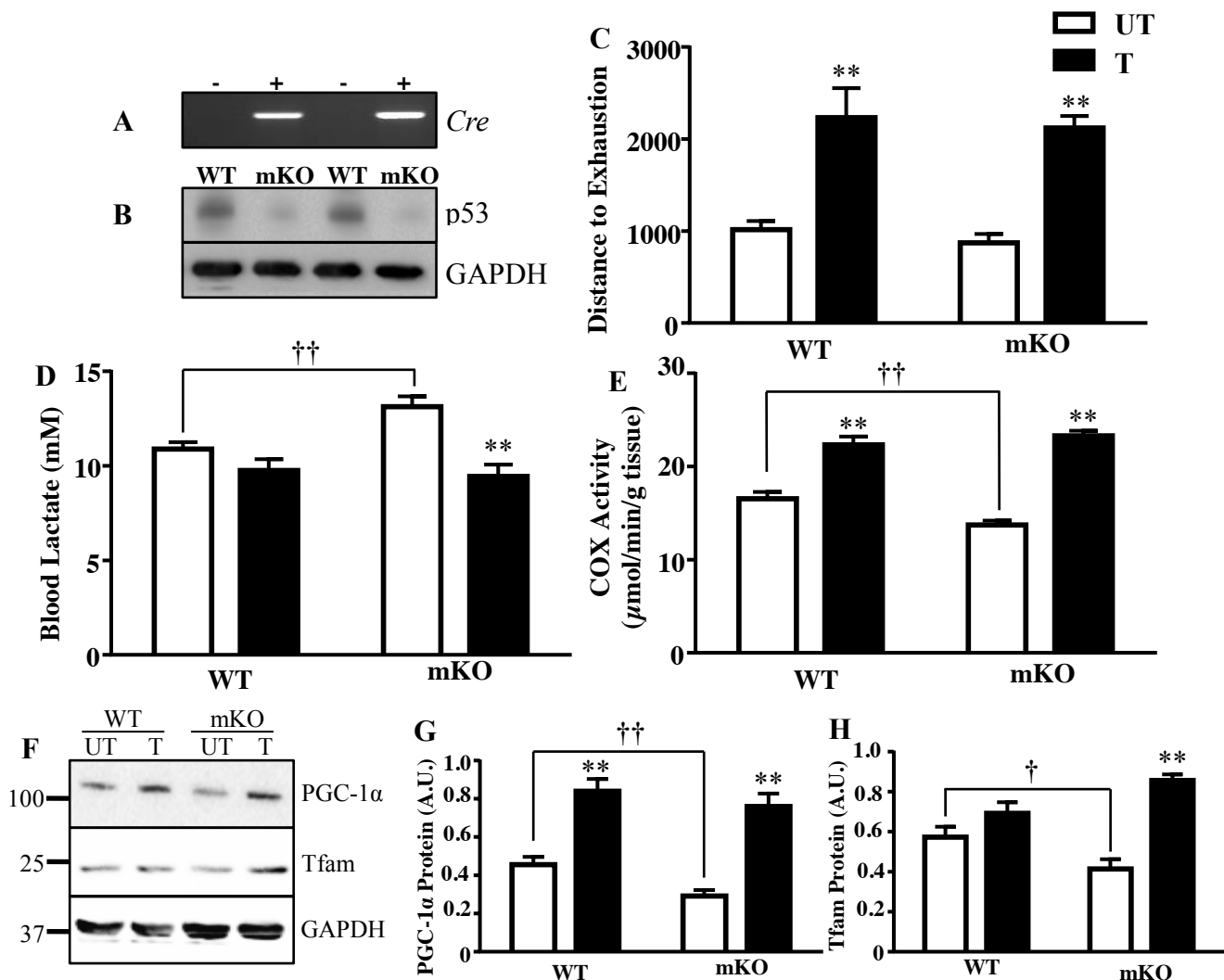


Figure 3. Mitochondrial content, exercise capacity, and lactate handling improves with exercise training. The deletion of p53 in skeletal muscle of MS mKO mice was examined through **A**) genotype against the Cre transcript, and **B**) total p53 protein in whole muscle. Following the 6-week training/sedentary protocol, mice were subjected to an exhaustive bout of exercise to determine training-induced adaptations by measuring **C**) distance to exhaustion (n=6-8/group); **p<0.01, UT vs. T, 2-way ANOVA, and **D**) final lactate production levels (n=6-17/group), **p<0.01, UT vs. T, Student's t-test. Mitochondrial biogenesis with training was measured through assessment of **E**) COX enzyme activity, a marker of mitochondrial content (n=6-8/group); **p<0.01, UT vs. T, 2-way ANOVA; ††p<0.01, UT WT vs. mKO, Student's t-test, and **F**) mitochondrial biogenesis markers **G**) PGC-1α protein (n=5-8/group); **p<0.01, UT vs. T, 2-way ANOVA; ††p<0.01, UT WT vs. mKO, Student's t-test, and **H**) Tfam protein (n=6-7/group); **p<0.01, UT vs. T, 2-way ANOVA; †p<0.05, UT WT vs. mKO, Student's t-test. Data are presented as mean ± SEM.

Table 1. Phenotypic alterations and exercise capacity under basal and exercise training conditions.

A. Pre-Training	WT		mKO	
<i>Initial Body wt, g</i>	30.4 ± 0.4		31.4 ± 1.0	
<i>Distance to Exhaustion (m)</i>	1,286 ± 51		1,156 ± 85	
B. Post-Training	WT		mKO	
	UT	T	UT	T
<i>Final Body wt, g</i>	33.2 ± 1.1	30.1 ± 0.3 *	34.8 ± 1.7	27.8 ± 0.4*
<i>TA wt/ body wt (mg/g)</i>	2.0 ± 0.08	1.6 ± 0.07 *	2.1 ± 0.08	1.8 ± 0.04*
<i>Gastrocnemius wt/ body wt, (mg/g)</i>	6.3 ± 0.3	5.8 ± 0.2	6.3 ± 0.3	6.2 ± 0.1
<i>Quadriceps wt/ body wt (mg/g)</i>	6.2 ± 0.1	6.2 ± 0.1	6.6 ± 0.2	6.6 ± 0.08
<i>Heart wt/body wt, (mg/g)</i>	5.4 ± 0.4	5.8 ± 0.2	4.8 ± 0.2	5.8 ± 0.1*
<i>Epididymal Fat wt/ body wt (mg/g)</i>	43.6 ± 3.3	31.5 ± 3.5 *	54.6 ± 3.4 †	23.9 ± 1.8 *
C. Mitochondrial Parameters				
<i>SS Mitochondrial Yield</i>	0.5 ± 0.07	0.8 ± 0.05 *	0.6 ± 0.09	0.8 ± 0.05 *
<i>IMF Mitochondrial Yield</i>	1.1 ± 0.02	1.3 ± 0.1	1.0 ± 0.1	1.4 ± 0.08*
<i>SS RCR</i>	3.8 ± 0.8	12.9 ± 5.3	4.6 ± 0.6	7.2 ± 1.8
<i>IMF RCR</i>	6.1 ± 0.2	10.1 ± 2.9	7.0 ± 1.1	12.1 ± 4.5

A) Pre-training variables (initial body mass and distance to exhaustion) were compared between genotype in the muscle specific (n=13-23/group). **B)** Phenotypic variables were measured following the training or sedentary program (n=6-10/group); *p≤0.05, UT vs. T; †p≤0.05, WT vs. mKO, 2-way ANOVA and Student's t-test. **C)** Mitochondrial parameters measured in SS and IMF mitochondrial subfractions (n=5-10/group); *p≤0.05, UT vs. T, 2-way ANOVA and Student's t-test. Data are presented as mean ± SEM. Abbreviations: RCR, respiratory control ratio; TA; tibialis anterior; SS, subsarcolemmal; IMF, intermyofibrillar.

Fig. 4

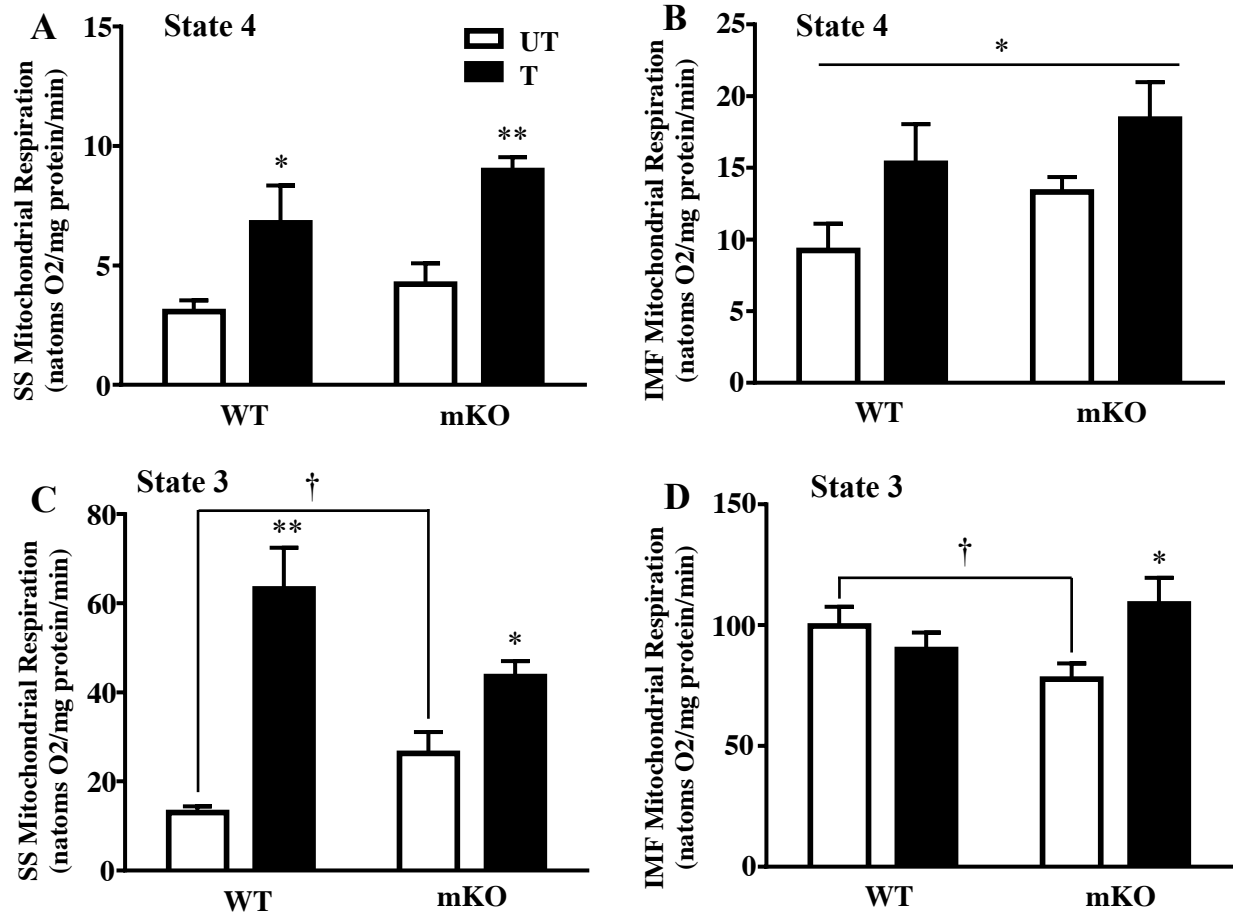


Figure 4. Mitochondrial respiration improves with exercise training. State 4 respiration was measured in **A**) SS (n=6-7/group); *p<0.05, **p<0.01, UT vs. T, Student's t-test and 2-way ANOVA, and **B**) IMF mitochondria (n=6-7/group); *p<0.05, main effect of genotype and training, 2-way ANOVA. State 3 respiration was further measured in **C**) SS (n=6/group);*p<0.05, **p<0.01, UT vs. T, Student's t-test and 2-way ANOVA; †p<0.05, UT WT vs. mKO, Student's t-test, and **D**) IMF mitochondria (n=6-7/group); *p<0.05, UT vs. T, Student's t-test; †p<0.05, UT WT vs. mKO, Student's t-test. Data are presented as mean ± SEM.

Fig. 5

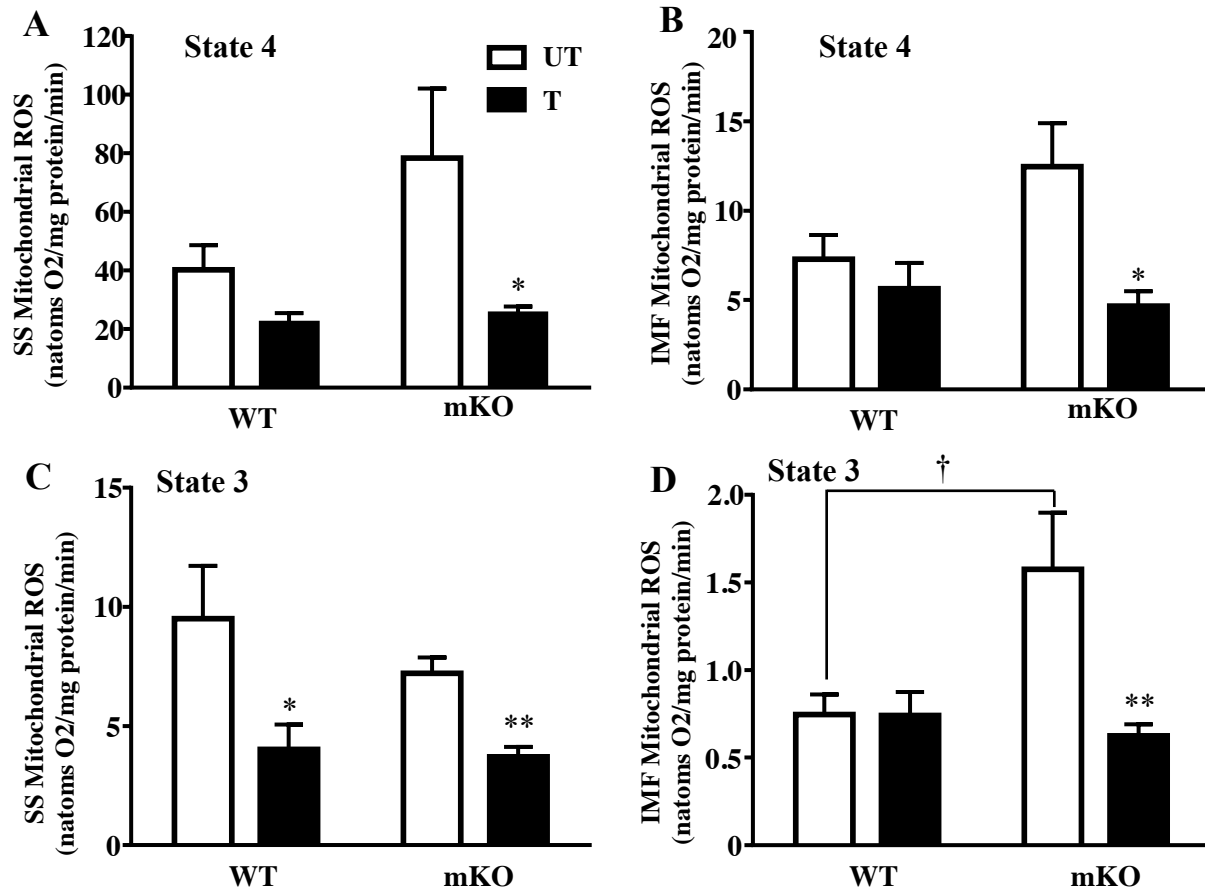


Figure 5. Mitochondrial reactive oxygen species (ROS) is reduced with exercise training.

State 4 ROS levels were measured in **A)** SS, and **B)** IMF mitochondria (n=6-8/group); *p<0.05, UT vs. T, 2-way ANOVA. State 3 ROS levels were measured in **C)** SS, and **D)** IMF mitochondria (n=6-8/group); *p<0.05, **p<0.01, UT vs. T, Student's t-test and 2-way ANOVA; †p<0.05, UT WT vs. mKO, 2-way ANOVA. Data are presented as mean \pm SEM.

Transcripts of genes related to downstream p53 signaling targets alter with exercise training.

The mRNA transcripts of numerous signaling pathways regulated by p53 were examined. Training downregulated *p53* (1.4-fold), *p21* (~1.4-fold), and *Bax* (1.2-fold) transcripts ($p < 0.05$; Fig. 6A). *TIGAR*, *Mdm2*, *Tfam*, *LC3*, *p62*, *SCO2*, and *PGC-1 α* mRNA transcripts were not significantly altered with training in WT mice. In the absence of p53 under basal conditions, there was a 1.2-1.6-fold reduction in the transcripts of genes involved in mitochondrial biogenesis (*Tfam*), autophagy (*LC3*, *p62*), and cell cycle arrest/cell death (*p21*, *Bax*) signaling pathways ($p < 0.05$; Fig. 6B). In contrast, *TIGAR* and *SCO2* mRNA levels increased in the absence of p53. The effect of training was evaluated to determine if exercise could reverse the gene expression pattern defined by the absence of p53. With training, the decrease in *PGC-1 α* mRNA was reversed, exhibiting a ~1.3-fold increase above WT untrained levels. The decrease in *Bax* mRNA and the increase in *SCO2* were further amplified with training ($p < 0.05$) while the reductions in *p21*, *Tfam*, and *LC3* transcripts were normalized. Thus, these training-induced alterations are not dependent on the presence of p53. Changes in the transcripts of *TIGAR* and *p62*, brought about by p53 deficiency, did not respond to training, indicating a strong dependence on p53 for basal expression. *Mdm2* expression was not significantly affected by either training, or the absence of p53, at the transcript level.

Targeted regulation of p53 protein. The effect of training was examined on proteins that determine p53 steady state levels (*Mdm2*) and mitochondrial localization (*CHCHD4*). *Mdm2* levels were unaffected by the absence of p53, and were increased by 1.7-2.1-fold with training (Fig. 7A). *CHCHD4* protein was reduced by 52% in the absence of p53 under basal conditions ($p < 0.05$; Fig. 7B). Training induced modest (1.5-fold) and large (4.6-fold) increases in *CHCHD4* expression in the WT and mKO mice, respectively.

Fig. 6

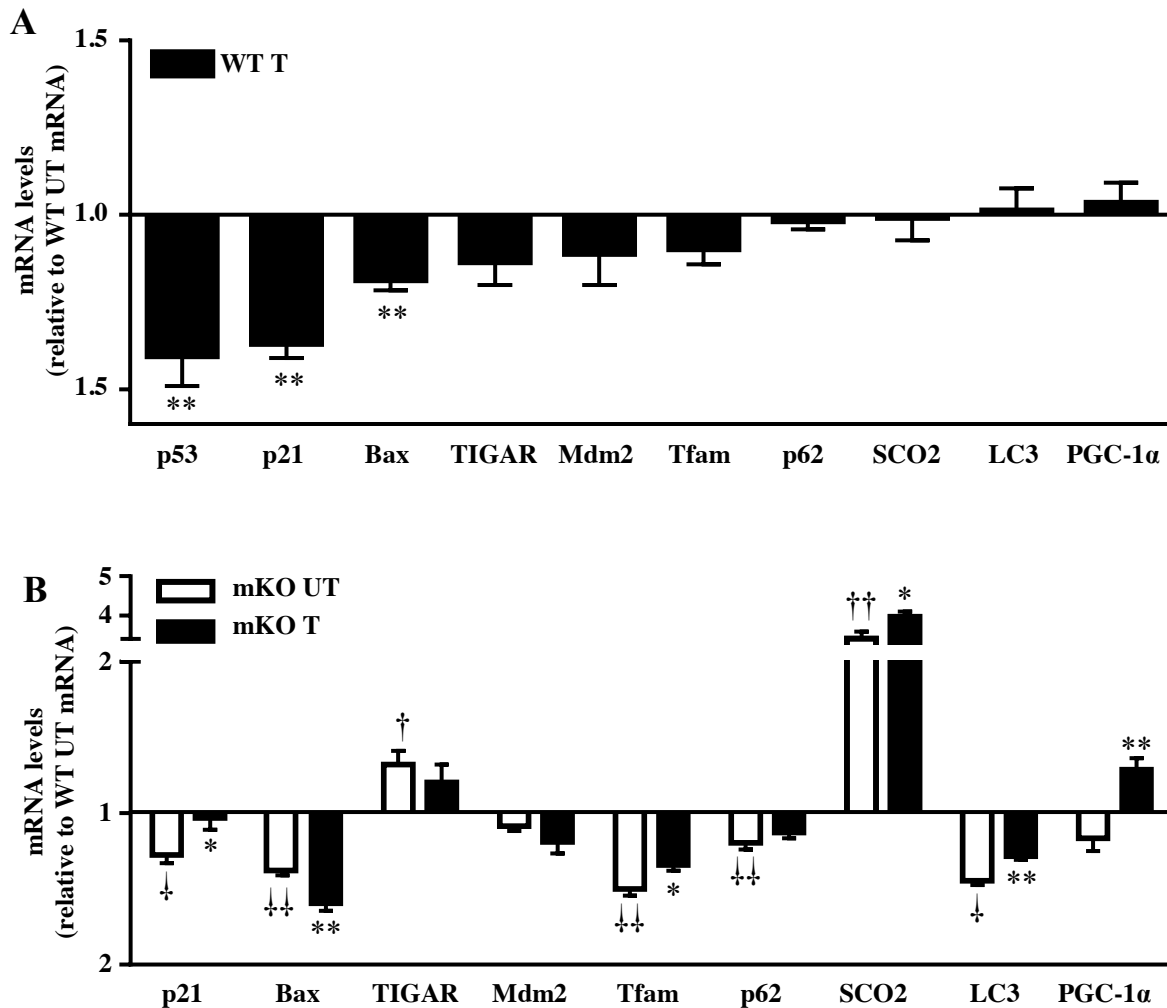


Figure 6. mRNA expression of downstream p53-regulated targets and the effect of training. **A)** The effect of training on mRNA transcripts of signaling pathways including cellular senescence (*p21*), apoptosis (*Bax*), metabolism (*TIGAR*), autophagy (*p62*, *LC3*), oxidative phosphorylation (*SCO2*), mitochondrial biogenesis (*PGC-1 α* , *Tfam*) and *p53* and its negative regulator *Mdm2*, in WT mice. Data are presented as fold change over WT control levels (n=8-10/group); *p<0.05, UT vs. T, Student's t-test. **B)** Effect of the absence of p53, and training on mRNA transcripts of signaling pathways. Data presented as fold change of mKO over WT untrained levels and as mKO trained over untrained levels (n=7-11/group); *p<0.05, mKO UT vs. T, Student's t-test; †p<0.05, UT WT vs. mKO, Student's t-test. Data are presented as mean \pm SEM.

Differential apoptotic release occurs in mitochondrial subfractions however, training reduces intrinsic mitochondrial apoptosis. To assess mitochondrial apoptotic susceptibility, we measured cytochrome c protein release from isolated organelles in the presence (H_2O_2) and absence (basal) of apoptotic stimuli. Under basal conditions, cytochrome c release from SS mitochondria was increased by 45% in the absence of p53, but was reduced by 44% in the IMF subfraction compared to WT counterparts (Fig. 8A, B). Training attenuated the elevated cytochrome c release rate in the SS subfraction of mKO mice to reach WT levels ($p < 0.05$; Fig. 8A). An attenuation of cytochrome c release from SS mitochondria by 42-60% in the WT and mKO mice was also observed in the presence of H_2O_2 (Fig. 8C). There was no effect of training or genotype on H_2O_2 -induced cytochrome c release in the IMF subfraction (Fig. 8D). Therefore, p53 and exercise training result in differential apoptotic adaptations, dependent on the mitochondrial subfraction.

To relate patterns of cytochrome c release to upstream activators, we measured p21, Bax, and Bcl-2 protein in whole muscle lysates. In the absence of p53, Bax protein levels increased by 2.3-fold, whereas Bcl-2 and p21 protein expression was reduced by 49% and 32%, respectively (Fig. 8, E-H). Training reduced Bax protein by 43% in the mKO mice, to values reaching WT control levels (Fig. 8F). Bcl-2 protein was reduced in both WT and mKO genotypes by ~34% with training (Fig. 8G). Though p21 expression was unaffected by training in WT mice, training induced a significant augmentation in p21 levels in the mKO mice by 2.1-fold (Fig. 8H). Therefore, p53 plays a role in regulating apoptotic protein signaling under basal conditions, but it does not appear to be required for the anti-apoptotic adaptations induced by exercise training.

Fig. 7

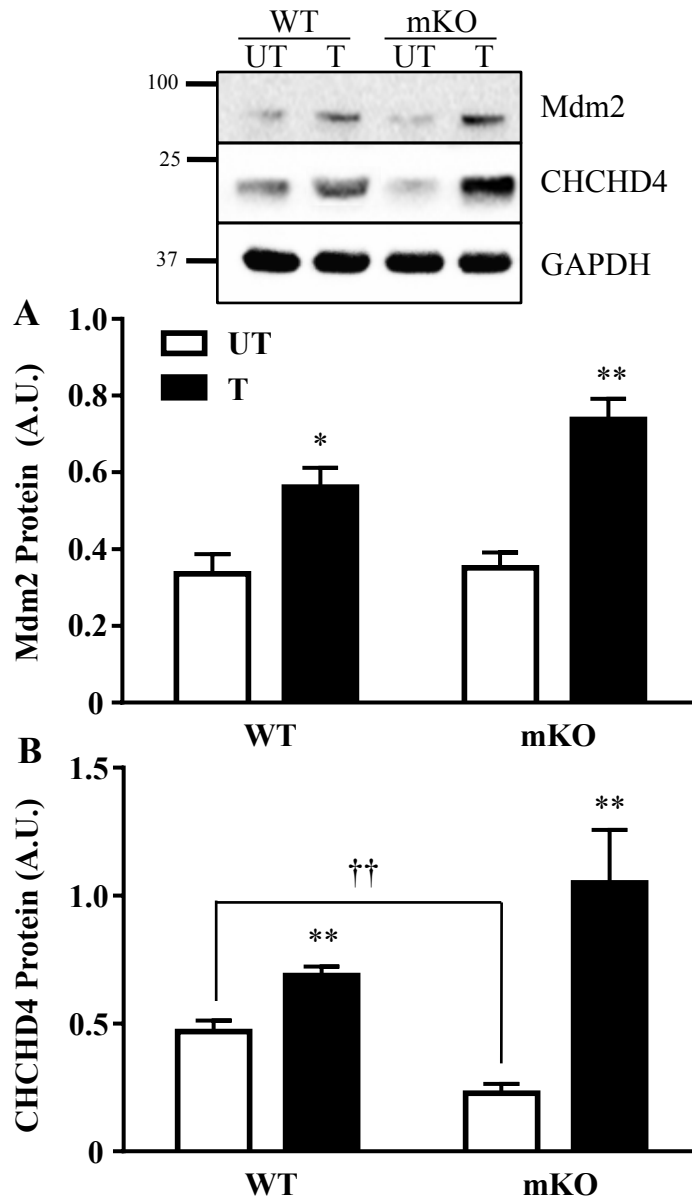


Figure 7. Regulators of p53 expression (Mdm2) and its mitochondrial localization (CHCHD4). Whole muscle protein expression of **A) Mdm2** (n=5-6/group); *p<0.05, **p<0.01, UT vs. T, 2-way ANOVA, and **B) CHCHD4** (n=5-6/group); **p<0.01, UT vs. T, Student's t-test and 2-way ANOVA; ††p<0.01, UT WT vs. mKO, Student's t-test, was measured. Data are presented as mean \pm SEM.

Exercise training increases autophagy signaling. We evaluated the potential role of p53 in mediating autophagy signaling through the examination of LC3, p62, Parkin and Beclin-1 proteins. In the absence of p53 under basal conditions, the autophagy protein markers p62, Parkin, and Beclin-1 were upregulated by 2.4-3-fold (Fig. 9, *B-D*). LC3-I and LC3-II levels were unaffected (Fig. 9A). Training induced relatively similar 1.7-2.2-fold increases in all of these autophagy proteins in WT mice. This increase was attenuated for LC3-II, and reversed for p62, Parkin, and Beclin-1 in the absence of p53, suggesting that training can normalize the aberrant expression of these proteins in p53 null mice, through a potential substrate clearance mechanism.

Signaling pathways and mitochondrial properties in muscle-specific and whole body p53 deletion models. Since a large number of studies have utilized whole-body (WB) p53 KO animals to examine mitochondrial content and function in (32, 33, 35, 37–39) muscle, we conducted a limited comparison of mitochondrial parameters between WB and mKO p53 knockout models under basal conditions. Mitochondrial content in the mKO and WB p53 KO mice was reduced by 17% and 27% respectively, with no difference in levels between models (Fig. 10A). *PGC-1 α* mRNA was not altered in the mKO mice, however it was reduced by 47% in WB KO mice compared to WT counterparts ($p < 0.05$; Fig. 10B). Furthermore, *PGC-1 α* mRNA and protein in WB WT mice was higher when compared to their muscle-specific counterparts. *PGC-1 α* protein was reduced in the absence of p53 by 36% and 40% in the mKO and WB mice, respectively (Fig. 10C). Differences in state 3 respiration were observed in the absence of p53 in SS mitochondria whereby mKO mice had 2-fold higher respiration, while WB KO mice had a 1.4-fold lower state 3 respiration compared to their WT counterparts (Fig. 10D). State 3 ROS in SS mitochondria was not elevated in the absence of p53 in either model, however the WB mice displayed greater (2.5-4.1-fold) ROS levels overall (Fig. 10E). Basal cytochrome c release

Fig. 8

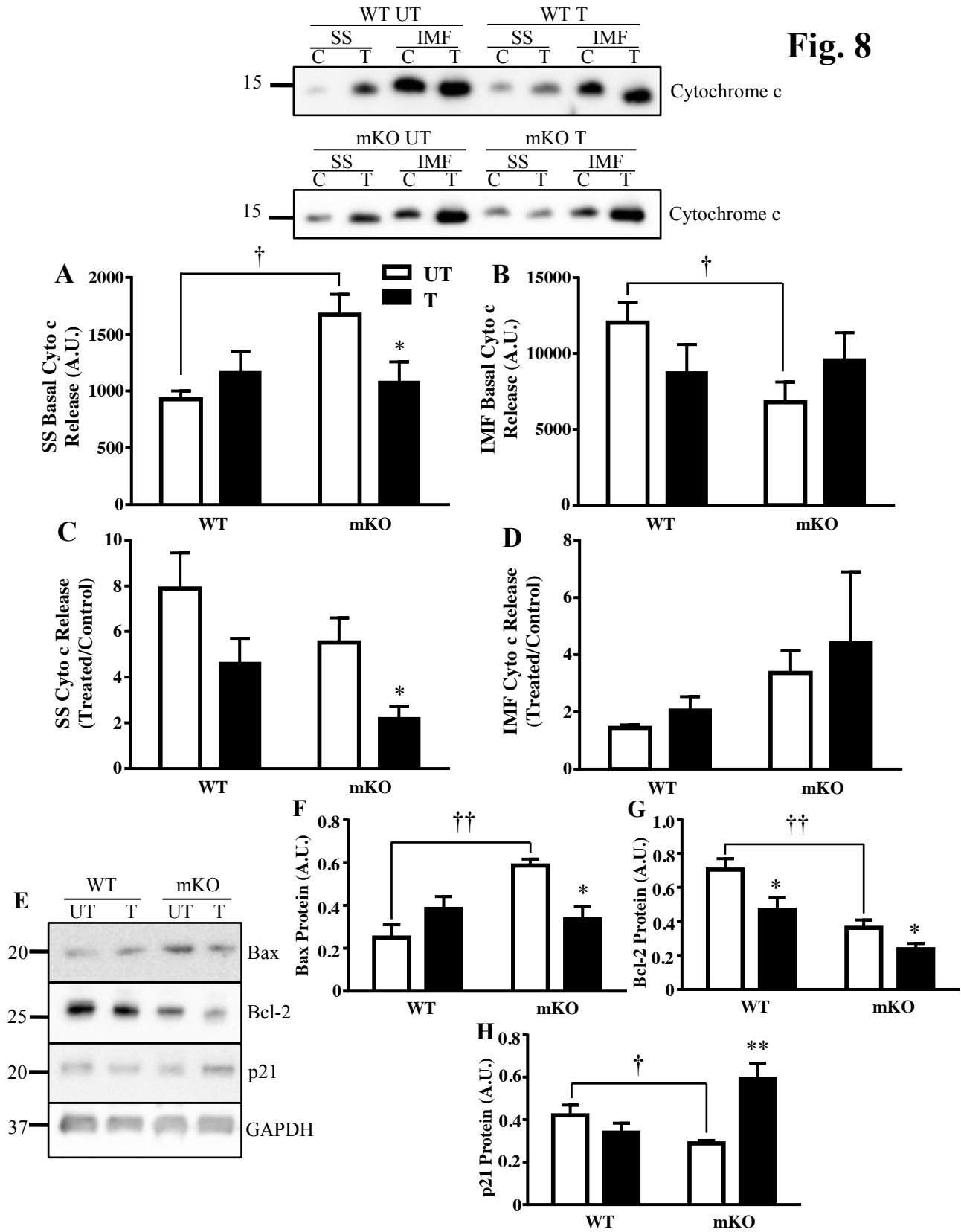


Figure 8. Effect of training and p53 on mitochondrially-mediated apoptosis. In the absence of p53 basally, **A**) greater cytochrome c release is observed in SS mitochondria with training reducing release (n=5-8/group); *p<0.05, UT vs. T, One-way ANOVA; †p<0.05, UT WT vs. mKO, Student's t-test, and **B**) reduced basal release is observed in IMF mitochondria (n=7-14/group); †p<0.05, UT WT vs. mKO, Student's t-test. Under apoptotic stimuli (H₂O₂), cytochrome c release was reduced with training in **C**) SS mitochondria (n=6-10/group); *p<0.05, UT vs. T, One-way ANOVA, and **D**) did not change in IMF mitochondria (n=6-12/group). **E**) Apoptosis, anti-apoptosis, and cellular senescent proteins were measured in whole muscle; **F**) Bax protein (n=4-6/group); *p<0.05; UT vs. T, 2-way ANOVA; ††p<0.01, UT WT vs. mKO, 2-way ANOVA; **G**) Bcl-2 protein (n=5-8/group); *p<0.05, UT vs. T, Student's t-test; ††p<0.01, UT WT vs. mKO, 2-way ANOVA; **H**) p21 cellular senescent protein (n=5-6/group); **p<0.01, UT vs. T, 2-way ANOVA; †p<0.05, UT WT vs. mKO, Student's t-test. Data are presented as mean ± SEM.

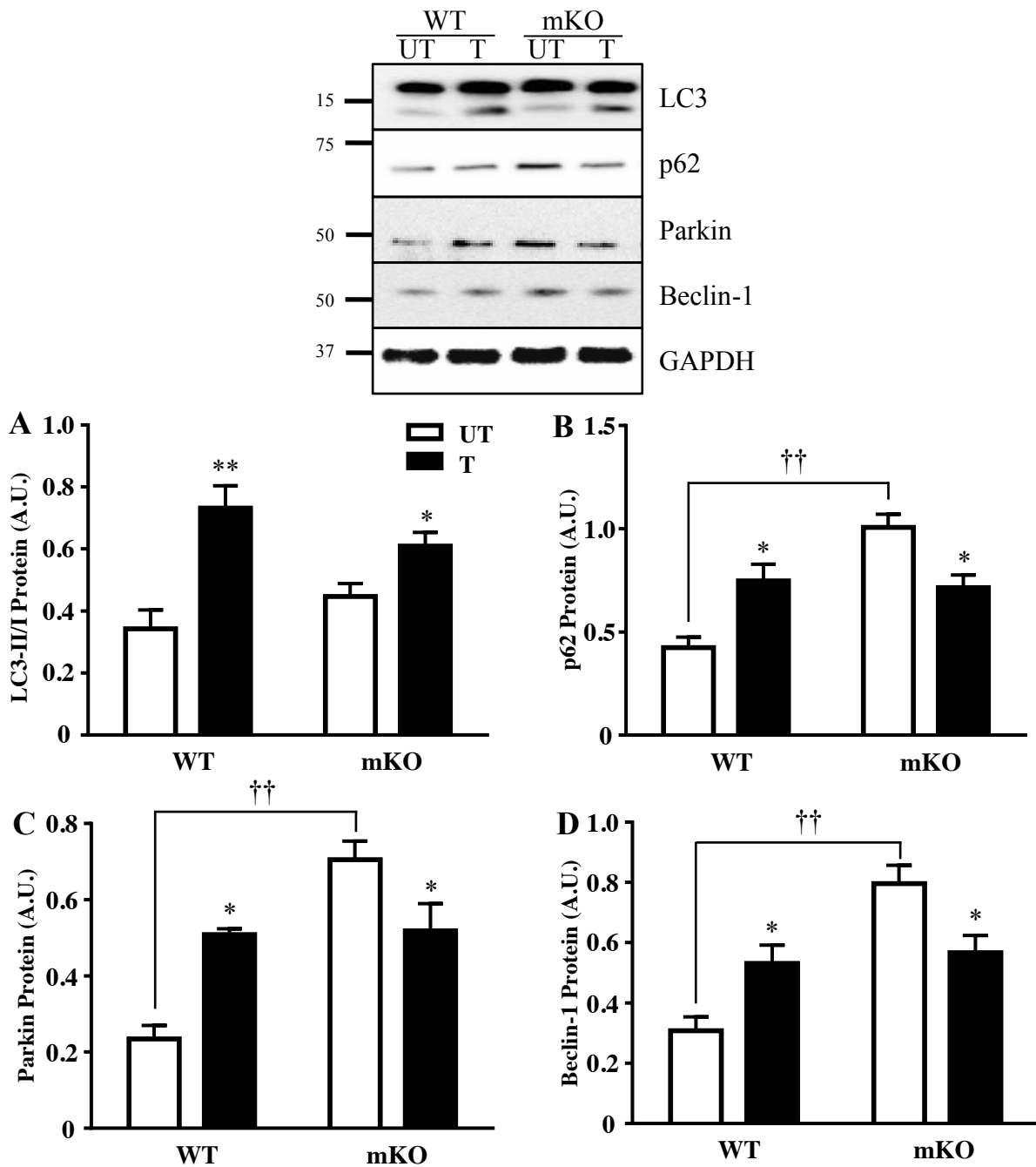
Fig. 9

Figure 9. Autophagic protein responses in the absence of p53 and with training. A) LC3-II/LC3-I ratio (n=6-8/group); * $p < 0.05$, ** $p < 0.01$, UT vs. T, 2-way ANOVA, B) p62 (n=5-8/group), * $p < 0.05$, UT vs. T, 2-way ANOVA; †† $p < 0.01$, UT WT vs. mKO, 2-way ANOVA, C) Parkin (n=5-7/group); * $p < 0.05$, UT vs. T, Student's t-test and 2-way ANOVA; †† $p < 0.01$, UT WT vs. mKO, 2-way ANOVA, and D) Beclin-1 (n=5-7/group); * $p < 0.05$, UT vs. T, Student's t-test; †† $p < 0.01$, UT WT vs. mKO, 2-way ANOVA. Data are presented as mean \pm SEM.

in SS mitochondria was elevated by ~45% in the absence of p53 in both models compared to WT mice (Fig. 10F). Therefore, some differences in gene expression, respiration, and ROS production exist between mouse models in the absence of p53.

The autophagy signaling pathway was measured through the examination of LC3, p62, and Beclin-1 proteins. Though LC3-I remained relatively constant between genotypes, activated LC3-II protein was increased in the WB KO mice, leading to an elevation in the LC3 II/I ratio ($p < 0.05$; Fig. 11A, B). p62 protein was elevated by 2.4- and 1.6-fold in the mKO and WB KO mice (Fig. 11A, C). Beclin-1 protein was increased in the mKO mice by 2.6-fold, but the higher level evident in the WB WT control mice precluded a significant increase in the WB KO animals (Fig. 11A, D).

Understanding the combined effect of genotype, training, and mouse model on exercise capacity adaptations and mitochondrial biogenesis. We sought to understand whether the adaptive response to training would be similar in WB p53 KO and mKO mice. Exercise capacity was significantly improved (~2.5-fold) following the training program in all mice regardless of genotype or model (Fig. 12A). Training increased mitochondrial content by 27-43% in the KO and WT mice, attaining similar levels post-training (Fig. 12B). In the WB mice, training increased mitochondrial content by 43% in the WT mice, and by 36% in the KO mice. In the absence of p53, training elevated PGC-1 α protein levels to a similar extent in both WB p53 KO and mKO mice, thus attenuating the deficit induced by p53. Thus, the absence of p53 does not impact the improvements in performance, mitochondrial content, or expression of PGC-1 α in response to training.

Fig. 10

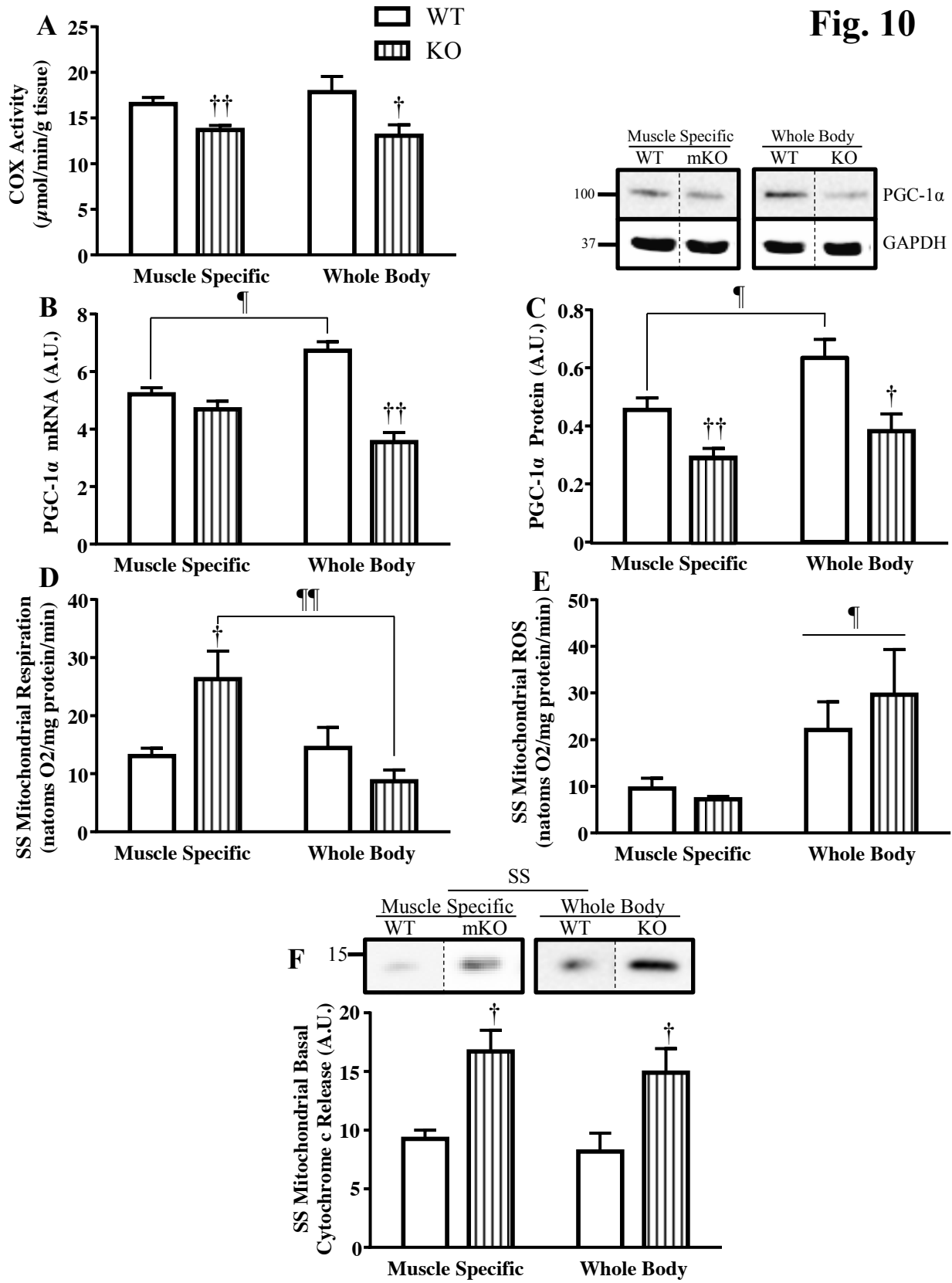


Figure 10. Basal mitochondrial biogenesis and apoptotic signaling comparisons in mouse models. Muscle specific (mKO) and whole body (WB) WT and p53 deletion models were compared under basal conditions. Mitochondrial biogenesis was measured through **A)** COX enzyme activity (n=6-8/group); †p<0.05, ††p<0.01, UT WT vs. KO, Student's t-test and 2-way ANOVA, and whole muscle **B)** *PGC-1 α* mRNA (n=5-10/group); ††p<0.01, UT WT vs. KO, 2-way ANOVA; ¶p<0.05, WT MS vs. WB, 2-way ANOVA, and **C)** PGC-1 α protein (n=5-7/group); †p<0.05, ††p<0.01, UT WT vs. KO, Student's t-test and 2-way ANOVA; ¶p<0.05, WT MS vs. WB, Student's t-test. Immunoblots were retrieved from the same blot but were spliced for direct comparison of untrained animals. SS mitochondrial state 3 **D)** respiration (n=6/group); †p<0.05, UT WT vs. KO, Student's t-test; ¶¶p<0.01, KO MS vs. WB, 2-way ANOVA, and **E)** ROS emission (n=6-7/group); ¶p<0.05, MS vs. WB, Student's t-test and 2-way ANOVA. **F)** Basal cytochrome c release in SS mitochondria (n=5-9/group); †p<0.05, UT WT vs. KO, Student's t-test and 2-way ANOVA. Data are presented as mean \pm SEM.

Fig. 11

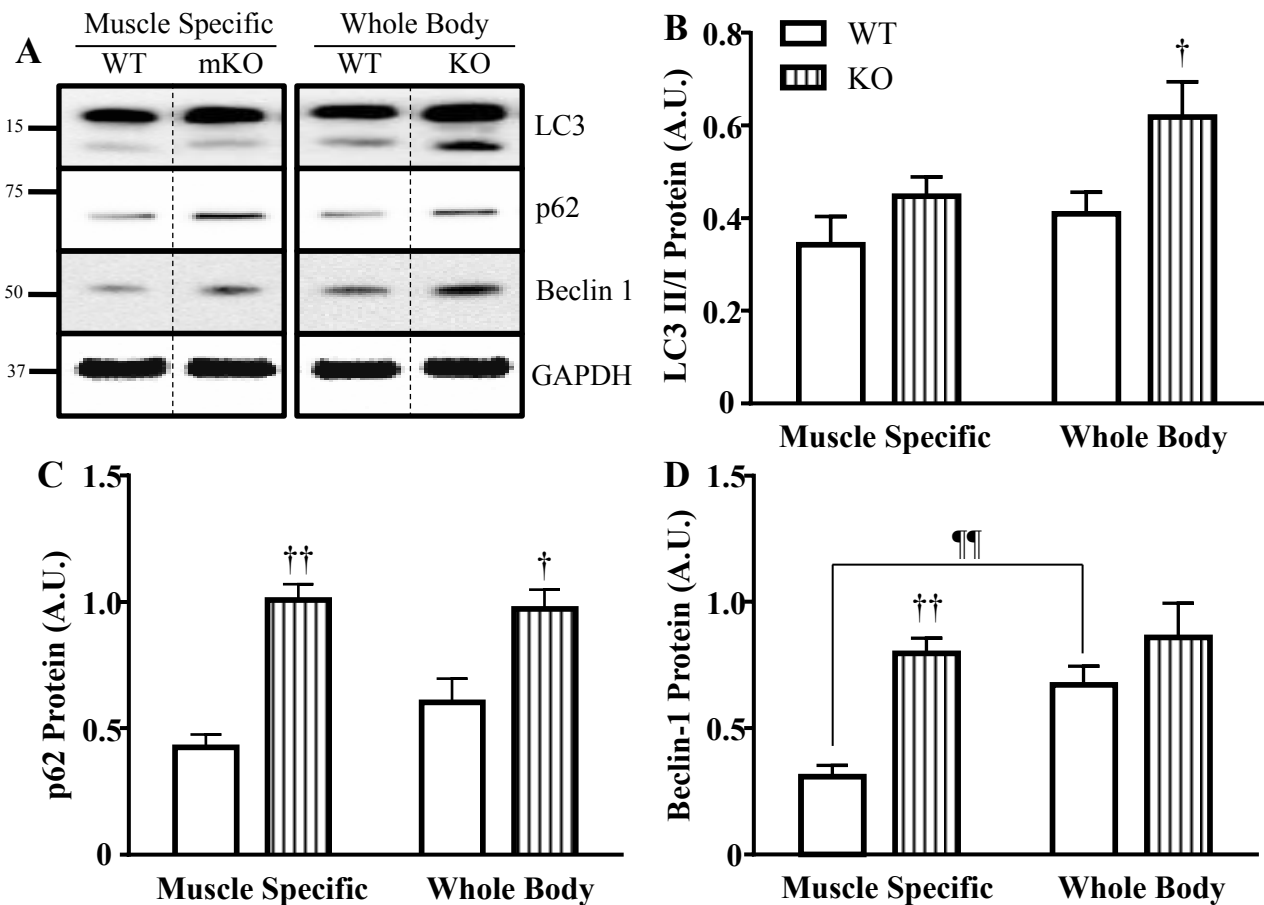


Figure 11. Autophagic signaling occurs similarly between mouse models in the absence of p53. The alterations in the autophagy signaling pathway in the absence of p53 was compared between MS and WB mouse models. **A)** Immunoblots of whole muscle autophagic proteins including **B)** LC3-II/LC3-I ratio (n=6-8/group); †p<0.05, UT WT vs. KO, Student's t-test, **C)** p62 (n=5-8/group); †p<0.05, ††p<0.01, UT WT vs. KO, 2-way ANOVA, and **D)** Beclin-1 were measured (n=5-7/group); ††p<0.01, UT WT vs. KO, 2-way ANOVA; ¶¶p<0.01, WT MS vs. WB, Student's t-test. Data are presented as mean ± SEM.

Fig. 12

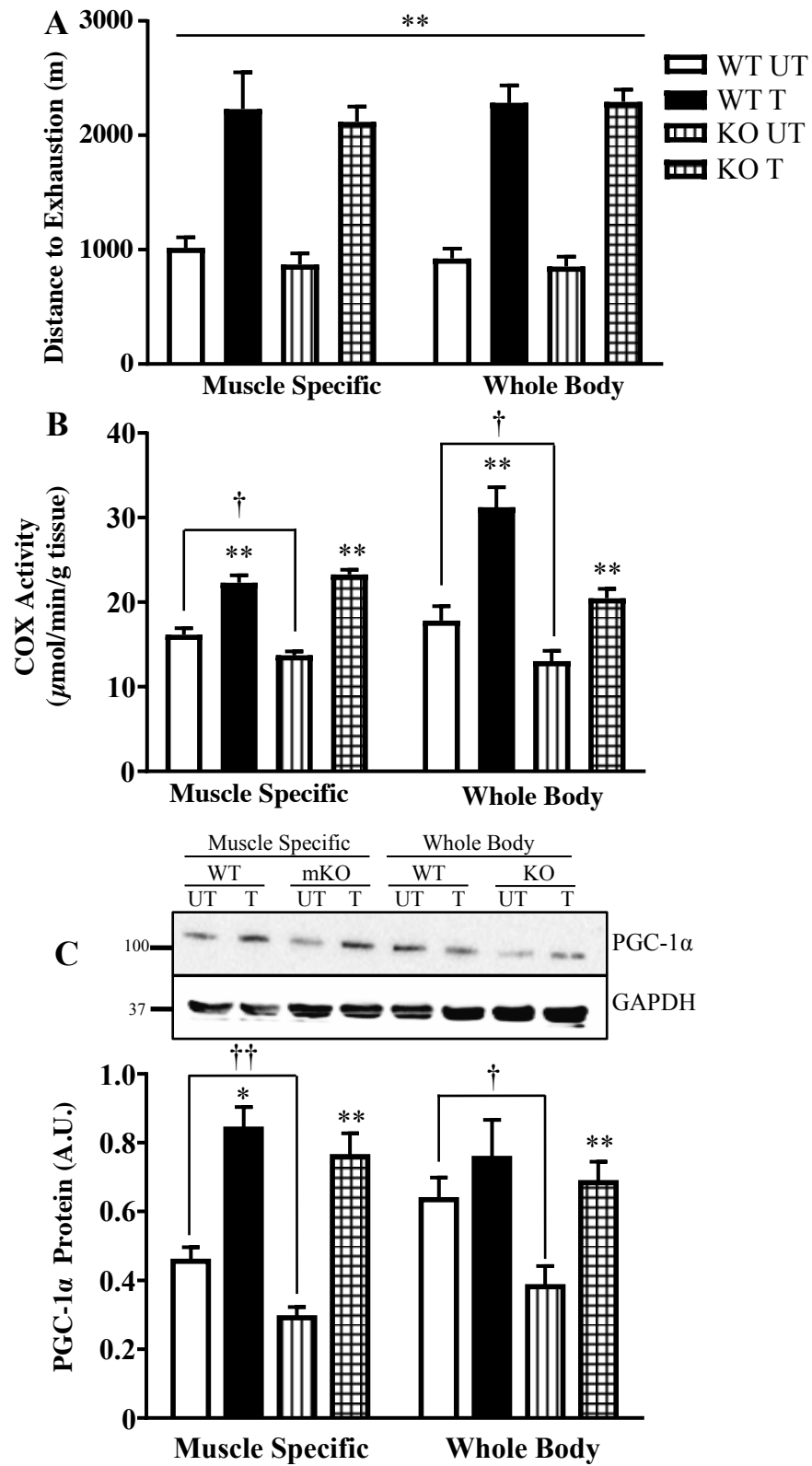


Figure 12. Adaptive mitochondrial responses with training in two mouse models. Following the 6-week training/sedentary protocol, MS and WB mice were subjected to an exhaustive exercise test. **A)** Distance to exhaustion in both mouse models (n=6-9/group); **p<0.01, UT vs. T, 2-way ANOVA. **B)** COX activity (n=6-8/group); *p<0.05, **p<0.01, UT vs. T, Student's t-test and 2-way ANOVA; †p<0.05, UT WT vs. KO, Student's t-test. **C)** PGC-1 α protein (n=5-10/group); *p<0.05, **p<0.01, UT vs. T, Student's t-test and 2-way ANOVA; †p<0.05, UT WT vs. KO, Student's t-test; ¶p<0.05, WT MS vs. WB, Student's t-test. Data are presented as mean \pm SEM.

Discussion

The function of p53 in the transcriptional regulation of numerous signaling pathways is well established. However, its role in maintaining mitochondrial content and function, as well as the adaptive responses to endurance training remains unresolved. Thus, we sought to comprehensively evaluate this function of p53 by using muscle-specific p53 knockout animals. Our results reveal that 1) training reduces p53 at the mRNA and protein levels, but increases the proportion of activated p53, particularly within mitochondria, 2) p53 is important for regulating basal mitochondrial biogenesis, respiration, ROS emission and apoptosis, but is not essential for training-induced adaptations in mitochondrial content, exercise capacity, and lactate handling, 3) p53 is not required for autophagy signaling but may be necessary for substrate clearance (21, 37), a process improved with training, 4) p53 is important for maintaining the expression of specific transcripts regulating mitochondrial biogenesis, metabolism, autophagy, apoptosis and cellular senescence, both basally and with training, and 5) training can improve mitochondrial content and function, as well as attenuate the deficits in mitochondrial function induced by the absence of p53.

It is well-established that acute exercise results in p53 re-localization. We and others have shown that p53 can be redirected to the mitochondria (34, 38) and nucleus (17, 44, 50) with acute exercise, concomitant with the activation of both AMPK and p38 MAPK kinases (5, 25, 38) and the phosphorylation of p53 on Ser¹⁵ (4, 38). This is important for the transcriptional activation of nuclear and mitochondrial gene products, as well as for the dissociation of p53 from its negative regulator Mdm2 (20, 24, 36, 38, 41). The results presented in our study extend these findings to show that endurance training modifies this subcellular redistribution during acute exercise. Though nuclear accumulation of p53 does occur with acute exercise (17, 27, 29, 38, 44, 50),

training resulted in the re-localization of activated p53 out of the nucleus, leading to its cytosolic accumulation (Fig. 1F) where it can then localize to mitochondria (Fig. 1J, K). p53 mitochondrial accumulation was likely facilitated by enhanced CHCHD4 levels (Fig. 5H), a component of the mitochondrial import machinery, which specifically targets p53 to increase trafficking into the organelle (50). Once inside, p53 can maintain mitochondrial genome integrity by interacting with Tfam, increasing mtDNA transcription, and enhancing polymerase- γ activity (1, 18, 38, 39, 48).

We sought to identify the mitochondrial impairments in muscle consequent to the absence of p53, and the potential corrective effects of a chronic endurance training program. Under basal conditions, the presence of a genome-wide p53 deletion has been shown to result in morphological disruptions of SS and IMF mitochondria, reduced mitochondrial content and mtDNA copy number, and decreases in numerous transcriptional targets including PGC-1 α and Tfam (28, 33, 35, 38, 39). Functional deficits include impaired state 3 respiration and elevated ROS levels in IMF mitochondria, altered DNA fragmentation and enhanced apoptotic potential, evidenced through increased cytochrome c release from SS mitochondria (10, 32, 35). Our data reveal that the muscle-specific absence of p53 results in a modest, but significant reduction in mitochondrial content, along with decreases in both Tfam and PGC-1 α mRNA and protein. Functional mitochondrial deficits were also observed, including impaired state 3 respiration, elevated ROS levels and increased pro-apoptotic signaling, accompanied by an increase in the Bax:Bcl-2 protein ratio. Interestingly, a recent study employing 8-week old muscle-specific p53 mKO mice (43) observed no deficits in mitochondrial proteins or mRNA. This difference in results may be developmentally-related, as our study was conducted using ~3 month old mice for comparison. This would suggest that the influence of p53 on mitochondrial function is dependent

on age. Although cage activity, based on voluntary running wheel data, differs markedly between whole body p53 knockout and WT animals (35), we found no differences in voluntary wheel running activity over a 2-week period between mKO and WT mice (n=3-4). Thus, differences in activity level do not appear to be the cause of the reduced mitochondrial content in mKO mice.

We additionally probed the autophagy pathway, known to be altered in the absence of p53 (9, 21, 31, 35, 37, 45, 49). Elevations in p62, Parkin, and Beclin-1 autophagy proteins were observed in the absence of p53, with a trend for an increase in the LC3 II/I ratio. These data suggest that autophagic signaling is enhanced in the absence of p53, but that clearance of autophagosomes, and substrates such as p62, is impaired. Similar results have previously been shown (37), whereby the absence of p53 led to elevated p62 protein and reduced ubiquitination. This impaired clearance could contribute to the accumulation of dysfunctional mitochondria that we observed in the mKO mice (Fig. 3D, H).

We also examined the consequences of muscle-specific p53 deletion on muscle mass and physiological performance. Analogous to previous work (15), our mKO mice revealed no baseline differences in body or hindlimb mass, indicating that p53 is not required for the maintenance of skeletal muscle mass. While one study identified significant reductions in whole body exercise performance and aerobic capacity, evidenced by 3-fold higher lactate levels and impaired aerobic swimming performance as a result of p53 deletion (33, 35), another investigation revealed no effect on performance during an acute bout of exhaustive exercise (38). We confirmed these findings, whereby our mKO mice displayed similar pre-training exercise performance as the WT mice. However, the lower oxidative capacity of these mice resulted in higher blood lactate following their exercise test, suggesting a greater reliance on glycolysis to achieve this same performance.

We sought to determine whether p53 is necessary for adaptations to exercise training. In contrast to a previous study using a whole body p53 knockout model in which a reduced adaptive capacity was noted (33), we observed that WT and mKO mice respond with similar phenotypic and physiological adaptations to training, as shown by >2-fold improvement in exercise capacity and an attenuation in final lactate levels. Mitochondrial content was increased in the mKO mice by 42%, to attain similar levels as the WT trained mice, which increased their COX activity by 27%. In the absence of p53, we observed similar elevations in PGC-1 α and Tfam proteins. Furthermore, mitochondrial respiration was increased while ROS emission was reduced in the mKO mice, indicating that training improved the mitochondrial deficits induced basally by the absence of p53. Apoptosis was down-regulated with exercise training, as evidenced by reduced cytochrome c release from SS mitochondria and attenuated Bax protein levels in the mKO mice. Proteins of the autophagy pathway, including Parkin, Beclin-1, and LC3-II were significantly upregulated in the WT mice with training, as shown in other models of chronic exercise (7, 8, 22). In contrast, training reduced the already elevated levels of these proteins in mKO mice toward levels observed in the WT trained mice. Of particular relevance is the training-induced reduction in p62 protein, in the absence of a change in *p62* mRNA, signifying enhanced p62 degradation via autophagic flux. Thus, training induces the activation of redundant signals to increase mitochondrial biogenesis and autophagy, and reduce apoptosis, to compensate for the loss of p53, resulting in similar final adaptations between groups.

As most literature on the role of p53 in skeletal muscle has been performed using a whole body (WB) p53 deletion model, we inquired as to whether deficits observed in the WB model are a result of the loss of p53 in muscle, or a consequence of its absence in alternative tissues. Though we observed similar directional alterations in mitochondrial content, autophagy proteins,

PGC-1 α mRNA and protein, state 3 respiration and ROS emission in SS mitochondria of both WB p53 KO and mKO models basally, the magnitude of change was less pronounced in the mKO mice (33, 35, 37, 38). This may be a result of the lingering, yet vanishingly low, p53 protein in the mKO mice, or a consequence of blood-borne metabolic, endocrine, or immunological influences on muscle as a result of a genome-wide p53 deletion. Whatever the cause, it is evident that chronic exercise is able to combat these defects to produce similar adaptations in performance, mitochondrial function, and PGC-1 α protein between these two experimental models.

This study has sought to provide a greater understanding of the role of p53 in mediating exercise-induced adaptations in muscle. Though p53 is required for mitochondrial maintenance and function, autophagy and apoptotic regulation, its absence in muscle does not cause an impairment in endurance exercise performance. Thus, redundant signaling exists to compensate for its loss, allowing for beneficial exercise-induced mitochondrial adaptations to occur, thereby improving muscle health. Our data also indicate that exercise, in the form of a progressive and regulated endurance training program, can be a viable therapeutic option for individuals with mutated or non-functional p53.

References:

1. **Achanta G, Sasaki R, Feng L, Carew JS, Lu W, Pelicano H, Keating MJ, Huang P.** Novel role of p53 in maintaining mitochondrial genetic stability through interaction with DNA Pol γ . *EMBO J* 24: 3482–3492, 2005.
2. **Adhihetty PJ, Irrcher I, Joseph AM, Ljubcic V, Hood DA.** Plasticity of skeletal muscle mitochondria in response to contractile activity. *Exp Physiol* 88: 99–107, 2003.
3. **Adhihetty PJ, Ljubcic V, Hood DA.** Effect of chronic contractile activity on SS and IMF mitochondrial apoptotic susceptibility in skeletal muscle. *Am J Physiol Endocrinol Metab* 292: E748-55, 2007.
4. **Bartlett JD, Hwa Joo C, Jeong TS, Louhelainen J, Cochran AJ, Gibala MJ, Gregson W, Close GL, Drust B, Morton J.** Matched work high-intensity interval and continuous running induce similar increases in PGC-1 α mRNA, AMPK, p38, and p53 phosphorylation in human skeletal muscle. *J Appl Physiol* 112: 1135–1143, 2012.
5. **Bartlett JD, Louhelainen J, Iqbal Z, Cochran AJ, Gibala MJ, Gregson W, Close GL, Drust B, Morton J.** Reduced carbohydrate availability enhances exercise-induced p53 signaling in human skeletal muscle: implications for mitochondrial biogenesis. *AJP Regul Integr Comp Physiol* 304: R450–R458, 2013.
6. **Bradford, MM.** A rapid and sensitive method for the quantitation of microgram quantities of protein utilizing the principle of protein-dye binding. *Anal Biochem* 72: 248–254, 1976.
7. **Carter HN, Pauly H, Tryon LD, Hood DA.** Effect of contractile activity on PGC-1 α transcription in young and aged skeletal muscle. *J Appl Physiol*, 2018.
8. **Chen CCW, Erlich AT, Hood DA.** Role of Parkin and endurance training on mitochondrial turnover in skeletal muscle. *Skelet Muscle* 8: 1–14, 2018.
9. **Chipuk JE, Green D.** Dissecting p53-dependent apoptosis. *Cell Death Differ* 13: 994–1002, 2006.
10. **Chipuk JE, Kuwana T, Bouchier-Hayes L, Droin NM, Newmeyer DD, Schuler M, Green D.** Direct activation of Bax by p53 mediates mitochondrial membrane permeabilization and apoptosis. *Science (80)* 303: 1010–1014, 2004.
11. **Cogswell AM, Stevens RJ, Hood DA.** Properties of skeletal muscle mitochondria isolated from subsarcolemmal and intermyofibrillar regions. *Am J Physiol* 264: C383-9, 1993.
12. **Cooperstein SJ, Lazarow A.** A microspectrophotometric method for the determination of cytochrome oxidase. *J Biol Chem* 189: 665–670, 1951.
13. **Crighton D, Wilkinson S, O’Prey J, Syed N, Smith P, Harrison PR, Gasco M, Garrone O, Crook T, Ryan K.** DRAM, a p53-induced modulator of autophagy, is critical for apoptosis. *Cell* 126: 121–134, 2006.

14. **Feng Z, Hu W, De Stanchina E, Teresky AK, Jin S, Lowe S, Levine A.** The regulation of AMPK β 1, TSC2, and PTEN expression by p53: Stress, cell and tissue specificity, and the role of these gene products in modulating the IGF-1-AKT-mTOR pathways. *Cancer Res* 67: 3043–3053, 2007.
15. **Fox DK, Ebert SM, Bongers KS, Dyle MC, Bullard SA, Dierdorff JM, Kunkel SD, Adams C.** p53 and ATF4 mediate distinct and additive pathways to skeletal muscle atrophy during limb immobilization. *AJP Endocrinol Metab* 307: E245–E261, 2014.
16. **Fridman JS, Lowe S.** Control of apoptosis by p53. *Oncogene* 22: 9030–9040, 2003.
17. **Granata C, Oliveira RSF, Little JP, Renner K, Bishop D.** Sprint-interval but not continuous exercise increases PGC-1 α protein content and p53 phosphorylation in nuclear fractions of human skeletal muscle. *Sci Rep* 7: 44227, 2017.
18. **Heyne K Mannebach S, Wuertz E, Knaup KX, Mahyar-Roemer M, Roemer K.** Identification of a putative p53 binding sequence within the human mitochondrial genome. *FEBS Lett* 578: 198–202, 2004.
19. **Hood DA, Irrcher I, Ljubicic V, Joseph A.** Coordination of metabolic plasticity in skeletal muscle. *J Exp Biol* 209: 2265–2275, 2006.
20. **Irrcher I, Ljubicic V, Kirwan A, Hood DA.** AMP-activated protein kinase-regulated activation of the PGC-1 α promoter in skeletal muscle cells. *PLoS One* 3: e6314, 2008.
21. **Kenzelmann Broz D, Mello SS, Biegging KT, Jiang D, Dusek RL, Brady CA, Sidow A, Attardi L.** Global genomic profiling reveals an extensive p53-regulated autophagy program contributing to key p53 responses. *Genes Dev* 27: 1016–1031, 2013.
22. **Kim Y, Hood DA.** Regulation of the autophagy system during chronic contractile activity-induced muscle adaptations. *Physiol Rep* 5: 1–11, 2017.
23. **Levine AJ, Oren M.** The first 30 years of p53: growing every more complex. *Nat Rev Cancer* 9: 749–758, 2009.
24. **Liang SH, Clarke M.** Regulation of p53 localization. *Eur J Biochem* 268: 2779–2783, 2001.
25. **Ljubicic V, Hood DA.** Specific attenuation of protein kinase phosphorylation in muscle with a high mitochondrial content. *Am J Physiol Endocrinol Metab* 297: E749–E758, 2009.
26. **Ljubicic V, Joseph AM, Adhietty PJ, Huang JH, Saleem A, Ugucioni G, Hood DA.** Molecular basis for an attenuated mitochondrial adaptive plasticity in aged skeletal muscle. *Aging (Albany NY)* 1: 818–830, 2009.
27. **Lohrum MA, Woods DB, Ludwig RL, Bálint E, Vousden K.** C-terminal ubiquitination of p53 contributes to nuclear export. *Mol Cell Biol* 21: 8521–8532, 2001.
28. **Macleod KF, Sherry N, Hannon G, Beach D, Tokino T, Kinzler K, Vogelstein B,**

- Jacks T.** p53-dependent and independent expression of p21 during cell growth, differentiation, and DNA damage. *Genes Dev* 9: 935–944, 1995.
29. **Marchenko ND, Wolff S, Erster S, Becker K, Moll U.** Monoubiquitylation promotes mitochondrial p53 translocation. *EMBO J* 26: 923–934, 2007.
 30. **Marchenko ND, Zaika A, Moll U.** Death signal-induced localization of p53 protein to mitochondria: A potential role in apoptotic signaling. *J Biol Chem* 275: 16202–16212, 2000.
 31. **Marino G, Niso-Santano M, Baehrecke EH, Kroemer G.** Self-consumption: the interplay of autophagy and apoptosis. *Nat Rev Mol Cell Biol* 15: 81–94, 2014.
 32. **Matoba S, Kang JG, Patino WD, Wragg A, Boehm M, Gravrilova O, Hurley PJ, Bunz F, Hwang P.** p53 regulates mitochondrial respiration. *Science* (80) 312: 1650–1653, 2006.
 33. **Park JY, Wang PY, Matsumoto T, Sung HJ, Choi JW, Anderson SA, Leary SC, Balaban RS, Hwang P.** p53 improves aerobic exercise capacity and augments skeletal muscle mitochondrial DNA content. *Circ Res* 105: 705–712, 2009.
 34. **Safdar A, Khrapko K, Flynn JM, Saleem A, De Lisio M, Johnston APW, Kratysberg Y, Samjoo IA, Kitaoka Y, Ogborn DI, Little JP, Raha S, Parise G, Akhtar M, Hettinga BP, Rowe G, Arany Z, Prolla TA, Tarnopolsky MA.** Exercise-induced mitochondrial p53 repairs mtDNA mutations in mutator mice. *Skelet Muscle* 6: 7, 2016.
 35. **Saleem A, Adhietty PJ, Hood DA.** Role of p53 in mitochondrial biogenesis and apoptosis in skeletal muscle. *Physiol Genomics* 37: 58–66, 2009.
 36. **Saleem A, Carter H, Iqbal S, Hood DA.** Role of p53 within the regulatory network controlling muscle mitochondrial biogenesis. *Exerc Sport Sci Rev* 39: 199–205, 2011.
 37. **Saleem A, Carter HN, Hood DA.** p53 is necessary for the adaptive changes in cellular milieu subsequent to an acute bout of endurance exercise. *AJP Cell Physiol* 306: C241–C249, 2014.
 38. **Saleem A, Hood DA.** Acute exercise induces tumour suppressor protein p53 translocation to the mitochondria and promotes a p53-Tfam-mitochondrial DNA complex in skeletal muscle. *J Physiol* 591: 3625–3636, 2013.
 39. **Saleem A, Iqbal S, Zhang Y, Hood DA.** Effect of p53 on mitochondrial morphology, import, and assembly in skeletal muscle. *Am J Physiol - Cell Physiol* 308: C319–C329, 2015.
 40. **Scherz-Shouval R, Weidberg H, Gonen C, Wilder S, Elazar Z, Oren M.** p53-dependent regulation of autophagy protein LC3 supports cancer cell survival under prolonged starvation. *PNAS* 107: 18511–18516, 2010.
 41. **Shieh SY, Ikeda M, Taya Y, Prives C.** DNA damage-induced phosphorylation of p53 alleviates inhibition by MDM2. *Cell* 91: 325–334, 1997.

42. **Siu PM, Bryner RW, Martyn JK, Alway S.** Apoptotic adaptations from exercise training in skeletal and cardiac muscles. *FASEB J* 18: 1150–1152, 2004.
43. **Stocks B, Dent JR, Joanisse S, McCurdy CE, Philp A.** Skeletal muscle fibre-specific knockout of p53 does not reduce mitochondrial content or enzyme activity. *Front Physiol* 8: 1–10, 2017.
44. **Tachtsis B, Smiles WJ, Lane SC, Hawley JA, Camera D.** Acute endurance exercise induces nuclear p53 abundance in human skeletal muscle. *Front Physiol* 7: 144, 2016.
45. **Tasdemir E, Maiuri MC, Galluzzi L, Vitale I, Djavaheri-mergny M, Amelio MD, Criollo A, Morselli E, Zhu C, Harper F, Nannmark U, Samara C, Pinton P, Vicencio JM, Carnuccio R, Moll U, Madeo F, Paterlini-Brechot P, Rizzuto R, Szabadkai G, Pierron G, Blomgren K, Tavernarakis N, Codogno P, Cecconi F, Kroemer G.** Regulation of autophagy by cytoplasmic p53. *Nat Cell Biol* 10: 676–687, 2008.
46. **Vainshtein A, Kazak L, Hood DA.** Effects of endurance training on apoptotic susceptibility in striated muscle. *J Appl Physiol* 110: 1638–1645, 2011.
47. **Vaseva AV, Moll U.** The mitochondrial p53 pathway. *Biochim Biophys Acta* 1787: 414–420, 2009.
48. **Yoshida Y, Izumi H, Torigoe T, Ishiguchi H, Itoh H, Kang D.** p53 physically interacts with mitochondrial transcription factor A and differentially regulates binding to damaged DNA. *Cancer Res* 63: 3729–3734, 2003.
49. **Yu X, Munoz-Alarcon A, Ajayi A, Webling K, Steinhof A, Langel U, Strom A.** Inhibition of autophagy via p53-mediated disruption of ULK1 in a SCA7 polyglutamine disease model. *J Mol Neurosci* 50: 586–599, 2013.
50. **Zhuang J, Kamp WM, Li J, Liu C, Kang JG, Wang PY, Hwang P.** Forkhead box O3A (FOXO3) and the mitochondrial disulfide relay carrier (CHCHD4) regulate p53 protein nuclear activity in response to exercise. *J Biol Chem* 291: 24819–24827, 2016.

Acknowledgements

The authors would like to thank Dr. Christopher Adams for his donation of the Muscle Specific WT and p53 mKO mice. We would like to thank D. Posluns, A. Akhtar, M. Khalid, and N. Barazi for technical assistance during this project. KB was funded by an OGS QEII-GSST scholarship. DAH holds a Canada Research Chair in Cell Physiology. This work was funded by an NSERC grant to DAH.

Manuscript Author Contributions

KB and DAH developed the concept for the study and designed the experimental outline. KB performed all of the experiments, except for nuclear/cytosolic extractions. This extraction procedure was performed by ATE and MT. ATE assisted also with the exercise training program. KB and DAH analyzed the data and interpreted the results. KB prepared the figures and drafted the manuscript. KB and DAH edited and revised the manuscript and approved the final version.

Future Work

Based on the present findings and on previous research performed in the field of p53 and mitochondrial signaling with exercise, future research could focus on:

Short-Term Goals

- Examining glycolytic proteins through immunoblotting to determine metabolic reliance on glycolysis rather than oxidative phosphorylation in the mKO mice, basally;
- Measuring mitophagy flux and lysosomal biogenesis to understand mitochondrial turnover with exercise training, and its dependency on p53;
- Understanding the role of p53 on additional mechanisms that regulate cellular homeostasis through protein analysis via immunoblotting for the antioxidant and ROS pathways;
- Evaluating whether additional post-translational modifications are facilitating the subcellular re-localization of p53 by immunoblotting for residue modifications.
- Elucidating transcription factors that may compensate for the loss of p53, allowing for training-induced adaptations in mitochondrial biogenesis and gene transcription;

Long-Term

- Determining the transcription factors that may compensate for the loss of p53 with exercise training by performing a microarray;
- Ascertaining the mechanisms that assist in the re-localization of p53 to alternate cellular compartments with exercise, accomplished through in vitro inhibition of channels and additional fluorescent tagging to determine transport proteins;
- Discovering an ideal exercise program by creating a time course with altered exercise parameters (length of program, intensity, frequency, duration), to determine the point for optimal skeletal muscle mitochondrial adaptations, and the whether there is a dependency on p53 within the variable exercise regimens.

Appendices

Appendix A: Manuscript Data and Statistical Analysis

Table 3A: Pre-training body mass and performance test, distance to exhaustion

Initial Body Mass (g) – Muscle Specific Mice		
N	WT	mKO
1	30.8	38.4
2	30.4	28.5
3	29.6	29.5
4	26.8	27.2
5	31.0	29.4
6	31.4	44.4
7	31.5	34.6
8	30.1	27.0
9	31.2	36.7
10	31.3	32.0
11	30.4	32.8
12	29.2	29.2
13	31.7	27.8
14		28.8
15		27.8
16		28.2
17		27.7
18		36.9
19		31.1
20		31.4
21		29.5
X	30.415	31.376
SEM	0.367	0.985

Pre-Training Distance to Exhaustion (m) – Muscle Specific Mice		
N	WT	mKO
1	1144.22	1381.40
2	1322.50	1012.56
3	1597.00	1546.42
4	1150.00	1322.50
5	970.00	1387.88
6	1559.00	477.00
7	1578.00	523.25
8	962.00	855.23
9	1287.50	1466.50
10	1189.44	1616.00
11	1012.56	1635.00
12	1201.00	804.80
13	1509.42	922.50
14	1394.00	876.00
15	1192.50	970.00
16	1301.50	1313.75
17	1485.00	1503.50
18		1201.00
X	1285.626	1156.405
SEM	50.830	85.428

Unpaired T-test – WT versus KO	
P value	0.4621
P value summary	ns
Significantly different? (P<0.05)	No

Unpaired T-test – WT versus KO	
P value	0.2091
P value summary	ns
Significantly different? (P<0.05)	No

Table 3B: Post-training body mass measurement

Final Body Mass (g) - Muscle Specific Mice				
	WT		mKO	
N	UT	T	UT	T
1	31.52	29.02	42.40	27.10
2	31.23	30.52	30.60	27.72
3	34.03	30.35	33.40	25.61
4	30.07	30.74	30.40	28.42
5	36.13	30.07	30.40	28.92
6	36.15	29.75	43.00	27.06
7			38.40	26.82
8			29.10	29.41
9			38.40	30.10
10			32.30	27.00
X	33.188	30.075	34.840	27.816
SEM	1.072	0.254	1.660	0.434

Two-Way ANOVA			
Source of Variation	P value	P value summary	Significance
Interaction	0.1138	ns	No
Mouse Model	0.8017	ns	No
Genotype/Training	0.0002	***	Yes

Post-Hoc Test				
Bonferroni	Mean Diff.	t-value	P-value	Summary
WT:UT vs. WT:T	3.113	1.644	>0.05	ns
WT:UT vs. KO:UT	-1.652	0.9750	> 0.05	ns
WT:UT vs. KO:T	5.372	3.171	≤ 0.05	*
WT:T vs. KO:UT	-4.765	2.813	> 0.05	ns
WT:T vs. KO:T	2.259	1.333	> 0.05	ns
KO:UT vs. KO:T	7.024	4.788	<0.005	***

Unpaired T-test – WT UT versus WT T	
P value	0.0180
P value summary	*
Significantly different? (P<0.05)	Yes

Table 3B: Post-training tibialis anterior (TA) mass measurement, corrected for body mass

Tibialis Anterior (TA) Skeletal Muscle Mass/Body Mass (mg/g) – Muscle Specific Mice				
	WT		mKO	
N	UT	T	UT	T
1	2.00	1.51	2.57	1.93
2	2.20	1.62	1.98	1.64
3	2.20	1.69	1.91	1.82
4	1.95	1.49	2.06	1.85
5	1.86	1.83	1.91	1.62
6	1.68	1.30	2.05	1.72
7			2.01	1.78
8			2.21	1.94
X	1.982	1.573	2.088	1.788
SEM	0.0822	0.0747	0.0768	0.0429

Two-Way ANOVA			
Source of Variation	P value	P value summary	Significance
Interaction	0.4457	ns	No
Mouse Model	0.0311	*	Yes
Genotype/Training	< 0.0001	****	Yes

Post-Hoc Test				
Bonferroni	Mean Diff.	t-value	P-value	Summary
WT:UT vs. WT:T	0.4083	3.866	≤ 0.01	**
WT:UT vs. KO:UT	-0.1058	1.071	> 0.05	ns
WT:UT vs. KO:T	0.1942	1.965	> 0.05	ns
WT:T vs. KO:UT	-0.5142	5.204	≤ 0.005	***
WT:T vs. KO:T	-0.2142	2.168	> 0.05	ns
KO:UT vs. KO:T	0.3000	3.280	≤ 0.05	*

Table 3B: Post-training gastrocnemius mass measurement, corrected for body mass

Gastrocnemius Skeletal Muscle Mass/Body Mass (mg/g) – Muscle Specific Mice				
	WT		mKO	
N	UT	T	UT	T
1	7.42	6.32	8.13	6.24
2	6.73	6.28	5.88	6.32
3	5.89	5.56	6.18	6.52
4	6.10	5.74	6.15	6.14
5	5.90	5.81	6.16	6.36
6	6.00	5.34	5.88	5.19
7			6.25	6.45
8			5.83	6.19
X	6.340	5.842	6.308	6.176
SEM	0.251	0.160	0.267	0.148

Two-Way ANOVA			
Source of Variation	P value	P value summary	Significance
Interaction	0.4092	ns	No
Mouse Model	0.4961	ns	No
Genotype/Training	0.1626	ns	No

Post-Hoc Test				
Bonferroni	Mean Diff.	t-value	P-value	Summary
WT:UT vs. WT:T	0.4983	1.508	> 0.05	ns
WT:UT vs. KO:UT	0.03250	0.1052	> 0.05	ns
WT:UT vs. KO:T	0.1638	0.5299	> 0.05	ns
WT:T vs. KO:UT	-0.4658	1.507	> 0.05	ns
WT:T vs. KO:T	-0.3346	1.083	> 0.05	ns
KO:UT vs. KO:T	0.1313	0.4588	> 0.05	ns

Unpaired T-test – WT UT versus WT T	
P value	0.1246
P value summary	ns
Significantly different? (P<0.05)	No

Table 3B: Post-training quadriceps mass measurement, corrected for body mass

Quadriceps Skeletal Muscle Mass/Body Mass (mg/g) – Muscle Specific Mice				
	WT		mKO	
N	UT	T	UT	T
1	6.56	5.65	7.28	6.56
2	6.51	5.95	6.96	6.50
3	5.87	6.58	6.64	6.56
4	6.15	6.08	6.52	6.45
5	6.18	6.57	6.05	6.52
6	6.15	6.22	6.05	6.60
7			7.61	7.15
8			5.93	6.73
X	6.237	6.175	6.630	6.634
SEM	0.105	0.148	0.218	0.0793

Two-Way ANOVA			
Source of Variation	P value	P value summary	Significance
Interaction	0.8358	ns	No
Mouse Model	0.0117	*	Yes
Genotype/Training	0.8544	ns	No

Post-Hoc Test				
Bonferroni	Mean Diff.	t-value	P-value	Summary
WT:UT vs. WT:T	0.06167	0.2614	> 0.05	ns
WT:UT vs. KO:UT	-0.3933	1.782	> 0.05	ns
WT:UT vs. KO:T	-0.3971	1.799	> 0.05	ns
WT:T vs. KO:UT	-0.4550	2.062	> 0.05	ns
WT:T vs. KO:T	-0.4588	2.078	> 0.05	ns
KO:UT vs. KO:T	-0.003750	0.01835	> 0.05	ns

Unpaired T-test – WT UT versus KO UT	
P value	0.1708
P value summary	ns
Significantly different? (P<0.05)	No

Table 3B: Post-training heart mass measurement, corrected for body mass

Heart Mass/Body Mass (mg/g) – Muscle Specific Mice				
	WT		mKO	
N	UT	T	UT	T
1	6.14	6.04	3.69	5.42
2	5.71	6.26	4.29	5.69
3	4.89	5.69	5.07	6.01
4	3.99	5.13	4.76	5.51
5	6.59	5.76	5.06	6.13
6	4.94	5.66	5.14	5.64
7			5.04	6.10
8			5.11	6.00
X	5.377	5.757	4.770	5.813
SEM	0.388	0.157	0.184	0.0989

Two-Way ANOVA			
Source of Variation	P value	P value summary	Significance
Interaction	0.1388	ns	No
Mouse Model	0.2151	ns	No
Genotype/Training	0.0031	**	Yes

Post-Hoc Test				
Bonferroni	Mean Diff.	t-value	P-value	Summary
WT:UT vs. WT:T	-0.3800	1.162	> 0.05	ns
WT:UT vs. KO:UT	0.6067	1.983	> 0.05	ns
WT:UT vs. KO:T	-0.4358	1.425	> 0.05	ns
WT:T vs. KO:UT	0.9867	3.225	≤ 0.05	*
WT:T vs. KO:T	-0.05583	0.1825	> 0.05	ns
KO:UT vs. KO:T	-1.043	3.681	≤ 0.01	**

Unpaired T-test – WT UT versus WT T	
P value	0.3853
P value summary	ns
Significantly different? (P<0.05)	No

Table 3B: Post-training epididymal fat mass measurement, corrected for body mass

Epididymal Fat Mass /Body Mass (mg/g) – Muscle Specific Mice				
	WT		mKO	
N	UT	T	UT	T
1	33.60	22.25	67.17	26.68
2	43.06	24.78	59.87	27.04
3	51.42	29.34	41.71	30.32
4	38.65	39.98	53.59	24.04
5	39.77	44.16	39.43	19.37
6	54.89	28.43	58.87	27.07
7			59.64	14.52
8			56.22	22.32
X	43.565	31.490	54.563	23.920
SEM	3.307	3.545	3.352	1.792

Two-Way ANOVA			
Source of Variation	P value	P value summary	Significance
Interaction	0.0054	**	Yes
Mouse Model	0.5773	ns	No
Genotype/Training	< 0.0001	****	Yes

Post-Hoc Test				
Bonferroni	Mean Diff.	t-value	P-value	Summary
WT:UT vs. WT:T	12.08	2.633	> 0.05	ns
WT:UT vs. KO:UT	-11.00	2.564	> 0.05	ns
WT:UT vs. KO:T	19.65	4.579	≤ 0.005	***
WT:T vs. KO:UT	-23.07	5.378	≤ 0.001	****
WT:T vs. KO:T	7.570	1.765	> 0.05	ns
KO:UT vs. KO:T	30.64	7.715	≤ 0.001	****

Unpaired T-test – WT UT versus WT T	
P value	0.0319
P value summary	*
Significantly different? (P<0.05)	Yes

Unpaired T-test – WT UT versus KO UT	
P value	0.0417
P value summary	*
Significantly different? (P<0.05)	Yes

Table 3C: Post-training SS mitochondrial yield

SS Mitochondrial Yield ($\mu\text{g}/\text{mg}$) - Muscle Specific Mice				
	WT		mKO	
N	UT	T	UT	T
1	0.47	0.95	0.58	0.80
2	0.62	0.83	0.44	1.03
3	0.71	0.89	0.83	0.90
4	0.22	0.79	0.69	0.76
5	0.56	0.87	0.036	0.85
6	0.67	0.61	0.6	0.69
7			0.59	0.64
8			0.72	
X	0.542	0.823	0.561	0.81
SEM	0.0730	0.0481	0.0853	0.0498

Two-Way ANOVA			
Source of Variation	P value	P value summary	Significance
Interaction	0.8178	ns	No
Mouse Model	0.9674	ns	No
Genotype/Training	0.0009	***	Yes

Post-Hoc Test				
Bonferroni	Mean Diff.	t-value	P-value	Summary
WT:UT vs. WT:T	-0.2817	2.719	> 0.05	ns
WT:UT vs. KO:UT	-0.01908	0.1969	> 0.05	ns
WT:UT vs. KO:T	-0.2683	2.688	> 0.05	ns
WT:T vs. KO:UT	0.2626	2.710	> 0.05	ns
WT:T vs. KO:T	0.01333	0.1336	> 0.05	ns
KO:UT vs. KO:T	-0.2493	2.684	> 0.05	ns

Unpaired T-test – WT UT versus WT T	
P value	0.0091
P value summary	**
Significantly different? (P<0.05)	Yes

Unpaired T-test – KO UT versus KO T	
P value	0.0304
P value summary	*
Significantly different? (P<0.05)	Yes

Table 3C: Post-training IMF mitochondrial yield

IMF Mitochondrial Yield ($\mu\text{g}/\text{mg}$) - Muscle Specific Mice				
	WT		mKO	
N	UT	T	UT	T
1	1.11	1.05	0.98	1.10
2	1.00	1.06	1.18	1.17
3	1.09	1.56	1.15	1.35
4	1.08	1.58	1.06	1.21
5	1.04	1.14	1.15	1.61
6		1.38	0.12	1.54
7			0.96	1.76
8			0.99	1.44
X	1.064	1.295	0.949	1.398
SEM	0.0196	0.0999	0.122	0.0820

Two-Way ANOVA			
Source of Variation	P value	P value summary	Significance
Interaction	0.2909	ns	No
Mouse Model	0.9521	ns	No
Genotype/Training	0.0027	**	Yes

Post-Hoc Test				
Bonferroni	Mean Diff.	t-value	P-value	Summary
WT:UT vs. WT:T	-0.2305	1.481	> 0.05	ns
WT:UT vs. KO:UT	0.1153	0.7864	> 0.05	ns
WT:UT vs. KO:T	-0.3335	2.276	> 0.05	ns
WT:T vs. KO:UT	0.3458	2.490	> 0.05	ns
WT:T vs. KO:T	-0.1030	0.7419	> 0.05	ns
KO:UT vs. KO:T	-0.4488	3.491	≤ 0.05	*

Unpaired T-test – WT UT versus WT T	
P value	0.0694
P value summary	ns
Significantly different? (P<0.05)	No

Table 3C: Post-training Respiratory Control Ratio (RCR) (state 3/4) in SS Mitochondria

SS Respiratory Control Ratio (RCR)- Muscle Specific Mice				
	WT		mKO	
N	UT	T	UT	T
1	2.09	4.56	3.19	5.00
2	0.70	3.62	2.52	4.22
3	5.82	10.30	4.33	5.55
4	3.56	37.00	7.35	5.64
5	7.20	17.00	5.44	9.32
6	3.15	4.71	4.90	4.39
7	3.93		6.45	4.31
8			2.75	19.00
X	3.779	12.865	4.616	7.179
SEM	0.826	5.251	0.621	1.787

Two-Way ANOVA			
Source of Variation	P value	P value summary	Significance
Interaction	0.1917	ns	No
Mouse Model	0.3282	ns	No
Genotype/Training	0.0244	*	Yes

Post-Hoc Test				
Bonferroni	Mean Diff.	t-value	P-value	Summary
WT:UT vs. WT:T	-9.086	2.513	> 0.05	ns
WT:UT vs. KO:UT	-0.8377	0.2490	> 0.05	ns
WT:UT vs. KO:T	-3.400	1.011	> 0.05	ns
WT:T vs. KO:UT	8.249	2.350	> 0.05	ns
WT:T vs. KO:T	5.686	1.620	> 0.05	ns
KO:UT vs. KO:T	-2.563	0.7885	> 0.05	ns

Unpaired T-test – WT UT versus WT T	
P value	0.0911
P value summary	ns
Significantly different? (P<0.05)	No

Unpaired T-test – KO UT versus KO T	
P value	0.1971
P value summary	ns
Significantly different? (P<0.05)	No

Table 3C: Post-training Respiratory Control Ratio (RCR) (state 3/4) in IMF Mitochondria

IMF Respiratory Control Ratio (RCR)- Muscle Specific Mice				
	WT		KO	
N	UT	T	UT	T
1	6.59	2.82	8.62	7.89
2	5.43	18.47	5.22	7.97
3	6.89	4.74	5.77	8.17
4	5.86	19.06	12.36	1.80
5	5.64	7.49	7.80	6.27
6	5.89	8.04	6.66	4.97
7			2.85	18.36
8				41.50
X	6.0500	10.103	7.0400	12.116
SEM	0.232	2.847	1.134	4.521

Two-Way ANOVA			
Source of Variation	P value	P value summary	Significance
Interaction	0.8692	ns	No
Mouse Model	0.6296	ns	No
Genotype/Training	0.1508	ns	No

Post-Hoc Test				
Bonferroni	Mean Diff.	t-value	P-value	Summary
WT:UT vs. WT:T	-4.053	0.8862	> 0.05	ns
WT:UT vs. KO:UT	-0.9900	0.2246	> 0.05	ns
WT:UT vs. KO:T	-6.066	1.418	> 0.05	ns
WT:T vs. KO:UT	3.063	0.6950	> 0.05	ns
WT:T vs. KO:T	-2.013	0.4705	> 0.05	ns
KO:UT vs. KO:T	-5.076	1.238	> 0.05	ns

Unpaired T-test –WT UT versus WT T	
P value	0.1863
P value summary	ns
Significantly different? (P<0.05)	No

Unpaired T-test – KO UT versus KO T	
P value	0.3257
P value summary	ns
Significantly different? (P<0.05)	No

Figure 2B: Whole muscle total p53 protein – WT Muscle-Specific Mice

Total-p53 Protein Expression – Whole Muscle Extracts - Muscle Specific Mice		
WT		
N	UT	T
1	0.74	0.29
2	0.35	0.41
3	1.29	0.28
4	0.63	0.13
5	0.47	0.050
6	0.75	0.44
7		0.28
X	0.704	0.269
SEM	0.133	0.0528

Unpaired T-test- WT UT versus T	
P value	0.0080
P value summary	**
Significantly different? (P<0.05)	Yes

Figure 2C: Whole muscle phosphorylated-p53 (Ser¹⁵) protein – WT Muscle-Specific Mice

Phospho-p53/ Total p53 Protein Expression – Whole Muscle Extracts - Muscle Specific Mice		
WT		
N	UT	T
1	0.60	0.67
2	0.11	0.66
3	0.48	0.58
4	0.24	0.65
5	0.60	1.55
6	0.42	2.039
X	0.407	1.0254
SEM	0.0809	0.251

Unpaired T-test- WT UT versus T	
P value	0.0413
P value summary	*
Significantly different? (P<0.05)	Yes

Figure 2E: Total p53 protein in nuclear and cytosolic cellular compartments - WT Muscle-Specific Mice

Nuclear/Cytosolic – Total p53 Protein - Muscle Specific Mice				
	Nuclear		Cytosolic	
N	UT	T	UT	T
1	1.012	0.32	1.25	0.65
2	0.74	0.50	0.96	1.22
3	0.43	0.22	1.29	0.83
4	0.47	0.13	1.54	0.41
5				0.98
X	0.661	0.295	1.257	0.816
SEM	0.136	0.0793	0.119	0.139

Two-Way ANOVA			
Source of Variation	P value	P value summary	Significance
Interaction	0.9730	ns	No
Mouse Model	0.0025	**	Yes
Genotype/Training	0.0086	**	Yes

Post-Hoc Test				
Bonferroni	Mean Diff.	t-value	P-value	Summary
Nuc:UT vs. Nuc:T	0.3659	2.018	> 0.05	ns
Nuc:UT vs. Cyto:UT	-0.5968	3.291	≤ 0.05	#
Nuc:UT vs. Cyto:T	-0.1554	0.9033	> 0.05	ns
Nuc:T vs. Cyto:UT	-0.9627	5.309	≤ 0.005	***
Nuc:T vs. Cyto:T	-0.5213	3.030	> 0.05	ns
Cyto:UT vs. Cyto:T	0.4414	2.566	> 0.05	ns

Unpaired T-test- Nuc UT versus Nuc T	
P value	0.0552
P value summary	*
Significantly different? (P<0.05)	Yes

Unpaired T-test- Cyto UT versus Cyto T	
P value	0.0525
P value summary	*
Significantly different? (P<0.05)	Yes

Unpaired T-test- Nuc T versus Cyto T	
P value	0.0194
P value summary	#
Significantly different? (P<0.05)	Yes

Figure 2E: Phosphorylated p53 (Ser¹⁵) protein in nuclear and cytosolic cellular compartments, percentage of total - WT Muscle-Specific Mice

Phospho-p53 (% Total) Nuc/Cyto - Muscle Specific Mice				
	UT		T	
N	NUC	CYTO	NUC	CYTO
1	0.73 – 73.0%	0.27 – 27.0%	0.31 – 31.0%	0.69 – 69.0%
2	0.62 – 62.0%	0.38 – 38.0%	0.43 – 43.0%	0.57 – 57.0%
3	0.71 – 71.0%	0.29 – 29.0%	0.33 – 33.0%	0.67 – 67.0%
4	0.82 – 82.0%	0.18 – 18.0%	0.44 – 44.0%	0.56 – 56.0%
X	0.722 – 72.2%	0.278 – 27.8%	0.378 – 37.8%	0.623 – 62.3%
SEM	0.0418	0.0418	0.0345	0.0345

Two-Way ANOVA			
Source of Variation	P value	P value summary	Significance
Interaction	< 0.0001	****	Yes
Mouse Model	> 0.9999	ns	No
Genotype/Training	0.0222	*	Yes

Post-Hoc Test				
Bonferroni	Mean Diff.	t-value	P-value	Summary
UT:Nuc vs. UT:Cyto	0.4443	3.428	≤ 0.001	####
UT:Nuc vs. T:Nuc	0.3436	3.006	≤ 0.005	***
UT:Nuc vs. T:Cyto	0.1006	2.049	> 0.05	ns
UT:Cyto vs. T:Nuc	-0.1006	0.2590	> 0.05	ns
UT:Cyto vs. T:Cyto	-0.3436	1.267	≤ 0.005	***
T:Nuc vs. T:Cyto	-0.2430	0.9566	≤ 0.01	##

Figure 2H: Total p53 protein in IMF mitochondria - WT Muscle-Specific Mice

IMF Mitochondria –Total p53 Protein - Muscle Specific Mice		
WT		
N	UT	T
1	0.81	0.31
2	1.09	0.42
3	0.93	0.36
4	1.50	0.48
5	0.73	
X	1.0124	0.393
SEM	0.136	0.0368

Unpaired T-test – WT UT versus WT T	
P value	0.0056
P value summary	**
Significantly different? (P<0.05)	Yes

Figure 2I: Total p53 protein in SS mitochondria - WT Muscle-Specific Mice

SS Mitochondria –Total p53 Protein - Muscle Specific Mice		
WT		
N	UT	T
1	0.95	0.78
2	0.56	0.20
3	0.69	0.38
4	1.36	0.30
5	0.75	
X	0.863	0.416
SEM	0.139	0.128

Unpaired T-test- WT UT versus WT T	
P value	0.0544
P value summary	*
Significantly different? (P<0.05)	Yes

Figure 2J: Phosphorylated p53 (Ser¹⁵) protein in IMF mitochondria - WT Muscle-Specific Mice

IMF Mitochondria – Phospho-p53/ Total p53 Protein - Muscle Specific Mice		
WT		
N	UT	T
1	0.34	1.85
2	0.41	1.62
3	0.56	0.78
4	0.68	0.71
5	0.41	0.91
X	0.479	1.173
SEM	0.0418	0.0345

Unpaired T-test – WT UT versus WT T	
P value	0.0209
P value summary	*
Significantly different? (P<0.05)	Yes

Figure 2K: Phosphorylated p53 (Ser¹⁵) protein in SS mitochondria - WT Muscle-Specific Mice

SS Mitochondria – Phospho-p53/ Total p53 Protein - Muscle Specific Mice		
WT		
N	UT	T
1	0.63	1.29
2	0.66	1.79
3	0.34	0.73
4	0.50	0.82
5	0.53	
X	0.530	1.160
SEM	0.0560	0.244

Unpaired T-test- WT UT versus WT T	
P value	0.0257
P value summary	*
Significantly different? (P<0.05)	Yes

Figure 3C: Post-training performance test, distance to exhaustion

Post-Training Performance Stress Test – Distance to Exhaustion (m)- Muscle Specific Mice				
	WT		mKO	
N	UT	T	UT	T
1	891.50	1623.60	726.00	1731.50
2	1349.00	2990.30	1067.00	2555.00
3	922.50	1376.00	1059.00	2117.00
4	852.80	1578.00	1084.00	2465.00
5	1252.50	2834.00	1150.00	2487.50
6	830.00	2992.70	926.00	1946.90
7			400.00	2112.80
8			557.00	1533.10
X	1016.383	2232.433	871.125	2118.600
SEM	91.705	318.679	98.330	131.523

Two-Way ANOVA			
Source of Variation	P value	P value summary	Significance
Interaction	0.9275	ns	No
Mouse Model	0.4559	ns	No
Genotype/Training	< 0.0001	****	Yes

Post-Hoc Test				
Bonferroni	Mean Diff.	t-value	P-value	Summary
WT:UT vs. WT:T	-1216	4.705	≤ 0.005	***
WT:UT vs. KO:UT	145.3	0.6009	> 0.05	ns
WT:UT vs. KO:T	-1102	4.559	≤ 0.005	***
WT:T vs. KO:UT	1361	5.631	≤ 0.001	****
WT:T vs. KO:T	113.8	0.4709	> 0.05	ns
KO:UT vs. KO:T	-1247	5.574	≤ 0.001	****

Figure 3D: Post-training performance test, final lactate levels

Post-Training Performance Stress Test - Post-Exercise Lactate Levels (mM)- Muscle Specific Mice				
	WT		mKO	
N	UT	T	UT	T
1	12.3	10.9	11.9	7.9
2	11.4	7.8	11.5	8
3	12.2	10.7	12.2	7.4
4	9.5	8.8	10.8	11.3
5	11.1	11.7	17.8	9.5
6	11.5	11.8	13.9	9.3
7	10.6		10.9	12.6
8	10.5		12.7	9.4
9	8.8		13.4	
10	10		12	
11	11.8		10.9	
12	12.8		18.6	
13	9		13.2	
14			14.2	
15			12.2	
16			13.8	
17			13.3	
X	10.885	10.283	13.135	9.425
SEM	0.356	0.664	0.531	0.628

Two-Way ANOVA			
Source of Variation	P value	P value summary	Significance
Interaction	0.0268	*	Yes
Mouse Model	0.0972	ns	No
Genotype/Training	0.0001	***	Yes

Post-Hoc Test				
Bonferroni	Mean Diff.	t-value	P-value	Summary
WT:UT vs. WT:T	1.122	1.375	> 0.05	ns
WT:UT vs. KO:UT	-2.251	3.364	≤ 0.01	**
WT:UT vs. KO:T	1.46	1.789	> 0.05	ns
WT:T vs. KO:UT	-3.373	4.332	≤ 0.005	***
WT:T vs. KO:T	0.3375	0.3717	> 0.05	ns
KO:UT vs. KO:T	3.71	4.765	≤ 0.005	***

Unpaired T-test – WT UT versus WT T	
P value	0.1002
P value summary	ns
Significantly different? (P<0.05)	No

Figure 3E: Post-Training COX Enzyme Activity, marker of mitochondrial content

COX Enzyme Activity ($\mu\text{mol}/\text{min}/\text{g}$ tissue)– Mitochondrial Content - Muscle Specific Mice					
		WT		mKO	
N	UT	T	UT	T	
1	19.21	19.63	14.84	22.22	
2	16.66	21.86	11.04	22.61	
3	13.76	21.52	12.21	24.46	
4	16.87	20.65	14.41	22.49	
5	15.90	24.89	13.29	25.42	
6	16.80	20.09	14.65	22.34	
7		22.98	14.66	21.18	
8		26.86	14.50	25.49	
X	16.533	22.310	13.700	23.276	
SEM	0.718	0.881	0.495	0.572	

Two-Way ANOVA			
Source of Variation	P value	P value summary	Significance
Interaction	0.0105	*	Yes
Mouse Model	0.1868	ns	No
Genotype/Training	< 0.0001	****	Yes

Post-Hoc Test				
Bonferroni	Mean Diff.	t-value	P-value	Summary
WT:UT vs. WT:T	-5.777	5.716	≤ 0.001	****
WT:UT vs. KO:UT	2.833	2.804	> 0.05	ns
WT:UT vs. KO:T	-6.743	6.672	≤ 0.001	****
WT:T vs. KO:UT	8.610	9.203	≤ 0.001	****
WT:T vs. KO:T	-0.9662	1.033	> 0.05	ns
KO:UT vs. KO:T	-9.576	10.24	≤ 0.001	****

Unpaired T-test –WT UT versus KO UT	
P value	0.0056
P value summary	††
Significantly different? (P<0.05)	Yes

Figure 3G: Post-training whole muscle PGC-1 α protein

Whole Muscle PGC-1α Protein - Muscle Specific Mice				
	WT		mKO	
N	UT	T	UT	T
1	0.35	0.93	0.39	0.69
2	0.40	0.74	0.27	0.89
3	0.43	0.71	0.21	0.41
4	0.58	1.17	0.42	0.93
5	0.52	0.73	0.30	0.93
6		0.88	0.24	0.69
7		0.71	0.21	0.61
8				0.91
X	0.456	0.840	0.291	0.759
SEM	0.0410	0.0641	0.0321	0.0675

Two-Way ANOVA			
Source of Variation	P value	P value summary	Significance
Interaction	0.4746	ns	No
Mouse Model	0.0452	*	Yes
Genotype/Training	< 0.0001	****	Yes

Post-Hoc Test				
Bonferroni	Mean Diff.	t-value	P-value	Summary
WT:UT vs. WT:T	-0.3841	4.429	≤ 0.01	**
WT:UT vs. KO:UT	0.1646	1.898	> 0.05	ns
WT:UT vs. KO:T	-0.3036	3.596	≤ 0.01	**
WT:T vs. KO:UT	0.5487	6.931	≤ 0.001	****
WT:T vs. KO:T	0.08049	1.050	> 0.05	ns
KO:UT vs. KO:T	-0.4682	6.108	≤ 0.001	****

Unpaired T-test- WT UT versus KO UT	
P value	0.0094
P value summary	††
Significantly different? (P<0.05)	Yes

Figure 3H: Post-training whole muscle Tfam protein

Whole Muscle Tfam Protein Expression - Muscle Specific Mice				
	WT		mKO	
N	UT	T	UT	T
1	0.56	0.55	0.47	0.72
2	0.52	0.65	0.31	0.80
3	0.74	0.75	0.59	0.92
4	0.71	0.53	0.30	0.91
5	0.43	0.78	0.49	0.95
6	0.47	0.88	0.33	0.89
7				0.81
X	0.573	0.691	0.414	0.855
SEM	0.0512	0.0559	0.0479	0.0314

Two-Way ANOVA			
Source of Variation	P value	P value summary	Significance
Interaction	0.0023	**	Yes
Mouse Model	0.9634	ns	No
Genotype/Training	< 0.0001	****	Yes

Post-Hoc Test				
Bonferroni	Mean Diff.	t-value	P-value	Summary
WT:UT vs. WT:T	-0.1180	1.762	> 0.05	ns
WT:UT vs. KO:UT	0.1594	2.381	> 0.05	ns
WT:UT vs. KO:T	-0.2818	4.366	≤ 0.01	**
WT:T vs. KO:UT	0.2774	4.143	≤ 0.01	**
WT:T vs. KO:T	-0.1637	2.537	> 0.05	ns
KO:UT vs. KO:T	-0.4412	6.837	≤ 0.001	****

Unpaired T-test- WT UT versus WT T	
P value	0.1505
P value summary	ns
Significantly different? (P<0.05)	No

Unpaired T-test- WT UT versus KO UT	
P value	0.0462
P value summary	†
Significantly different? (P<0.05)	Yes

Figure 4A: Post-training state 4 (basal) respiration in SS mitochondria

State 4 Respiration (natoms O₂/mg protein/min) – SS Mitochondria- Muscle Specific Mice				
	WT		mKO	
N	UT	T	UT	T
1	4.08	2.63	3.05	7.75
2	3.26	3.54	7.49	8.48
3	4.87	8.87	2.82	7.80
4	1.28	3.96	2.43	11.15
5	3.06	11.01	3.23	8.39
6	1.67	10.68	6.32	11.07
7	3.26			8.18
X	3.069	6.782	4.223	8.974
SEM	0.476	1.561	0.868	0.561

Two-Way ANOVA			
Source of Variation	P value	P value summary	Significance
Interaction	0.5755	ns	No
Mouse Model	0.0803	ns	No
Genotype/Training	0.0001	***	Yes

Post-Hoc Test				
Bonferroni	Mean Diff.	t-value	P-value	Summary
WT:UT vs. WT:T	-3.713	2.876	> 0.05	ns
WT:UT vs. KO:UT	-1.155	0.8944	> 0.05	ns
WT:UT vs. KO:T	-5.906	4.761	≤ 0.005	***
WT:T vs. KO:UT	2.558	1.909	> 0.05	ns
WT:T vs. KO:T	-2.193	1.698	> 0.05	ns
KO:UT vs. KO:T	-4.751	3.680	≤ 0.01	**

Unpaired T-test – WT UT versus WT T	
P value	0.0331
P value summary	*
Significantly different? (P<0.05)	Yes

Unpaired T-test – WT UT versus KO UT	
P value	0.2499
P value summary	ns
Significantly different? (P<0.05)	No

Figure 4B: Post-training state 4 (basal) respiration in IMF mitochondria

State 4 Respiration (natoms O₂/mg protein/min) – IMF Mitochondria - Muscle Specific Mice				
	WT		mKO	
N	UT	T	UT	T
1	16.12	23.62	12.68	27.73
2	6.77	19.64	16.96	19.67
3	4.12	6.04	15.10	13.61
4	5.61	19.13	10.36	13.05
5	10.39	14.11	10.19	12.55
6	12.46	9.24	11.77	27.66
7			16.20	14.64
X	9.245	15.297	13.323	18.416
SEM	1.867	2.748	1.047	2.556

Two-Way ANOVA			
Source of Variation	P value	P value summary	Significance
Interaction	0.8249	ns	No
Mouse Model	0.1069	ns	No
Genotype/Training	0.0162	*	Yes

Post-Hoc Test				
Bonferroni	Mean Diff.	t-value	P-value	Summary
WT:UT vs. WT:T	-6.052	1.926	> 0.05	ns
WT:UT vs. KO:UT	-4.078	1.347	> 0.05	ns
WT:UT vs. KO:T	-9.171	3.029	≤ 0.05	*
WT:T vs. KO:UT	1.974	0.6519	> 0.05	ns
WT:T vs. KO:T	-3.119	1.030	> 0.05	ns
KO:UT vs. KO:T	-5.093	1.751	> 0.05	ns

Unpaired T-test – WT UT versus WT T	
P value	0.0985
P value summary	ns
Significantly different? (P<0.05)	No

Unpaired T-test – WT UT versus KO UT	
P value	0.0732
P value summary	ns
Significantly different? (P<0.05)	No

Unpaired T-test – KO UT versus KO T	
P value	0.0900
P value summary	ns
Significantly different? (P<0.05)	No

Figure 4C: Post-training state 3 (active) respiration in SS mitochondria

State 3 Respiration (natoms O₂/mg protein/min) – SS Mitochondria - Muscle Specific Mice				
	WT		mKO	
N	UT	T	UT	T
1	8.53	84.37	31.93	42.97
2	10.89	91.41	34.80	47.79
3	17.80	55.31	13.20	48.98
4	12.01	67.38	25.16	26.79
5	16.16	30.21	11.91	47.67
6	12.82	50.28	40.79	47.03
X	13.035	63.160	26.298	43.538
SEM	1.396	9.271	4.809	3.453

Two-Way ANOVA			
Source of Variation	P value	P value summary	Significance
Interaction	0.0076	**	Yes
Mouse Model	0.5728	ns	No
Genotype/Training	< 0.0001	****	Yes

Post-Hoc Test				
Bonferroni	Mean Diff.	t-value	P-value	Summary
WT:UT vs. WT:T	-50.13	6.392	≤ 0.001	****
WT:UT vs. KO:UT	-13.26	1.691	> 0.05	ns
WT:UT vs. KO:T	-30.50	3.890	≤ 0.01	**
WT:T vs. KO:UT	36.86	4.701	≤ 0.005	***
WT:T vs. KO:T	19.62	2.502	> 0.05	ns
KO:UT vs. KO:T	-17.24	2.199	> 0.05	ns

Unpaired T-test – KO UT versus KO T	
P value	0.0155
P value summary	†
Significantly different? (P<0.05)	Yes

Unpaired T-test – MS WT UT versus KO UT	
P value	0.0244
P value summary	*
Significantly different? (P<0.05)	Yes

Figure 4D: Post-training state 3 (active) respiration in IMF mitochondria

State 3 Respiration (natoms O2/mg protein/min) – IMF Mitochondria - Muscle Specific Mice				
	WT		mKO	
N	UT	T	UT	T
1	106.21	66.68	88.48	67.67
2	122.63	111.53	87.14	107.29
3	94.36	90.78	79.44	103.95
4	110.43	90.34	86.33	102.55
5	120.03	105.65	78.36	130.77
6	71.54	74.30	46.20	91.83
7	73.03			157.57
X	99.747	89.880	77.658	108.804
SEM	7.912	7.070	6.520	10.808

Two-Way ANOVA			
Source of Variation	P value	P value summary	Significance
Interaction	0.0249	*	Yes
Mouse Model	0.8543	ns	No
Genotype/Training	0.2247	ns	No

Post-Hoc Test				
Bonferroni	Mean Diff.	t-value	P-value	Summary
WT:UT vs. WT:T	9.867	0.8193	> 0.05	ns
WT:UT vs. KO:UT	22.09	1.834	> 0.05	ns
WT:UT vs. KO:T	-9.057	0.7827	> 0.05	ns
WT:T vs. KO:UT	12.22	0.9779	> 0.05	ns
WT:T vs. KO:T	-18.92	1.571	> 0.05	ns
KO:UT vs. KO:T	-31.15	2.586	> 0.05	ns

Unpaired T-test – WT UT versus WT T	
P value	0.3796
P value summary	ns
Significantly different? (P<0.05)	No

Unpaired T-test – KO UT versus KO T	
P value	0.0377
P value summary	*
Significantly different? (P<0.05)	Yes

Unpaired T-test – MS WT UT versus KO UT	
P value	0.0549
P value summary	†
Significantly different? (P<0.05)	Yes

Figure 5A: Post-training state 4 (basal) reactive oxygen species (ROS) in SS mitochondria

State 4 ROS (natoms O₂/mg protein/min) – SS Mitochondria - Muscle Specific Mice				
WT			mKO	
N	UT	T	UT	T
1	56.33	19.14	32.69	30.67
2	8.58	32.07	36.12	25.32
3	50.22	9.38	36.87	30.52
4	20.80	28.67	43.90	22.53
5	47.18	22.45	62.50	16.15
6	58.54	22.18	187.55	30.91
7			148.74	16.64
8				30.95
X	40.275	22.315	78.339	25.461
SEM	8.410	3.230	23.858	2.259

Two-Way ANOVA			
Source of Variation	P value	P value summary	Significance
Interaction	0.1987	ns	No
Mouse Model	0.1319	ns	No
Genotype/Training	0.0132	*	Yes

Post-Hoc Test				
Bonferroni	Mean Diff.	t-value	P-value	Summary
WT:UT vs. WT:T	17.96	0.9143	> 0.05	ns
WT:UT vs. KO:UT	-38.06	2.011	> 0.05	ns
WT:UT vs. KO:T	14.81	0.8062	> 0.05	ns
WT:T vs. KO:UT	-56.02	2.960	> 0.05	*
WT:T vs. KO:T	-3.146	0.1712	> 0.05	ns
KO:UT vs. KO:T	52.88	3.003	> 0.05	*

Unpaired T-test – WT UT versus WT T	
P value	0.0742
P value summary	ns
Significantly different? (P<0.05)	No

Unpaired T-test – WT UT versus KO UT	
P value	0.1872
P value summary	ns
Significantly different? (P<0.05)	No

Figure 5B: Post-training state 4 (basal) reactive oxygen species (ROS) in IMF mitochondria

State 4 ROS (natoms O₂/mg protein/min) – IMF Mitochondria- Muscle Specific Mice				
	WT		mKO	
N	UT	T	UT	T
1	5.83	1.51	10.27	3.09
2	6.24	5.46	5.31	2.50
3	10.07	6.74	5.67	6.52
4	11.93	3.49	8.29	5.68
5	7.06	4.78	10.75	4.95
6	2.59	11.82	17.61	9.05
7			16.26	2.92
8			25.46	2.70
X	7.287	5.633	12.453	4.676
SEM	1.350	1.436	2.436	0.822

Two-Way ANOVA			
Source of Variation	P value	P value summary	Significance
Interaction	0.0877	ns	No
Mouse Model	0.2329	ns	No
Genotype/Training	0.0114	*	Yes

Post-Hoc Test				
Bonferroni	Mean Diff.	t-value	P-value	Summary
WT:UT vs. WT:T	1.653	0.6359	> 0.05	ns
WT:UT vs. KO:UT	-5.166	2.124	> 0.05	ns
WT:UT vs. KO:T	2.610	1.073	> 0.05	ns
WT:T vs. KO:UT	-6.819	2.804	> 0.05	ns
WT:T vs. KO:T	0.9571	0.3936	> 0.05	ns
KO:UT vs. KO:T	7.776	3.454	≤ 0.05	*

Unpaired T-test – WT UT versus WT T	
P value	0.4211
P value summary	ns
Significantly different? (P<0.05)	No

Unpaired T-test – WT UT versus KO UT	
P value	0.1179
P value summary	ns
Significantly different? (P<0.05)	No

Figure 5C: Post-training state 3 (active) reactive oxygen species (ROS) in SS mitochondria

State 3 ROS (natoms O ₂ /mg protein/min) – SS Mitochondria - Muscle Specific Mice				
	WT		mKO	
N	UT	T	UT	T
1	1.91	7.07	6.56	3.41
2	11.94	7.32	5.36	2.85
3	3.91	1.91	5.81	2.49
4	16.04	1.33	9.40	3.01
5	10.95	1.35	5.70	4.23
6	12.26	1.19	8.99	5.00
7		7.72	8.66	5.81
8		4.22		2.89
X	9.502	4.014	7.211	3.711
SEM	2.216	1.042	0.657	0.419

Two-Way ANOVA			
Source of Variation	P value	P value summary	Significance
Interaction	0.3953	ns	No
Mouse Model	0.2700	ns	No
Genotype/Training	0.0006	***	Yes

Post-Hoc Test				
Bonferroni	Mean Diff.	t-value	P-value	Summary
WT:UT vs. WT:T	5.488	3.307	≤ 0.05	*
WT:UT vs. KO:UT	2.290	1.340	> 0.05	ns
WT:UT vs. KO:T	5.790	3.489	≤ 0.05	*
WT:T vs. KO:UT	-3.198	2.011	> 0.05	ns
WT:T vs. KO:T	0.3025	0.1969	> 0.05	ns
KO:UT vs. KO:T	3.500	2.201	> 0.05	ns

Unpaired T-test – KO UT versus KO T	
P value	0.0005
P value summary	***
Significantly different? (P<0.05)	Yes

Unpaired T-test – WT UT versus KO UT	
P value	0.3112
P value summary	ns
Significantly different? (P<0.05)	No

Figure 5D: Post-training state 3 (active) reactive oxygen species (ROS) in IMF mitochondria

State 3 ROS (natoms O₂/mg protein/min) – IMF Mitochondria - Muscle Specific Mice				
	WT		mKO	
N	UT	T	UT	T
1	0.78	0.68	1.19	0.63
2	0.60	0.69	1.05	0.60
3	0.85	0.90	1.09	0.65
4	0.66	0.48	1.38	0.53
5	0.40	0.39	1.58	0.66
6	1.38	1.31	1.35	1.03
7	0.94		3.80	0.39
8	0.35		1.15	0.51
X	0.745	0.742	1.574	0.625
SEM	0.116	0.135	0.324	0.0660

Two-Way ANOVA			
Source of Variation	P value	P value summary	Significance
Interaction	0.0237	*	Yes
Mouse Model	0.0818	ns	No
Genotype/Training	0.0228	*	Yes

Post-Hoc Test				
Bonferroni	Mean Diff.	t-value	P-value	Summary
WT:UT vs. WT:T	0.003333	0.01155	> 0.05	ns
WT:UT vs. KO:UT	-0.8288	3.101	≤ 0.05	†
WT:UT vs. KO:T	0.1200	0.4491	> 0.05	ns
WT:T vs. KO:UT	-0.8321	2.883	≤ 0.05	*
WT:T vs. KO:T	0.1167	0.4042	> 0.05	ns
KO:UT vs. KO:T	0.9488	3.550	≤ 0.01	**

Figure 6: mRNA expression (ΔC_t) of genes examined basally in the absence of p53, under the influence of training, and training reversal of basal p53-induced deficits

p53 mRNA – Muscle Specific Mice		
WT		
N	UT	T
1	4.32	2.74
2	3.99	3.47
3	3.96	1.74
4	3.81	3.62
5	3.53	1.43
6	3.85	1.25
7		2.90
8		3.67
9		1.033
10		1.43
X	3.910	2.327
SEM	0.106	0.334

Unpaired T-test – p53 WT UT versus WT T	
P value	0.0031
P value summary	**
Significantly different? (P<0.05)	Yes

p21 mRNA – Muscle Specific Mice				
WT			mKO	
N	UT	T	UT	T
1	6.53	3.50	3.50	6.04
2	6.66	2.99	4.71	5.41
3	4.61	4.40	4.69	3.65
4	5.38	3.74	4.20	3.81
5	4.90	3.69	4.76	5.79
6		2.92	3.73	7.08
7		4.35	4.41	5.09
8		2.70	1.93	6.65
9			4.68	
X	5.614	3.536	4.068	5.441
SEM	0.419	0.226	0.307	0.436

Unpaired T-test – p21 WT UT versus WT T	
P value	0.0006
P value summary	***
Significantly different? (P<0.05)	Yes

Unpaired T-test – p21 WT UT versus KO UT	
P value	0.0112
P value summary	†
Significantly different? (P<0.05)	Yes

Unpaired T-test – p21 KO UT versus KO T	
P value	0.0193
P value summary	*
Significantly different? (P<0.05)	Yes

Bax mRNA – Muscle Specific Mice				
N	WT		mKO	
	UT	T	UT	T
1	8.81	5.18	4.78	4.93
2	7.48	6.48	5.33	4.54
3	8.00	7.21	4.11	4.21
4	9.00	7.20	5.30	4.93
5	8.00	6.64	6.09	2.08
6		7.16	4.79	2.28
7		6.90	6.02	2.34
8		6.93	4.86	2.34
9			4.38	2.59
10			4.97	
X	8.260	6.712	5.065	3.361
SEM	0.282	0.239	0.202	0.417

Unpaired T-test – Bax WT UT versus WT T	
P value	0.0017
P value summary	**
Significantly different? (P<0.05)	Yes

Unpaired T-test – Bax WT UT versus KO UT	
P value	< 0.0001
P value summary	††††
Significantly different? (P<0.05)	Yes

Unpaired T-test – Bax KO UT versus KO T	
P value	0.0014
P value summary	**
Significantly different? (P<0.05)	Yes

TIGAR mRNA – Muscle Specific Mice				
N	WT		mKO	
	UT	T	UT	T
1	3.70	3.22	6.72	5.49
2	4.90	4.19	5.25	5.84
3	4.40	3.62	5.59	5.38
4	3.84	4.14	5.98	5.84
5	3.93	4.50	6.36	5.70
6	3.75	3.85	6.91	2.99
7		3.64	5.90	3.22
8		2.00	5.17	
9		2.62	5.17	
10			3.18	
11			3.16	
X	4.089	3.533	5.398	4.922
SEM	0.193	0.267	0.377	0.475

Unpaired T-test – TIGAR WT UT versus WT T	
P value	0.1524
P value summary	ns
Significantly different? (P<0.05)	No

Unpaired T-test – TIGAR WT UT versus KO UT	
P value	0.0276
P value summary	†
Significantly different? (P<0.05)	Yes

Unpaired T-test – TIGAR KO UT versus KO T	
P value	0.4428
P value summary	ns
Significantly different? (P<0.05)	No

Mdm2 mRNA – Muscle Specific Mice					
		WT		mKO	
N	UT	T	UT	T	
1	3.41	2.28	2.84	2.84	
2	3.72	2.50	2.78	2.63	
3	3.37	3.02	2.58	2.46	
4	3.01	3.99	3.21	2.56	
5	2.86	3.50	2.47	3.53	
6	2.21	3.06	2.92	3.23	
7		3.21	3.03	3.25	
8		1.36		1.52	
9		1.85		1.80	
X	3.098	2.752	2.834	2.648	
SEM	0.217	0.277	0.0953	0.221	

Unpaired T-test – Mdm2 WT UT versus WT T	
P value	0.3842
P value summary	ns
Significantly different? (P<0.05)	No

Unpaired T-test – Mdm2 WT UT versus KO UT	
P value	0.2649
P value summary	ns
Significantly different? (P<0.05)	No

Unpaired T-test – Mdm2 KO UT versus KO T	
P value	0.4957
P value summary	ns
Significantly different? (P<0.05)	No

Tfam mRNA – Muscle Specific Mice					
		WT		mKO	
N	UT	T	UT	T	
1	6.38	5.19	3.84	3.93	
2	6.52	5.67	3.71	3.69	
3	6.93	5.42	3.55	3.76	
4	6.86	6.76	4.07	4.72	
5	6.32	6.88	3.85	3.72	
6	5.53	5.57	3.71	4.06	
7		5.04	3.33	4.90	
8			3.56	5.95	
9			2.10	3.12	
10			2.61	4.52	
11			1.05		
X	6.425	5.790	3.216	4.237	
SEM	0.206	0.278	0.279	0.256	

Unpaired T-test – Tfam WT UT versus WT T	
P value	0.1023
P value summary	ns
Significantly different? (P<0.05)	No

Unpaired T-test – Tfam WT UT versus KO UT	
P value	< 0.0001
P value summary	††††
Significantly different? (P<0.05)	Yes

Unpaired T-test – Tfam KO UT versus KO T	
P value	0.0148
P value summary	*
Significantly different? (P<0.05)	Yes

SCO2 mRNA – Muscle Specific Mice				
WT		mKO		
N	UT	T	UT	T
1	1.76	1.22	5.11	6.53
2	1.83	1.49	5.84	5.70
3	1.61	1.90	5.85	6.42
4	1.40	1.86	4.85	7.64
5	1.62	1.88	6.70	7.23
6		1.86	6.95	6.34
7		2.17	4.46	6.53
8		1.27	4.76	6.46
9		1.32	6.00	5.92
10		1.34		
X	1.645	1.631	5.614	6.531
SEM	0.0747	0.107	0.292	0.199

Unpaired T-test – SCO2 WT UT versus WT T	
P value	0.9306
P value summary	ns
Significantly different? (P<0.05)	No

Unpaired T-test – SCO2 WT UT versus KO UT	
P value	< 0.0001
P value summary	††††
Significantly different? (P<0.05)	Yes

Unpaired T-test – SCO2 KO UT versus KO T	
P value	0.0194
P value summary	*
Significantly different? (P<0.05)	Yes

p62 mRNA – Muscle Specific Mice				
WT		mKO		
N	UT	T	UT	T
1	5.68	5.21	5.34	4.75
2	5.38	5.51	4.85	3.78
3	5.64	5.47	4.31	5.34
4	6.05	5.95	5.10	4.17
5	5.51	5.91	4.59	4.89
6		5.04	4.57	5.36
7		5.76	4.29	5.92
8			3.43	5.61
9			3.26	4.75
10			5.73	4.76
X	5.655	5.550	4.548	4.934
SEM	0.113	0.131	0.246	0.205

Unpaired T-test – p62 WT UT versus WT T	
P value	0.5791
P value summary	ns
Significantly different? (P<0.05)	No

Unpaired T-test – p62 WT UT versus KO UT	
P value	0.0093
P value summary	††
Significantly different? (P<0.05)	Yes

Unpaired T-test – p62 KO UT versus KO T	
P value	0.2440
P value summary	ns
Significantly different? (P<0.05)	No

LC3 mRNA – Muscle Specific Mice				
		WT		mKO
N	UT	T	UT	T
1	4.93	4.37	3.30	2.92
2	6.66	4.39	1.86	3.17
3	4.70	4.77	2.67	3.85
4	3.51	4.50	2.91	3.89
5	4.51	6.69	3.05	3.69
6		5.81	2.85	3.70
7		4.19	3.01	3.58
8		4.69	2.84	3.85
9			2.86	3.02
10			2.50	3.21
11			1.83	
X	4.863	4.927	2.699	3.487
SEM	0.510	0.307	0.141	0.117

Unpaired T-test – LC3 WT UT versus WT T	
P value	0.9116
P value summary	ns
Significantly different? (P<0.05)	No

Unpaired T-test – LC3 WT UT versus KO UT	
P value	< 0.0001
P value summary	††††
Significantly different? (P<0.05)	Yes

Unpaired T-test – LC3 KO UT versus KO T	
P value	0.0004
P value summary	***
Significantly different? (P<0.05)	Yes

PGC-1 α mRNA – Muscle Specific Mice				
		WT		mKO
N	UT	T	UT	T
1	5.76	6.29	4.64	7.27
2	5.56	4.43	3.92	5.70
3	4.46	4.70	5.44	6.99
4	5.08	5.53	5.42	6.59
5	5.20	5.81	4.74	5.55
6		6.31	5.45	5.36
7		4.66	4.58	8.31
8			2.83	7.88
9			5.11	
10			1.28	
X	5.212	5.391	4.342	6.706
SEM	0.225	0.299	0.426	0.390

Unpaired T-test – PGC-1 α WT UT versus WT T	
P value	0.6668
P value summary	ns
Significantly different? (P<0.05)	No

Unpaired T-test – PGC-1 α WT UT versus KO UT	
P value	0.1921
P value summary	ns
Significantly different? (P<0.05)	No

Unpaired T-test – PGC-1 α KO UT versus KO T	
P value	0.0010
P value summary	**
Significantly different? (P<0.05)	Yes

Figure 6A: mRNA expression of genes in response to exercise training in WT mice, expressed as fold change

mRNA WT T/ mRNA WT UT (Fold Change) - Muscle Specific Mice										
N	p53	p21	Bax	TIGAR	Mdm2	Tfam	p62	SCO2	LC3	PGC-1α
1	0.70	0.62	0.63	0.79	0.73	0.81	0.92	0.74	0.90	1.21
2	0.89	0.53	0.78	1.026	0.81	0.88	0.97	0.91	0.90	0.85
3	0.45	0.78	0.87	0.88	0.98	0.84	0.97	1.15	0.98	0.90
4	0.92	0.67	0.87	1.014	1.29	1.052	1.053	1.13	0.93	1.060
5	0.37	0.66	0.80	1.099	1.13	1.071	1.044	1.14	1.38	1.12
6	0.32	0.52	0.87	0.94	0.99	0.87	0.89	1.13	1.19	1.21
7	0.74	0.77	0.84	0.89	1.04	0.78	1.019	1.32	0.86	0.89
8	0.94	0.48	0.84	0.49	0.44			0.77	0.96	
9	0.26			0.64	0.60			0.80		
10	0.36							0.82		
X	0.595	0.630	0.813	0.864	0.890	0.901	0.981	0.991	1.0130	1.0344
SEM	0.0854	0.0403	0.0289	0.0653	0.0892	0.0432	0.0231	0.0650	0.0631	0.0575
Δ	↓1.405	↓1.370	↓1.187	↓1.136	↓1.110	↓1.099	↓1.019	↓1.009	↑1.013	↑1.034

Figure 6B: mRNA expression of genes in the absence of p53 basally, and the response of training on restoring deficits induced by the absence of p53 basally; expressed as fold change

mRNA KO UT/ mRNA WT UT and mRNA KO T/mRNA WT T – Muscle Specific Mice																		
N	p21		Bax		TIGAR		Mdm2		Tfam		p62		SCO2		LC3		PGC-1α	
	KO UT	KO T	KO UT	KO T	KO UT	KO T	KO UT	KO UT	KO UT	KO T	KO UT	KO T	KO UT	KO T	KO UT	KO T	KO UT	KO T
1	0.62	1.077	0.58	0.60	1.64	1.34	0.92	0.92	0.60	0.61	0.94	0.84	3.11	3.97	0.68	0.60	0.89	1.39
2	0.84	0.96	0.65	0.55	1.29	1.43	0.90	0.85	0.58	0.57	0.86	0.67	3.55	3.46	0.38	0.65	0.75	1.09
3	0.84	0.65	0.50	0.51	1.37	1.32	0.83	0.79	0.55	0.59	0.76	0.95	3.55	3.90	0.55	0.79	1.04	1.34
4	0.75	0.68	0.64	0.60	1.46	1.43	1.04	0.83	0.63	0.74	0.90	0.74	2.95	4.65	0.60	0.80	1.04	1.27
5	0.85	1.031	0.74	0.25	1.56	1.39	0.80	1.14	0.60	0.58	0.81	0.87	4.07	4.40	0.63	0.76	0.91	1.07
6	0.66	1.26	0.58	0.28	1.69	0.73	0.94	1.04	0.58	0.63	0.81	0.95	4.23	3.86	0.59	0.76	1.05	1.03
7	0.79	0.91	0.73	0.28	1.44	0.79	0.98	1.05	0.52	0.76	0.76	1.05	2.71	3.97	0.62	0.74	0.88	1.60
8	0.34	1.19	0.59	0.28	1.27			0.49	0.55	0.93	0.61	0.99	2.89	3.93	0.58	0.79	0.54	1.51
9	0.83		0.53	0.31	1.26			0.58	0.33	0.49	0.58	0.84	3.65	3.60	0.60	0.62	0.98	
10			0.60		0.78				0.41	0.70	1.01	0.84			0.51	0.66	0.25	
11					0.77				0.16						0.38			
X	0.725	0.969	0.613	0.407	1.321	1.204	0.915	0.855	0.501	0.659	0.804	0.873	3.412	3.970	0.555	0.717	0.833	1.287
SEM	0.055	0.078	0.025	0.051	0.092	0.116	0.031	0.072	0.043	0.040	0.044	0.036	0.177	0.121	0.029	0.024	0.082	0.075
Δ	↓1.28	↓1.03	↓1.39	↓1.59	↑1.32	↑1.20	↓1.09	↓1.15	↓1.50	↓1.34	↓1.20	↓1.13	↑3.41	↑3.97	↓1.45	↓1.28	↓1.17	↑1.29

Figure 7A: Post-training whole muscle Mdm2 protein

Whole Muscle - Mdm2 Protein - Muscle Specific Mice				
	WT		mKO	
N	UT	T	UT	T
1	0.32	0.69	0.34	0.65
2	0.48	0.48	0.46	0.94
3	0.40	0.44	0.40	0.63
4	0.19	0.47	0.34	0.74
5	0.44	0.55	0.22	0.73
6	0.18	0.74		
X	0.336	0.561	0.352	0.738
SEM	0.0519	0.0510	0.0395	0.0542

Two-Way ANOVA			
Source of Variation	P value	P value summary	Significance
Interaction	0.1267	ns	No
Mouse Model	0.0712	ns	No
Genotype/Training	< 0.0001	****	Yes

Post-Hoc Test				
Bonferroni	Mean Diff.	t-value	P-value	Summary
WT:UT vs. WT:T	-0.2253	3.320	≤ 0.05	*
WT:UT vs. KO:UT	-0.01588	0.2232	> 0.05	ns
WT:UT vs. KO:T	-0.4024	5.654	≤ 0.005	***
WT:T vs. KO:UT	0.2094	2.943	> 0.05	ns
WT:T vs. KO:T	-0.1771	2.488	> 0.05	ns
KO:UT vs. KO:T	-0.3865	5.199	≤ 0.005	***

Figure 7B: Post-training whole muscle CHCHD4 protein

Whole Muscle - CHCHD4 Protein - Muscle Specific Mice				
	WT		mKO	
N	UT	T	UT	T
1	0.44	0.84	0.22	0.99
2	0.33	0.67	0.38	0.73
3	0.45	0.65	0.19	0.98
4	0.54	0.67	0.16	1.84
5	0.58	0.71	0.18	0.70
6		0.60		
X	0.469	0.688	0.226	1.0492
SEM	0.0431	0.0336	0.0386	0.206

Two-Way ANOVA			
Source of Variation	P value	P value summary	Significance
Interaction	0.0096	**	Yes
Mouse Model	0.5762	ns	No
Genotype/Training	0.0001	***	Yes

Post-Hoc Test				
Bonferroni	Mean Diff.	t-value	P-value	Summary
WT:UT vs. WT:T	-0.2190	1.530	> 0.05	ns
WT:UT vs. KO:UT	0.2430	1.625	> 0.05	ns
WT:UT vs. KO:T	-0.5799	3.879	≤ 0.01	**
WT:T vs. KO:UT	0.4620	3.227	≤ 0.05	*
WT:T vs. KO:T	-0.3609	2.521	> 0.05	ns
KO:UT vs. KO:T	-0.8229	5.504	≤ 0.005	***

Unpaired T-test- WT UT versus WT T	
P value	0.0028
P value summary	**
Significantly different? (P<0.05)	Yes

Unpaired T-test- WT UT versus KO UT	
P value	0.0030
P value summary	††
Significantly different? (P<0.05)	Yes

Figure 8A: Post-training cytochrome c protein release from SS mitochondria under basal conditions

Cytochrome C Protein Release – Basal – SS Mitochondrial - Muscle Specific Mice				
N	WT		mKO	
	UT	T	UT	T
1	639.36	635.94	2459.55	887.55
2	1087.31	1021.79	1042.72	1048.89
3	1000.00	1674.26	1129.84	739.48
4	1044.012	1020.21	1340.31	1110.96
5	1024.033	1475.38	1719.96	704.21
6	757.033		2238.96	1065.89
7			1519.79	836.50
8			1911.43	2252.13
X	925.290	1165.513	1670.319	1080.701
SEM	74.329	183.991	180.495	175.740

One-Way ANOVA	
P value	0.0195
P value summary	*
Significantly different? (P<0.05)	Yes

Post-Hoc Test				
Bonferroni	Mean Diff.	t-value	P-value	Summary
WT UT versus WT T	-240.2	0.9074	> 0.05	ns
WT UT versus KO UT	-745	3.155	≤ 0.05	†
WT UT versus KO T	-155.4	0.6582	> 0.05	ns
WT T versus KO UT	-504.8	2.025	> 0.05	ns
WT T versus KO T	84.81	0.3403	> 0.05	ns
KO UT versus KO T	589.6	2.697	> 0.05	ns

Unpaired T-test – KO UT versus KO T	
P value	0.0346
P value summary	*
Significantly different? (P<0.05)	Yes

Figure 8B: Post-training cytochrome c protein release from IMF mitochondria under basal conditions

Cytochrome C Protein Release - Basal - IMF Mitochondria – Muscle Specific Mice				
	WT		mKO	
N	UT	T	UT	T
1	14777.075	4417.15	11805.23	8125.28
2	10879.30	13339.98	876.77	8153.28
3	5276.39	8788.91	8269.96	8690.47
4	10847.033	13100.61	7693.74	11403.33
5	12690.50	10239.98	15333.42	9175.10
6	16205.13	15551.18	840.96	18378.42
7	13608.81	2707.55	10962.15	15938.78
8		1727.67	10698.42	13659.49
9			2861.15	958.89
10			790.69	1353.72
11			9118.45	
12			3422.40	
13			1381.96	
14			11137.79	
X	12040.605	8734.129	6799.506	9583.675
SEM	1347.328	1856.789	1327.0812	1779.248

One-Way ANOVA	
P value	0.1636
P value summary	ns
Significantly different? (P<0.05)	No

Post-Hoc Test				
Bonferroni	Mean Diff.	t-value	P-value	Summary
WT UT versus WT T	3306	1.278	> 0.05	ns
WT UT versus KO UT	5241	2.265	> 0.05	ns
WT UT versus KO T	2457	0.9973	> 0.05	ns
WT T versus KO UT	1935	0.8731	> 0.05	ns
WT T versus KO T	-849.5	0.3583	> 0.05	ns
KO UT versus KO T	-2784	1.345	> 0.05	ns

Unpaired T-test - WT UT versus KO UT	
P value	0.0228
P value summary	†
Significantly different? (P<0.05)	Yes

Figure 8C: Post-training cytochrome c protein release from SS mitochondria treated with apoptotic stimulus (H₂O₂), presented as fold change

Cytochrome C Protein Release - Treated/Control - SS Mitochondria – Muscle Specific Mice				
	WT		mKO	
N	UT	T	UT	T
1	11.063	3.22	2.14	1.12
2	5.13	2.63	5.73	1.70
3	2.29	2.33	1.58	3.27
4	10.80	9.39	8.15	1.75
5	11.60	4.42	7.98	1.022
6	6.45	5.75	1.79	4.32
7			1.73	
8			8.076	
9			10.66	
10			7.41	
X	7.888	4.624	5.524	2.197
SEM	1.564	1.0830	1.0783	0.536

One-Way ANOVA	
P value	0.0276
P value summary	*
Significantly different? (P<0.05)	Yes

Post-Hoc Test				
Bonferroni	Mean Diff.	t-value	P-value	Summary
WT UT versus WT T	3.263	1.859	> 0.05	ns
WT UT versus KO UT	2.364	1.506	> 0.05	ns
WT UT versus KO T	5.69	3.242	≤ 0.05	*
WT T versus KO UT	-0.8998	0.5732	> 0.05	ns
WT T versus KO T	2.427	1.383	> 0.05	ns
KO UT versus KO T	3.327	2.119	> 0.05	ns

Unpaired T-test – KO UT versus KO T	
P value	0.0399
P value summary	*
Significantly different? (P<0.05)	Yes

Unpaired T-test – WT UT versus WT T	
P value	0.1170
P value summary	ns
Significantly different? (P<0.05)	No

Figure 8D: Post-training cytochrome c protein release from IMF mitochondria treated with apoptotic stimulus (H₂O₂), presented as fold change

Cytochrome C Protein Release - Treated/Control - IMF Mitochondria - Muscle Specific Mice				
	WT		mKO	
N	UT	T	UT	T
1	1.19	4.20	1.24	2.56
2	1.61	1.31	2.21	1.54
3	1.75	2.26	1.95	2.97
4	1.69	1.22	1.27	1.16
5	1.19	2.13	6.50	1.53
6	1.23	1.32	1.49	16.74
7			1.52	
8			4.90	
9			8.00	
10			1.38	
11			8.076	
12			1.84	
X	1.443	2.0717	3.362	4.417
SEM	0.110	0.464	0.785	2.481

One-Way ANOVA	
P value	0.3852
P value summary	ns
Significantly different? (P<0.05)	No

Post-Hoc Test				
Bonferroni	Mean Diff.	t-value	P-value	Summary
WT UT versus WT T	-0.6284	0.3361	> 0.05	ns
WT UT versus KO UT	-1.919	1.185	> 0.05	ns
WT UT versus KO T	-2.974	1.59	> 0.05	ns
WT T versus KO UT	-1.291	0.797	> 0.05	ns
WT T versus KO T	-2.345	1.254	> 0.05	ns
KO UT versus KO T	-1.055	0.6514	> 0.05	ns

Unpaired T-test –WT UT versus KO UT	
P value	0.1087
P value summary	ns
Significantly different? (P<0.05)	No

Unpaired T-test –WT UT versus WT T	
P value	0.2165
P value summary	ns
Significantly different? (P<0.05)	No

Figure 8F: Post-training whole muscle Bax protein

Whole Muscle - Bax Protein - Muscle Specific Mice				
	WT		mKO	
N	UT	T	UT	T
1	0.31	0.5	0.59	0.57
2	0.2	0.29	0.64	0.31
3	0.38	0.24	0.65	0.32
4	0.11	0.41	0.49	0.38
5		0.27	0.64	0.11
6		0.59	0.5	0.32
X	0.25	0.383	0.585	0.335
SEM	0.0596	0.0575	0.0297	0.0603

Two-Way ANOVA			
Source of Variation	P value	P value summary	Significance
Interaction	0.0022	**	Yes
Mouse Model	0.0157	*	Yes
Genotype/Training	0.2920	ns	No

Post-Hoc Test				
Bonferroni	Mean Diff.	t-value	P-value	Summary
WT:UT vs. WT:T	-0.1333	1.664	> 0.05	ns
WT:UT vs. KO:UT	-0.3350	4.182	≤ 0.01	††
WT:UT vs. KO:T	-0.08500	1.061	> 0.05	ns
WT:T vs. KO:UT	-0.2017	2.815	> 0.05	ns
WT:T vs. KO:T	0.04833	0.6746	> 0.05	ns
KO:UT vs. KO:T	0.2500	3.489	≤ 0.05	*

Unpaired T-test – WT UT versus WT T	
P value	0.1593
P value summary	ns
Significantly different? (P<0.05)	No

Figure 8G: Post-training whole muscle Bcl-2 protein

Whole Muscle - Bcl-2 Protein - Muscle Specific Mice				
	WT		mKO	
N	UT	T	UT	T
1	0.59	0.21	0.22	0.16
2	0.84	0.71	0.16	0.27
3	0.86	0.73	0.52	0.24
4	0.54	0.29	0.46	0.14
5	0.70	0.55	0.41	0.24
6		0.23	0.30	0.38
7		0.58	0.48	0.34
8		0.44	0.35	0.11
X	0.705	0.468	0.363	0.237
SEM	0.0640	0.0738	0.0457	0.0333

Two-Way ANOVA			
Source of Variation	P value	P value summary	Significance
Interaction	0.3394	ns	No
Mouse Model	< 0.0001	****	Yes
Genotype/Training	0.0039	**	Yes

Post-Hoc Test				
Bonferroni	Mean Diff.	t-value	P-value	Summary
WT:UT vs. WT:T	0.2369	2.761	> 0.05	ns
WT:UT vs. KO:UT	0.3422	3.989	≤ 0.01	††
WT:UT vs. KO:T	0.4679	5.455	≤ 0.001	****
WT:T vs. KO:UT	0.1053	1.400	> 0.05	ns
WT:T vs. KO:T	0.2310	3.071	≤ 0.05	*
KO:UT vs. KO:T	0.1257	1.671	> 0.05	ns

Unpaired T-test- WT UT versus WT T	
P value	0.0488
P value summary	*
Significantly different? (P<0.05)	Yes

Unpaired T-test- KO UT versus KO T	
P value	0.0431
P value summary	*
Significantly different? (P<0.05)	Yes

Figure 8H: Post-training whole muscle p21 protein

Whole Muscle - p21 Protein - Muscle Specific Mice				
	WT		mKO	
N	UT	T	UT	T
1	0.35	0.24	0.28	0.53
2	0.23	0.24	0.29	0.53
3	0.56	0.33	0.34	0.54
4	0.46	0.42	0.28	0.88
5	0.42	0.46	0.30	0.48
6	0.51		0.24	
X	0.420	0.339	0.288	0.592
SEM	0.0491	0.0447	0.0134	0.0724

Two-Way ANOVA			
Source of Variation	P value	P value summary	Significance
Interaction	0.0008	***	Yes
Mouse Model	0.2182	ns	No
Genotype/Training	0.0308	*	Yes

Post-Hoc Test				
Bonferroni	Mean Diff.	t-value	P-value	Summary
WT:UT vs. WT:T	0.08095	1.202	> 0.05	ns
WT:UT vs. KO:UT	0.1317	2.052	> 0.05	ns
WT:UT vs. KO:T	-0.1723	2.559	> 0.05	ns
WT:T vs. KO:UT	0.05079	0.7544	> 0.05	ns
WT:T vs. KO:T	-0.2532	3.601	≤ 0.05	*
KO:UT vs. KO:T	-0.3040	4.515	≤ 0.01	**

Unpaired T-test- WT UT versus WT T	
P value	0.2621
P value summary	ns
Significantly different? (P<0.05)	No

Unpaired T-test- WT UT versus KO UT	
P value	0.0271
P value summary	†
Significantly different? (P<0.05)	Yes

Figure 9A: Post-training whole muscle LC3 II/ LC3 I protein

Whole Muscle - LC3 II/LC3 I Protein - Muscle Specific Mice				
	WT		mKO	
N	UT	T	UT	T
1	0.37	0.57	0.62	0.66
2	0.60	1.087	0.32	0.60
3	0.34	0.57	0.35	0.62
4	0.16	0.80	0.37	0.77
5	0.22	0.59	0.46	0.69
6	0.36	0.79	0.45	0.51
7		0.93	0.56	0.41
8		0.52		
X	0.343	0.732	0.447	0.609
SEM	0.0613	0.0718	0.0419	0.0446

Two-Way ANOVA			
Source of Variation	P value	P value summary	Significance
Interaction	0.0618	ns	No
Mouse Model	0.8749	ns	No
Genotype/Training	< 0.0001	****	Yes

Post-Hoc Test				
Bonferroni	Mean Diff.	t-value	P-value	Summary
WT:UT vs. WT:T	-0.3896	4.728	≤ 0.005	***
WT:UT vs. KO:UT	-0.1044	1.229	> 0.05	ns
WT:UT vs. KO:T	-0.2668	3.143	≤ 0.05	*
WT:T vs. KO:UT	0.2853	3.612	≤ 0.01	**
WT:T vs. KO:T	0.1228	1.555	> 0.05	ns
KO:UT vs. KO:T	-0.1625	1.992	> 0.05	ns

Unpaired T-test- WT UT versus KO UT	
P value	0.1777
P value summary	ns
Significantly different? (P<0.05)	No

Unpaired T-test- KO UT versus KO T	
P value	0.0222
P value summary	*
Significantly different? (P<0.05)	Yes

Figure 9B: Post-training whole muscle p62 protein

Whole Muscle - p62 Protein - Muscle Specific Mice				
	WT		mKO	
N	UT	T	UT	T
1	0.24	0.87	0.93	0.63
2	0.47	0.76	1.17	0.76
3	0.53	0.74	0.76	0.54
4	0.47	0.51	0.88	0.59
5	0.41	0.47	0.85	0.74
6		1.10	1.27	0.73
7		0.78	1.13	1.024
8			1.079	
X	0.425	0.747	1.00699	0.715
SEM	0.0505	0.0809	0.0633	0.0605

Two-Way ANOVA			
Source of Variation	P value	P value summary	Significance
Interaction	0.0002	***	Yes
Mouse Model	0.0005	***	Yes
Genotype/Training	0.8279	ns	No

Post-Hoc Test				
Bonferroni	Mean Diff.	t-value	P-value	Summary
WT:UT vs. WT:T	-0.3225	3.149	≤ 0.05	*
WT:UT vs. KO:UT	-0.5824	5.840	≤ 0.005	††††
WT:UT vs. KO:T	-0.2900	2.831	> 0.05	ns
WT:T vs. KO:UT	-0.2599	2.871	> 0.05	ns
WT:T vs. KO:T	0.03257	0.3483	> 0.05	ns
KO:UT vs. KO:T	0.2925	3.230	≤ 0.05	*

Figure 9A: Post-training whole muscle Parkin protein

Whole Muscle - Parkin Protein - Muscle Specific Mice				
	WT		mKO	
N	UT	T	UT	T
1	0.19	0.49	0.77	0.46
2	0.30	0.49	0.72	0.47
3	0.25	0.55	0.69	0.31
4	0.31	0.54	0.63	0.84
5	0.12	0.47	0.62	0.48
6			0.56	0.55
7			0.95	
X	0.234	0.509	0.705	0.518
SEM	0.0360	0.0153	0.0489	0.0717

Two-Way ANOVA			
Source of Variation	P value	P value summary	Significance
Interaction	0.0003	***	Yes
Mouse Model	0.0002	***	Yes
Genotype/Training	0.4081	ns	No

Post-Hoc Test				
Bonferroni	Mean Diff.	t-value	P-value	Summary
WT:UT vs. WT:T	-0.2745	3.543	≤ 0.05	*
WT:UT vs. KO:UT	-0.4710	6.566	≤ 0.001	††††
WT:UT vs. KO:T	-0.2837	3.825	≤ 0.01	**
WT:T vs. KO:UT	-0.1964	2.738	> 0.05	ns
WT:T vs. KO:T	-0.009180	0.1238	> 0.05	ns
KO:UT vs. KO:T	0.1872	2.747	> 0.05	ns

Unpaired T-test- KO UT versus KO T	
P value	0.0490
P value summary	*
Significantly different? (P<0.05)	Yes

Figure 9A: Post-training whole muscle Beclin-1 protein

Whole Muscle - Beclin-1 Protein - Muscle Specific Mice				
	WT		mKO	
N	UT	T	UT	T
1	0.24	0.76	0.69	0.31
2	0.18	0.50	0.69	0.48
3	0.32	0.55	1.028	0.56
4	0.40	0.73	0.65	0.60
5	0.41	0.41	0.99	0.75
6		0.40	0.85	0.54
7		0.36	0.67	0.72
X	0.308	0.531	0.796	0.567
SEM	0.0453	0.0612	0.0608	0.0563

Two-Way ANOVA			
Source of Variation	P value	P value summary	Significance
Interaction	0.0009	***	Yes
Mouse Model	0.0002	***	Yes
Genotype/Training	0.9582	ns	No

Post-Hoc Test				
Bonferroni	Mean Diff.	t-value	P-value	Summary
WT:UT vs. WT:T	-0.2227	2.558	> 0.05	ns
WT:UT vs. KO:UT	-0.4880	5.605	≤ 0.001	††††
WT:UT vs. KO:T	-0.2590	2.975	≤ 0.05	*
WT:T vs. KO:UT	-0.2653	3.338	≤ 0.05	*
WT:T vs. KO:T	-0.03636	0.4574	> 0.05	ns
KO:UT vs. KO:T	0.2289	2.880	> 0.05	ns

Unpaired T-test- WT UT versus WT T	
P value	0.0223
P value summary	*
Significantly different? (P<0.05)	Yes

Unpaired T-test- KO UT versus KO T	
P value	0.0171
P value summary	*
Significantly different? (P<0.05)	Yes

Figure 10A: COX Enzyme Activity, marker of mitochondrial content, in untrained Muscle Specific (MS) versus Whole Body (WB) mice

COX Enzyme Activity ($\mu\text{mol}/\text{min}/\text{g}$ tissue) – Untrained MS versus WB Mice				
	Muscle Specific Mice		Whole Body Mice	
N	WT	mKO	WT	KO
1	19.21	14.84	22.49	11.59
2	16.66	11.04	19.12	12.30
3	13.76	12.21	12.88	13.00
4	16.87	14.41	22.31	14.93
5	15.90	13.29	16.76	17.58
6	16.80	14.65	13.56	8.88
7		14.66		
8		14.50		
X	16.533	13.700	17.853	13.047
SEM	0.718	0.495	1.706	1.213

Two-Way ANOVA			
Source of Variation	P value	P value summary	Significance
Interaction	0.3657	ns	No
Mouse Model	0.7579	ns	No
Genotype/Training	0.0017	**	Yes

Post-Hoc Test				
Bonferroni	Mean Diff.	t-value	P-value	Summary
Muscle Specific:WT vs. Muscle Specific:KO	2.833	1.941	> 0.05	ns
Muscle Specific:WT vs. Whole Body:WT	-1.320	0.8461	> 0.05	ns
Muscle Specific:WT vs. Whole Body:KO	3.487	2.235	> 0.05	ns
Muscle Specific:KO vs. Whole Body:WT	-4.153	2.846	> 0.05	ns
Muscle Specific:KO vs. Whole Body:KO	0.6533	0.4477	> 0.05	ns
Whole Body:WT vs. Whole Body:KO	4.807	3.081	≤ 0.05	†

Unpaired T-test- MS WT UT versus mKO UT	
P value	0.0056
P value summary	††
Significantly different? (P<0.05)	Yes

Figure 10B: PGC-1 α mRNA in untrained Muscle Specific (MS) versus Whole Body (WB) mice

PGC-1α mRNA – Untrained MS versus WB Mice				
	Muscle Specific Mice		Whole Body Mice	
N	WT	mKO	WT	KO
1	5.76	4.64	6.89	2.61
2	5.56	3.92	7.21	4.43
3	4.46	5.44	5.31	3.47
4	5.08	5.42	6.64	1.23
5	5.20	4.74	7.94	3.66
6		5.45	7.19	4.48
7		4.58	5.51	4.75
8		2.83	7.10	3.61
9		5.11		4.10
10				3.19
X	5.212	4.342	6.722	3.553
SEM	0.225	0.426	0.316	0.330

Two-Way ANOVA			
Source of Variation	P value	P value summary	Significance
Interaction	0.0004	***	Yes
Mouse Model	0.5619	ns	No
Genotype/Training	< 0.0001	****	Yes

Post-Hoc Test				
Bonferroni	Mean Diff.	t-value	P-value	Summary
Muscle Specific:WT vs. Muscle Specific:KO	0.5309	1.066	> 0.05	ns
Muscle Specific:WT vs. Whole Body:WT	-1.512	2.971	≤ 0.05	¶
Muscle Specific:WT vs. Whole Body:KO	1.659	3.394	≤ 0.05	*
Muscle Specific:KO vs. Whole Body:WT	-2.043	4.710	≤ 0.005	***
Muscle Specific:KO vs. Whole Body:KO	1.128	2.751	> 0.05	ns
Whole Body:WT vs. Whole Body:KO	3.171	7.490	≤ 0.001	††††

Unpaired T-test- MS WT UT versus mKO UT	
P value	0.2340
P value summary	ns
Significantly different? (P<0.05)	No

Figure 10C: PGC-1 α protein in untrained Muscle Specific (MS) versus Whole Body (WB) mice

PGC-1α Protein – Untrained MS versus WB Mice				
	Muscle Specific Mice		Whole Body Mice	
N	WT	mKO	WT	KO
1	0.35	0.39	0.43	0.50
2	0.40	0.27	0.37	0.33
3	0.43	0.21	0.70	0.50
4	0.58	0.42	0.66	0.077
5	0.52	0.30	0.70	0.52
6		0.24	0.83	0.40
7		0.21	0.75	0.35
X	0.456	0.291	0.633	0.382
SEM	0.0410	0.0321	0.0650	0.059

Two-Way ANOVA			
Source of Variation	P value	P value summary	Significance
Interaction	0.4194	ns	No
Mouse Model	0.0183	*	Yes
Genotype/Training	0.0007	***	Yes

Post-Hoc Test				
Bonferroni	Mean Diff.	t-value	P-value	Summary
Muscle Specific:WT vs. Muscle Specific:KO	0.1646	2.102	> 0.05	ns
Muscle Specific:WT vs. Whole Body:WT	-0.1787	2.282	> 0.05	ns
Muscle Specific:WT vs. Whole Body:KO	0.07319	0.9348	> 0.05	ns
Muscle Specific:KO vs. Whole Body:WT	-0.3433	4.803	\leq 0.005	***
Muscle Specific:KO vs. Whole Body:KO	-0.09143	1.279	> 0.05	ns
Whole Body:WT vs. Whole Body:KO	0.2519	3.524	\leq 0.05	†

Unpaired T-test- MS WT UT versus mKO UT	
P value	0.0094
P value summary	††
Significantly different? (P<0.05)	Yes

Unpaired T-test- MS WT UT versus WB WT UT	
P value	0.0133
P value summary	¶
Significantly different? (P<0.05)	Yes

Figure 10D: State 3 respiration in the SS mitochondria of untrained Muscle Specific (MS) versus Whole Body (WB) mice

State 3 Respiration – SS Mitochondria – Untrained MS versus WB Mice				
	Muscle Specific Mice		Whole Body Mice	
N	WT	mKO	WT	KO
1	8.53	31.93	5.50	6.47
2	10.89	34.80	6.51	15.24
3	17.80	13.20	27.50	9.51
4	12.01	25.16	21.37	2.34
5	16.16	11.91	14.40	12.89
6	12.82	40.79	11.46	5.80
X	13.035	26.298	14.457	8.708
SEM	1.396	4.809	3.513	1.956

Two-Way ANOVA			
Source of Variation	P value	P value summary	Significance
Interaction	0.0077	**	Yes
Mouse Model	0.0205	*	Yes
Genotype/Training	0.2557	ns	No

Post-Hoc Test				
Bonferroni	Mean Diff.	t-value	P-value	Summary
Muscle Specific:WT vs. Muscle Specific:KO	-13.26	2.921	> 0.05	ns
Muscle Specific:WT vs. Whole Body:WT	-1.422	0.3130	> 0.05	ns
Muscle Specific:WT vs. Whole Body:KO	4.327	0.9527	> 0.05	ns
Muscle Specific:KO vs. Whole Body:WT	11.84	2.608	> 0.05	ns
Muscle Specific:KO vs. Whole Body:KO	17.59	3.873	≤ 0.01	¶¶
Whole Body:WT vs. Whole Body:KO	5.748	1.266	> 0.05	ns

Unpaired T-test- MS WT UT versus mKO UT	
P value	0.0244
P value summary	†
Significantly different? (P<0.05)	Yes

Unpaired T-test- MS WT UT versus WB WT UT	
P value	0.7147
P value summary	ns
Significantly different? (P<0.05)	No

Unpaired T-test- WB WT UT versus KO UT	
P value	0.1833
P value summary	ns
Significantly different? (P<0.05)	No

Figure 10E: State 3 reactive oxygen species (ROS) in the SS mitochondria of untrained Muscle Specific (MS) versus Whole Body (WB) mice

State 3 ROS - SS Mitochondria - Untrained MS versus WB Mice				
	Muscle Specific Mice		Whole Body Mice	
N	WT	mKO	WT	KO
1	1.91	6.56	18.25	26.02
2	11.94	5.36	15.58	18.63
3	3.91	5.81	47.29	62.22
4	16.04	9.40	17.70	7.39
5	10.95	5.70	12.46	8.34
6	12.26	8.99	31.39	55.22
7		8.66		
X	9.502	7.211	23.778	29.637
SEM	2.216	0.657	5.396	9.659

Two-Way ANOVA			
Source of Variation	P value	P value summary	Significance
Interaction	0.4605	ns	No
Mouse Model	0.0028	**	Yes
Genotype/Training	0.7453	ns	No

Post-Hoc Test				
Bonferroni	Mean Diff.	t-value	P-value	Summary
Muscle Specific:WT vs. Muscle Specific:KO	2.290	0.3045	> 0.05	ns
Muscle Specific:WT vs. Whole Body:WT	-14.28	1.829	> 0.05	ns
Muscle Specific:WT vs. Whole Body:KO	-20.14	2.580	> 0.05	ns
Muscle Specific:KO vs. Whole Body:WT	-16.57	2.203	> 0.05	ns
Muscle Specific:KO vs. Whole Body:KO	-22.43	2.982	≤ 0.05	¶
Whole Body:WT vs. Whole Body:KO	-5.858	0.7506	> 0.05	ns

Unpaired T-test- MS WT UT versus WB WT UT	
P value	0.0344
P value summary	¶
Significantly different? (P<0.05)	Yes

Figure 10F: Basal cytochrome c protein release in the SS mitochondria of untrained Muscle Specific (MS) versus Whole Body (WB) mice

Cytochrome C Protein Release – Basal - SS Mitochondria – Untrained MS versus WB Mice				
	Muscle Specific Mice		Whole Body Mice	
N	WT	mKO	WT	KO
1	639.36	2459.55	877.48	1246.67
2	1087.31	1042.72	571.96	1907.21
3	1000.00	1129.84	554.55	1279.26
4	1044.012	1340.31	1399.13	972.77
5	1024.033	1719.96	688.26	2038.98
6	757.033	2238.96		
7		1519.79		
8		1911.43		
X	925.290	1670.319	818.275	1488.976
SEM	74.329	180.495	156.210	205.741

Two-Way ANOVA			
Source of Variation	P value	P value summary	Significance
Interaction	0.8287	ns	No
Mouse Model	0.4052	ns	No
Genotype/Training	0.0005	***	Yes

Post-Hoc Test				
Bonferroni	Mean Diff.	t-value	P-value	Summary
Muscle Specific:WT vs. Muscle Specific:KO	-745.0	3.383	≤ 0.05	†
Muscle Specific:WT vs. Whole Body:WT	107.0	0.4335	> 0.05	ns
Muscle Specific:WT vs. Whole Body:KO	-563.7	2.283	> 0.05	ns
Muscle Specific:KO vs. Whole Body:WT	852.0	3.666	≤ 0.01	**
Muscle Specific:KO vs. Whole Body:KO	181.3	0.7802	> 0.05	ns
Whole Body:WT vs. Whole Body:KO	-670.7	2.601	> 0.05	ns

Unpaired T-test- WB WT UT versus KO UT	
P value	0.0318
P value summary	†
Significantly different? (P<0.05)	Yes

Figure 11B: Whole muscle LC3 II/ LC3 I protein in untrained Muscle Specific (MS) versus Whole Body (WB) mice

LC3 II/ LC3 I Protein- Untrained MS versus WB Mice					
		Muscle Specific Mice		Whole Body Mice	
N	WT	mKO	WT	KO	
1	0.37	0.62	0.30	0.41	
2	0.60	0.32	0.45	0.96	
3	0.34	0.35	0.56	0.60	
4	0.16	0.37	0.48	0.53	
5	0.22	0.46	0.47	0.66	
6	0.36	0.45	0.54	0.55	
7		0.56	0.21		
8			0.27		
X	0.343	0.447	0.411	0.619	
SEM	0.0613	0.0419	0.0465	0.0770	

Two-Way ANOVA			
Source of Variation	P value	P value summary	Significance
Interaction	0.3641	ns	No
Mouse Model	0.0443	*	Yes
Genotype/Training	0.0105	*	Yes

Post-Hoc Test				
Bonferroni	Mean Diff.	t-value	P-value	Summary
Muscle Specific:WT vs. Muscle Specific:KO	-0.1044	1.295	> 0.05	ns
Muscle Specific:WT vs. Whole Body:WT	-0.06748	0.8627	> 0.05	ns
Muscle Specific:WT vs. Whole Body:KO	-0.2758	3.298	≤ 0.05	*
Muscle Specific:KO vs. Whole Body:WT	0.03687	0.4919	> 0.05	ns
Muscle Specific:KO vs. Whole Body:KO	-0.1715	2.128	> 0.05	ns
Whole Body:WT vs. Whole Body:KO	-0.2083	2.663	> 0.05	ns

Unpaired T-test- MS mKO UT versus WB KO UT	
P value	0.0649
P value summary	ns
Significantly different? (P<0.05)	No

Unpaired T-test- WB WT UT versus KO UT	
P value	0.0302
P value summary	†
Significantly different? (P<0.05)	Yes

Figure 11C: Whole muscle p62 protein in untrained Muscle Specific (MS) versus Whole Body (WB) mice

p62 Protein- Untrained MS versus WB Mice				
	Muscle Specific Mice		Whole Body Mice	
N	WT	mKO	WT	KO
1	0.24	0.93	0.64	1.033
2	0.47	1.17	0.75	1.021
3	0.53	0.76	0.81	1.29
4	0.47	0.88	0.44	0.84
5	0.41	0.85	0.21	0.90
6		1.27	0.76	0.75
7		1.13		
8		1.08		
X	0.425	1.007	0.601	0.971
SEM	0.0505	0.0633	0.0949	0.0771

Two-Way ANOVA			
Source of Variation	P value	P value summary	Significance
Interaction	0.1750	ns	No
Mouse Model	0.3558	ns	No
Genotype/Training	< 0.0001	****	Yes

Post-Hoc Test				
Bonferroni	Mean Diff.	t-value	P-value	Summary
Muscle Specific:WT vs. Muscle Specific:KO	-0.5824	5.495	≤ 0.005	†††
Muscle Specific:WT vs. Whole Body:WT	-0.1771	1.573	> 0.05	ns
Muscle Specific:WT vs. Whole Body:KO	-0.5478	4.865	≤ 0.005	***
Muscle Specific:KO vs. Whole Body:WT	0.4053	4.036	≤ 0.01	**
Muscle Specific:KO vs. Whole Body:KO	0.03465	0.3451	> 0.05	ns
Whole Body:WT vs. Whole Body:KO	-0.3707	3.453	≤ 0.05	†

Unpaired T-test- MS WT UT versus WB WT UT	
P value	0.1567
P value summary	ns
Significantly different? (P<0.05)	No

Figure 11D: Whole muscle Beclin-1 protein in untrained Muscle Specific (MS) versus Whole Body (WB) mice

Beclin-1 Protein- Untrained MS versus WB Mice				
	Muscle Specific Mice		Whole Body Mice	
N	WT	mKO	WT	KO
1	0.24	0.69	0.40	0.73
2	0.18	0.69	0.73	1.59
3	0.32	1.03	0.56	0.75
4	0.40	0.65	0.58	0.80
5	0.41	0.99	0.79	0.67
6		0.85	0.62	0.99
7		0.67	1.018	0.49
X	0.308	0.796	0.671	0.859
SEM	0.0453	0.0608	0.0751	0.134

Two-Way ANOVA			
Source of Variation	P value	P value summary	Significance
Interaction	0.1185	ns	No
Mouse Model	0.0302	*	Yes
Genotype/Training	0.0013	**	Yes

Post-Hoc Test				
Bonferroni	Mean Diff.	t-value	P-value	Summary
Muscle Specific:WT vs. Muscle Specific:KO	-0.4880	3.589	≤ 0.01	††
Muscle Specific:WT vs. Whole Body:WT	-0.3629	2.669	> 0.05	ns
Muscle Specific:WT vs. Whole Body:KO	-0.5517	4.058	≤ 0.01	**
Muscle Specific:KO vs. Whole Body:WT	0.1251	1.008	> 0.05	ns
Muscle Specific:KO vs. Whole Body:KO	-0.06377	0.5138	> 0.05	ns
Whole Body:WT vs. Whole Body:KO	-0.1889	1.522	> 0.05	ns

Unpaired T-test- MS WT UT versus WB WT UT	
P value	0.0039
P value summary	¶¶
Significantly different? (P<0.05)	Yes

Unpaired T-test- WB WT UT versus KO UT	
P value	0.2423
P value summary	ns
Significantly different? (P<0.05)	No

Figure 12A: Post-training performance test, exercise capacity comparison between Muscle Specific (MS) versus Whole Body (WB) mice

Post-Training Performance Stress Test – Distance to Exhaustion (m)								
Muscle Specific Mice					Whole Body Mice			
WT		mKO			WT		KO	
N	UT	T	UT	T	UT	T	UT	T
1	891.5	1623.6	726.0	1731.5	1258.1	2382.6	661.0	2317.04
2	1349.0	2990.3	1067.0	2555.0	477.0	3002.5	1111.0	1715.9
3	922.5	1376.0	1059.0	2117.0	980.6	2202.0	755.0	2033.0
4	852.8	1578.0	1084.0	2465.0	662.4	1836.0	332.0	2345.2
5	1252.5	2834.0	1150.0	2487.5	982.8	1830.0	970.0	2127.5
6	830.0	2992.7	926.0	1946.9	944.4	2064.5	733.0	2210.6
7			400.0	2112.8	726.0	3027.0	1117.0	2810.5
8			557.0	1533.1	1043.9	1946.9	1084.0	2519.0
9					1245.5	2270.8	915.0	2568.8
X	1016.383	2232.433	871.125	2118.600	924.522	2284.700	853.111	2294.171
SEM	91.705	318.679	98.330	131.523	86.913	151.545	86.559	107.565

Two-Way ANOVA			
Source of Variation	P value	P value summary	Significance
Interaction	0.7933	ns	No
Mouse Model	0.7646	ns	No
Genotype/Training	<0.0001	****	Yes

Post-Hoc Test				
Bonferroni	Mean Diff.	t-value	P-value	Summary
Muscle Specific:WT UT vs. Muscle Specific:WT T	-1216	5.445	≤ 0.001	****
Muscle Specific:WT UT vs. Muscle Specific:KO UT	145.4	0.696	> 0.05	ns
Muscle Specific:WT UT vs. Whole Body:WT UT	91.86	0.4506	> 0.05	ns
Muscle Specific:WT T vs. Muscle Specific:KO T	113.8	0.5449	> 0.05	ns
Muscle Specific:WT T vs. Whole Body:WT T	-52.28	0.2564	> 0.05	ns
Muscle Specific:KO UT vs. Muscle Specific:KO T	-1248	6.451	≤ 0.001	****
Muscle Specific:KO UT vs. Whole Body:KO UT	17.99	0.0957	> 0.05	ns
Muscle Specific:KO T vs. Whole Body:KO T	-175.6	0.9342	> 0.05	ns
Whole Body:WT UT vs. Whole Body:WT T	-1360	7.46	≤ 0.001	****
Whole Body:WT UT vs. Whole Body:KO UT	71.53	0.3923	> 0.05	ns
Whole Body:WT T vs. Whole Body:KO T	-9.471	0.0519	> 0.05	ns
Whole Body:KO UT vs. Whole Body:KO T	-1441	7.904	≤ 0.001	****

Figure 12B: Post-training COX Enzyme Activity, a marker of mitochondrial content, and the comparison between Muscle Specific (MS) versus Whole Body (WB) mice

COX Enzyme Activity – Muscle Specific Mice versus Whole Body Mice								
Muscle Specific Mice					Whole Body Mice			
N	WT		mKO		WT		KO	
	UT	T	UT	T	UT	T	UT	T
1	19.21	19.63	14.84	22.22	22.49	37.96	11.59	19.80
2	16.66	21.86	11.04	22.61	19.12	39.13	12.30	26.16
3	13.76	21.52	12.21	24.46	12.88	37.71	13.00	19.82
4	16.87	20.65	14.41	22.49	22.31	31.72	14.93	18.66
5	15.90	24.89	13.29	25.42	16.76	28.80	17.58	24.33
6	16.80	20.09	14.65	22.34	13.56	22.79	8.88	17.83
7		22.98	14.66	21.18		30.12		19.34
8		26.86	14.50	25.49		21.53		18.03
X	16.533	22.310	13.700	23.276	17.853	31.220	13.047	20.496
SEM	0.718	0.881	0.495	0.572	1.706	2.399	1.213	1.082

Two-Way ANOVA			
Source of Variation	P value	P value summary	Significance
Interaction	0.0001	***	Yes
Mouse Model	0.0604	ns	No
Genotype/Training	<0.0001	****	Yes

Post-Hoc Test				
Bonferroni	Mean Diff.	t-value	P-value	Summary
Muscle Specific:WT UT vs. Muscle Specific:WT T	-6.111	3.233	> 0.05	ns
Muscle Specific:WT UT vs. Muscle Specific:KO UT	2.499	1.322	> 0.05	ns
Muscle Specific:WT UT vs. Whole Body:WT UT	-1.656	0.8193	> 0.05	ns
Muscle Specific:WT T vs. Muscle Specific:KO T	-0.9663	0.5522	> 0.05	ns
Muscle Specific:WT T vs. Whole Body:WT T	-8.909	5.091	≤ 0.005	***
Muscle Specific:KO UT vs. Muscle Specific:KO T	-9.576	5.472	≤ 0.001	****
Muscle Specific:KO UT vs. Whole Body:KO UT	0.6516	0.3448	> 0.05	ns
Muscle Specific:KO T vs. Whole Body:KO T	2.779	1.588	> 0.05	ns
Whole Body:WT UT vs. Whole Body:WT T	-13.36	7.071	≤ 0.001	****
Whole Body:WT UT vs. Whole Body:KO UT	4.806	2.379	> 0.05	ns
Whole Body:WT T vs. Whole Body:KO T	10.72	6.127	≤ 0.001	****
Whole Body:KO UT vs. Whole Body:KO T	-7.448	3.941	≤ 0.01	**

Unpaired T-test – MS WT UT versus MS WT T	
P value	0.0003
P value summary	***
Significantly different? (P<0.05)	Yes

Unpaired T-test – MS WT UT versus MS KO UT	
P value	0.0140
P value summary	†
Significantly different? (P<0.05)	Yes

Unpaired T-test – WB WT UT versus WB KO UT	
P value	0.0446
P value summary	†
Significantly different? (P<0.05)	Yes

Figure 12C: Post-training whole muscle PGC-1 α protein comparison between Muscle Specific (MS) versus Whole Body (WB) mice

Whole Muscle PGC-1 α Protein Expression								
N	Muscle Specific Mice				Whole Body Mice			
	WT		mKO		WT		KO	
	UT	T	UT	T	UT	T	UT	T
1	0.35	0.93	0.39	0.69	0.43	0.38	0.50	0.66
2	0.40	0.74	0.27	0.89	0.37	0.38	0.33	0.51
3	0.43	0.71	0.21	0.41	0.70	0.47	0.50	0.93
4	0.58	1.17	0.42	0.93	0.66	0.85	0.077	0.73
5	0.52	0.73	0.30	0.93	0.70	0.66	0.52	0.93
6		0.88	0.24	0.69	0.83	1.24	0.40	0.66
7		0.71	0.21	0.61	0.75	1.31	0.35	0.80
8				0.91		0.78		0.40
9						0.43		0.53
10						1.05		
X	0.456	0.840	0.291	0.759	0.633	0.755	0.382	0.683
SEM	0.041	0.064	0.0321	0.068	0.0650	0.112	0.0585	0.0611

Two-Way ANOVA			
Source of Variation	P value	P value summary	Significance
Interaction	0.2697	ns	No
Mouse Model	0.6093	ns	No
Genotype/Training	< 0.0001	****	Yes

Post-Hoc Test					
Bonferroni		Mean Diff.	t-value	P-value	Summary
Muscle Specific:WT UT vs. Muscle Specific:WT T		-0.3841	3.182	> 0.05	ns
Muscle Specific:WT UT vs. Muscle Specific:KO UT		0.1646	1.364	> 0.05	ns
Muscle Specific:WT UT vs. Whole Body:WT UT		-0.1787	1.480	> 0.05	ns
Muscle Specific:WT T vs. Muscle Specific:KO T		0.08049	0.7543	> 0.05	ns
Muscle Specific:WT T vs. Whole Body:WT T		0.08471	0.8337	> 0.05	ns
Muscle Specific:KO UT vs. Muscle Specific:KO T		-0.4682	4.388	\leq 0.01	**
Muscle Specific:KO UT vs. Whole Body:KO UT		-0.09143	0.8296	> 0.05	ns
Muscle Specific:KO T vs. Whole Body:KO T		0.07589	0.7575	> 0.05	ns
Whole Body:WT UT vs. Whole Body:WT T		-0.1207	1.188	> 0.05	ns
Whole Body:WT UT vs. Whole Body:KO UT		0.2519	2.285	> 0.05	ns
Whole Body:WT T vs. Whole Body:KO T		0.07167	0.7565	> 0.05	ns
Whole Body:KO UT vs. Whole Body:KO T		-0.3009	2.896	> 0.05	ns

Unpaired T-test- MS WT UT versus T	
P value	0.0011
P value summary	**
Significantly different? (P<0.05)	Yes

Unpaired T-test- MS WT UT versus KO UT	
P value	0.0095
P value summary	††
Significantly different? (P<0.05)	Yes

Unpaired T-test- WB KO UT versus T	
P value	0.0038
P value summary	**
Significantly different? (P<0.05)	Yes

Unpaired T-test- WB WT UT versus KO UT	
P value	0.0133
P value summary	†
Significantly different? (P<0.05)	Yes

Unpaired T-test- WB WT UT versus T	
P value	0.4166
P value summary	ns
Significantly different? (P<0.05)	No

Unpaired T-test- MS WT UT versus WB WT UT	
P value	0.0604
P value summary	ns
Significantly different? (P<0.05)	No

Appendix B: Supplementary and Additional Data

Table 1. Antibody concentrations for western blot analyses.

Antibody	Molecular Weight	Company/Product Number	Protein Loaded (μg)	Primary Concentration	Secondary Concentration
Upstream Regulators of p53					
Mdm2	90 kDa	Antibody provided by Dr. O. Birot	75	1:100	1:3000 M
Phospho-p53 (ser15)	53 kDa	Cell Signaling (9284S)	60	1:100 (WM)	1:6000 R (WM)
Total - p53	53 kDa	PAB 421 antibody provided by Dr. S. Benchimol	50	1:50	1:3000 M
CHCHD4	21 kDa	Santa Cruz Biotechnology (sc-98628)	60	1:250	1:3000 R
Autophagy Markers					
LC3 A/B	12-17 kDa	Cell Signaling (4108S)	75	1:200	1:1000 R
SQSTM1/p62	62 kDa	Abcam (ab65416)	75	1:200	1:1000 M
Parkin	52 kDa	Cell Signaling (4211S)	60	1:1000	1:1000 M
Beclin 1	53 kDa	Cell Signaling (3738S)	60	1:1000	1:1000 R
Antioxidant Markers					
KEAP1	32 kDa	Proteintech (10503-2-AP)	60	1:1000	1:1000 R
Nrf2	102 kDa	Santa Cruz Biotechnology (sc-722)	60	1:250	1:1500 R
Mitochondrial Biogenesis Marker					
PGC-1 α	100 kDa	EMD Millipore (ab3242)	40	1: 1500	1:3000 R
Tfam	25 kDa	Made in House	40	1:1000	1:3000 R
COX IV	15 kDa	Abcam (ab14744)	40	1:2000	1:2000 M
Cellular Senescent and Apoptosis Markers					
p21	21-25 kDa	Santa Cruz Biotechnology (sc-397)	60	1:100	1:1500 R
Bcl-2	26 kDa	Santa Cruz Biotechnology (sc-7382)	75	1:200	1:2000 M
Bax	20 kDa	Santa Cruz Biotechnology (sc-493)	75	1:200	1:1500 R
AIF	67 kDa	Santa Cruz Biotechnology (sc-9416)	150	1:1000	1:3000 G
Cytochrome C	12-15 kDa	BD Pharmingen (556433)	150	1:1000	1:1000 M
Loading Controls					
GAPDH	32-37 kDa	Abcam (ab8245)	60	1:100 000	1:5000 M
α -Tubulin	50 kDa	Calbiochem (CP06-100UG)	60	1:3000	1: 1000 M
VDAC	32-37 kDa	Abcam (ab14734)	60	1:3000	1:5000 M
H2B	12-15 kDa	Cell Signaling (2934S)	60	1:1000 (2%)	1:1000 M (2%)

Table 2. Phenotypic alterations and exercise capacity under basal and exercise training conditions in MS and WB mice.

A. Pre-Training	Muscle Specific (MS) Mice				Whole Body (WB) Mice			
	WT		KO		WT		KO	
<i>Initial Body wt, g</i>	30.4 ± 0.4 ¶¶		31.4 ± 1.0 ¶		24.3 ± 0.7		28.6 ± 0.8 ††	
<i>Distance to Exhaustion (m)</i>	1286 ± 51		1156 ± 85		1262 ± 48		1208 ± 48	
B. Post-Training	WT		KO		WT		KO	
	UT	T	UT	T	UT	T	UT	T
<i>Final Body wt, g</i>	32.9 ± 1.3 ¶	30.1 ± 0.3 *	34.8 ± 1.7 ¶	27.8 ± 0.4 *	28.1 ± 1.1	23.1 ± 1.1 *	30.4 ± 0.7	25.8 ± 1.1 **
<i>TA wt/body wt (mg/g)</i>	2.0 ± 0.08	1.6 ± 0.07 **	2.1 ± 0.08	1.8 ± 0.04 **	1.9 ± 0.07	1.6 ± 0.03**	1.9 ± 0.2	1.7 ± 0.04
<i>Gastrocnemius wt/body wt, (mg/g)</i>	6.3 ± 0.3	5.8 ± 0.2	6.3 ± 0.3	6.2 ± 0.1	6.3 ± 0.2	6.3 ± 0.1	5.9 ± 0.2	6.2 ± 0.1
<i>Quadriceps wt/body wt (mg/g)</i>	6.2 ± 0.1	6.2 ± 0.1	6.6 ± 0.2	6.6 ± 0.08	7.1 ± 0.4	6.7 ± 0.3	6.4 ± 0.3	6.5 ± 0.1
<i>Heart wt/body wt, (mg/g)</i>	5.4 ± 0.4	5.8 ± 0.2	4.8 ± 0.2	5.8 ± 0.1 **	5.4 ± 0.2	7.2 ± 0.4 **	5.4 ± 0.3	6.9 ± 0.2 **
<i>Epididymal Fat wt/body wt (mg/g)</i>	43.6 ± 3.3 ¶¶	31.5 ± 3.5 *	54.6 ± 3.4 † ¶¶	23.9 ± 1.8 **	30.2 ± 2.4	21.8 ± 0.6 **	40.5 ± 3.8	17.6 ± 0.8 **
C. Mitochondrial Parameters	Muscle Specific (MS) Mice				Whole Body (WB) Mice			
	WT		KO		WT		KO	
<i>SS Mitochondrial Yield</i>	0.5 ± 0.07	0.8 ± 0.05 **	0.6 ± 0.09	0.8 ± 0.05 *	0.7 ± 0.1	1.2 ± 0.1 *	0.7 ± 0.05	0.7 ± 0.03
<i>IMF Mitochondrial Yield</i>	1.1 ± 0.03	1.3 ± 0.09	1.0 ± 0.08	1.4 ± 0.08**	1.1 ± 0.1	1.5 ± 0.2	1.0 ± 0.07	1.3 ± 0.03 **
<i>SS RCR</i>	3.8 ± 0.8	12.9 ± 5.3	4.6 ± 0.6	7.2 ± 1.8	3.4 ± 1.2	8.4 ± 1.4 *	3.1 ± 1.4	5.3 ± 1.2
<i>IMF RCR</i>	6.1 ± 0.2	10.1 ± 2.8	7.0 ± 1.1	12.1 ± 4.5	11.3 ± 2.0 ¶	16.3 ± 2.8	11.0 ± 2.4	17.1 ± 4.0

A) Pre-training variables (initial body mass and distance to exhaustion) were compared in the absence of p53 between mouse models (n=13-23/group); ¶p≤0.05, ¶¶p≤0.01, MS vs. WB; ††p≤0.01, WT vs. KO, 2-way ANOVA. **B)** Phenotypic variables were measured following the training or sedentary program (n=6-10/group); *p≤0.05, **p≤0.01, UT vs. T; ¶p≤0.05, ¶¶p≤0.01, MS vs. WB; †p≤0.05, MS WT vs. KO, Student's t-test and 2-way ANOVA. **C)** Mitochondrial parameters including yield and RCR values in both SS and IMF mitochondrial subfractions were measured (n=6-11/group); *p≤0.05, **p≤0.01, UT vs. T; ¶p≤0.05, MS vs. WB, Student's t-test. Data are presented as mean± SEM. Abbreviations: RCR, respiratory control ratio; TA; tibialis anterior; SS, subsarcolemmal; IMF, intermyofibrillar.

Table 3. mRNA and protein fold-change comparison to examine the effect of genotype and training in muscle-specific mice.

mRNA and Protein Expression Comparison – Muscle Specific Mice			
mRNA or Protein	UT WT vs. mKO	WT UT vs. T	mKO UT vs. T
<i>p53</i> mRNA		↓ 41.0% **	
<i>p53</i> protein		↓ 61.4% **	
<i>p21</i> mRNA	↓ 26.8% †	↓ 37.5 % **	↑ 1.3-fold *
<i>p21</i> protein	↓ 31.0 % †	NS	↑ 2.0-fold **
<i>Bax</i> mRNA	↓ 38.6 % ††	↓ 19.3% **	↓ 33.3% **
<i>Bax</i> protein	↑ 2.4-fold ††	NS	↓ 42.4% *
<i>Mdm2</i> mRNA	NS	NS	NS
<i>Mdm2</i> protein	NS	↑ 1.6-fold *	↑ 2.1-fold **
<i>Tfam</i> mRNA	↓ 50% ††	NS	↑ 1.3-fold *
<i>Tfam</i> protein	↓ 28.1% †	NS	↑ 2.1-fold **
<i>PGC-1α</i> mRNA	NS	NS	↑ 1.6-fold **
<i>PGC-1α</i> protein	↓ 37.0% ††	↑ 1.8-fold **	↑ 2.6-fold **
<i>p62</i> mRNA	↓ 21.1% ††	NS	NS
<i>p62</i> protein	↑ 2.3-fold ††	↑ 1.7-fold *	↓ 28.7% *
<i>LC3</i> mRNA	↓ 44.9 % ††	NS	↑ 1.3-fold **
<i>LC3</i> protein	NS	↑ 2.1-fold **	↑ 1.4-fold *

Increased expression is measured through fold change and reduced expression is measured as a percent difference. Patterns in mRNA and protein regulation are similar for p53, p21, Tfam, PGC-1 α , LC3, but are different for Bax and Mdm2 (n=4-11/group); *p \leq 0.05, **p \leq 0.01, UT vs. T, Student's t-test and 2-way ANOVA; †p \leq 0.05, ††p \leq 0.01, Student's t-test and 2-way ANOVA. NS= non-significant.

Table 4. Structural protein analysis to determine analogous features to the p53 transcription factor.

Protein	Search Strategy		
	Dali Server/PSI-BLAST Search	Z Score	Literature Search
p63	680 aa, 63 kDA, 16 exons, chr 3q28, 12 isoforms	31.2	
p73	636 aa, 73 kDA, 27 exons, chr 1p36.32, no isoforms	31.0	
Bcl-2A1	175 aa, 20.1 kDA, 7 exons, chr 15q25.1, 2 isoforms	28.9	
NFATC1	943 aa, 101.2 kDA, 23 exons, chr 18q23, 4 isoforms	8.2	
p65 (NF- κ B)	968 aa, 105.36 kDA, 37 exons, chr 4q24, 3 isoforms	6.2	
RELB	579 aa, 62.1 kDA, 16 exons, chr 19q13.32, 2 isoforms	5.4	
SIRT1			747 aa, 81.68 kDA, 20 exons, chr 10q21.3, 3 isoforms
FOXO1			655 aa, 69.66 kDA, 13 exons, chr 13q14.11, 6 isoforms
E2F1			437 aa, 46.92 kDA, 9 exons, chr 20q11.22, 5 isoforms
IGF-1			195 aa, 21.84 kDA, 13 exons, chr 12q23.2, 9 isoforms
NR4A1			598 aa, 64.46 kDA, 26 exons, chr 12q13.13, 3 isoforms
JUNB			347 aa, 35.88 kDA, 3 exons, chr 19p13.13, no isoforms
MYC			439 aa, 48.80 kDA, 5 exons, chr 8q24.21, 3 isoforms
FOS			380 aa, 40.70 kDA, 6 exons, chr 14q24.3, 2 isoforms
ATF3			181 aa, 20.58 kDA, 18 exons, chr 1q32.3, 7 isoforms
ID1-3			119 aa, 12.99 kDA, 5 exons, chr 1p36.12, 3 isoforms
CTGF			343 aa, 38.09 kDA, 7 exons, chr 6q23.2, no isomers
HIF1a			826 aa, 92.67 kDA, 22 exons, chr 14q23.2, no isomers
MEF2A			507 aa, 54.81 kDA, 42 exons, chr 15q26.3, 3 isomers
HDAC1			482 aa, 55.10 kDA, 20 exons, chr 1p35.2, 11 isomers
NRF1			503 aa, 53.54 kDA, 19 exons, chr 7q32.2, 2 isoforms
CREB1			341 aa, 36.69 kDA, 37 exons, chr 2q33.3, 5 isomers

To examine the transcription factors that may compensate for the lack of p53 with exercise, structural similarities were compared from similar proteins to p53 (393 aa, chr 17p13.1, 53 kDA, 28 exons). Using the Dali Server and PSI-BLAST search against the p53 2GEQA region, which contains the DNA binding region in *mus musculus*, and examined the structural similarities of proteins. This server utilizes a sum of pairs method which analyzes intramolecular distances; a high z score indicates similar distances between structures. This analysis concluded six noteworthy transcription factors. Additional transcriptional regulators, determined through review of literature, include 16 proteins (12, 20, 35, 49). Further analysis is required to provide a complete inquiry into viable compensatory mechanisms. Details on the aforementioned proteins are listed in the order of amino acid (aa) length, kilo dalton size, number of exons, chromosome (chr) location, and number of isomers. **Abbreviations:** Bcl-2A1, BCL2 related protein 1; NFATC1, Nuclear factor of activated T-cells 1; p65/NF- κ B1, Nuclear factor kappa B subunit 1;

RELB, RELB proto-oncogene, NF-kB subunit; SIRT1, Sirtuin 1; FOXO1, Forkhead Box O1; IGF-1, Insulin like growth factor 1; NR4A1, Nuclear receptor subfamily 4 group 1 member 1; JUNB, JunB proto-oncogene; Myc, Myc proto-oncogene; FOS, Fos proto-oncogene, ATF3, Activating transcription factor 3; ID1-3, Inhibitor of DNA binding 3, HLH protein; CTGF, Connective tissue growth factor; HIF1-a, Hypoxia inducible factor 1 alpha subunit; MEF2A, Myocyte enhancer factor 2A; HDAC1, histone de-acetylase 1; NRF1, nuclear respiratory factor 1; CREB1, CAMP responsive element binding protein 1.

Fig 1.

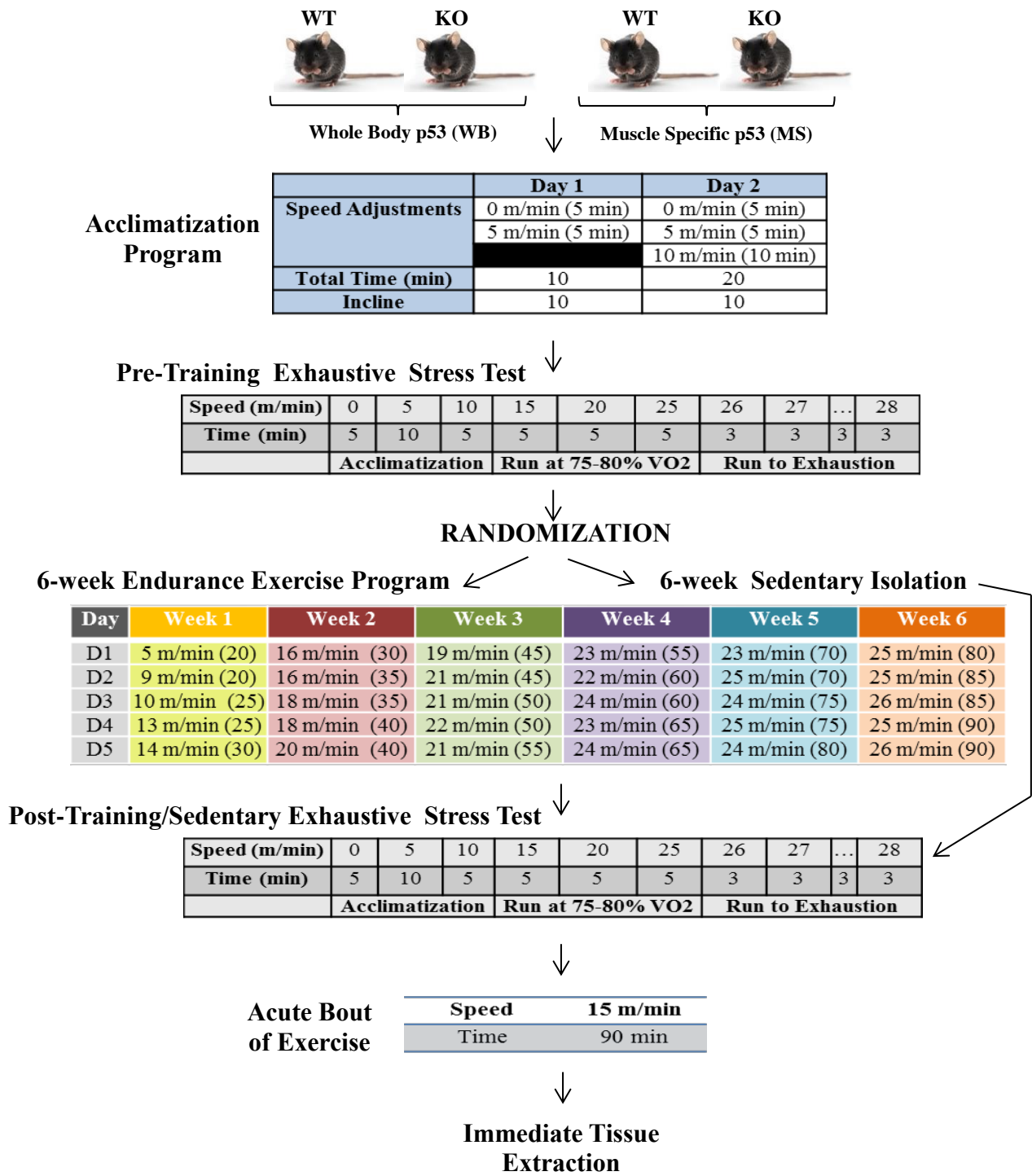


Figure 1. Detailed exercise protocol for sedentary and exercise grouped mice. Muscle specific and whole body WT and KO mice underwent a two-day acclimatization program to the treadmill. 24 hours following the second day of acclimatization, all mice underwent a pre-training exhaustive stress test. A 48 hour time delay occurred between the first exhaustive stress test and the initiation of the 6-week exercise training or sedentary program. 48 hours following the exercise/sedentary intervention, a second exhaustive exercise stress test was performed to measure the adaptations with training. After a 48 hour wait period, all mice were subjected to an acute bout of exercise prior to euthanization and tissue extraction immediately following the 90 min bout. Acute exercise was employed prior to tissue extraction to upregulate signaling transcription for mRNA analysis.

Fig 2.

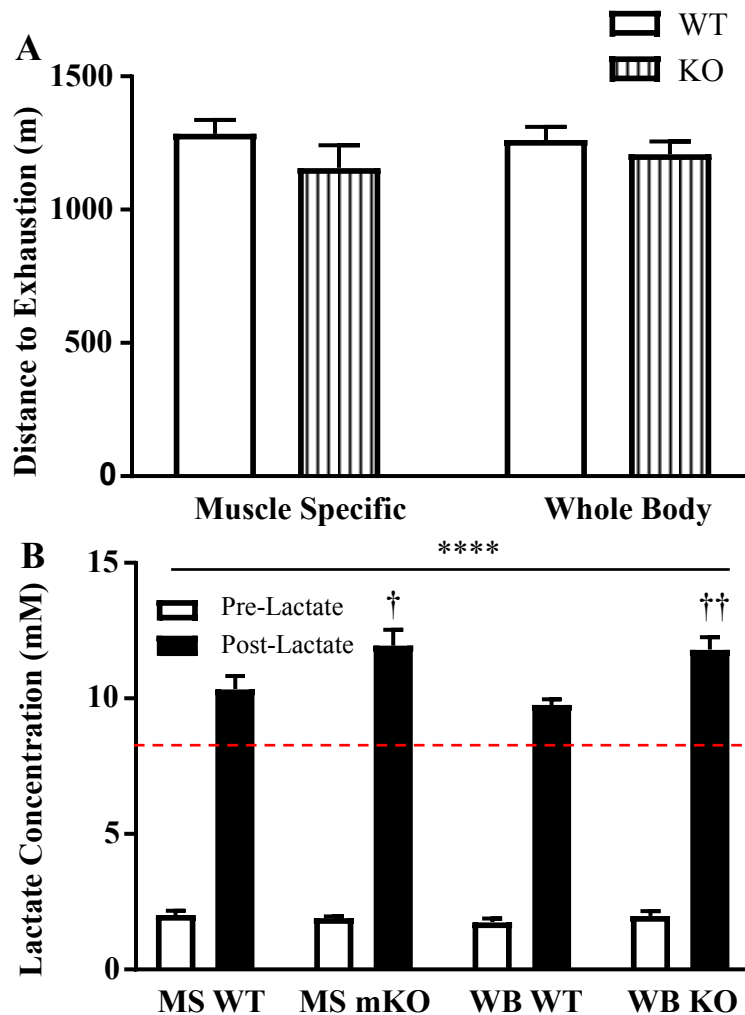


Figure 2. Differences in baseline exercise performance. MS and WB mice were subjected to a pre-training exhaustive bout of exercise. Exercise performance was measured by recording **A**) distance to exhaustion (n=17-18/group); N.S. $p > 0.05$, 2-way ANOVA, and **B**) lactate production before and after exercise (n=7-20/group); † $p \leq 0.05$, †† $p \leq 0.01$, WT vs. KO, 2-way ANOVA; **** $p \leq 0.001$, Pre-lactate vs. Post-lactate (effect of exercise), 2-way ANOVA. Red line indicates an exhaustive lactate threshold (> 8 mM). Data are presented as mean \pm SEM.

Fig 3.

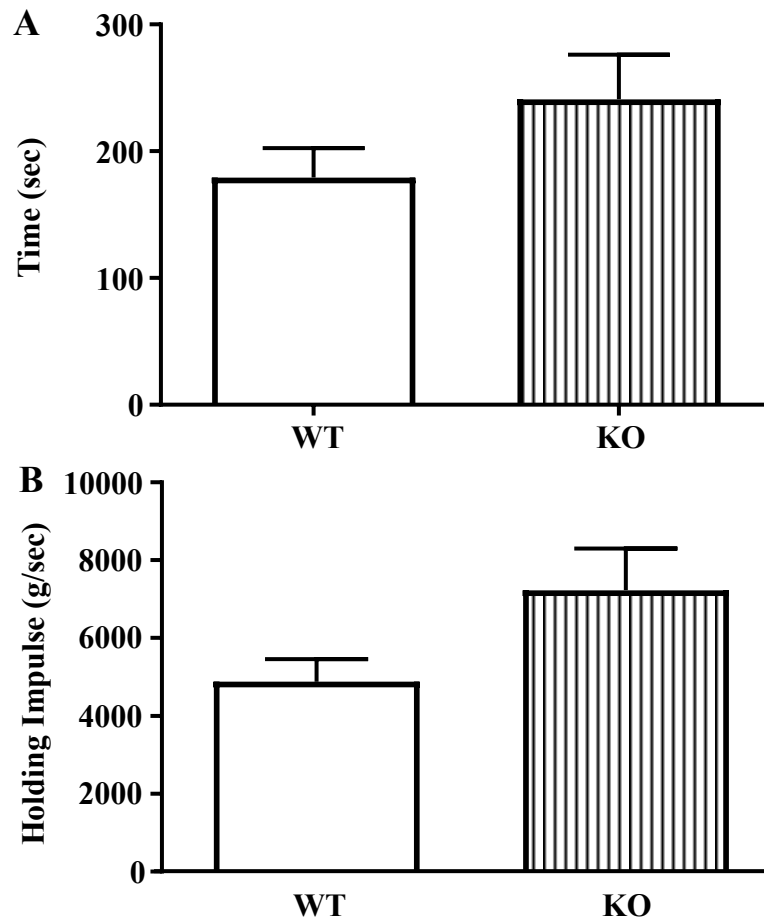


Figure 3. The absence of p53 does not impact skeletal muscle strength. Skeletal muscle strength in whole body mice was measured through a cage hanging test. Strength was measured by **A)** length of time spent hanging (n=14/group). N.S., $p>0.05$, WT vs KO, student's T-test, and by the **B)** holding impulse (n=14/group). N.S., $p>0.05$, WT vs KO, student's T-test. Data are presented as mean \pm SEM. This model for resistance exercise indicated that WB KO mice, though not significantly different from the WT mice, did display an increased trend for improved strength capacity. N.S.= non-significant.

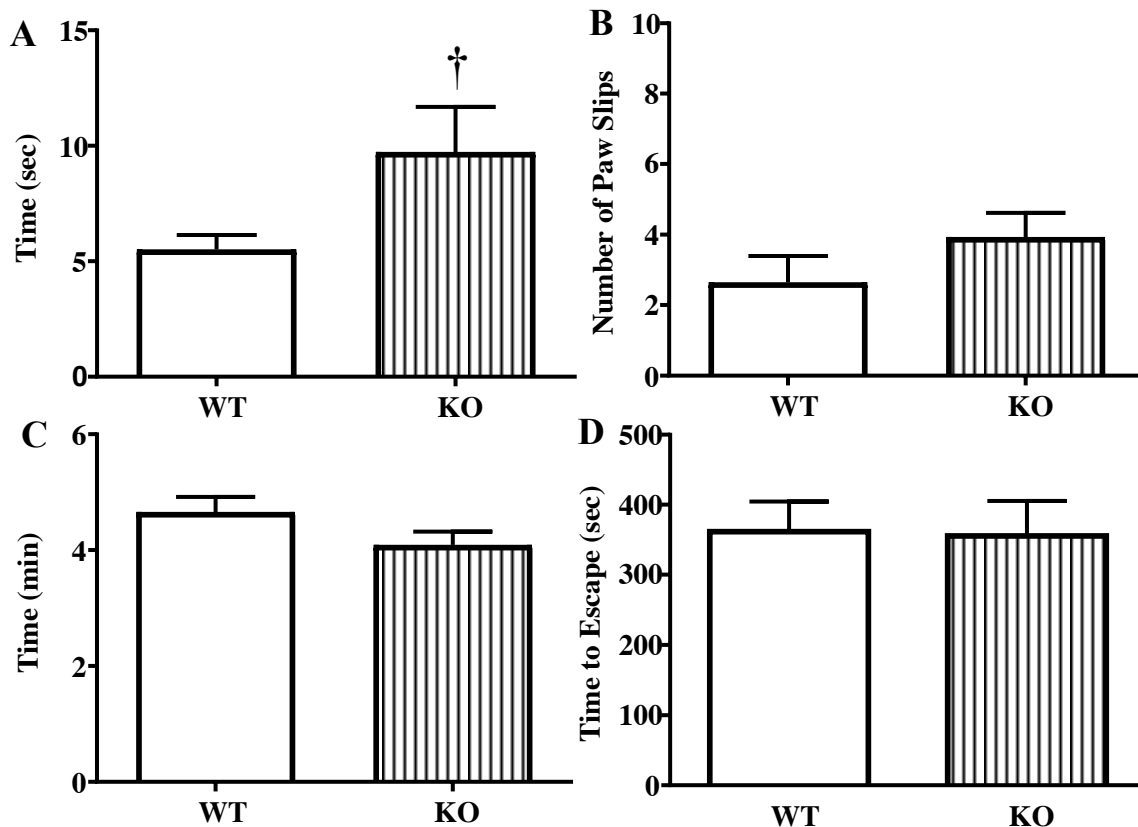
Fig 4.

Figure 4. Neurological testing to assess cerebral function in the absence of p53. To examine walking synchronization in the WB mice, a balance beam test was employed to measure the **A)** time to cross (n=14/group); †p≤0.05, WT vs. KO, Student's t-test, and the **B)** number of paw slips (n=14/group); N.S., p>0.05, Student's t-test. A pole test was employed to examine motor coordination and synchronization for correct paw placement during vertical navigation down a pole by measuring **C)** the time to traverse down the pole (n=14/group); N.S., p>0.05, Student's t-test. To establish central neural activity for voluntary movement identified through spatial learning, memory, and behavioural parameters, a cylinder escape test was employed. **D)** The time to escape the cylinder was measured (n=14/group); N.S., p>0.05. Data are presented as mean ± SEM. N.S. = non-significant

Fig 5.

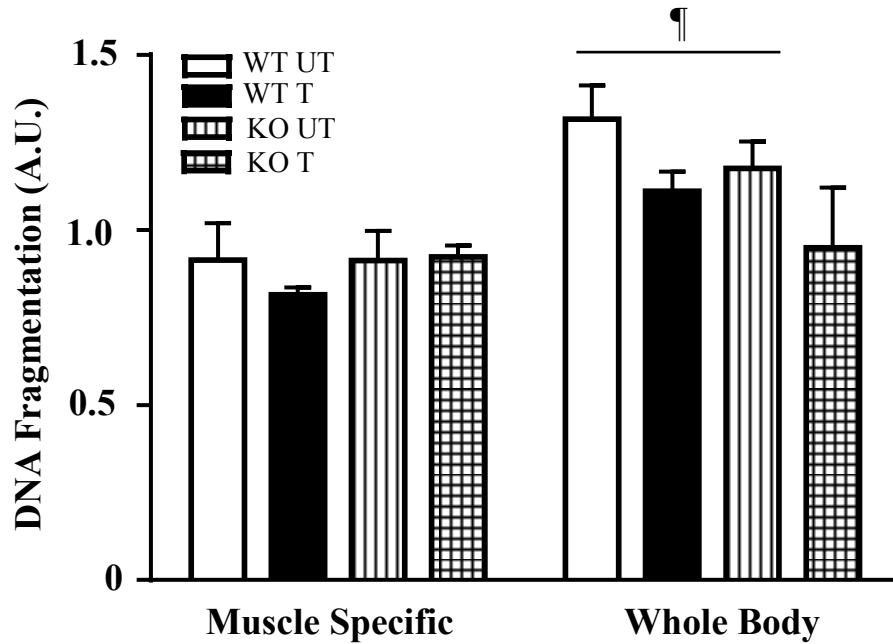


Figure 5. Reduced DNA fragmentation and apoptosis with training. DNA fragmentation was measured following training in both mouse models. Though no significant differences are detected with training and genotype, the WB mice do experience greater apoptosis than the MS mice (n=6-8/group); ¶ $p \leq 0.05$, WB vs. MS, Student's t-test. Furthermore, a trend for reduced DNA fragmentation with training in the WB WT and KO mice was observed. Data are presented as mean \pm SEM.

Fig 6.

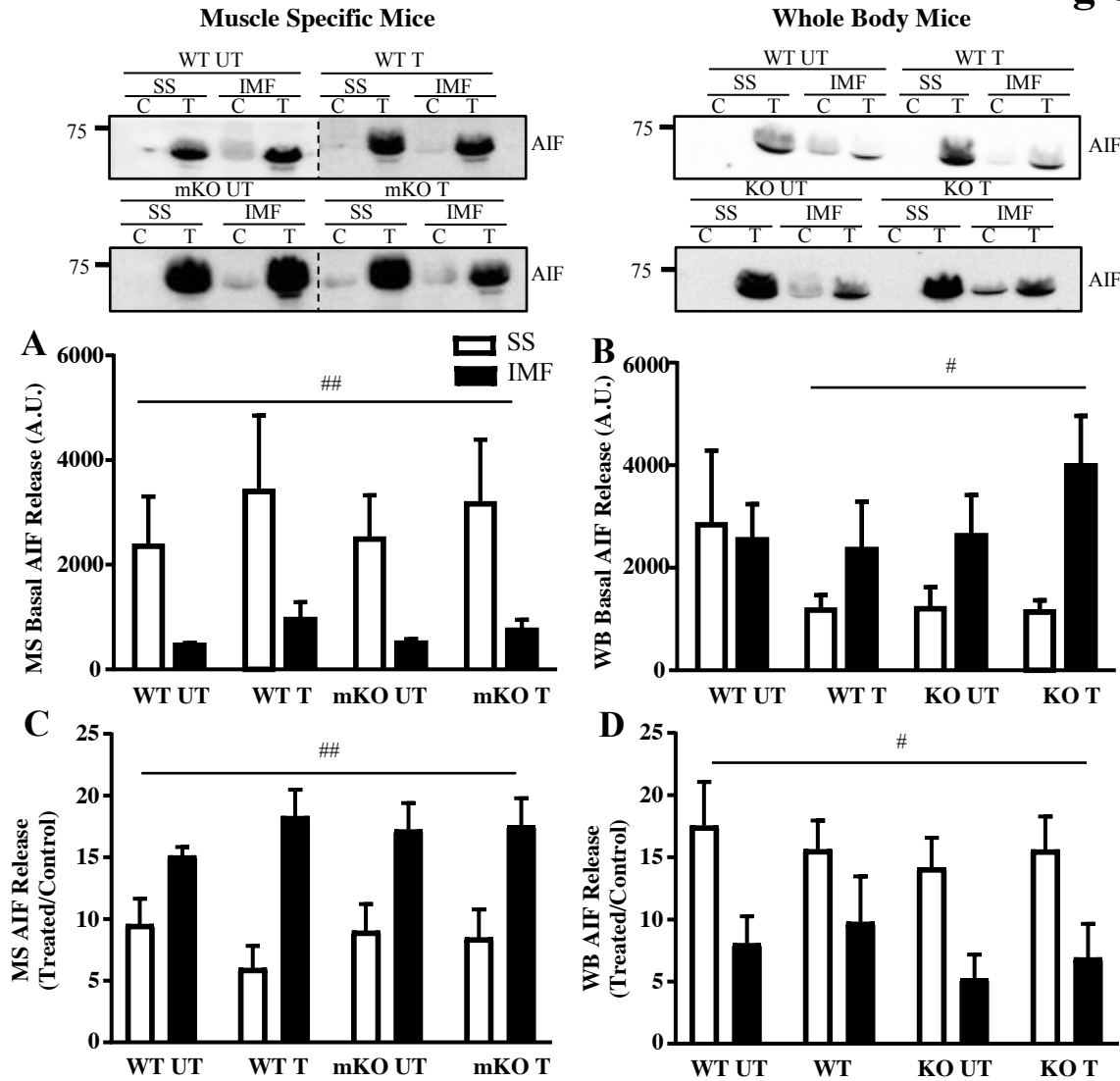


Figure 6. AIF mitochondrial protein release. Mitochondrial AIF protein release was measured from SS and IMF subfractions under basal conditions in **A**) MS mice (n=7-14/group); ###p≤0.01, main effect of SS mitochondria, 2-way ANOVA, and **B**) WB mice (n=10-13/group); #p≤0.05, main effect of IMF mitochondria, 2-way ANOVA. AIF protein release was further measured in SS and IMF mitochondria when activated through apoptotic stimuli (H₂O₂) in **C**) MS mice (n=6-11/group); ###p≤0.01, main effect of IMF mitochondria, 2-way ANOVA, and **D**) WB mice (n=8-12/group); #p≤0.05, main effect of SS mitochondria, 2-way ANOVA. Data are presented as mean ± SEM.

Fig 7.

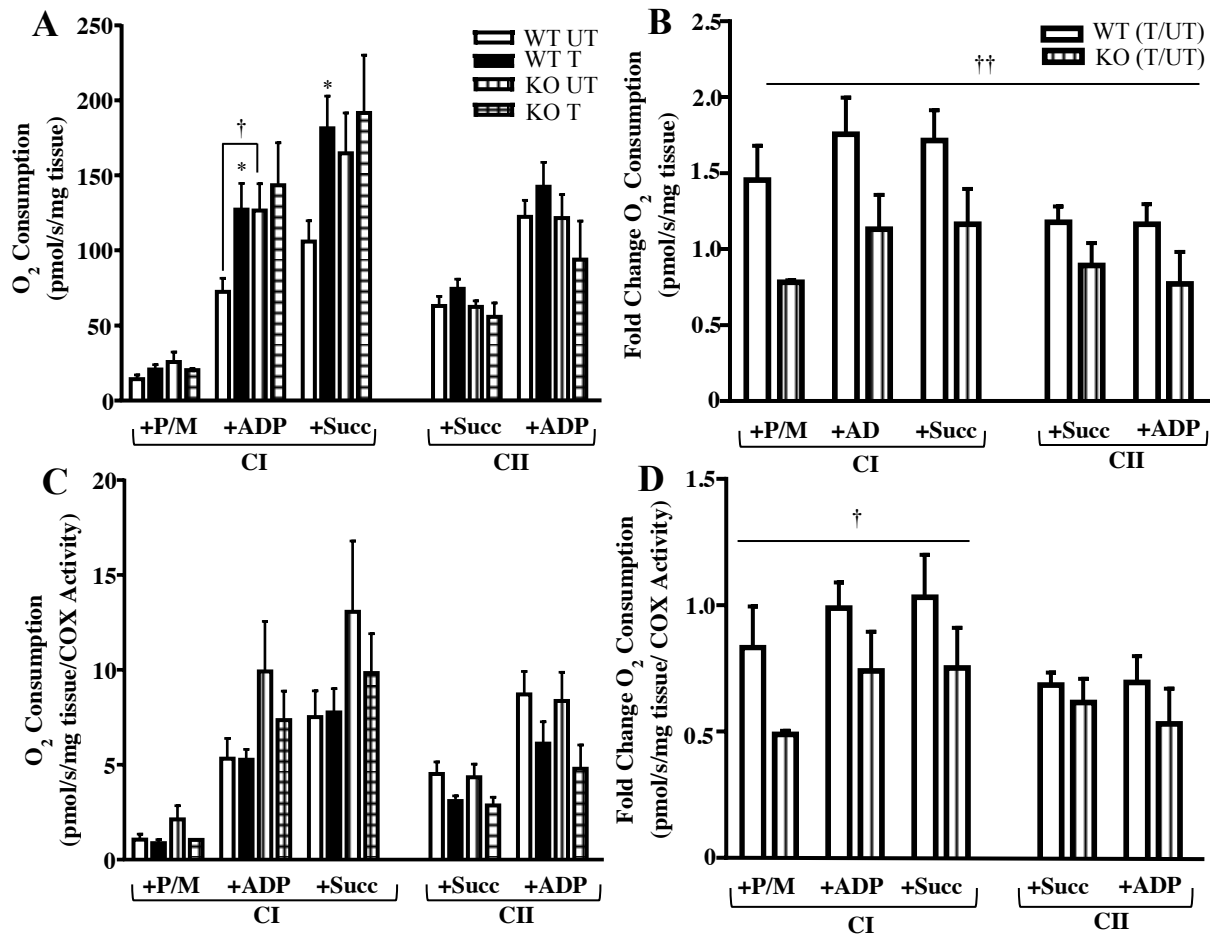


Figure 7. Respiration analysis of permeabilized fibres in WB mice. **A)** Mitochondrial respiration for Complex I (state 4 and state 3) Complex I & II (state 3), and Complex II (state 3) was performed on a subset of whole body mice (n=2-5/group); *p≤0.05, UT vs. T; †p≤0.05, WT vs. KO, Student's t-test and 2-way ANOVA. **B)** The fold change on the effect of training on respiration was calculated between WT and KO mice (n=2-5/group); ††p≤0.01, main effect of genotype, 2-way ANOVA. **C)** Mitochondrial respiration corrected for total mitochondrial volume was measured (n=2-5/group); N.S., p>0.05, 2-way ANOVA. **D)** Fold change on the effect of training on corrected respiration was measured (n=2-5/group); ††p≤0.01, main effect of genotype, 2-way ANOVA. Data are presented as mean ± SEM. N.S. = non-significant. Abbreviations: P/M, pyruvate/malate; ADP, adenosine diphosphate; Succ, succinate; CI, Complex I; CII, Complex 2.

Fig 8.

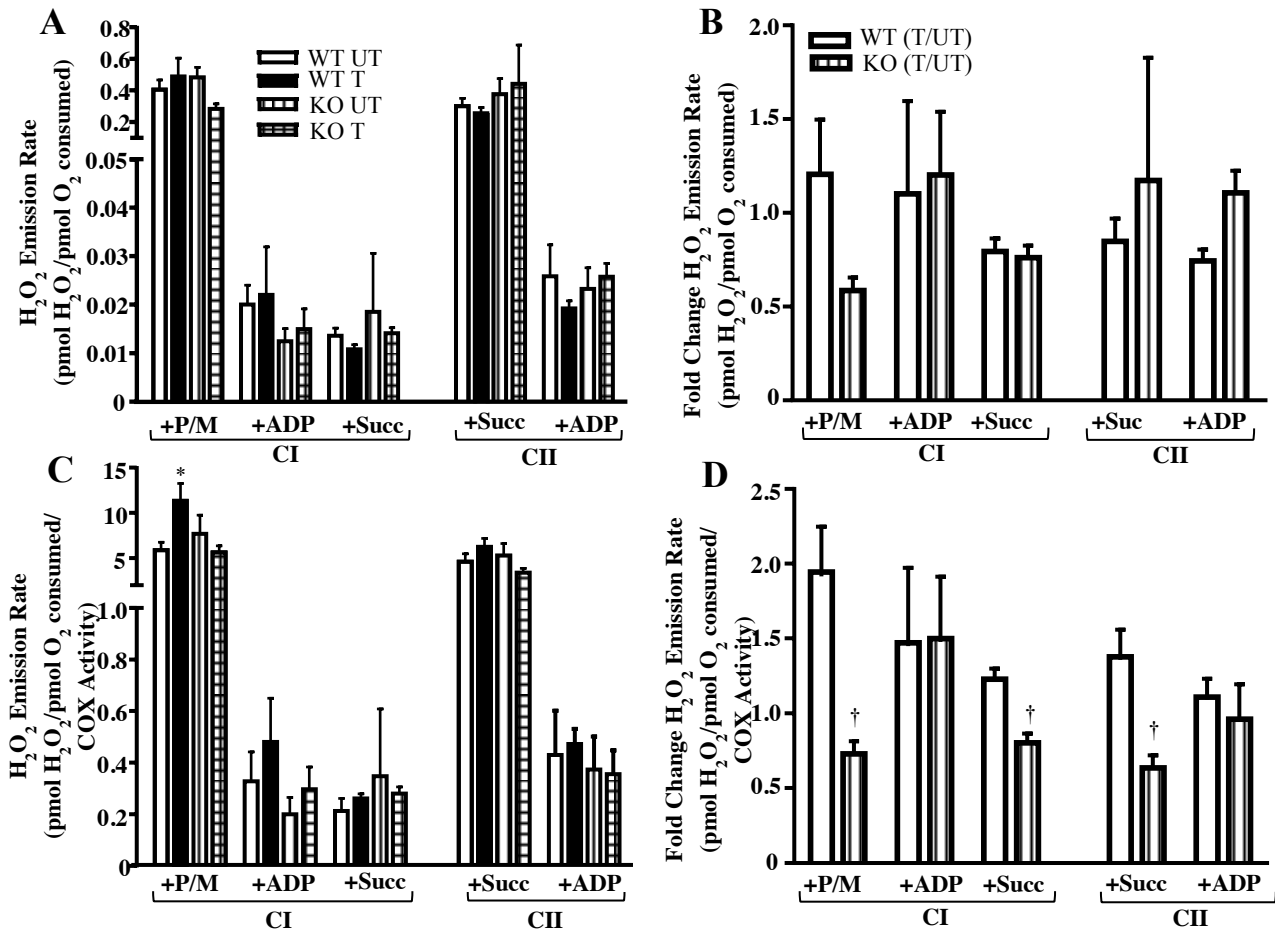


Figure 8. Reactive Oxygen Species (ROS) analysis in permeabilized fibers in WB mice. A) Mitochondrial ROS in Complex I (state 4 and state 3), Complex I & II (state 3), and Complex II (state 3) was measured using the Oroboros instrument on a subset of whole body mice (n=2-5/group); N.S., p>0.05, 2-way ANOVA. **B)** The fold change on the effect of training on ROS was calculated between WT and KO mice (n=2-5/group); N.S., p>0.05, 2-way ANOVA. **C)** Mitochondrial ROS corrected for total mitochondrial volume was measured (n=2-5/group); *p≤0.05, UT vs. T, Student's t-test. **D)** Fold change on the effect of training on corrected ROS was measured (n=2-5/group); †p≤0.05, WT vs. KO, Student's t-test. Data are presented as mean ± SEM. N.S.= non-significant. **Abbreviations:** P/M, pyruvate/malate; ADP, adenosine diphosphate; Succ, succinate; CI, Complex I; CII, Complex 2.

Fig 9.

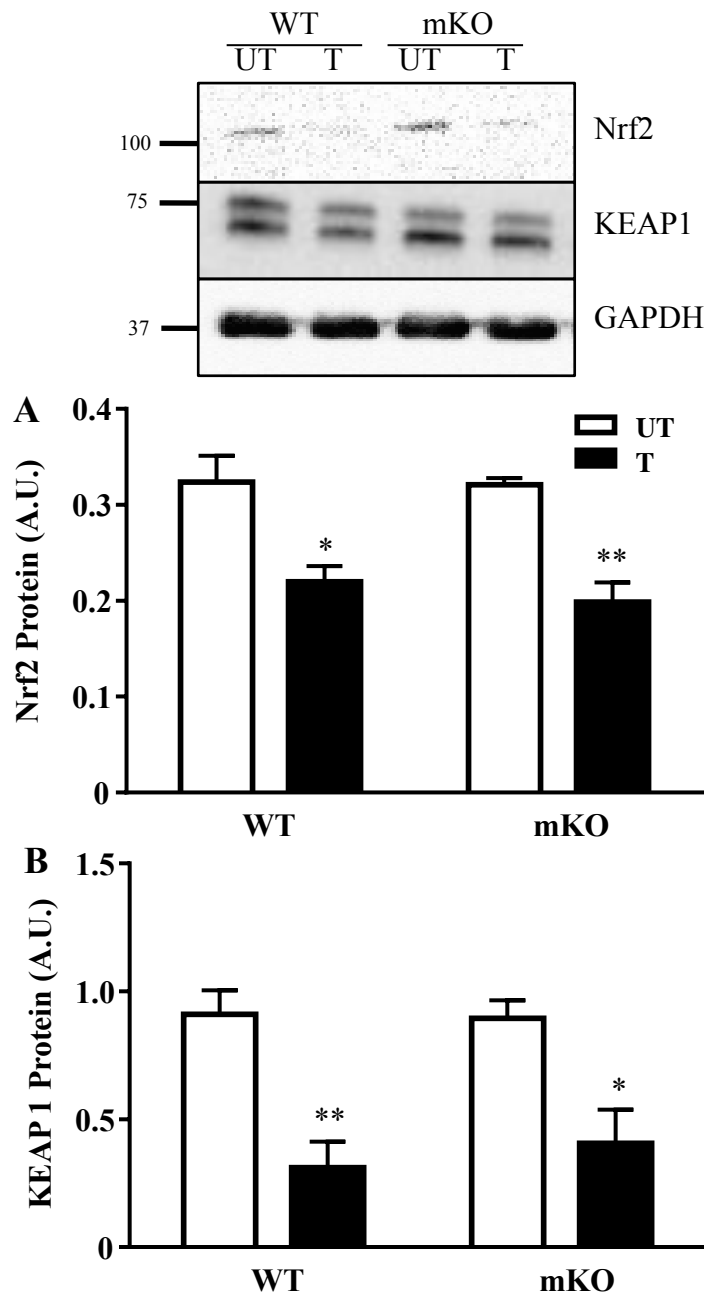


Figure 9. Antioxidant regulation with exercise training. A) The major antioxidant transcriptional regulator Nrf2, and its B) negative regulator KEAP1 were examined in the context of exercise training (n=4-5/group); *p<0.05, **p<0.05, UT vs. T, 2-way ANOVA. Data are presented as mean \pm SEM.

Fig 10.

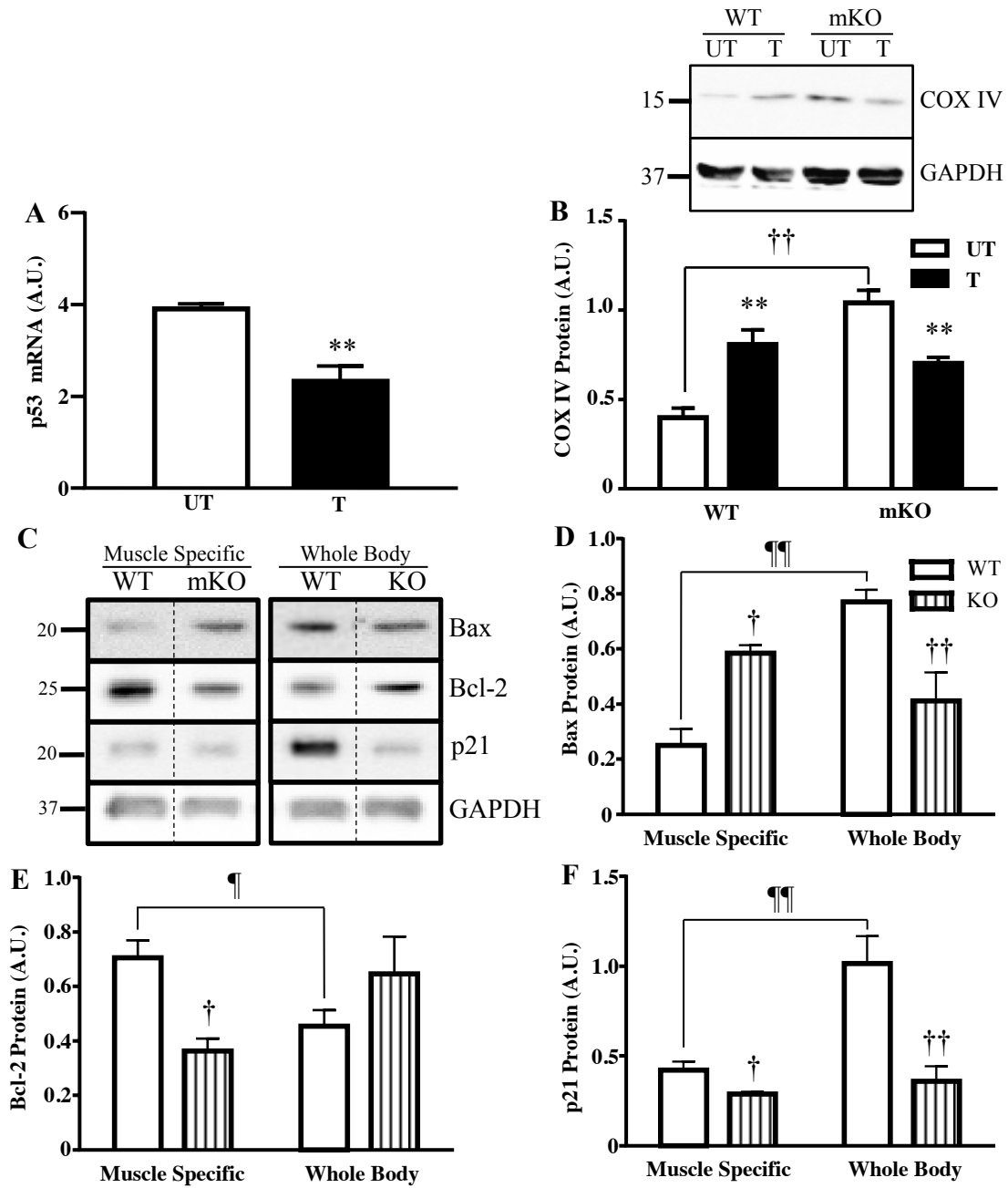


Figure 10. Signaling regulation in untrained and trained MS and WB mice. **A)** p53 mRNA was reduced with training in MS mice (n=6-10/group); **p≤0.01, UT vs. T, Student's t-test. **B)** Mitochondrial biogenesis was measured through COX IV protein in whole muscle lysates of MS mice (n=5-7/group); **p≤0.01, UT vs. T, 2-way ANOVA; †† p≤0.01, UT WT vs. KO, 2-way ANOVA. **C)** The effects of the absence of p53 on apoptotic signaling in untrained MS and WB mice was measured through protein analysis of **D)** Bax (n=4-6/group); †p≤0.05; ††p≤0.01, UT WT vs. KO; ¶¶p≤0.01, MS vs. WB, 2-way ANOVA, **E)** Bcl-2 (n=5-8/group); †p≤0.05, UT WT vs. KO, 2-way ANOVA; ¶p≤0.05, MS vs. WB, Student's t-test, and **F)** p21 (n=6-8/group); †p≤0.05, ††p≤0.01, UT WT vs. KO, Student's t-test and 2-way ANOVA; ¶¶p≤0.01, MS vs. WB, 2-way ANOVA. Data are presented as mean ± SEM.

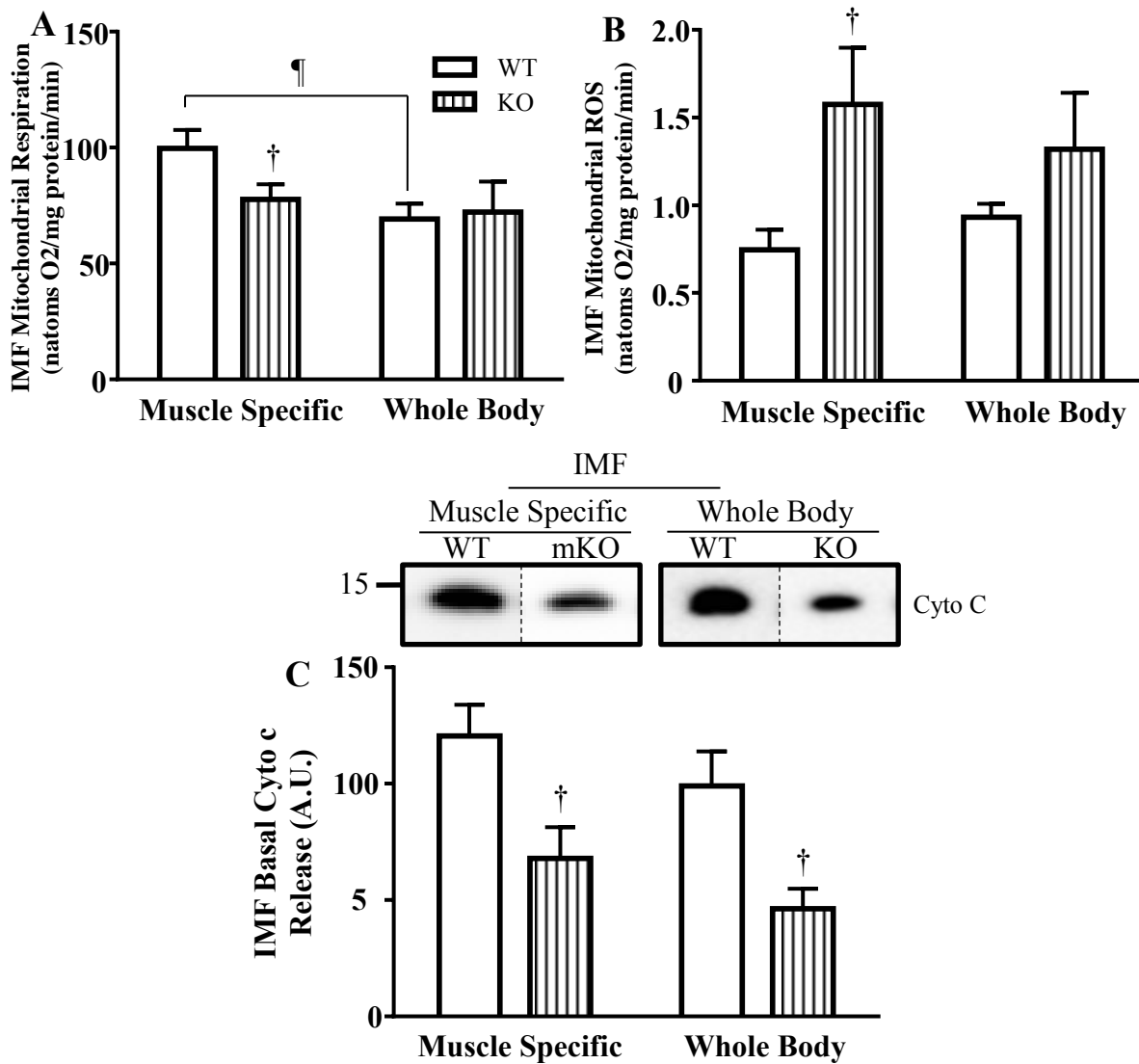
Fig 11

Figure 11. IMF mitochondrial functional (respiration and ROS) and apoptosis signaling comparison between MS and WB mice in the absence of p53. IMF mitochondrial function was measured through state 3 **A**) respiration (n=6-8/group); [†]p≤0.05, UT WT vs, KO; [¶]p≤0.05, MS vs. WB, Student's t-test, and **B**) ROS (n=7-8/group); [†]p≤0.05, UT WT vs, KO, Student's t-test. **C**) Apoptosis was basally measured through cytochrome c release from IMF mitochondria (n=6-14/group); [†]p≤0.05, UT WT vs, KO, Student's t-test. Data are presented as mean ± SEM.

Appendix C: Data and Statistical Analysis for Supplementary

Table 2A: Pre-training initial body mass measurement, comparison between Muscle-Specific (MS) and Whole-Body (WB) Mice

N	Pre-Training Initial Body Mass – MS versus WB Mice			
	Muscle Specific Mice		Whole Body Mice	
	WT	mKO	WT	KO
1	30.8	38.4	28.4	34.1
2	30.4	28.5	17.7	25.5
3	29.6	29.5	19.5	33.5
4	26.8	27.2	23.4	39.5
5	31.0	29.4	27.6	30.3
6	31.4	44.4	26.2	29.3
7	31.5	34.6	23.9	25.6
8	30.1	27.0	25.4	28.8
9	31.2	36.7	28.8	24.8
10	31.3	32.0	25.6	25.1
11	30.4	32.8	26.3	26.9
12	29.2	29.2	20.3	27.6
13	31.7	27.8	20.2	25.9
14		28.8	25.6	29.4
15		27.8	19.5	30.7
16		28.2	19.8	29.4
17		27.7	24.8	29.1
18		36.9	24.2	28.2
19		31.1	26.4	27.7
20		31.4	26.5	29.5
21		29.5	26.0	
22			27.2	
23			25.0	
X	30.415	31.376	24.274	29.045
SEM	0.367	0.984	0.667	0.789

Two-Way ANOVA			
Source of Variation	P value	P value summary	Significance
Interaction	0.0329	*	Yes
Mouse Model	<0.0001	****	Yes
Genotype/Training	0.0010	***	Yes

Post-Hoc Test				
Bonferroni	Mean Diff.	t-value	P-value	Summary
Muscle Specific:WT vs. Muscle Specific:KO	-0.9608	0.8352	> 0.05	ns
Muscle Specific:WT vs. Whole Body:WT	6.141	5.429	≤ 0.001	¶¶¶¶
Muscle Specific:KO vs. Whole Body:KO	2.831	2.78	≤ 0.05	¶
Whole Body:WT vs. Whole Body:KO	-4.271	4.285	≤ 0.005	†††

Table 2A: Pre-training initial body mass measurement, comparison between Muscle-Specific (MS) and Whole-Body (WB) Mice

Pre-Training Performance Test – Distance to Exhaustion (m) - MS versus WB Mice				
	Muscle-Specific Mice		Whole-Body Mice	
N	WT	mKO	WT	KO
1	1144.22	1381.40	1173.80	1067.00
2	1322.50	1012.56	1124.75	1277.00
3	1597.00	1546.42	1102.00	1485.00
4	1150.00	1322.50	1091.75	1439.00
5	970.00	1387.88	1077.89	668.00
6	1559.00	477.00	1261.25	1167.00
7	1578.00	523.25	1394.00	894.60
8	962.00	855.23	794.00	1129.70
9	1287.50	1466.50	1067.00	1197.60
10	1189.44	1616.00	1150.00	1218.00
11	1012.56	1635.00	1386.80	1422.80
12	1201.00	804.80	1503.50	1386.80
13	1509.42	922.50	1444.40	1433.60
14	1394.00	876.00	1496.10	1175.50
15	1192.50	970.00	1577.50	1235.00
16	1301.50	1313.75	1397.60	1291.00
17	1485.00	1503.50	1322.50	1221.40
18		1201.00	1358.00	1042.25
X	1285.626	1156.405	1262.380	1208.403
SEM	50.830	85.428	47.654	48.436

Two-Way ANOVA			
Source of Variation	P value	P value summary	Significant?
Interaction	0.5361	ns	No
Mouse Model	0.8129	ns	No
Genotype	0.1347	ns	No

Post-Hoc Test				
Bonferroni	Mean Diff.	t-value	P-value	Summary
Muscle Specific:WT vs. Muscle Specific:KO	129.2	1.5	> 0.05	ns
Muscle Specific:WT vs. Whole Body:WT	23.25	0.2698	> 0.05	ns
Muscle Specific:KO vs. Whole Body:KO	-52	0.6123	> 0.05	ns
Whole Body:WT vs. Whole Body:KO	53.98	0.6356	> 0.05	ns

Table 2B: Post-training final body mass measurement, comparison between Muscle-Specific (MS) and Whole-Body (WB) Mice

Post-Training Final Body Mass (g) – MS versus WB Mice								
N	Muscle Specific Mice				Whole Body Mice			
	WT		mKO		WT		KO	
	UT	T	UT	T	UT	T	UT	T
1	31.52	29.02	42.40	27.10	22.83	20.09	33.40	22.76
2	31.23	30.52	30.60	27.72	22.82	20.46	28.90	26.32
3	34.03	30.35	33.40	25.61	28.70	23.30	31.50	25.79
4	28.07	30.74	30.40	28.42	29.30	19.39	32.50	21.29
5	36.13	30.07	30.40	28.92	28.10	19.28	29.60	28.80
6	36.15	29.75	43.00	27.06	28.50	26.50	31.40	28.50
7			38.40	26.82	31.70	25.80	28.20	30.00
8			29.10	29.41	30.00	27.00	27.90	22.80
9			38.40	30.10	30.6	26.30		
10			32.30	27.00				
X	32.855	30.075	34.840	27.816	28.061	23.124	30.425	25.783
SEM	1.295	0.254	1.660	0.434	1.057	1.110	0.727	1.140

Two-Way ANOVA			
Source of Variation	P value	P value summary	Significance
Interaction	0.1983	ns	No
Mouse Model	<0.0001	****	Yes
Genotype/Training	<0.0001	****	Yes

Post-Hoc Test				
Bonferroni	Mean Diff.	t-value	P-value	Summary
Muscle Specific:WT UT vs. Muscle Specific:WT T	2.78	1.511	> 0.05	ns
Muscle Specific:WT UT vs. Muscle Specific:KO UT	-1.98	1.203	> 0.05	ns
Muscle Specific:WT UT vs. Whole Body:WT UT	4.794	2.854	> 0.05	ns
Muscle Specific:WT T vs. Muscle Specific:KO T	2.259	1.373	> 0.05	ns
Muscle Specific:WT T vs. Whole Body:WT T	6.951	4.139	≤ 0.01	¶¶
Muscle Specific:KO UT vs. Muscle Specific:KO T	7.019	4.925	≤ 0.005	***
Muscle Specific:KO UT vs. Whole Body:KO UT	4.416	2.922	> 0.05	ns
Muscle Specific:KO T vs. Whole Body:KO T	2.034	1.346	> 0.05	ns
Whole Body:WT UT vs. Whole Body:WT T	4.937	3.287	≤0.05	*
Whole Body:WT UT vs. Whole Body:KO UT	-2.357	1.522	> 0.05	ns
Whole Body:WT T vs. Whole Body:KO T	-2.658	1.716	> 0.05	ns
Whole Body:KO UT vs. Whole Body:KO T	4.637	2.91	> 0.05	ns

Unpaired T-test – MS WT UT versus MS WT T	
P value	0.0478
P value summary	*
Significantly different? (P<0.05)	Yes

Unpaired T-test – WB KO UT versus WB KO T	
P value	0.0041
P value summary	**
Significantly different? (P<0.05)	Yes

Unpaired T-test - MS WT UT versus WB WT UT	
P value	0.0132
P value summary	¶
Significantly different? (P<0.05)	Yes

Unpaired T-test - MS KO UT versus WB KO UT	
P value	0.0401
P value summary	¶
Significantly different? (P<0.05)	Yes

Unpaired T-test – WB WT UT versus KO UT	
P value	0.0926
P value summary	ns
Significantly different? (P<0.05)	No

Table 2B: Post-training tibialis anterior (TA) mass, corrected for body mass, comparison between Muscle-Specific (MS) and Whole-Body (WB) Mice

Tibialis Anterior (TA) Skeletal Muscle Mass/Body Mass (mg/g) – MS versus WB Mice								
Muscle Specific Mice					Whole Body Mice			
N	WT		mKO		WT		KO	
	UT	T	UT	T	UT	T	UT	T
1	2.00	1.51	2.57	1.93	2.09	1.65	2.37	1.72
2	2.20	1.62	1.98	1.64	2.03	1.61	2.87	1.52
3	2.20	1.69	1.91	1.82	2.11	1.62	1.69	1.83
4	1.95	1.49	2.06	1.85	1.84	1.57	1.70	1.63
5	1.86	1.83	1.91	1.62	1.95	1.40	1.55	1.59
6	1.68	1.30	2.05	1.72	1.70	1.54	1.61	1.55
7			2.01	1.78	1.69	1.54	1.56	1.80
8			2.21	1.94			1.62	1.70
X	1.982	1.573	2.088	1.788	1.916	1.561	1.871	1.668
SEM	0.0822	0.0747	0.0768	0.0429	0.0665	0.0311	0.171	0.0403

Two-Way ANOVA			
Source of Variation	P value	P value summary	Significance
Interaction	0.6817	ns	No
Mouse Model	0.1068	ns	No
Genotype/Training	<0.0001	****	Yes

Post-Hoc Test				
Bonferroni	Mean Diff.	t-value	P-value	Summary
Muscle Specific:WT UT vs. Muscle Specific:WT T	0.4076	3.003	> 0.05	ns
Muscle Specific:WT UT vs. Muscle Specific:KO UT	-0.1059	0.8344	> 0.05	ns
Muscle Specific:WT UT vs. Whole Body:WT UT	0.06336	0.4844	> 0.05	ns
Muscle Specific:WT T vs. Muscle Specific:KO T	-0.2138	1.684	> 0.05	ns
Muscle Specific:WT T vs. Whole Body:WT T	0.01088	0.0832	> 0.05	ns
Muscle Specific:KO UT vs. Muscle Specific:KO T	0.2998	2.55	> 0.05	ns
Muscle Specific:KO UT vs. Whole Body:KO UT	0.2153	1.832	> 0.05	ns
Muscle Specific:KO T vs. Whole Body:KO T	0.1188	1.011	> 0.05	ns
Whole Body:WT UT vs. Whole Body:WT T	0.3551	2.826	> 0.05	ns
Whole Body:WT UT vs. Whole Body:KO UT	0.04604	0.3784	> 0.05	ns
Whole Body:WT T vs. Whole Body:KO T	-0.1058	0.8697	> 0.05	ns
Whole Body:KO UT vs. Whole Body:KO T	0.2033	1.729	> 0.05	ns

Unpaired T-test – MS WT UT versus MS WT T	
P value	0.0045
P value summary	**
Significantly different? (P<0.05)	Yes

Unpaired T-test – MS KO UT versus MS KO T	
P value	0.0043
P value summary	**
Significantly different? (P<0.05)	Yes

Unpaired T-test – WB WT UT versus WB WT T	
P value	0.0004
P value summary	***
Significantly different? (P<0.05)	Yes

Table 2B: Post-training gastrocnemius mass, corrected for body mass, comparison between Muscle-Specific (MS) and Whole-Body (WB) Mice

Gastrocnemius Muscle Mass/Body Mass (mg/g) – MS versus WB Mice								
Muscle Specific Mice					Whole Body Mice			
WT			mKO		WT		KO	
N	UT	T	UT	T	UT	T	UT	T
1	7.42	6.32	8.13	6.24	6.58	6.94	6.50	6.20
2	6.73	6.28	5.88	6.32	6.57	6.35	6.37	6.65
3	5.89	5.56	6.18	6.52	6.90	6.22	5.50	6.31
4	6.10	5.74	6.15	6.14	5.98	5.97	5.00	5.78
5	5.90	5.81	6.16	6.36	5.90	6.05	5.70	6.03
6	6.00	5.34	5.88	5.19	6.71	6.39	6.14	5.95
7			6.25	6.45	5.48	6.39	5.76	6.42
8			5.83	6.19			6.29	6.43
X	6.340	5.842	6.308	6.176	6.303	6.330	5.908	6.221
SEM	0.251	0.160	0.267	0.148	0.196	0.120	0.180	0.102

Two-Way ANOVA			
Source of Variation	P value	P value summary	Significance
Interaction	0.1415	ns	No
Mouse Model	0.8459	ns	No
Genotype/Training	0.5897	ns	No

Post-Hoc Test				
Bonferroni	Mean Diff.	t-value	P-value	Summary
Muscle Specific:WT UT vs. Muscle Specific:WT T	0.5022	1.745	> 0.05	ns
Muscle Specific:WT UT vs. Muscle Specific:KO UT	0.03814	0.1417	> 0.05	ns
Muscle Specific:WT UT vs. Whole Body:WT UT	0.03465	0.1249	> 0.05	ns
Muscle Specific:WT T vs. Muscle Specific:KO T	-0.3361	1.248	> 0.05	ns
Muscle Specific:WT T vs. Whole Body:WT T	-0.4899	1.766	> 0.05	ns
Muscle Specific:KO UT vs. Muscle Specific:KO T	0.1279	0.5133	> 0.05	ns
Muscle Specific:KO UT vs. Whole Body:KO UT	0.3969	1.592	> 0.05	ns
Muscle Specific:KO T vs. Whole Body:KO T	-0.04472	0.1794	> 0.05	ns
Whole Body:WT UT vs. Whole Body:WT T	-0.02235	0.0839	> 0.05	ns
Whole Body:WT UT vs. Whole Body:KO UT	0.4004	1.552	> 0.05	ns
Whole Body:WT T vs. Whole Body:KO T	0.1091	0.4227	> 0.05	ns
Whole Body:KO UT vs. Whole Body:KO T	-0.3137	1.259	> 0.05	ns

Table 2B: Post-training quadriceps mass, corrected for body mass, comparison between Muscle-Specific (MS) and Whole-Body (WB) Mice

Quadriceps Muscle Mass/Body Mass (mg/g) – MS versus WB Mice								
Muscle Specific Mice					Whole Body Mice			
WT		mKO			WT		KO	
N	UT	T	UT	T	UT	T	UT	T
1	6.56	5.65	7.28	6.56	8.49	7.75	7.53	5.85
2	6.51	5.95	6.96	6.50	7.58	7.48	6.29	6.65
3	5.87	6.58	6.64	6.56	8.32	6.08	5.54	6.70
4	6.15	6.08	6.52	6.45	6.54	7.51	5.44	6.56
5	6.18	6.57	6.05	6.52	6.22	5.46	5.89	6.37
6	6.15	6.22	6.05	6.60	7.16	6.65	7.91	6.38
7			7.61	7.15	5.33	6.13	5.79	6.19
8			5.93	6.73			6.73	6.95
X	6.237	6.175	6.630	6.634	7.091	6.723	6.390	6.456
SEM	0.105	0.148	0.218	0.0793	0.433	0.331	0.327	0.120

Two-Way ANOVA			
Source of Variation	P value	P value summary	Significance
Interaction	0.0966	ns	No
Mouse Model	0.1771	ns	No
Genotype/Training	0.8766	ns	No

Post-Hoc Test				
Bonferroni	Mean Diff.	t-value	P-value	Summary
Muscle Specific:WT UT vs. Muscle Specific:WT T	0.06081	0.1542	> 0.05	ns
Muscle Specific:WT UT vs. Muscle Specific:KO UT	-0.3929	1.065	> 0.05	ns
Muscle Specific:WT UT vs. Whole Body:WT UT	-0.8553	2.251	> 0.05	ns
Muscle Specific:WT T vs. Muscle Specific:KO T	-0.4573	1.24	> 0.05	ns
Muscle Specific:WT T vs. Whole Body:WT T	-0.5487	1.444	> 0.05	ns
Muscle Specific:KO UT vs. Muscle Specific:KO T	-0.003661	0.0107	> 0.05	ns
Muscle Specific:KO UT vs. Whole Body:KO UT	0.239	0.6997	> 0.05	ns
Muscle Specific:KO T vs. Whole Body:KO T	0.1759	0.515	> 0.05	ns
Whole Body:WT UT vs. Whole Body:WT T	0.3675	1.007	> 0.05	ns
Whole Body:WT UT vs. Whole Body:KO UT	0.7014	1.984	> 0.05	ns
Whole Body:WT T vs. Whole Body:KO T	0.2672	0.7559	> 0.05	ns
Whole Body:KO UT vs. Whole Body:KO T	-0.06675	0.1955	> 0.05	ns

Unpaired T-test – MS WT UT versus KO UT	
P value	0.1708
P value summary	ns
Significantly different? (P<0.05)	No

Table 2B: Post-training heart mass, corrected for body mass, comparison between Muscle-Specific (MS) and Whole-Body (WB) Mice

Heart Mass/Body Mass (mg/g) – MS versus WB Mice								
Muscle Specific Mice					Whole Body Mice			
WT		mKO			WT		KO	
N	UT	T	UT	T	UT	T	UT	T
1	6.14	6.04	3.69	5.42	4.44	6.87	6.11	6.48
2	5.71	6.26	4.29	5.69	6.00	6.56	6.07	6.33
3	4.89	5.69	5.07	6.01	5.65	7.15	6.64	6.23
4	3.99	5.13	4.76	5.51	5.82	7.04	5.56	6.99
5	6.59	5.76	5.06	6.13	5.67	6.79	4.78	7.76
6	4.94	5.66	5.14	5.64	5.46	9.62	4.56	7.09
7			5.04	6.10	4.98	6.30	5.13	7.33
8			5.11	6.00			4.32	6.59
X	5.377	5.757	4.770	5.813	5.431	7.190	5.396	6.850
SEM	0.388	0.157	0.184	0.0989	0.205	0.419	0.294	0.189

Two-Way ANOVA			
Source of Variation	P value	P value summary	Significance
Interaction	0.0772	ns	No
Mouse Model	<0.0001	****	Yes
Genotype/Training	<0.0001	****	Yes

Post-Hoc Test					
Bonferroni		Mean Diff.	t-value	P-value	Summary
Muscle Specific:WT UT vs. Muscle Specific:WT T		-0.3815	0.9603	> 0.05	ns
Muscle Specific:WT UT vs. Muscle Specific:KO UT		0.6059	1.63	> 0.05	ns
Muscle Specific:WT UT vs. Whole Body:WT UT		-0.05545	0.1448	> 0.05	ns
Muscle Specific:WT T vs. Muscle Specific:KO T		-0.05429	0.1461	> 0.05	ns
Muscle Specific:WT T vs. Whole Body:WT T		-1.433	3.743	≤ 0.05	*
Muscle Specific:KO UT vs. Muscle Specific:KO T		-1.042	3.028	> 0.05	ns
Muscle Specific:KO UT vs. Whole Body:KO UT		-0.6252	1.817	> 0.05	ns
Muscle Specific:KO T vs. Whole Body:KO T		-1.039	3.019	> 0.05	ns
Whole Body:WT UT vs. Whole Body:WT T		-1.759	4.782	≤ 0.005	***
Whole Body:WT UT vs. Whole Body:KO UT		0.03617	0.1016	> 0.05	ns
Whole Body:WT T vs. Whole Body:KO T		0.34	0.9547	> 0.05	ns
Whole Body:KO UT vs. Whole Body:KO T		-1.455	4.23	≤ 0.01	**

Unpaired T-test – MS KO UT versus MS KO T	
P value	0.0002
P value summary	***
Significantly different? (P<0.05)	Yes

Table 2B: Post-training epididymal fat mass, corrected for body mass, comparison between Muscle-Specific (MS) and Whole-Body (WB) Mice

Epididymal Fat Muscle Mass/Body Mass (mg/g) – MS versus WB Mice								
Muscle Specific Mice					Whole Body Mice			
WT		mKO		WT		KO		
N	UT	T	UT	T	UT	T	UT	T
1	33.60	22.25	67.17	26.68	29.06	18.64	49.44	17.50
2	43.06	24.78	59.87	27.04	35.80	21.60	40.08	14.09
3	51.42	29.34	41.71	30.32	22.18	23.89	39.33	16.55
4	38.65	39.98	53.59	24.04	29.74	21.75	52.07	17.03
5	39.77	44.16	39.43	19.37	22.51	22.73	46.69	17.33
6	54.89	28.43	58.87	27.07	33.29	22.14	23.70	20.86
7			59.64	14.52	38.43	21.57	32.48	20.58
8			56.22	22.32				17.18
X	43.565	31.490	54.563	23.920	30.144	21.760	40.541	17.640
SEM	3.307	3.545	3.352	1.792	2.358	0.606	3.780	0.773

Two-Way ANOVA			
Source of Variation	P value	P value summary	Significance
Interaction	0.4031	ns	No
Mouse Model	<0.0001	****	Yes
Genotype/Training	<0.0001	****	Yes

Post-Hoc Test				
Bonferroni	Mean Diff.	t-value	P-value	Summary
Muscle Specific:WT UT vs. Muscle Specific:WT T	12.07	2.989	> 0.05	ns
Muscle Specific:WT UT vs. Muscle Specific:KO UT	-11	2.911	> 0.05	ns
Muscle Specific:WT UT vs. Whole Body:WT UT	13.42	3.447	≤ 0.05	*
Muscle Specific:WT T vs. Muscle Specific:KO T	7.569	2.003	> 0.05	ns
Muscle Specific:WT T vs. Whole Body:WT T	9.731	2.5	> 0.05	ns
Muscle Specific:KO UT vs. Muscle Specific:KO T	30.64	8.76	≤ 0.001	****
Muscle Specific:KO UT vs. Whole Body:KO UT	14.02	3.872	≤ 0.01	¶¶
Muscle Specific:KO T vs. Whole Body:KO T	6.282	1.796	> 0.05	ns
Whole Body:WT UT vs. Whole Body:WT T	8.387	2.243	> 0.05	ns
Whole Body:WT UT vs. Whole Body:KO UT	-10.4	2.78	> 0.05	ns
Whole Body:WT T vs. Whole Body:KO T	4.12	1.138	> 0.05	ns
Whole Body:KO UT vs. Whole Body:KO T	22.9	6.326	≤ 0.001	****

Unpaired T-test – MS WT UT versus MS WT T	
P value	0.0320
P value summary	*
Significantly different? (P<0.05)	Yes

Unpaired T-test – WB WT UT versus WB WT T	
P value	0.0049
P value summary	**
Significantly different? (P<0.05)	Yes

Unpaired T-test – MS WT UT versus WB WT UT	
P value	0.0062
P value summary	¶¶
Significantly different? (P<0.05)	Yes

Unpaired T-test – MS WT UT versus KO UT	
P value	0.0417
P value summary	†
Significantly different? (P<0.05)	Yes

Table 2C: Post-training SS mitochondrial yield comparison between Muscle-Specific (MS) and Whole-Body (WB) Mice

SS Mitochondrial Yield ($\mu\text{g}/\text{mg}$) – MS versus WB Mice								
Muscle Specific Mice					Whole Body Mice			
N	WT		mKO		WT		KO	
	UT	T	UT	T	UT	T	UT	T
1	0.47	0.95	0.58	0.8	0.46	0.76	0.51	0.6
2	0.62	0.83	0.44	1.03	0.69	1	0.85	0.54
3	0.71	0.89	0.83	0.9	0.59	1.01	0.69	0.59
4	0.22	0.79	0.69	0.76	1.14	0.72	0.78	0.74
5	0.56	0.87	0.036	0.85	0.73	0.8	0.43	0.58
6	0.67	0.61	0.6	0.69	0.5	1.5	0.6	0.72
7			0.59	0.64	0.61	1.15	0.76	0.73
8			0.72		1.55	1.81	0.59	0.72
9					0.52	1.82		0.72
10					0.54			0.66
11								0.91
X	0.541	0.823	0.561	0.81	0.733	1.174	0.651	0.683
SEM	0.0730	0.0481	0.0852	0.0498	0.110	0.144	0.0508	0.0314

Two-Way ANOVA			
Source of Variation	P value	P value summary	Significance
Interaction	0.0358	*	Yes
Mouse Model	0.0141	*	Yes
Genotype/Training	0.0027	**	Yes

Post-Hoc Test				
Bonferroni	Mean Diff.	t-value	P-value	Summary
Muscle Specific:WT UT vs. Muscle Specific:WT T	-0.2809	1.763	> 0.05	ns
Muscle Specific:WT UT vs. Muscle Specific:KO UT	-0.01550	0.104	> 0.05	ns
Muscle Specific:WT UT vs. Whole Body:WT UT	-0.3908	2.743	> 0.05	ns
Muscle Specific:WT T vs. Muscle Specific:KO T	0.01575	0.1026	> 0.05	ns
Muscle Specific:WT T vs. Whole Body:WT T	-0.3502	2.408	> 0.05	ns
Muscle Specific:KO UT vs. Muscle Specific:KO T	-0.2496	1.748	> 0.05	ns
Muscle Specific:KO UT vs. Whole Body:KO UT	-0.09303	0.6742	> 0.05	ns
Muscle Specific:KO T vs. Whole Body:KO T	0.1256	0.9411	> 0.05	ns
Whole Body:WT UT vs. Whole Body:WT T	-0.2402	1.895	> 0.05	ns
Whole Body:WT UT vs. Whole Body:KO UT	0.2823	2.157	> 0.05	ns
Whole Body:WT T vs. Whole Body:KO T	0.4915	3.963	≤ 0.01	**
Whole Body:KO UT vs. Whole Body:KO T	-0.03101	0.2418	> 0.05	ns

Unpaired T-test – MS WT UT versus T	
P value	0.0089
P value summary	**
Significantly different? (P<0.05)	Yes

Unpaired T-test – MS KO UT versus T	
P value	0.0166
P value summary	*
Significantly different? (P<0.05)	Yes

Unpaired T-test – WB WT UT versus WT T	
P value	0.0247
P value summary	*
Significantly different? (P<0.05)	Yes

Unpaired T-test – MS WT UT versus WB WT UT	
P value	0.2339
P value summary	ns
Significantly different? (P<0.05)	No

Table 2C: Post-training IMF mitochondrial yield comparison between Muscle-Specific (MS) and Whole-Body (WB) Mice

IMF Mitochondrial Yield ($\mu\text{g}/\text{mg}$) – MS versus WB								
Muscle Specific Mice					Whole Body Mice			
N	WT		mKO		WT		KO	
	UT	T	UT	T	UT	T	UT	T
1	1.11	1.047	0.98	1.1	0.7	1.17	0.67	1.35
2	1.00	1.017	1.18	1.17	1.04	1.45	0.78	1.4
3	1.22	1.06	1.22	1.35	0.94	1.21	1.26	1.1
4	1.09	1.56	1.15	1.21	1.51	0.85	1.16	1.31
5	1.08	1.58	1.06	1.61	0.5	1.24	0.97	1.35
6	1.04	1.14	1.15	1.76	1.15	1.29	1.05	1.31
7		1.38	0.12	1.54	1.42	1.3	1.25	1.41
8			0.96	1.76	1.82	1.15	1.21	1.2
9			1.23	1.44	0.73	2.11	1.25	1.37
10			0.99		0.55	2.58	0.89	
11					1.78	2.18		
X	1.0903	1.255	1.004	1.438	1.104	1.503	1.049	1.311
SEM	0.0308	0.0933	0.103	0.0828	0.143	0.162	0.0676	0.0336

Two-Way ANOVA			
Source of Variation	P value	P value summary	Significance
Interaction	0.2100	ns	No
Mouse Model	0.2508	ns	No
Genotype/Training	0.0008	***	Yes

Post-Hoc Test					
Bonferroni		Mean Diff.	t-value	P-value	Summary
Muscle Specific:WT UT vs. Muscle Specific:WT T		-0.1655	0.9203	> 0.05	ns
Muscle Specific:WT UT vs. Muscle Specific:KO UT		0.08605	0.5155	> 0.05	ns
Muscle Specific:WT UT vs. Whole Body:WT UT		-0.1042	0.6351	> 0.05	ns
Muscle Specific:WT T vs. Muscle Specific:KO T		-0.1820	1.117	> 0.05	ns
Muscle Specific:WT T vs. Whole Body:WT T		-0.3376	2.16	> 0.05	ns
Muscle Specific:KO UT vs. Muscle Specific:KO T		-0.4335	2.919	> 0.05	ns
Muscle Specific:KO UT vs. Whole Body:KO UT		-0.04359	0.3015	> 0.05	ns
Muscle Specific:KO T vs. Whole Body:KO T		0.1274	0.836	> 0.05	ns
Whole Body:WT UT vs. Whole Body:WT T		-0.3989	2.894	> 0.05	ns
Whole Body:WT UT vs. Whole Body:KO UT		0.1467	1.038	> 0.05	ns
Whole Body:WT T vs. Whole Body:KO T		0.2830	1.948	> 0.05	ns
Whole Body:KO UT vs. Whole Body:KO T		-0.2625	1.768	> 0.05	ns

Unpaired T-test – MS WT UT versus WT T	
P value	0.1455
P value summary	ns
Significantly different? (P<0.05)	No

Unpaired T-test – WB WT UT versus WT T	
P value	0.0796
P value summary	ns
Significantly different? (P<0.05)	No

Unpaired T-test – MS KO UT versus KO T	
P value	0.0050
P value summary	**
Significantly different? (P<0.05)	Yes

Unpaired T-test – WB KO UT versus KO T	
P value	0.0038
P value summary	**
Significantly different? (P<0.05)	Yes

Table 2C: Post-training respiratory control ratio (RCR) in SS mitochondria, comparison between Muscle-Specific (MS) and Whole-Body (WB) Mice

SS Mitochondria RCR – MS versus WB Mice								
N	Muscle Specific Mice				Whole Body Mice			
	WT		mKO		WT		KO	
	UT	T	UT	T	UT	T	UT	T
1	2.09	4.56	3.19	5.00	1.36	11.00	1.09	4.25
2	0.70	3.62	2.52	4.22	1.05	7.50	9.13	2.32
3	5.82	10.30	4.33	5.55	10.00	8.29	2.00	4.00
4	3.56	37.00	7.35	5.64	8.70	13.00	0.14	11.2
5	7.20	17.00	5.44	9.32	3.56	11.00	1.50	7.25
6	3.15	4.71	4.90	4.39	1.00	2.60	4.57	5.29
7	3.93		6.45	4.31	0.40	5.08		2.67
8			2.75	19.00	0.50			
9					3.67			
X	3.779	12.865	4.616	7.179	3.360	8.353	3.072	5.283
SEM	0.826	5.251	0.621	1.787	1.205	1.381	1.355	1.167

Two-Way ANOVA			
Source of Variation	P value	P value summary	Significance
Interaction	0.7667	ns	No
Mouse Model	0.1352	ns	No
Genotype/Training	0.0029	**	Yes

Post-Hoc Test				
Bonferroni	Mean Diff.	t-value	P-value	Summary
Muscle Specific:WT UT vs. Muscle Specific:WT T	-9.086	3.139	> 0.05	ns
Muscle Specific:WT UT vs. Muscle Specific:KO UT	-0.8377	0.3111	> 0.05	ns
Muscle Specific:WT UT vs. Whole Body:WT UT	0.4186	0.1597	> 0.05	ns
Muscle Specific:WT T vs. Muscle Specific:KO T	5.686	2.024	> 0.05	ns
Muscle Specific:WT T vs. Whole Body:WT T	4.512	1.559	> 0.05	ns
Muscle Specific:KO UT vs. Muscle Specific:KO T	-2.563	0.9851	> 0.05	ns
Muscle Specific:KO UT vs. Whole Body:KO UT	1.545	0.5497	> 0.05	ns
Muscle Specific:KO T vs. Whole Body:KO T	1.896	0.7041	> 0.05	ns
Whole Body:WT UT vs. Whole Body:WT T	-4.993	1.904	> 0.05	ns
Whole Body:WT UT vs. Whole Body:KO UT	0.2883	0.1052	> 0.05	ns
Whole Body:WT T vs. Whole Body:KO T	3.070	1.104	> 0.05	ns
Whole Body:KO UT vs. Whole Body:KO T	-2.211	0.7640	> 0.05	ns

Unpaired T-test – MS WT UT versus WT T	
P value	0.0911
P value summary	ns
Significantly different? (P<0.05)	No

Unpaired T-test – WB WT UT versus WT T	
P value	0.0164
P value summary	*
Significantly different? (P<0.05)	Yes

Unpaired T-test – MS KO UT versus KO T	
P value	0.1971
P value summary	ns
Significantly different? (P<0.05)	No

Table 2C: Post-training respiratory control ratio (RCR) in SS mitochondria, comparison between Muscle-Specific (MS) and Whole-Body (WB) Mice

IMF Mitochondria RCR – MS versus WB Mice								
N	Muscle Specific Mice				Whole Body Mice			
	WT		mKO		WT		KO	
	UT	T	UT	T	UT	T	UT	T
1	6.59	2.82	8.62	7.89	20.14	12.36	21.47	11.3
2	5.43	18.47	5.22	7.97	15.9	12.33	3.82	9.72
3	6.89	4.74	5.77	8.17	3.83	7.43	7.06	9.42
4	5.86	19.06	12.36	1.80	4.50	13.04	11.22	15.64
5	5.64	7.49	7.80	6.27	9.14	27.87	10.49	22.12
6	5.89	8.04	6.66	4.97	11.37	25.04	11.98	12.73
7			2.85	18.36	15.88	15.77		39.1
8				41.50	9.66			
X	6.0500	10.103	7.0400	12.116	11.303	16.263	11.007	17.147
SEM	0.232	2.847	1.134	4.521	2.025	2.808	2.436	4.016

Two-Way ANOVA			
Source of Variation	P value	P value summary	Significance
Interaction	0.9879	ns	No
Mouse Model	0.0199	*	Yes
Genotype/Training	0.1217	ns	No

Post-Hoc Test				
Bonferroni	Mean Diff.	t-value	P-value	Summary
Muscle Specific:WT UT vs. Muscle Specific:WT T	-4.053	0.9000	> 0.05	ns
Muscle Specific:WT UT vs. Muscle Specific:KO UT	-0.9900	0.2281	> 0.05	ns
Muscle Specific:WT UT vs. Whole Body:WT UT	-5.253	1.247	> 0.05	ns
Muscle Specific:WT T vs. Muscle Specific:KO T	-2.013	0.4778	> 0.05	ns
Muscle Specific:WT T vs. Whole Body:WT T	-6.160	1.419	> 0.05	ns
Muscle Specific:KO UT vs. Muscle Specific:KO T	-5.076	1.257	> 0.05	ns
Muscle Specific:KO UT vs. Whole Body:KO UT	-3.967	0.9140	> 0.05	ns
Muscle Specific:KO T vs. Whole Body:KO T	-5.031	1.246	> 0.05	ns
Whole Body:WT UT vs. Whole Body:WT T	-4.960	1.229	> 0.05	ns
Whole Body:WT UT vs. Whole Body:KO UT	0.2958	0.07023	> 0.05	ns
Whole Body:WT T vs. Whole Body:KO T	-0.8843	0.2121	> 0.05	ns
Whole Body:KO UT vs. Whole Body:KO T	-6.140	1.415	> 0.05	ns

Unpaired T-test – MS WT UT versus WT T	
P value	0.1863
P value summary	ns
Significantly different? (P<0.05)	No

Unpaired T-test – MS WT UT versus WB WT UT	
P value	0.0468
P value summary	¶
Significantly different? (P<0.05)	Yes

Unpaired T-test – WB WT UT versus WT T	
P value	0.1682
P value summary	ns
Significantly different? (P<0.05)	No

Unpaired T-test – WB KO UT versus KO T	
P value	0.2367
P value summary	ns
Significantly different? (P<0.05)	No

Table 3: mRNA and protein fold comparison, average values and fold change

mRNA and Protein Comparison – Muscle Specific Mice							
mRNA/protein	WT		KO		Δ WT UT vs. mKO	Δ WT UT vs. T	Δ mKO UT vs. T
	UT	T	UT	T			
<i>p53 mRNA</i>	3.9	2.3	n/a	n/a	n/a	↓ 41.0%	n/a
p53 protein	0.70	0.27	n/a	n/a	n/a	↓ 61.4%	n/a
<i>p21 mRNA</i>	5.6	3.5	4.1	5.4	↓ 26.8%	↓ 37.5%	↑ 1.3-fold
p21 protein	0.42	0.34	0.29	0.59	↓ 31.0 %	NS	↑ 2.0-fold
<i>Bax mRNA</i>	8.3	6.7	5.1	3.4	↓ 38.6 %	↓ 19.3%	↓ 33.3%
Bax protein	0.25	0.38	0.59	0.34	↑ 2.4-fold	NS	↓ 42.4%
<i>Mdm2 mRNA</i>	3.1	2.8	2.8	2.6	NS	NS	NS
Mdm2 protein	0.34	0.56	0.35	0.74	NS	↑ 1.6-fold	↑ 2.1-fold
<i>Tfam mRNA</i>	6.4	5.8	3.2	4.2	↓ 50%	NS	↑ 1.3-fold
Tfam protein	0.57	0.69	0.41	0.86	↓ 28.1%	NS	↑ 2.1-fold
<i>PGC-1α mRNA</i>	5.2	5.4	4.3	6.7	NS	NS	↑ 1.6-fold
PGC-1α protein	0.46	0.84	0.29	0.76	↓ 37.0%	↑ 1.8-fold	↑ 2.6-fold
<i>p62 mRNA</i>	5.7	5.6	4.5	4.9	↓ 21.1%	NS	NS
p62 protein	0.43	0.75	1.01	0.72	↑ 2.3-fold	↑ 1.7-fold	↓ 28.7%
<i>LC3 mRNA</i>	4.9	4.9	2.7	3.5	↓ 44.9 %	NS	↑ 1.3-fold
LC3 protein	0.34	0.73	0.45	0.61	NS	↑ 2.1-fold	↑ 1.4-fold

Figure 2B: Pre-Training performance test, initial and final blood lactate comparison between Muscle-Specific (MS) and Whole-Body (WB) mice

Pre-Training Stress Performance Test – Lactate Production (mM) – MS versus WB Mice								
N	MS WT		MS mKO		WB WT		WB KO	
	Pre-Lactate	Post-Lactate	Pre-Lactate	Post-Lactate	Pre-Lactate	Post-Lactate	Pre-Lactate	Post-Lactate
1	2.9	11.1	1.5	12.7	1.1	10.6	1.1	14.7
2	1.1	11.5	2.0	13.4	1.4	9.6	2.3	9.1
3	2.1	10.6	1.8	12.0	1.3	9.2	1.9	11.2
4	2.2	10.5	2.0	10.9	2.2	8.5	2.4	15.3
5	2.3	8.4	1.8	9.5	1.4	9.2	1.9	11.4
6	2.3	8.8	1.6	18.6	1.7	10.8	2.3	10.6
7	2.3	10.0	1.5	13.2	2.1	10.0	2.0	10.9
8	2.6	11.8	1.8	9.3	2.6	8.7		11.5
9	1.2	12.8	2.1	14.2	1.9	9.6		10.3
10	2.5	13.5	2.3	12.2	1.6	11.9		14.4
11	1.6	9.0	2.3	13.8	1.5	10.3		10.3
12	1.3	8.7	2.6	13.3	2.2	8.8		11.0
13	2.9	7.8	1.7	9.4		9.5		15.0
14	2.4		1.5	9.7		10.3		10.6
15	1.2		1.9	10.7		9.2		11.7
16	2.1		2.1	9.7		10.3		12.0
17	1.3		2.1	10.7		9.9		10.8
18			1.6			8.8		
19						9.4		
20						10.8		
X	2.018	10.346	1.900	11.959	1.750	9.770	1.986	11.812
SEM	0.148	0.490	0.0741	0.584	0.130	0.193	0.167	0.451

Two-Way ANOVA			
Source of Variation	P value	P value summary	Significance
Interaction	0.0071	**	Yes
Mouse Model/Genotype	0.0025	**	Yes
Pre/Post Lactate	<0.0001	****	Yes

Post-Hoc Test				
Bonferroni	Mean Diff.	t-value	P-value	Summary
MS WT:Pre-Lactate vs. MS WT:Post-Lactate	-8.329	16.56	≤0.001	****
MS WT:Pre-Lactate vs. MS KO:Pre-Lactate	0.1176	0.2548	> 0.05	ns
MS WT:Pre-Lactate vs. WB WT:Pre-Lactate	0.2676	0.5199	> 0.05	ns
MS WT:Post-Lactate vs. MS KO:Post-Lactate	-1.613	3.206	≤ 0.05	†
MS WT:Post-Lactate vs. WB WT:Post-Lactate	0.5762	1.184	> 0.05	ns
MS KO:Pre-Lactate vs. MS KO:Post-Lactate	-10.06	21.78	≤0.001	****
MS KO:Pre-Lactate vs. WB KO:Pre-Lactate	-0.08571	0.1409	> 0.05	ns
MS KO:Post-Lactate vs. WB KO:Post-Lactate	0.1471	0.314	> 0.05	ns
WB WT:Pre-Lactate vs. WB WT:Post-Lactate	-8.02	16.09	≤0.001	****
WB WT:Pre-Lactate vs. WB KO:Pre-Lactate	-0.2357	0.363	> 0.05	ns
WB WT:Post-Lactate vs. WB KO:Post-Lactate	-2.042	4.533	≤0.005	†††
WB KO:Pre-Lactate vs. WB KO:Post-Lactate	-9.826	16.02	≤0.001	****

Figure 3A: Cage hanging grip strength test, time hanging

Cage Hanging Grip Strength Test – Time (sec) – Whole Body Mice		
N	WT	KO
1	105.17	278.02
2	84.42	123.30
3	171.70	129.30
4	42.62	551.30
5	254.38	143.67
6	172.60	332.29
7	179.80	156.71
8	232.91	354.34
9	114.77	280.00
10	212.09	262.00
11	272.90	85.99
12	129.59	271.78
13	164.75	334.33
14	375.14	74.11
X	179.489	241.224
SEM	23.066	35.180

Unpaired T-test – WT versus KO	
P value	0.1542
P value summary	ns
Significantly different? (P<0.05)	No

Figure 3B: Cage hanging grip strength test, holding impulse

Cage Hanging Grip Strength Test – Holding Impulse –Whole Body Mice		
N	WT	KO
1	3018.379	7562.144
2	2237.13	3723.66
3	5030.81	4072.95
4	1099.596	17035.17
5	6944.574	4381.935
6	4850.06	10799.43
7	5124.3	5375.153
8	6288.57	10204.99
9	3638.209	7980
10	5577.967	7755.2
11	7422.88	2700.086
12	3317.504	8153.4
13	4332.925	9428.106
14	9378.5	2067.669
X	4875.815	7231.421
SEM	586.216	1062.210

Unpaired T-test – WT versus KO	
P value	0.0631
P value summary	ns
Significantly different? (P<0.05)	No

Figure 4A: Balance Beam Test, time to cross

Balance Beam Test – Time to Cross (sec) – Whole Body Mice		
N	WT	KO
1	6	5
2	12	6
3	4	9
4	4	6
5	8	27
6	5	25
7	4	14
8	5	9
9	5	5
10	3	8
11	3	5
12	5	5
13	7	8
14	6	4
X	5.500	9.714
SEM	0.627	1.971

Unpaired T-test – WT versus KO	
P value	0.0519
P value summary	†
Significantly different? (P<0.05)	Yes

Figure 4B: Balance Beam Test, number of paw slips

Balance Beam Test – Number of Paw Slips – Whole Body Mice		
N	WT	KO
1	0	1
2	2	4
3	0	3
4	0	2
5	4	2
6	2	5
7	1	5
8	9	2
9	8	2
10	4	9
11	2	8
12	1	1
13	1	7
14	3	4
X	2.643	3.929
SEM	0.753	0.691

Unpaired T-test – WT versus KO	
P value	0.2196
P value summary	ns
Significantly different? (P<0.05)	No

Figure 4C: Vertical pole test, time traversing down the pole

Vertical Pole Test – Time (sec) – Whole Body Mice		
N	WT	KO
1	4.077	4.157
2	4.753	3.393
3	3.403	4.137
4	4.377	4.347
5	3.630	5.013
6	4.543	3.750
7	3.840	3.987
8	5.577	6.073
9	3.710	4.033
10	6.083	4.310
11	6.760	4.583
12	5.200	4.027
13	4.087	2.947
14	5.090	2.443
X	4.652	4.086
SEM	0.265	0.232

Unpaired T-test – WT versus KO	
P value	0.1195
P value summary	ns
Significantly different? (P<0.05)	No

Figure 4D: Cylinder escape test, time to escape cylinder

Cylinder Escape Test – Time (sec) – Whole Body Mice		
N	WT	KO
1	231.00	600.00
2	537.75	600.00
3	343.85	186.53
4	588.04	98.62
5	366.31	177.40
6	345.82	600.00
7	108.16	265.69
8	600.00	217.87
9	173.64	502.39
10	244.34	466.83
11	600.00	198.78
12	281.10	403.9
13	320.48	499.00
14	319.83	162.96
X	361.451	355.712
SEM	43.021	49.788

Unpaired T-test – WT versus KO	
P value	0.9312
P value summary	ns
Significantly different? (P<0.05)	No

Figure 5: Post-training DNA fragmentation, Muscle-Specific (MS) versus Whole-Body (WB) Mice

DNA Fragmentation – MS versus WB Mice								
N	Muscle Specific Mice				Whole Body Mice			
	WT		mKO		WT		KO	
	UT	T	UT	T	UT	T	UT	T
1	0.77	0.72	0.69	0.87	0.93	1.11	0.88	0.94
2	0.72	0.84	0.83	0.76	1.71	0.88	1.13	0.93
3	0.90	0.77	0.79	0.92	1.22	1.10	1.25	1.16
4	0.77	0.83	0.81	1.06	1.13	1.28	1.20	1.25
5	0.97	0.90	0.86	0.87	1.46	1.22	1.13	1.27
6	1.51	0.84	1.37	0.94	1.28	1.07	1.46	0.15
7	0.76	0.80	1.03	1.02	1.48			
8				0.94				
X	0.914	0.814	0.911	0.923	1.316	1.110	1.175	0.950
SEM	0.105	0.0218	0.0856	0.0330	0.0972	0.0565	0.0771	0.171

Two-Way ANOVA			
Source of Variation	P value	P value summary	Significance
Interaction	0.1921	ns	No
Mouse Model	0.0003	***	Yes
Genotype/Training	0.1729	ns	No

Post-Hoc Test				
Bonferroni	Mean Diff.	t-value	P-value	Summary
Muscle Specific:WT UT vs. Muscle Specific:WT T	0.1000	0.8194	> 0.05	ns
Muscle Specific:WT UT vs. Muscle Specific:KO UT	0.002857	0.02341	> 0.05	ns
Muscle Specific:WT UT vs. Whole Body:WT UT	-0.4014	3.289	> 0.05	ns
Muscle Specific:WT T vs. Muscle Specific:KO T	-0.1082	0.9158	> 0.05	ns
Muscle Specific:WT T vs. Whole Body:WT T	-0.2957	2.328	> 0.05	ns
Muscle Specific:KO UT vs. Muscle Specific:KO T	-0.01107	0.09369	> 0.05	ns
Muscle Specific:KO UT vs. Whole Body:KO UT	-0.2636	2.075	> 0.05	ns
Muscle Specific:KO T vs. Whole Body:KO T	-0.0275	0.2230	> 0.05	ns
Whole Body:WT UT vs. Whole Body:WT T	0.2057	1.619	> 0.05	ns
Whole Body:WT UT vs. Whole Body:KO UT	0.1407	1.108	> 0.05	ns
Whole Body:WT T vs. Whole Body:KO T	0.1600	1.214	> 0.05	ns
Whole Body:KO UT vs. Whole Body:KO T	0.2250	1.707	> 0.05	ns

Unpaired T-test – MS KO UT versus WB KO UT	
P value	0.0434
P value summary	¶
Significantly different? (P<0.05)	Yes

Unpaired T-test – WB WT UT versus WB WT T	
P value	0.1084
P value summary	ns
Significantly different? (P<0.05)	No

Unpaired T-test – MS WT T versus WB WT T	
P value	0.0003
P value summary	¶¶¶
Significantly different? (P<0.05)	Yes

Unpaired T-test – MS KO T versus WB KO T	
P value	0.8585
P value summary	ns
Significantly different? (P<0.05)	No

Unpaired T-test – MS WT UT versus WB WT UT	
P value	0.0158
P value summary	¶
Significantly different? (P<0.05)	Yes

Figure 6A: Post-training AIF protein release from SS and IMF mitochondria under basal conditions

AIF Protein Release - Basal – SS & IMF Mitochondria – Muscle-Specific Mice								
N	SS				IMF			
	WT		mKO		WT		mKO	
	UT	T	UT	T	UT	T	UT	T
1	2294.13	340.41	2919.26	12049.57	693.06	1564.26	826.01	2765.08
2	2016.72	9556.91	11410.15	7472.45	495.58	3846.26	280.09	698.86
3	1291.48	13763.81	345.53	520.36	251.97	354.305	340.24	337.48
4	784.72	3254.91	319.46	496.65	451.01	729.8	426.68	137.97
5	556.31	610.6	5800.08	291.49	459.58	367.94	162.26	426.44
6	7734.15	446.82	353.6	949.41	283.23	351.16	50.9	300.85
7	1074.89	2492.26	4672.5	1976.18	522.89	355.9	237.87	113.78
8		1212.77	416.06	1178.53		294.26	202.7	332.09
9		1678.79	923.28	629.28		719.79	230.11	961.48
10		573.72	694.06	510.68		819.28	836.06	690.58
11			1026.16	10476.57			868.06	1102.35
12			1386.43	1372.08			892.81	
13			1057.96				939.21	
14			3592.03				599.34	
X	2250.343	3393.100	2494.04	3160.271	451.046	940.296	492.310	715.178
SEM	944.250	1444.369	831.900	1231.770	56.396	345.100	85.674	226.692

Two-Way ANOVA			
Source of Variation	P value	P value summary	Significance
Interaction	0.9826	ns	No
Genotype/Training	0.7779	ns	No
Mitochondrial Subfraction	0.0005	###	Yes

Post-Hoc Test				
Bonferroni	Mean Diff.	t-value	P-value	Summary
WT UT:SS vs. WT UT:IMF	1904	1.316	> 0.05	ns
WT UT:SS vs. WT T:SS	-1049	0.7869	> 0.05	ns
WT UT:SS vs. KO UT:SS	-139.3	0.1112	> 0.05	ns
WT UT:IMF vs. WT T:IMF	-489.2	0.3669	> 0.05	ns
WT UT:IMF vs. KO UT:IMF	-41.26	0.03294	> 0.05	ns
WT T:SS vs. WT T:IMF	2464	2.036	> 0.05	ns
WT T:SS vs. KO T:SS	243.7	0.2104	> 0.05	ns
WT T:IMF vs. KO T:IMF	202.3	0.1746	> 0.05	ns
KO UT:SS vs. KO UT:IMF	2002	1.957	> 0.05	ns
KO UT:SS vs. KO T:SS	-666.3	0.6259	> 0.05	ns
KO UT:IMF vs. KO T:IMF	-245.7	0.2308	> 0.05	ns
KO T:SS vs. KO T:IMF	2422	2.193	> 0.05	ns

Unpaired T-test – IMF WT UT versus WT T	
P value	0.2614
P value summary	ns
Significantly different? (P<0.05)	No

Unpaired T-test – IMF KO UT versus T	
P value	0.2607
P value summary	ns
Significantly different? (P<0.05)	No

Figure 6B: Post-training AIF protein release from SS and IMF mitochondria under basal conditions

AIF Protein Release - Basal – SS & IMF Mitochondria – Whole-Body Mice								
SS					IMF			
WT			KO		WT		KO	
N	UT	T	UT	T	UT	T	UT	T
1	663.82	2670.5	632.06	675.01	5741.9	501.28	5772.6	1960.7
2	16699.1	788.01	526.31	1099.52	791.5	2701.52	2591.62	10169.21
3	561.58	874.06	527.75	535.53	6295.62	10118.69	1675.84	808.84
4	610.33	951.33	758.26	866.5	5981.9	650.26	827.03	3626.3
5	510.33	641.43	4921.03	1486.03	4618.21	661.89	541.91	2328.4
6	1471.69	709.77	1121.4	926.91	4663.08	780.84	6607.03	6676.62
7	4572.26	666.06	537.74	147.21	388.23	9439.4	775.79	8036.15
8	691.96	671.67	765.5	637.74	850.67	801.96	6063.18	6102.81
9	590.77	4176.13	1229.15	1247.23	788.94	401.97	790.36	2182.45
10	976.5	807.13	1004.82	2108.15	544.46	476.48	540.89	418.87
11	3780.55	727.23		2785.05	245.97	428.16		1520.27
12		551.36				671.06		
13		1058.31				2872.55		
X	2829.899	1176.384	1202.402	1137.716	2810.044	2346.620	2618.625	3984.602
SEM	1450.087	291.828	420.872	227.956	780.908	943.402	797.131	979.268

Two-Way ANOVA			
Source of Variation	P value	P value summary	Significance
Interaction	0.3131	ns	No
Genotype/Training	0.5861	ns	No
Mitochondrial Subfraction	0.0306	*	Yes

Post-Hoc Test				
Bonferroni	Mean Diff.	t-value	P-value	Summary
WT UT:SS vs. WT UT:IMF	300.7	0.2561	> 0.05	ns
WT UT:SS vs. WT T:SS	1662	1.473	> 0.05	ns
WT UT:SS vs. KO UT:SS	1636	1.360	> 0.05	ns
WT UT:IMF vs. WT T:IMF	190.7	0.1691	> 0.05	ns
WT UT:IMF vs. KO UT:IMF	-81.31	0.06759	> 0.05	ns
WT T:SS vs. WT T:IMF	-1170	1.084	> 0.05	ns
WT T:SS vs. KO T:SS	38.67	0.03428	> 0.05	ns
WT T:IMF vs. KO T:IMF	-1638	1.452	> 0.05	ns
KO UT:SS vs. KO UT:IMF	-1416	1.150	> 0.05	ns
KO UT:SS vs. KO T:SS	64.68	0.05376	> 0.05	ns
KO UT:IMF vs. KO T:IMF	-1366	1.135	> 0.05	ns
KO T:SS vs. KO T:IMF	-2847	2.425	> 0.05	ns

Figure 6C: Post-training AIF protein release from SS and IMF mitochondria treated with apoptotic stimulus (H₂O₂), presented as fold change

AIF Protein Release – Treated/Control – SS & IMF Mitochondria – Muscle-Specific Mice								
N	SS				IMF			
	WT		mKO		WT		mKO	
	UT	T	UT	T	UT	T	UT	T
1	6.04	2.76	6.16	1.43	16.95	10.63	11.10	4.61
2	7.79	1.36	1.04	2.29	15.88	20.34	19.75	14.91
3	10.75	1.20	2.88	8.30	11.95	19.88	8.27	22.45
4	15.91	5.24	3.38	18.17	14.97	21.32	29.12	18.24
5	2.67	8.10	6.85	7.40	14.91	7.31	25.87	23.96
6	14.35	9.50	9.00	15.36	16.12	21.73	11.58	22.69
7		14.10	15.59	1.91		24.72	14.80	22.96
8			20.45	13.00		20.74	7.12	17.86
9			18.97				22.05	10.64
10			5.98				21.60	
11							18.31	
X	9.585	6.037	9.030	8.483	15.130	18.334	17.234	17.591
SEM	2.063	1.812	2.181	2.291	0.708	2.131	2.182	2.184

Two-Way ANOVA			
Source of Variation	P value	P value summary	Significance
Interaction	0.5493	ns	No
Genotype/Training	0.9603	ns	No
Mitochondrial Subfraction	<0.0001	####	Yes

Post-Hoc Test				
Bonferroni	Mean Diff.	t-value	P-value	Summary
WT UT:SS vs. WT UT:IMF	-5.544	1.573	> 0.05	ns
WT UT:SS vs. WT T:SS	3.546	1.044	> 0.05	ns
WT UT:SS vs. KO UT:SS	0.5538	0.1757	> 0.05	ns
WT UT:IMF vs. WT T:IMF	-3.204	0.9717	> 0.05	ns
WT UT:IMF vs. KO UT:IMF	-2.103	0.6788	> 0.05	ns
WT T:SS vs. WT T:IMF	-12.29	3.891	≤ 0.01	**
WT T:SS vs. KO T:SS	-2.446	0.774	> 0.05	ns
WT T:IMF vs. KO T:IMF	0.7412	0.2498	> 0.05	ns
KO UT:SS vs. KO UT:IMF	-8.201	3.074	> 0.05	ns
KO UT:SS vs. KO T:SS	0.5466	0.1887	> 0.05	ns
KO UT:IMF vs. KO T:IMF	-0.3595	0.131	> 0.05	ns
KO T:SS vs. KO T:IMF	-9.107	3.07	> 0.05	ns

Unpaired T-test – WT UT IMF vs WT T IMF	
P value	0.2344
P value summary	ns
Significantly different? (P<0.05)	No

Figure 6D: Post-training AIF protein release from SS and IMF mitochondria treated with apoptotic stimulus (H₂O₂), presented as fold change

AIF Protein Release – Treated/Control – SS & IMF Mitochondria – Whole-Body Mice								
SS					IMF			
WT			KO		WT		KO	
N	UT	T	UT	T	UT	T	UT	T
1	9.73	4.23	10.56	12.75	1.78	4.01	2.13	8.47
2	23.62	22.91	9.31	22.25	8.80	1.63	3.42	1.63
3	28.80	17.62	4.47	6.28	1.05	10.51	7.56	3.06
4	39.74	14.15	8.90	19.97	3.16	13.28	2.08	8.26
5	13.18	21.18	24.49	29.89	2.54	1.17	1.10	2.33
6	3.62	21.95	17.73	14.19	2.19	6.40	5.22	0.57
7	5.28	7.90	19.69	10.20	18.49	1.30	2.81	1.96
8	17.79	8.90	18.21	11.39	20.95	4.70	17.72	4.85
9	12.57	2.09			6.36	15.00		30.01
10	21.16	25.31			8.21	43.64		8.03
11		24.44			15.60	6.06		
12		17.01						
X	17.549	15.641	14.170	15.865	8.103	9.791	5.255	6.917
SEM	3.525	2.338	2.407	2.709	2.159	3.672	1.923	2.732

Two-Way ANOVA			
Source of Variation	P value	P value summary	Significance
Interaction	0.9071	ns	No
Genotype/Training	0.6847	ns	No
Mitochondrial Subfraction	0.0001	###	Yes

Post-Hoc Test				
Bonferroni	Mean Diff.	t-value	P-value	Summary
WT UT:SS vs. WT UT:IMF	9.447	2.453	> 0.05	ns
WT UT:SS vs. WT T:SS	1.909	0.5059	> 0.05	ns
WT UT:SS vs. KO UT:SS	3.379	0.8083	> 0.05	ns
WT UT:IMF vs. WT T:IMF	-1.689	0.4495	> 0.05	ns
WT UT:IMF vs. KO UT:IMF	2.848	0.6953	> 0.05	ns
WT T:SS vs. WT T:IMF	5.848	1.59	> 0.05	ns
WT T:SS vs. KO T:SS	0.02642	0.0066	> 0.05	ns
WT T:IMF vs. KO T:IMF	2.873	0.746	> 0.05	ns
KO UT:SS vs. KO UT:IMF	8.915	2.023	> 0.05	ns
KO UT:SS vs. KO T:SS	-1.444	0.3276	> 0.05	ns
KO UT:IMF vs. KO T:IMF	-1.664	0.398	> 0.05	ns
KO T:SS vs. KO T:IMF	8.695	2.08	> 0.05	ns

Figure 7A: Post-training state 3 and 4 respiration in permeabilized fibers, WB Mice

N	O ₂ Consumption (pmol/s/mg tissue) - (Oroboros technology) – WB Mice									
	WT UT					WT T				
	+P/M (CI)	+ADP (CI)	+SUCC (CI&CII)	+Succ (CII)	+ADP (CII)	+P/M (CI)	+ADP (CI)	+SUCC (CI&CII)	+Succ (CII)	+ADP (CII)
1	23.38	101.4	145.31	63.25	138.09	26.79	190.1	236.4	98.54	191.48
2	6.25	57.35	68.2	77.32	138.95	17.18	139.48	170.87	60.67	107.11
3	12.21	53.82	119.12	53.16	121.45	27.87	95.74	226.5	68.72	170.57
4	15.6	85.7	116.32	76.62	134.1	21.02	103.58	137.22	76.07	119.36
5	13.66	64.08	80.52	45.4	79.6	10.6	108.05	136.86	68.24	124.38
X	14.22	72.47	105.89	63.15	122.4	20.69	127.39	181.57	74.45	142.58
SEM	2.772	9.107	13.968	6.313	11.157	3.186	17.351	21.337	6.497	16.283

N	KO UT					KO T				
	+P/M (CI)	+ADP (CI)	+SUCC (CI&CII)	+Succ (CII)	+ADP (CII)	+P/M (CI)	+ADP (CI)	+SUCC (CI&CII)	+Succ (CII)	+ADP (CII)
1	41.85	164.84	222.05	58.6	105.83	19.88	115.24	153.54	65	119.59
2	11.91	78.81	93.63	57.13	96.56	20.51	171.81	230.18	46.65	68.41
3	19.87	128.6	161.67	74.26	166.26					
4	29.57	134.46	181.73	59.87	117.99					
5										
X	25.80	126.68	164.77	62.47	121.66	20.20	143.52	191.86	55.83	94.00
SEM	17.823	26.831	3.971	15.501	0.315	28.285	38.320	9.175	25.590	17.823

Two-Way ANOVA			
Source of Variation	P value	P value summary	Significance
Interaction	0.0573	ns	No
Substrate	< 0.0001	****	Yes
Genotype/Training	0.0014	**	Yes

Post-Hoc Test				
Bonferroni	Mean Diff.	t-value	P-value	Summary
+P/M:WT UT vs. +P/M:WT T	-6.473	0.346	> 0.05	ns
+P/M:WT UT vs. +P/M:KO UT	-11.58	0.5835	> 0.05	ns
+P/M:WT T vs. +P/M:KO T	0.496	0.02004	> 0.05	ns
+P/M:KO UT vs. +P/M:KO T	5.603	0.2187	> 0.05	ns
+ADP:WT UT vs. +ADP:WT T	-54.92	2.935	> 0.05	ns
+ADP:WT UT vs. +ADP:KO UT	-54.2	2.731	> 0.05	ns
+ADP:WT T vs. +ADP:KO T	-16.13	0.6518	> 0.05	ns
+ADP:KO UT vs. +ADP:KO T	-16.85	0.6576	> 0.05	ns
+Succ:WT UT vs. +Succ:WT T	-75.68	4.044	≤ 0.05	*
+Succ:WT UT vs. +Succ:KO UT	-58.88	2.967	> 0.05	ns
+Succ:WT T vs. +Succ:KO T	-10.29	0.4157	> 0.05	ns
+Succ:KO UT vs. +Succ:KO T	-27.09	1.057	> 0.05	ns
+Succ:WT UT vs. +Succ:WT T	-11.3	0.604	> 0.05	ns
+Succ:WT UT vs. +Succ:KO UT	0.6853	0.03453	> 0.05	ns
+Succ:WT T vs. +Succ:KO T	18.63	0.7526	> 0.05	ns
+Succ:KO UT vs. +Succ:KO T	6.642	0.2592	> 0.05	ns
+ADP:WT UT vs. +ADP:WT T	-20.14	1.076	> 0.05	ns
+ADP:WT UT vs. +ADP:KO UT	0.7781	0.03921	> 0.05	ns
+ADP:WT T vs. +ADP:KO T	48.58	1.963	> 0.05	ns
+ADP:KO UT vs. +ADP:KO T	27.66	1.08	> 0.05	ns

Unpaired T-test – + ADP WT UT versus WT T	
P value	0.0231
P value summary	*
Significantly different? (P<0.05)	Yes

Unpaired T-test – + ADP WT UT versus KO UT	
P value	0.0233
P value summary	†
Significantly different? (P<0.05)	Yes

Unpaired T-test – + Succ WT UT versus KO UT	
P value	0.0768
P value summary	ns
Significantly different? (P<0.05)	No

Unpaired T-test – + P/M WT UT versus KO UT	
P value	0.1172
P value summary	ns
Significantly different? (P<0.05)	No

Figure 7B: Post-training fold change in state 3 and 4 respiration in permeabilized fibers, WB Mice

N	Fold Change O ₂ Consumption (pmol/s/mg tissue - (Oroboros technology) – WB Mice									
	WT T/UT					KO T/UT				
	+P/M (CI)	+ADP (CI)	+SUCC (CI&CII)	+Succ (CII)	+ADP (CII)	+P/M (CI)	+ADP (CI)	+SUCC (CI&CII)	+Succ (CII)	+ADP (CII)
1	1.88	2.62	2.23	1.56	1.56	0.77	0.91	0.93	1.04	0.98
2	1.21	1.92	1.61	0.96	0.87	0.8	1.36	1.4	0.75	0.56
3	1.96	1.32	2.14	1.09	0.39					
4	1.48	1.43	1.3	1.2	0.97					
5	0.75	1.49	1.29	1.08	1.02					
X	1.456	1.756	1.714	1.178	0.962	0.785	1.135	1.165	0.895	0.770
SEM	0.223	0.239	0.201	0.103	0.187	0.015	0.225	0.235	0.145	0.210

Two-Way ANOVA			
Source of Variation	P value	P value summary	Significance
Interaction	0.9108	ns	No
Substrate	0.1439	ns	No
Genotype/Training	0.0021	††	Yes

Post-Hoc Test				
Bonferroni	Mean Diff.	t-value	P-value	Summary
+P/M:WT (T/UT) vs. +P/M:KO (T/UT)	0.6725	2.043	> 0.05	ns
+ADP:WT (T/UT) vs. +ADP:KO (T/UT)	0.6248	1.899	> 0.05	ns
+Succ:WT (T/UT) vs. +Succ:KO (T/UT)	0.5502	1.672	> 0.05	ns
+Succ:WT (T/UT) vs. +Succ:KO (T/UT)	0.2853	0.8669	> 0.05	ns
+ADP:WT (T/UT) vs. +ADP:KO (T/UT)	0.3919	1.191	> 0.05	ns

Figure 7C: Post-training state 3 and 4 respiration in permeabilized fibers, corrected for mitochondrial content in WB Mice

N	O₂ Consumption/COX Activity (pmol/s/mg tissue/COX Activity) (Oroboros technology) – WB Mice									
	WT UT					WT T				
	+P/M (CI)	+ADP (CI)	+SUCC (CI&CII)	+Succ (CII)	+ADP (CII)	+P/M (CI)	+ADP (CI)	+SUCC (CI&CII)	+Succ (CII)	+ADP (CII)
1	2.06	8.93	12.8	5.57	12.17	0.93	6.6	8.21	3.42	6.65
2	0.49	4.45	5.29	6	10.79	0.75	6.12	7.5	2.66	4.7
3	0.55	2.41	5.34	2.38	5.44	1.49	5.13	12.14	3.68	9.14
4	0.93	5.11	6.94	4.57	8	0.7	3.44	4.56	2.53	3.96
5	1.22	5.72	7.19	4.05	7.11	0.49	5.02	6.36		
X	1.05	5.324	7.512	4.514	8.702	0.872	5.262	7.754	3.0725	6.1125
SEM	0.285	1.060	1.379	0.636	1.226	0.170	0.544	1.258	0.282	1.158

N	KO UT					KO T				
	+P/M (CI)	+ADP (CI)	+SUCC (CI&CII)	+Succ (CII)	+ADP (CII)	+P/M (CI)	+ADP (CI)	+SUCC (CI&CII)	+Succ (CII)	+ADP (CII)
	1	3.4	13.4	18.05	4.76	8.6	1	5.81	7.75	3.28
2	0.58	4.55	4.55	2.78	4.69	1.06	8.88	11.9	2.41	3.54
3	1.13	9.19	9.19	4.22	9.46					
4	3.33	20.46	20.46	6.74	13.28					
5				3.17	5.78					
X	2.11	11.9	13.0625	4.334	8.362	1.03	7.345	9.825	2.845	4.785
SEM	0.733	3.378	3.731	0.698	1.510	0.030	1.535	2.075	0.435	1.245

Two-Way ANOVA			
Source of Variation	P value	P value summary	Significance
Interaction	0.5030	ns	No
Substrate	< 0.0001	****	Yes
Genotype/Training	0.0073	**	Yes

Post-Hoc Test				
Bonferroni	Mean Diff.	t-value	P-value	Summary
+P/M:WT UT vs. +P/M:WT T	0.1749	0.09733	> 0.05	ns
+P/M:WT UT vs. +P/M:KO UT	-1.061	0.5569	> 0.05	ns
+P/M:WT T vs. +P/M:KO T	-0.1582	0.06655	> 0.05	ns
+P/M:KO UT vs. +P/M:KO T	1.078	0.4381	> 0.05	ns
+ADP:WT UT vs. +ADP:WT T	0.06488	0.0361	> 0.05	ns
+ADP:WT UT vs. +ADP:KO UT	-4.593	2.41	> 0.05	ns
+ADP:KO UT vs. +ADP:KO T	2.571	1.045	> 0.05	ns
+ADP:KO T vs. +Succ:WT T	-0.4024	0.1693	> 0.05	ns
+Succ:WT UT vs. +Succ:WT T	-0.238	0.1324	> 0.05	ns
+Succ:WT UT vs. +Succ:KO UT	-5.55	2.912	> 0.05	ns
+Succ:WT T vs. +Succ:KO T	-2.073	0.872	> 0.05	ns
+Succ:KO UT vs. +Succ:KO T	3.239	1.316	> 0.05	ns
+Succ:WT UT vs. +Succ:WT T	1.444	0.7574	> 0.05	ns
+Succ:WT UT vs. +Succ:KO UT	0.1821	0.1013	> 0.05	ns
+Succ:WT T vs. +Succ:KO T	0.2276	0.09251	> 0.05	ns
+Succ:KO UT vs. +Succ:KO T	1.489	0.6264	> 0.05	ns
+ADP:WT UT vs. +ADP:WT T	2.588	1.358	> 0.05	ns
+ADP:WT UT vs. +ADP:KO UT	0.339	0.1886	> 0.05	ns
+ADP:WT T vs. +ADP:KO T	1.328	0.5397	> 0.05	ns
+ADP:KO UT vs. +ADP:KO T	3.577	1.505	> 0.05	ns

Unpaired T-test – +P/M WT UT versus KO UT	
P value	0.1848
P value summary	ns
Significantly different? (P<0.05)	No

Unpaired T-test – +Succ (CII) WT UT versus WT T	
P value	0.1007
P value summary	ns
Significantly different? (P<0.05)	No

Figure 7C: Post-training fold change state 3 and 4 respiration in permeabilized fibers, corrected for mitochondrial content in WB Mice

N	Fold Change O ₂ Consumption (pmol/s/mg tissue/COX Activity) corrected for COX- (Oroboros technology) – WB Mice									
	WT T/UT					KO T/UT				
	+P/M (CI)	+ADP (CI)	+SUCC (CI&CII)	+Succ (CII)	+ADP (CII)	+P/M (CI)	+ADP (CI)	+SUCC (CI&CII)	+Succ (CII)	+ADP (CII)
1	0.89	1.24	1.09	0.76	0.76	0.48	0.59	0.59	0.71	0.67
2	0.72	1.15	1	0.59	0.54	0.5	0.9	0.91	0.52	0.39
3	1.42	0.96	1.62	0.82	1.05					
4	0.67	0.65	0.61	0.56	0.46					
5	0.47	0.94	0.85	0.7	0.66					
X	0.834	0.988	1.034	0.686	0.694	0.490	0.745	0.750	0.615	0.530
SEM	0.161	0.102	0.168	0.0494	0.103	0.01	0.155	0.160	0.095	0.140

Two-Way ANOVA			
Source of Variation	P value	P value summary	Significance
Interaction	0.9145	ns	No
Substrate	0.2508	ns	No
Genotype/Training	0.0331	†	Yes

Post-Hoc Test				
Bonferroni	Mean Diff.	t-value	P-value	Summary
+P/M:WT (T/UT) vs. +P/M:KO (T/UT)	0.3442	1.572	> 0.05	ns
+ADP:WT (T/UT) vs. +ADP:KO (T/UT)	0.2470	1.128	> 0.05	ns
+Succ:WT (T/UT) vs. +Succ:KO (T/UT)	0.2796	1.277	> 0.05	ns
+Succ:WT (T/UT) vs. +Succ:KO (T/UT)	0.06954	0.3176	> 0.05	ns
+ADP:WT (T/UT) vs. +ADP:KO (T/UT)	0.1637	0.7475	> 0.05	ns

Figure 8A: Post-training state 3 and 4 reactive oxygen species (ROS) emission rate from permeabilized fibers, WB Mice

N	H₂O₂ Emission Rate (pmol H₂O₂/pmol O₂ consumed) (Oroboros technology) – WB Mice									
	WT UT					WT T				
	+P/M (CI)	+ADP (CI)	+SUCC (CI&CII)	+Succ (CII)	+ADP (CII)	+P/M (CI)	+ADP (CI)	+SUCC (CI&CII)	+Succ (CII)	+ADP (CII)
1	0.52	0.019	0.011	0.47	0.017	0.48	0.0091	0.0076	0.29	0.015
2	0.57	0.02	0.017	0.2	0.012	0.28	0.0086	0.01	0.16	0.022
3	0.36	0.035	0.017	0.3	0.049	0.93	0.061	0.013	0.25	0.02
4	0.22	0.014	0.011	0.33	0.021	0.31	0.013	0.011	0.2	0.022
5	0.35	0.012	0.011	0.21	0.03	0.45	0.019	0.013	0.38	0.016
X	0.404	0.02	0.0134	0.302	0.0258	0.49	0.02214	0.01092	0.256	0.019
SEM	0.0631	0.00404	0.00147	0.0489	0.00651	0.117	0.00989	0.00101	0.0380	0.00148

N	KO UT					KO T				
	+P/M (CI)	+ADP (CI)	+SUCC (CI&CII)	+Succ (CII)	+ADP (CII)	+P/M (CI)	+ADP (CI)	+SUCC (CI&CII)	+Succ (CII)	+ADP (CII)
	1	0.52	0.015	0.0078	0.62	0.023	0.32	0.019	0.015	0.69
2	0.61	0.018	0.055	0.15	0.036	0.25	0.011	0.013	0.19	0.023
3	0.49	0.0086	0.0059	0.41	0.018					
4	0.3	0.0077	0.0055	0.32	0.016					
5										
X	0.48	0.0123	0.0186	0.375	0.0233	0.285	0.015	0.014	0.44	0.0255
SEM	0.0652	0.00249	0.0122	0.0979	0.00450	0.035	0.004	0.001	0.25	0.0025

Two-Way ANOVA			
Source of Variation	P value	P value summary	Significance
Interaction	0.5680	ns	No
Substrate	< 0.0001	****	Yes
Genotype/Training	0.8224	ns	No

Post-Hoc Test				
Bonferroni	Mean Diff.	t-value	P-value	Summary
+P/M:WT UT vs. +P/M:WT T	-0.0833	1.198	> 0.05	ns
+P/M:WT UT vs. +P/M:KO UT	-0.07751	1.051	> 0.05	ns
+P/M:WT T vs. +P/M:KO T	0.2053	2.232	> 0.05	ns
+P/M:KO UT vs. +P/M:KO T	0.1995	2.096	> 0.05	ns
+ADP:WT UT vs. +ADP:WT T	-0.002025	0.02913	> 0.05	ns
+ADP:WT UT vs. +ADP:KO UT	0.007556	0.1025	> 0.05	ns
+ADP:WT T vs. +ADP:KO T	0.00708	0.07698	> 0.05	ns
+ADP:KO UT vs. +ADP:KO T	-0.002502	0.02628	> 0.05	ns
+Succ:WT UT vs. +Succ:WT T	0.002804	0.04033	> 0.05	ns
+Succ:WT UT vs. +Succ:KO UT	-0.004937	0.06695	> 0.05	ns
+Succ:WT T vs. +Succ:KO T	-0.00332	0.0361	> 0.05	ns
+Succ:KO UT vs. +Succ:KO T	0.004421	0.04644	> 0.05	ns
+Succ:WT UT vs. +Succ:WT T	0.04617	0.664	> 0.05	ns
+Succ:WT UT vs. +Succ:KO UT	-0.07504	1.018	> 0.05	ns
+Succ:WT T vs. +Succ:KO T	-0.1859	2.022	> 0.05	ns
+Succ:KO UT vs. +Succ:KO T	-0.06473	0.68	> 0.05	ns
+ADP:WT UT vs. +ADP:WT T	0.006602	0.09496	> 0.05	ns
+ADP:WT UT vs. +ADP:KO UT	0.002576	0.03493	> 0.05	ns
+ADP:WT T vs. +ADP:KO T	-0.006496	0.07063	> 0.05	ns
+ADP:KO UT vs. +ADP:KO T	-0.00247	0.02594	> 0.05	ns

Figure 8B: Post-training fold change in state 3 and 4 reactive oxygen species (ROS) emission rate from permeabilized fibers, WB Mice

N	H₂O₂ Emission Rate Fold Change (pmol H₂O₂/pmol O₂ consumed) (Oroboros technology) – WB Mice									
	WT T/UT					KO T/UT				
	+P/M (CI)	+ADP (CI)	+SUCC (CI&CII)	+Succ (CII)	+ADP (CII)	+P/M (CI)	+ADP (CI)	+SUCC (CI&CII)	+Succ (CII)	+ADP (CII)
1	1.18	0.45	0.56	0.95	0.58	0.66	1.54	0.82	1.83	1.22
2	0.68	0.43	0.75	0.54	0.86	0.52	0.86	0.7	0.52	0.99
3	2.3	3.05	0.94	0.82	0.78					
4	0.75	0.65	0.79	0.67	0.87					
5	1.12	0.93	0.92	1.25	0.63					
X	1.206	1.102	0.792	0.846	0.744	0.59	1.2	0.76	1.175	1.105
SEM	0.291	0.495	0.0685	0.122	0.0594	0.0700	0.340	0.0600	0.655	0.115

Two-Way ANOVA			
Source of Variation	P value	P value summary	Significance
Interaction	0.6074	ns	No
Substrate	0.8499	ns	No
Genotype/Training	0.9015	ns	No

Post-Hoc Test				
Bonferroni	Mean Diff.	t-value	P-value	Summary
+P/M:WT (T/UT) vs. +P/M:KO (T/UT)	0.6203	1.298	> 0.05	ns
+ADP:WT (T/UT) vs. +ADP:KO (T/UT)	-0.09961	0.2084	> 0.05	ns
+Succ:WT (T/UT) vs. +Succ:KO (T/UT)	0.03231	0.06759	> 0.05	ns
+Succ:WT (T/UT) vs. +Succ:KO (T/UT)	-0.3250	0.68	> 0.05	ns
+ADP:WT (T/UT) vs. +ADP:KO (T/UT)	-0.3615	0.7562	> 0.05	ns

Figure 8C: Post-training state 3 and 4 reactive oxygen species (ROS) emission rate from permeabilized fibers, corrected for mitochondrial content, in WB Mice

N	H ₂ O ₂ Emission Rate (pmol H ₂ O ₂ /pmol O ₂ consumed/COX Activity) corrected for mitochondrial content (Oroboros technology) – WB Mice									
	WT UT					WT T				
	+P/M (CI)	+ADP (CI)	+SUCC (CI&CII)	+Succ (CII)	+ADP (CII)	+P/M (CI)	+ADP (CI)	+SUCC (CI&CII)	+Succ (CII)	+ADP (CII)
1	5.9	0.22	0.12	5.31	0.2	13.69	0.26	0.22	8.22	0.43
2	7.34	0.26	0.22	2.51	0.15	6.28	0.2	0.23	3.72	0.51
3	8.06	0.77	0.39	6.7	1.1	17.32	1.14	0.24	1.62	0.38
4	3.69	0.24	0.18	5.59	0.35	9.19	0.39	0.32	6.07	0.68
5	3.92	0.13	0.13	2.37	0.34	9.76	0.4	0.27	8.15	0.35
X	5.782	0.324	0.208	4.496	0.428	11.248	0.478	0.256	5.556	0.47
SEM	0.880	0.114	0.0489	0.871	0.172	1.923	0.170	0.0181	1.284	0.0591

N	KO UT					KO T				
	+P/M (CI)	+ADP (CI)	+SUCC (CI&CII)	+Succ (CII)	+ADP (CII)	+P/M (CI)	+ADP (CI)	+SUCC (CI&CII)	+Succ (CII)	+ADP (CII)
1	6.45	0.19	0.096	7.64	0.28	6.26	0.38	0.3	2.77	0.26
2	12.52	0.38	1.13	3.04	0.73	4.8	0.21	0.25	3.76	0.44
3	8.66	0.15	0.1	7.26	0.32					
4	2.68	0.068	0.049	2.87	0.15					
5										
X	7.578	0.197	0.344	5.203	0.370	5.530	0.295	0.275	3.265	0.350
SEM	2.0587	0.0661	0.262	1.300	0.125	0.730	0.0850	0.0250	0.495	0.0900

Two-Way ANOVA			
Source of Variation	P value	P value summary	Significance
Interaction	0.0814	ns	No
Substrate	< 0.0001	****	Yes
Genotype/Training	0.0166	*	Yes

Post-Hoc Test				
Bonferroni	Mean Diff.	t-value	P-value	Summary
+P/M:WT UT vs. +P/M:WT T	-5.466	-9.906 to -1.027	> 0.05	ns
+P/M:WT UT vs. +P/M:KO UT	-1.796	-6.505 to 2.913	> 0.05	ns
+P/M:WT T vs. +P/M:KO T	5.714	-0.1592 to 11.59	> 0.05	ns
+P/M:KO UT vs. +P/M:KO T	2.043	-4.036 to 8.123	> 0.05	ns
+ADP:WT UT vs. +ADP:WT T	-0.1529	-4.593 to 4.287	> 0.05	ns
+ADP:WT UT vs. +ADP:KO UT	0.1283	-4.581 to 4.837	> 0.05	ns
+ADP:WT T vs. +ADP:KO T	0.1834	-5.690 to 6.057	> 0.05	ns
+ADP:KO UT vs. +ADP:KO T	-0.09783	-6.177 to 5.982	> 0.05	ns
+Succ:WT UT vs. +Succ:WT T	-0.04779	-4.488 to 4.392	> 0.05	ns
+Succ:WT UT vs. +Succ:KO UT	-0.1352	-4.844 to 4.574	> 0.05	ns
+Succ:WT T vs. +Succ:KO T	-0.01951	-5.893 to 5.854	> 0.05	ns
+Succ:KO UT vs. +Succ:KO T	0.06787	-6.012 to 6.147	> 0.05	ns
+Succ:WT UT vs. +Succ:WT T	-1.663	-6.103 to 2.777	> 0.05	ns
+Succ:WT UT vs. +Succ:KO UT	-0.7127	-5.422 to 3.996	> 0.05	ns
+Succ:WT T vs. +Succ:KO T	2.891	-2.982 to 8.765	> 0.05	ns
+Succ:KO UT vs. +Succ:KO T	1.941	-4.139 to 8.020	> 0.05	ns
+ADP:WT UT vs. +ADP:WT T	-0.04265	-4.483 to 4.397	> 0.05	ns
+ADP:WT UT vs. +ADP:KO UT	0.05599	-4.653 to 4.765	> 0.05	ns
+ADP:WT T vs. +ADP:KO T	0.1161	-5.757 to 5.989	> 0.05	ns
+ADP:KO UT vs. +ADP:KO T	0.01745	-6.062 to 6.097	> 0.05	ns

Unpaired T-test – P/M (CI) WT UT versus WT T	
P value	0.0324
P value summary	*
Significantly different? (P<0.05)	Yes

Figure 8D: Post-training fold change in state 3 and 4 reactive oxygen species (ROS) emission rate from permeabilized fibers, corrected for mitochondrial content, in WB Mice

N	H ₂ O ₂ Emission Rate Fold Change (pmol H ₂ O ₂ /pmol O ₂ consumed/COX Activity) corrected for mitochondrial content (Oroboros technology) – WB Mice									
	WT T/UT					KO T/UT				
	+P/M (CI)	+ADP (CI)	+SUCC (CI&CII)	+Succ (CII)	+ADP (CII)	+P/M (CI)	+ADP (CI)	+SUCC (CI&CII)	+Succ (CII)	+ADP (CII)
1	2.37	0.81	1.05	1.83	1.01	0.83	1.94	0.88	0.53	0.7
2	1.09	0.6	1.11	0.83	1.19	0.63	1.06	0.73	0.72	1.2
3	3	3.51	1.15	1.03	0.88					
4	1.59	1.21	1.55	1.35	1.59					
5	1.69	1.23	1.29	1.81	0.82					
X	1.948	1.472	1.230	1.370	1.098	0.730	1.500	0.805	0.625	0.95
SEM	0.333	0.523	0.0892	0.202	0.138	0.100	0.440	0.075	0.095	0.25

Two-Way ANOVA			
Source of Variation	P value	P value summary	Significance
Interaction	0.4730	ns	No
Substrate	0.5680	ns	No
Genotype/Training	0.0406	†	Yes

Post-Hoc Test				
Bonferroni	Mean Diff.	t-value	P-value	Summary
+P/M:WT (T/UT) vs. +P/M:KO (T/UT)	1.215	2.344	> 0.05	ns
+ADP:WT (T/UT) vs. +ADP:KO (T/UT)	-0.02744	0.05294	> 0.05	ns
+Succ:WT (T/UT) vs. +Succ:KO (T/UT)	0.4255	0.8208	> 0.05	ns
+Succ:WT (T/UT) vs. +Succ:KO (T/UT)	0.7428	1.433	> 0.05	ns
+ADP:WT (T/UT) vs. +ADP:KO (T/UT)	0.1471	0.2839	> 0.05	ns

Figure 9A: Post-training whole muscle Nrf2 protein

Whole Muscle Nrf2 Protein - Muscle Specific Mice				
	WT		mKO	
N	UT	T	UT	T
1	0.31	0.26	0.32	0.19
2	0.38	0.25	0.34	0.22
3	0.22	0.20	0.30	0.15
4	0.34	0.22	0.32	0.24
5	0.36	0.17		
X	0.324	0.220	0.321	0.199
SEM	0.0276	0.016	0.007	0.020

Two-Way ANOVA			
Source of Variation	P value	P value summary	Significance
Interaction	0.6693	ns	No
Substrate	0.6022	ns	No
Genotype/Training	< 0.0001	****	Yes

Post-Hoc Test				
Bonferroni	Mean Diff.	t-value	P-value	Summary
WT:UT vs. WT:T	0.1020	3.708	≤ 0.05	*
WT:UT vs. KO:UT	0.002000	0.06855	> 0.05	ns
WT:UT vs. KO:T	0.1220	4.182	≤ 0.01	**
WT:T vs. KO:UT	-0.1000	3.428	≤ 0.05	*
WT:T vs. KO:T	0.0200	0.6855	> 0.05	ns
KO:UT vs. KO:T	0.1200	3.902	≤ 0.01	**

Figure 9B: Post-training whole muscle KEAP1 protein

Whole Muscle KEAP1 Protein - Muscle Specific Mice				
	WT		KO	
N	UT	T	UT	T
1	0.69	0.23	0.93	0.17
2	1.01	0.16	0.71	0.56
3	0.84	0.61	1.04	0.19
4	1.11	0.24	0.90	0.70
X	0.910	0.311	0.894	0.406
SEM	0.094	0.101	0.070	0.132

Two-Way ANOVA			
Source of Variation	P value	P value summary	Significance
Interaction	0.5961	ns	No
Substrate	0.7052	ns	No
Genotype/Training	0.0002	***	Yes

Post-Hoc Test				
Bonferroni	Mean Diff.	t-value	P-value	Summary
WT:UT vs. WT:T	0.5995	4.161	≤ 0.01	**
WT:UT vs. KO:UT	0.01600	0.1110	> 0.05	ns
WT:UT vs. KO:T	0.5046	3.502	≤ 0.05	*
WT:T vs. KO:UT	-0.5835	4.050	≤ 0.01	**
WT:T vs. KO:T	-0.09495	0.6590	> 0.05	ns
KO:UT vs. KO:T	0.4886	3.391	≤ 0.05	*

Figure 10A: Post-training p53 mRNA transcript

p53 mRNA - Muscle Specific Mice		
WT		
N	UT	T
1	4.32	2.74
2	3.99	3.47
3	3.96	1.74
4	3.81	3.62
5	3.53	1.43
6	3.85	1.25
7		2.90
8		3.67
9		1.03
10		1.43
X	3.910	2.327
SEM	0.106	0.334

Unpaired T-test – MS WT UT versus WT T	
P value	0.0032
P value summary	**
Significantly different? (P<0.05)	Yes

Figure 10B: Post-training whole muscle COX IV protein

Whole Muscle COX IV Protein - Muscle Specific Mice				
N	WT		KO	
	UT	T	UT	T
1	0.38	0.70	0.82	0.67
2	0.24	0.69	0.95	0.58
3	0.49	1.00	1.11	0.65
4	0.54	1.12	1.21	0.84
5	0.33	0.66	0.94	0.77
6		0.68	1.34	0.74
7			0.92	0.67
X	0.398	0.807	1.041	0.702
SEM	0.053	0.082	0.070	0.033

Two-Way ANOVA			
Source of Variation	P value	P value summary	Significance
Interaction	< 0.0001	****	Yes
Substrate	0.0003	***	Yes
Genotype/Training	0.5626	ns	No

Post-Hoc Test				
Bonferroni	Mean Diff.	t-value	P-value	Summary
WT:UT vs. WT:T	-0.4123	4.387	≤ 0.01	**
WT:UT vs. KO:UT	-0.6454	7.101	≤ 0.001	††††
WT:UT vs. KO:T	-0.3069	3.376	≤ 0.05	*
WT:T vs. KO:UT	-0.2331	2.699	> 0.05	ns
WT:T vs. KO:T	0.1055	1.221	> 0.05	ns
KO:UT vs. KO:T	0.3386	4.080	≤ 0.01	**

Figure 10D: Whole muscle Bax protein, untrained Muscle-Specific (MS) and Whole-Body (WB) Mice

Whole Muscle Bax Protein– Untrained MS versus WB Mice				
	Muscle Specific Mice		Whole Body Mice	
N	WT	mKO	WT	KO
1	0.31	0.59	0.61	0.17
2	0.20	0.64	0.73	0.56
3	0.38	0.65	0.83	0.24
4	0.11	0.49	0.70	0.73
5		0.64	0.91	0.36
6		0.50	0.84	
X	0.250	0.585	0.770	0.412
SEM	0.060	0.030	0.045	0.103

Two-Way ANOVA			
Source of Variation	P value	P value summary	Significance
Interaction	< 0.0001	****	Yes
Substrate	0.0134	*	Yes
Genotype/Training	0.8570	ns	No

Post-Hoc Test				
Bonferroni	Mean Diff.	t-value	P-value	Summary
MS:WT vs. MS:KO	-0.3350	3.652	≤ 0.05	†
MS:WT vs. WB:WT	-0.5200	5.669	≤ 0.005	†††
MS:WT vs. WB:KO	-0.1620	1.700	> 0.05	ns
MS:KO vs. WB:WT	-0.1850	2.255	> 0.05	ns
MS:KO vs. WB:KO	0.1730	2.011	> 0.05	ns
WB:WT vs. WB:KO	0.3580	4.161	≤ 0.01	††

Figure 10E: Whole muscle Bcl-2 protein, untrained Muscle-Specific (MS) and Whole-Body (WB) Mice

Whole Muscle Bcl-2 Protein– Untrained MS versus WB Mice				
	Muscle Specific Mice		Whole Body Mice	
N	WT	mKO	WT	KO
1	0.59	0.22	0.31	0.24
2	0.84	0.16	0.45	1.09
3	0.86	0.52	0.61	0.54
4	0.54	0.46	0.34	0.88
5	0.70	0.41	0.56	0.32
6		0.30		0.81
7		0.48		
8		0.36		
X	0.705	0.363	0.496	0.587
SEM	0.064	0.0457	0.0910	0.129

Two-Way ANOVA			
Source of Variation	P value	P value summary	Significance
Interaction	0.0049	**	Yes
Substrate	0.8493	ns	No
Genotype/Training	0.3847	ns	No

Post-Hoc Test				
Bonferroni	Mean Diff.	t-value	P-value	Summary
MS:WT vs. MS:KO	0.3422	2.954	≤ 0.05	†
MS:WT vs. WB:WT	0.2508	1.952	> 0.05	ns
MS:WT vs. WB:KO	0.05882	0.4781	> 0.05	ns
MS:KO vs. WB:WT	-0.09135	0.7886	> 0.05	ns
MS:KO vs. WB:KO	-0.2834	2.582	> 0.05	ns
WB:WT vs. WB:KO	-0.1920	1.561	> 0.05	ns

Unpaired T-test – MS WT UT versus WB WT UT	
P value	0.0202
P value summary	¶
Significantly different? (P<0.05)	Yes

Figure 10F: Whole muscle p21 protein, untrained Muscle-Specific (MS) and Whole-Body (WB) Mice

Whole Muscle p21 Protein– Untrained MS versus WB Mice				
	Muscle Specific Mice		Whole Body Mice	
N	WT	mKO	WT	KO
1	0.35	0.28	1.56	0.45
2	0.23	0.29	1.18	0.23
3	0.56	0.34	0.54	0.43
4	0.46	0.28	1.18	0.78
5	0.42	0.30	0.68	0.57
6	0.51	0.24	0.95	0.15
7				0.14
8				0.11
X	0.420	0.288	1.0154	0.357
SEM	0.049	0.013	0.152	0.0854

Two-Way ANOVA			
Source of Variation	P value	P value summary	Significance
Interaction	0.0088	**	Yes
Substrate	0.0015	**	Yes
Genotype/Training	0.0003	***	Yes

Post-Hoc Test				
Bonferroni	Mean Diff.	t-value	P-value	Summary
MS:WT vs. MS:KO	0.1317	0.9866	> 0.05	ns
MS:WT vs. WB:WT	-0.5948	4.455	≤ 0.01	¶¶
MS:WT vs. WB:KO	0.06267	0.5017	> 0.05	ns
MS:KO vs. WB:WT	-0.7266	5.441	≤ 0.005	***
MS:KO vs. WB:KO	-0.06907	0.5530	> 0.05	ns
WB:WT vs. WB:KO	0.6575	5.264	≤ 0.005	†††

Unpaired T-test – MS WT UT versus KO UT	
P value	0.0240
P value summary	†
Significantly different? (P<0.05)	Yes

Figure 11A: State 3 respiration in IMF mitochondria, untrained Muscle-Specific (MS) and Whole-Body (WB) Mice

State 3 Respiration (natoms O₂/mg protein/min) – IMF Mitochondria – Untrained MS versus WB Mice				
	Muscle Specific Mice		Whole Body Mice	
N	WT	mKO	WT	KO
1	106.21	88.48	61.28	18.35
2	122.63	87.14	78.42	79.49
3	94.36	79.44	44.38	60.10
4	110.43	86.33	46.17	104.98
5	120.03	78.36	60.22	65.81
6	71.54	46.20	79.56	104.27
7	73.03		91.24	
8			91.94	
X	99.747	77.658	69.151	72.167
SEM	7.912	6.520	6.661	13.220

Two-Way ANOVA			
Source of Variation	P value	P value summary	Significance
Interaction	0.1634	ns	No
Substrate	0.0499	*	Yes
Genotype/Training	0.2854	ns	No

Post-Hoc Test				
Bonferroni	Mean Diff.	t-value	P-value	Summary
MS:WT vs. MS:KO	22.09	1.765	> 0.05	ns
MS:WT vs. WB:WT	30.60	2.629	> 0.05	ns
MS:WT vs. WB:KO	27.58	2.204	> 0.05	ns
MS:KO vs. WB:WT	8.507	0.7004	> 0.05	ns
MS:KO vs. WB:KO	5.492	0.4229	> 0.05	ns
WB:WT vs. WB:KO	-3.015	0.2483	> 0.05	ns

Unpaired T-test – MS WT UT versus KO UT	
P value	0.0549
P value summary	†
Significantly different? (P<0.05)	Yes

Unpaired T-test – MS WT UT versus WB WT UT	
P value	0.0106
P value summary	¶
Significantly different? (P<0.05)	Yes

Figure 11B: State 3 reactive oxygen species (ROS) emission in IMF mitochondria, untrained Muscle-Specific (MS) and Whole-Body (WB) Mice

State 3 ROS (natoms O₂/mg protein/min) – IMF Mitochondria – Untrained MS versus WB Mice				
	Muscle Specific Mice		Whole Body Mice	
N	WT	mKO	WT	KO
1	0.78	1.19	1.03	0.92
2	0.60	1.05	1.20	1.04
3	0.85	1.09	0.94	3.24
4	0.66	1.38	0.77	1.11
5	0.40	1.58	1.24	0.86
6	1.38	1.35	0.93	1.08
7	0.94	3.80	0.70	0.98
8	0.35	1.15	0.65	
X	0.745	1.574	0.933	1.319
SEM	0.116	0.324	0.0774	0.322

Two-Way ANOVA			
Source of Variation	P value	P value summary	Significance
Interaction	0.3506	ns	No
Substrate	0.8856	ns	No
Genotype/Training	0.0147	*	Yes

Post-Hoc Test				
Bonferroni	Mean Diff.	t-value	P-value	Summary
MS:WT vs. MS:KO	-0.8288	2.559	> 0.05	ns
MS:WT vs. WB:WT	-0.1875	0.5790	> 0.05	ns
MS:WT vs. WB:KO	-0.5736	1.711	> 0.05	ns
MS:KO vs. WB:WT	0.6413	1.980	> 0.05	ns
MS:KO vs. WB:KO	0.2552	0.7613	> 0.05	ns
WB:WT vs. WB:KO	-0.3861	1.152	> 0.05	ns

Unpaired T-test – MS WT UT versus KO UT	
P value	0.0304
P value summary	†
Significantly different? (P<0.05)	Yes

Figure 11C: Cytochrome c protein release from IMF mitochondria under basal conditions, untrained Muscle-Specific (MS) and Whole-Body (WB) Mice

Cytochrome C Protein Release – Basal - IMF Mitochondria				
	Muscle Specific Mice		Whole Body Mice	
N	WT UT	KO UT	WT UT	KO T
1	14777.075	11805.23	8882.55	4828.72
2	10879.30	876.77	5446.012	5942.84
3	5276.39	8269.96	8798.84	821.31
4	10847.033	7693.74	10278.13	4366.74
5	12690.50	15333.42	9556.74	7076.21
6	16205.13	840.96	16467.20	4715.72
7	13608.81	10962.15		
8		10698.42		
9		2861.15		
10		790.69		
11		9118.45		
12		3422.40		
13		1381.96		
14		11137.79		
X	12040.605	6799.506	9904.910	4625.255
SEM	1347.328	1327.0812	1477.323	862.741

Two-Way ANOVA			
Source of Variation	P value	P value summary	Significance
Interaction	0.9899	ns	No
Substrate	0.1649	ns	No
Genotype/Training	0.0016	**	Yes

Post-Hoc Test				
Bonferroni	Mean Diff.	t-value	P-value	Summary
MS:WT vs. MS:KO	5241	2.770	> 0.05	ns
MS:WT vs. WB:WT	2136	0.9391	> 0.05	ns
MS:WT vs. WB:KO	7415	3.261	≤ 0.05	*
MS:KO vs. WB:WT	-3105	1.557	> 0.05	ns
MS:KO vs. WB:KO	2174	1.090	> 0.05	ns
WB:WT vs. WB:KO	5280	2.237	> 0.05	ns

Unpaired T-test – MS WT UT versus KO UT	
P value	0.0228
P value summary	†
Significantly different? (P<0.05)	Yes

Unpaired T-test – WB WT UT versus KO UT	
P value	0.0115
P value summary	†
Significantly different? (P<0.05)	Yes

Appendix D: Laboratory Methods and Protocols

Genotyping – p53 Whole Body mice and Muscle Specific Mice

Reagents:

1. **Proteinase K (Pro K) from Tritirachium Album** (Sigma-Aldrich, cat#: P6556-100 mg). Store at -20°C
2. **Sterile Molecular Grade Water** (Wisent Inc., cat#: 809-115-66). Store at room temperature.
3. **Lysis Buffer for DNA Extraction:** Measure out 10 mM TRIS HCl (0.121g/100 mL) (Hydroxymethyl) Aminomethane (TRIS), Bioshop, cat#: 77-86-1, store at room temperature), 150 mM NaCl (0.8766g/100 mL) (Sodium Chloride, Bioshop, cat#: 7647-14-5, stored at room temperature), and 20 mM EDTA (0.744g/100 mL) (Bioshop, cat#: 6381-92-6, store at room temperature) and add the appropriate amount of ddH₂O depending on measurements. Then pH to 8.0. Autoclave for 30 min and store at room temperature.
4. **Jumpstart REDTaq ReadyMix Reaction Mix for PCR** (cat#: P0982-100RXN, Sigma Life Sciences, Store at -20°C).
5. **Mineral Oil** (PE Express, material#: 01862302, cat#: 87200827, Store at room temperature).
6. **1.5% Agarose** (Bioshop, cat#: 9012-36-6). Store at room temperature.
7. **50X TAE:** Weigh out 242 g TRIS (Hydroxymethyl) Aminomethane (TRIS), Bioshop, cat#: 77-86-1, store at room temperature), add 500 mL ddH₂O, add 57.1 mL Acetic Acid (Glacial, cat#64-19-7, stored at room temperature) into a beaker. Then prepare the 0.5M EDTA by adding 93.06 g of EDTA (Bioshop, cat#: 6381-92-6, store at room temperature) in 300 mL ddH₂O, pH with NaOH to 8.0; volume up to 500 mL total. Then add 100 mL of the EDTA solution to the beaker with TRIS, ddH₂O, and acetic acid. Autoclave and split the solution into sterile bottles.
 - a. **1X TAE:** Combine 80 mL of 50X TAE with 4 L of ddH₂O.
8. **Ethidium Bromide** (Sigma-Aldrich, cat#: E-8751). Store at 4°C. Make 10 mg/mL of ddH₂O.

Procedure:

1. Prepare sterile 1.5 mL (MCT Graduated Natural Eppendorfs; cat# 05-408-129; Fischer Brand) labeled eppendorf tubes on ice.
2. Obtain a small ear clipping from each mouse using an ear-punch tool.

*Fischerbrand Animal Ear-Punch
and Tags tool (13-812-201)*



Mice should be held by pinching the skin along the spine and pulling back to prevent movement. Clippings should be placed in specified eppendorfs and placed on ice.

3. Next prepare a fresh mixture of ProK by first measuring out approximately 1 mg of ProK and adding the associated ratio of 1000 μ l of sterile ddH₂O. If more ProK is added, add the correct ratio of water (i.e. 1.3 mg ProK to 1300 μ l sterile ddH₂O).
4. Then make a 9:1 mixture of lysis buffer to the ProK solution made in step 3. This can be accomplished by adding 900 μ l of lysis buffer and 100 μ l of ProK solution to a new sterile 1.5 ml eppendorf. Vortex (Mini Vortex, cat#: 02215365, Fischer Scientific) this new ProK/Lysis buffer solution.
5. Then add 20 μ l of this ProK/Lysis buffer solution to each of the eppendorfs containing the ear clipping. Ensure that the ear clipping is submerged in solution. Then vortex to mix the solution with the ear clipping and tap the eppendorf on the bench to bring the ear clipping into the solution at the bottom of the eppendorf.
6. Next, incubate the ear clipping and solution in the 55°C water bath (model 1122S, cat#: 13271-138, VWR) for 30 min. Eppendorfs should be placed in floating foam pads. After the initial 15 min, take the ear clippings out of the water bath and vortex. Tap again to ensure the clipping is submerged in the fluid at the bottom of the eppendorf. Place back in the water bath for the remaining 15 min. Once completed, vortex one last time and place tubes on ice.
7. Then add 180 μ l of sterile ddH₂O to each of the ear clipping containing eppendorfs and mix up and down with the pipette.
8. Finally, place the tubes on the hot plate (VWR Block Heater, cat#: 12621-104) set to ~95-100°C for 5 min. Once completed, briefly tap the tubes to mix.
9. Then store at -20°C or use immediately for PCR.

PCR-Amplification Procedure:

1. The mastermix solution must first be created. This solution contains the specific primers required for mouse breed/brand. This information can be found on the animal companies website. Three different mastermixes were required as there were three mouse breed/brand (p53 muscle specific mice (donated by Dr. Christopher Adams), Taconic p53 whole body mice (Donehower et al., Nature, 1992), Jackson p53 whole body mice (B6.129S2-Trp53^{tm1Tyj}/J)). Mastermix contains: *solutions are made either in 1.5 mL sterile eppendorfs or sterile 15 mL polystyrene conical tubes (cat#: 352095, Falcon).
 - a. Jumpstart Taq Polymerase **added first*
 - b. Sterile ddH₂O **added second*
 - c. Forward and Reverse primers for specific mouse brand ** add last*
 - i. Taconic p53 Mice:

1. p53 WT Reverse: ATGGGAGGCTGCCAGTCCTAACCC
2. p53 WT Forward: GTGTTTCATTAGTTCCCCACCTTGAC
3. p53 KO Reverse: TTTACGGAGCCCTGGCGCTCGATGT
4. p53 KO Forward: GGAATTCTGGGACAGCCAAGTCTGT
- ii. p53 Muscle Specific Mice *Cre Recombinase (~357 bp band)
 1. Cre Forward: TGCAACGAGTGATGAGGTTTC
 2. Cre Reverse: ACGAACCTGGTCGAAATCAG
- iii. p53 Jackson Mice (Mutant band = 110 bp, HT = 110 & 321 bp, WT = 321 bp)
 1. Common: TGGATGGTGGTATACTCAGAGC
 2. Mutant Forward: CAGCCTCTGTTCCACATACT
 3. Wild Type Forward: AGGCTTAGAGGTGCAAGCTG
2. Prior to using the primers, the primers had to be diluted to a 500 μmol concentration according to the equation $X/1000/500*1000*1000$ where x equals the nmol concentration on the primer ordered from customdna@sial.com, and the value of this equation is the amount of sterile ddH₂O required to add in the primer bottle. Mix up and down repetitively for one minute.
3. To get a 50μM stock, in a sterile 1.5 ml eppendorf, add 180 μl of sterile ddH₂O and 20 μl of the 500 μM primer stock.

**** FULL MASTERMIX PLAN CAN BE OBSERVED BELOW****

p53 Taconic Mice			p53 Muscle Specific Mice			p53 Jackson Mice		
No. of Samples	Master Mix: p53 (WT vs. KO)		No. of Samples	Master Mix: p53 Cre (+ vs. -)		No. of Samples	Master Mix: p53 JAX WB (+ vs. -)	
10	One RX (ul)	Total Volume (ul)	10	One RX (ul)	Total Volume (ul)	10	One RX (ul)	Total Volume (ul)
	Jumpstart Mix	25 325		Jumpstart Mix	25 325		Jumpstart Mix	25 325
No. Samples + 3	Fwd primer of WT	1 13	No. Samples + 3	Fwd primer of WT	1 13	No. Samples + 3	KO Forward	1 13
13	Rvs primer of WT	1 13		Rvs primer of WT	1 13		WT Forward	1 13
	Sterile ddH ₂ O	3 39		Sterile ddH ₂ O	3 39		Common (Reverse)	2 26
	TOTAL MM Vol:	30 390		TOTAL MM Vol:	30 390		Sterile ddH ₂ O	19 247
							TOTAL MM Vol:	48 624
	DNA (ul)	20		DNA (ul)	20		DNA (ul)	2
	Total Volume	50		Total Volume	50		Total Volume	50
No. of Samples	Master Mix: p53 (WT vs. KO)							
10	One RX (ul)	Total Volume (ul)						
	Jumpstart Mix	25 325						
No. Samples + 3	Fwd primer of KO	2 26						
13	Rvs primer of KO	2 26						
	Sterile ddH ₂ O	1 13						
	TOTAL MM Vol:	30 390						
	DNA (ul)	20						
	Total Volume	50						

4. Next, label 0.5 mL Flat-Cap PCR Tubes (cat#: 87-C500-F, Ultident Scientific) microcentrifuge eppendorfs for each sample. If WT and KO primers exist such as for the

Taconic mice, two sets of tubes are required (one with the WT primers and one with the KO primers). For the muscle specific and Jackson mice, all primers go into one tube.

5. Then add the appropriate amount of mastermix to the 0.5 mL “mini” eppendorfs (30-48 μ l).
6. Next add 20 μ l of DNA from the ear clipping and solution eppendorf to the mastermix mini eppendorfs. Centrifuge the samples to ensure mixing using the eppendorf centrifuge 54150 (Brinkmann Instruments, 5425-41150) machine.
7. Add two drops of mineral oil to each tube to prevent evaporation of solution during PCR amplification cycling.
8. Turn on the DNA Thermal Cycler (Perkin Elmer, model TC480) and place the mini eppendorfs inside the rack. Cycling times are different for each mouse breed/brand and must be set appropriately:

a. p53 Taconic Mice:

Initial Denaturing: 94° C for 2 min

Amplification Cycles: Denaturing → 95°C for 30 sec
 Annealing → 60°C for 30 sec
 Extension → 72°C for 45 sec } 35 cycles

Final Extension: 72°C for 5 min

Hold at 4°C

b. p53 Muscle Specific Mice:

Initial Denaturing: 94° C for 3 min

Amplification Cycles: Denaturing → 94°C for 30 sec
 Annealing → 56°C for 1 min
 Extension → 72°C for 1 min } 35 cycles

Final Extension: 72°C for 2 min

Hold at 4 °C

c. p53 Jackson Mice:

Initial Denaturing: 94° C for 2 min

1st Amplification Cycle: Denaturing → 94°C for 20 sec
 Annealing → 65°C for 15 sec
 Extension → 68°C for 10 sec } 10 cycles

2nd Amplification Cycle: Denaturing → 94°C for 15 sec
 Annealing → 60°C for 15 sec
 Extension → 72°C for 10 sec } 28 cycles

Final Extension: 72°C for 2 min

Hold at 10 °C

9. Near the end of the PCR amplification, you can begin preparing the agarose gel required to visualize the genotype. The gel is prepared using the following recipe and ratio measured into an 500 mL Erlenmeyer flask:
 - a. 1.5 g of 1.5% Agarose
 - b. 3 mL of 50X TAE

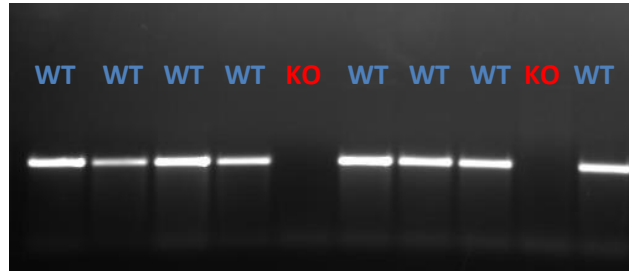
- c. 150 mL of sterile ddH₂O
- d. 25 µl of Ethidium Bromide ** added last to solidify the gel. Add once the mixture has cooled.

***these volumes are for a small gel. For one larger gel, double this amount. For two large gels, triple this amount.*

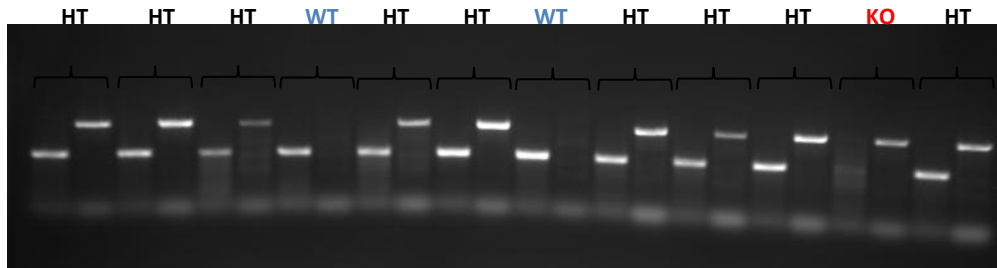
10. Microwave the mixture (Agarose powder, TAE, sterile ddH₂O) for 2 min, adding 30 second intervals until no more bubbles or opaque powder is visualized. Once sufficiently heated and mixed, leave on a stir plate (A. Thermo Scientific, model# S131125Q; B. Fischer Scientific, cat#: 11-000-49S; C. Fischer Scientific, cat# 11-600-49S) with a stirring rod to let it cool.
11. In the meantime, set up the electrophoresis machine (BioRad PowerPac HC, serial# 043BR59656) and apparatus (Electrophoresis Systems Large Horizontal System, FB-SB-2025, Fischer Scientific). Make sure the black end is at the back – this is the direction of the current so that it moves down the gel). Once ready and the solution is warm to the touch, add the ethidium bromide. Seal in the chamber of the apparatus to prevent any leakage and allow time to solidify. Once the seal is solidified, pour in the remainder of the solution. Add in the well comb. The solution will turn opaque once solidified.
12. Once solidified, pour 50x TAE around the gel so that it is submerged. Remove the well comb.
13. When the samples in the PCR machine are finished their cycles, remove the samples. Using a glass pipette (50 µl Hamilton glass syringe, cat# 1482432), pipette 30 µl of the sample into the wells of the gel.
14. Run the gel at 150-180 V until the sample has visually run approximately $\frac{3}{4}$ the length of the gel. Turn off the machine once at the appropriate distance.
15. Remove the gel and place on an imager (Bio/CAN Scientific, model# 3-3035) to view the genotype of the samples. Record values.

Example of gels:

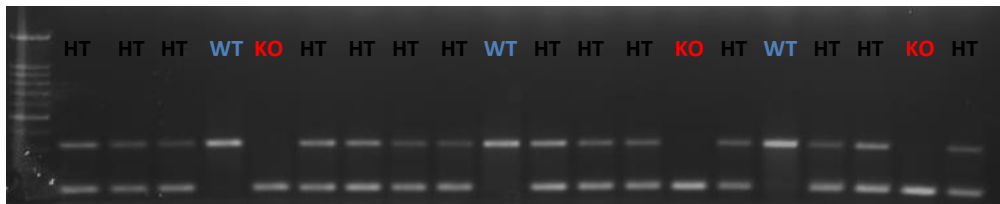
p53 Muscle Specific Mice



p53 Taconic Mice



p53 Jackson Mice



To visualize the molecular weights on the gel, use a 1 Kb DNA Ladder (Frogga Bio – BIO-HELIX, Cat # DM010-R500).

Mitochondrial Isolations from Skeletal Muscle

References: Cogswell et al. *Am J Physiol*, 1993, 264: C388-C389; Krieger et al. *J Appl Physiol*, 1980, 48: 23-28

Reagents:

1. **Potassium Chloride (KCl)** (Sigma-Aldrich, cat#: P3911-1kg, store at room temperature).
2. **Magnesium Sulfate Certified Anhydrous (MgSO₄)** (Fischer Scientific, cat#: M65-500, store at room temperature).
3. **Disodium Salt, Dihydrate (EDTA)** (Bioshop, cat#: 6381-92-6, store at room temperature).
4. **Tris (Hydroxymethyl) Aminomethane (TRIS)** (Bioshop, cat#: 77-86-1, store at room temperature).
5. **Adenosine 5'-Triphosphate Disodium Salt Hydrate (ATP)** (Sigma-Aldrich, cat#: A7699-10G, store at -20°C)
6. **Ethylene glycol-bis (2-amino-ethylether)- N, N, N, N'- tetraacetic acid (EGTA)** (Sigma-Aldrich, E4378-100C, store at room temperature).
7. **3-(N-morpholino) propanesulfonic acid (MOPS)** (Bioshop, cat# 1132-61-2, store at room temperature).
8. **Bovine Serum Albumin (BSA)** (Sigma-Aldrich, cat#: A2153-50G, store at 4°C).
9. **Sucrose (C₂H₂₂O₁₁)** (Caledon Laboratories Inc., cat# 8270-1, store at room temperature).
10. **Potassium Phosphate (K₂HPO₄)** (Fischer Scientific, cat#: P288-500, store at room temperature).
11. **Protease from Bacillus licheniformis (Nagarse)** (Sigma-Aldrich, cat#: P-5380-1G, store at -20°C).

Preparation:

1. Prepare one glass scintillation vial per mouse analyzed and fill with buffer 1. Label.
2. Label two 1.5 mL eppendorfs (MCT Graduated Natural Eppendorfs; cat# 05-408-129; Fischer Brand) for SS and IMF subfractions per mouse.
3. Prepare mitochondrial isolation buffers (only good for one week). Prepared in appropriate sized flasks. First measure out each powder into a labelled beaker. Add less volume of ddH₂O than final volume listed. pH to 7.4 for all solutions. Then pour solution into graduated cylinder and volume up to the appropriate volume listed. Pour into the labelled flask and store at 4°C.



	<u>100 mL</u>	<u>250 mL</u>	<u>500 mL</u>
Buffer 1			
100 mM KCl	0.745 g	1.863 g	3.725 g
5 mM MgSO ₄	0.06 g	0.15 g	0.30 g
5 mM EDTA	0.186 g	0.465 g	0.93 g
50 mM Tris base	0.604 g	1.51 g	3.02 g
Buffer 1 + ATP			
100 mM KCl	0.745 g	1.863 g	3.725 g
5 mM MgSO ₄	0.06 g	0.15 g	0.30 g
5 mM EDTA	0.186 g	0.465 g	0.93 g
50 mM Tris base	0.604 g	1.51 g	3.02 g
1 mM ATP	0.055 g	0.138 g	0.275 g
	<u>100 mL</u>	<u>500 mL</u>	<u>1000 mL</u>
Buffer 2			
100 mM KCl	0.745 g	3.725 g	7.45 g
5 mM MgSO ₄	0.06 g	0.300 g	0.600 g
5 mM EGTA	0.19 g	0.95 g	1.900 g
1 mM ATP	0.055 g	0.275 g	0.550 g
50 mM Tris Base	0.604 g	3.02 g	6.040 g
	<u>10 mL</u>	<u>20 mL</u>	<u>60 mL</u>
Resuspension Buffer			
100 mM KCl	0.075 g	0.15 g	0.45 g
10 mM MOPS	0.021 g	0.042 g	0.063 g
0.2% BSA	0.02 g	0.04 g	0.120 g
	<u>20 mL</u>	<u>40 mL</u>	<u>60 mL</u>
VO₂ Buffer			
250 mM sucrose	1.71 g	3.42 g	5.13 g
50 mM KCl	0.074 g	0.148 g	0.222 g
25 mM Tris Base	0.06 g	0.12 g	0.18 g
10 mM K ₂ HPO ₄	0.034 g	0.068 g	0.104 g

Procedure:

1. Obtain all hindlimb and forelimb muscle masses and place into the Buffer 1 scintillation vial at the time of extraction. Must be kept on ice.
2. Next, place the tissue onto a curved watch glass dish on ice. Dab away extra Buffer 1 solution. Trim away any fat and connective tissue. Then using tweezers and scissors, proceed mince the muscle with forceps and scissors until it resembles the consistency of jam and no large pieces remain.
3. Prepare a 50 mL plastic centrifuge tube (Nalgene, Thermo Scientific, cat#: 3119-0050) with 2 mL of Buffer 1 + ATP. Zero the scale using this filled plastic tube. Then place the minced tissue into the vial using the tweezers, ensuring that it is placed within the liquid at the bottom. Then place on the scale (Mettler-Toledo Scale, Fischer Scientific, cat#: MS104TS) to record the final weight. Volume up with Buffer 1 + ATP (i.e. if weight of

minced tissue is 895 mg \rightarrow 0.895 g \rightarrow 10 x mince tissue = 8.95 mL; 8.95 mL – 2 mL (previously added) = 6.95 mL Buffer 1+ATP to now add to volume up).

4. Next, homogenize with the IKA T25 Digital Ultra-Turrax polytron machine (model# T25DS1) at 40% power output (9.8 Hz) for 10 seconds moving the tube around rapidly. Between samples, rinse the homogenizing tip with ddH₂O.
5. Then place the plastic centrifuge tube into the Beckman JA 25.50 rotor and spin in the ultracentrifuge (Beckman Coulter Avanti J-25 Centrifuge, Sys ID: 297812, CAN: 605169-AA) at 800 g for 10 min. This step divides the IMF and SS mitochondrial subfractions. The supernate will contain the SS mitochondria and the pellet will contain the IMF mitochondria.

* SS and IMF Isolations are performed simultaneously

SS Mitochondrial Isolation:

1. Filter the supernate through a double layer of cheesecloth gauze into a second set of 50 ml plastic centrifuge tubes.
2. Spin tubes at 9000 g for 10 min. Upon completion of the spin discard the supernate and gently resuspend the pellet in 3.5 ml of Buffer 1 + ATP with a p-1000. Since the mitochondria are easily damaged, it is important that the resuspension of the pellet is done carefully.
3. Repeat the centrifugation of the previous step (9000 g for 10 min) and discard the supernate.
4. Resuspend the pellet in 100 μ l of Resuspension medium (using the p-200 to dispense the 100 μ l; use the p-1000 to resuspend), being gentle so as to prevent damage to the SS mitochondria. Some extra time is needed during this final resuspension to ensure the SS pellet is completely resuspended (there should be no large chunks left).
5. Keep the SS samples on ice while proceeding to isolate the IMF subfraction.

IMF mitochondrial isolation:

1. Gently resuspend the pellet (from step 5) in a 10-fold dilution of Buffer 1 + ATP using a teflon pestle (i.e. if the weight of the minced tissue is 0.895 g \rightarrow 10 x mince = 8.95 mL to add). Pour in the 10-fold dilution and then use the P-1000 to spray the pellet gentle of the wall. Once off, use the pestle to lightly break apart the pellet.
2. Using the Ultra-Turrax polytron set at 40% power output (9.8 Hz), homogenize and mix around the resuspended pellet for 10 sec. Rinse the shaft with ddH₂O in between samples.
3. Spin at 800 g for 10 min. Discard the resulting supernate.
4. Resuspend the pellet in a 10-fold dilution of Buffer 2 (i.e. 8.95 mL). Use the p-1000 to lift the pellet of the wall and then use the teflon pestle to lightly break apart the pellet.
5. Next, add the appropriate amount of nagarse which is 25x the minced weight. To make the nagarse solution, weigh out between 7 – 10 mg nagarse into a 1.5 ml eppendorf and then add the appropriate ratio of Buffer 2. For example, if 9.8 mg of nagarse is weighed out, add 980 μ l of Buffer 2. Then add this solution to the plastic centrifuge tube. For example, if the amount of tissue you have is 895 mg \rightarrow 0.895 g \rightarrow 0.895 x 25 = 22.375 μ l of the nagarse solution. The calculation for the appropriate volume is 0.025 ml/g of tissue. Mix gently back and forth 3-4 times and let it lie flat on ice for exactly 5 min. Every 1 min, gentle 3-4 times mix the tube back and forth.

6. After the 5 min, dilute the nagarse by adding 20 ml of Buffer 2. Mix back and forth 3-4 times.
7. Then, spin the diluted samples at 5000 g for 5 min. Discard the resulting supernate.
8. Resuspend the pellet in a 10-fold dilution of Buffer 2 (i.e 8.95 mL). Use the P-1000 to lift the pellet off the wall and then gently resuspend with a teflon pestle until the pellet is broken down.
9. Spin the samples at 800 g for 15 min.
10. Upon the completion of the spin, the supernate is poured into a new set of 50 ml plastic tubes (on ice); the pellet is discarded.
11. Spin the supernate at 9000 g for 10 min. The supernate is then discarded and the pellet is resuspended in 3.5 ml of Buffer 2. Use the p-1000 to lift the pellet off the wall and then mix up and down with the p-1000 to break apart the pellet.
12. Spin samples at 9000 g for 10 min. Discard the supernate.
13. Gently resuspend the pellet in 200 μ l of Resuspension medium (use the p-200 to deliver the resuspension buffer and use the p-1000 to break down the pellet until no large pieces remain).

Mitochondrial Respiration

Reference: Estabrook, R.W., *Meth. Enzymol.*, **10**: 41-47 (1967)

The rate of mitochondrial respiration is an important consideration in the biochemical analysis of mitochondria. There are three phases of interest in analyzing the respiratory ability of mitochondria. Mitochondria produce ATP in the presence of oxygen. The respiratory ability of the freshly isolated IMF and SS mitochondrial fractions and the homogenates can be illustrated by measuring the rate of oxygen consumption using a Clark oxygen electrode in the presence of a) the substrate alone (e.g. glutamate for state 4 or resting respiration); b) ADP, (state 3 or active respiration); and c) NADH⁺, which is used to measure the amount of damage that has occurred to the mitochondria, since the inner membrane is impermeable to NADH⁺.

Reagents (prepare first):

1. **VO₂ Buffer** for muscle mitochondria (please see instructions to make this buffer in the mitochondrial isolation protocol). Leave in the 4°C fridge until ready to use. Take out 30 min before use to allow it to reach room temperature.
2. **Glutamate:** measure 123.34 mg of glutamate (L-glutamic acid potassium salt monohydrate, Sigma-Aldrich, cat#: G1501-100G, Store at room temperature) into a 1.5 mL eppendorf (MCT Graduated Natural Eppendorfs; cat# 05-408-129; Fischer Brand). Add 1 mL of ddH₂O. Vortex (Mini Vortex, cat#: 02215365, Fischer Scientific) to ensure adequate mixing. The final concentration will be a 11.1 mM solution. Discard after use.
3. **ADP:** measure 11.29 mg of ADP (Adenosine 5'-diphosphate sodium salt, Sigma-Aldrich, cat#: A2754-500 mg, store at -20°C) into a 1.5 mL eppendorf. Add 1 mL of ddH₂O. Vortex to ensure adequate mixing. The final concentration will be a 0.44 mM solution. Discard after use.
4. **NADH:** measure 30 mg of NADH (β-nicotinamide adenine dinucleotide reduced disodium salt hydrate, Sigma-Aldrich, cat#: N8129-1G, store at -20°C) into a 1.5 mL eppendorf. Add 250 μl of ddH₂O. Vortex to ensure adequate mixing. The final concentration will be a 2.8 mM solution. Discard after use.

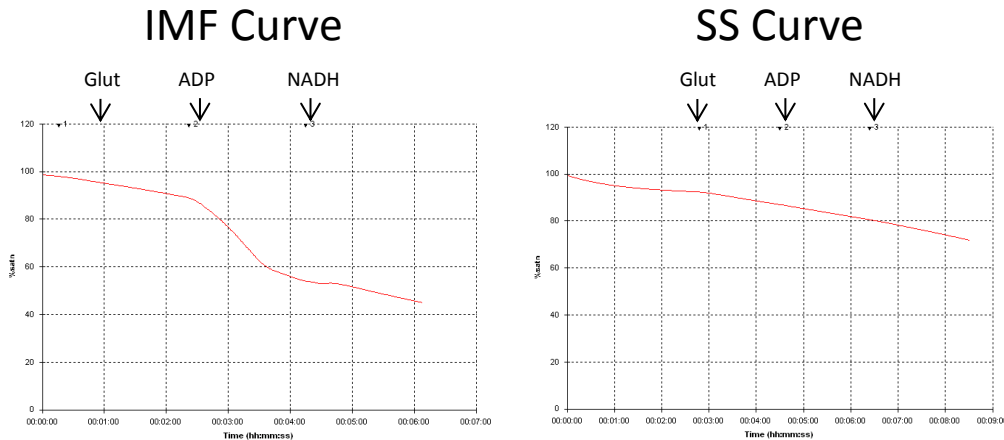
Procedure:

1. Set the water bath to 25-30°C. Turn this on prior to opening the system. Take out the VO₂ buffer 30 min prior to using to allow to reach room temperature.
2. Then turn on the computer. Go to START → Windows Virtual PC → Windows XP mode. Turn on the Strathkelvin 928 Oxygen Meter System (Strathkelvin Instruments, Model 782,

serial# 2214) and ensure that it is plugged into the computer. Go to USB → Attach 782 → Open 782 Oxygen System → Open Experiment.

3. Then take off the parafilm cover on the Clark oxygen electrode (Strathkelvin Instruments, Mitocell-MT200, serial# 2158). Clean out the chamber with ddH₂O and suction repeatedly (~3 times). Prepare the respiration glass 25 µl Hamilton glass syringe, mini stir bar, metal rod to remove the stir bar and plastic stopper.
4. Into the electrode, add 250 µl of VO₂ Buffer and then very slowly add 50 µl of the mitochondrial subfraction (add slow to not damage the mitochondria). Insert the stir bar and press the button on the electrode to turn on. Then insert the rubber stopper slowly making sure the volume that moves up the stopper is about half-way up canula in the centre of the stopper.
5. Then calibrate: Set-up Experiment → Calibrate → Calibrate High → Continue
 - a. Will take approximately 1 min to calibrate. Then click Accept Values → Calibration Complete → press START
6. Let the electrode run for the first 2 minutes. This is the drift which analyzes basal mitochondrial respiration.
7. After 2 minutes, you will then pick up 5 µl of the glutamate solution with the 25 µl Hamilton glass syringe and insert the syringe through the canula into the solution located at the base of the electrode. Make sure not to touch the stir bar as it could stall. Then press MARKER and type in glutamate to identify where is has been added. Then let it run with glutamate for 2 min. This is **STATE 4 RESPIRATION**.
8. After 2 minutes, you will then pick up 5 µl of the ADP solution with the 25 µl Hamilton glass syringe and insert the syringe through the canula into the solution located at the base of the electrode. Make sure not to touch the stir bar as it could stall. Then press MARKER and type in ADP to identify where is has been added. Then let it run with ADP for 2 min. This is **STATE 3 RESPIRATION**.
9. After 2 minutes, you will then pick up 5 µl of the NADH solution with the 25 µl Hamilton glass syringe and insert the syringe through the canula into the solution located at the base of the electrode. Make sure not to touch the stir bar as it could stall. Then press MARKER and type in NADH to identify where is has been added. Then let it run with NADH for 2 min. This is a control check to assess the integrity of the mitochondria. If NADH decreases rapidly, it may mean that the mitochondria may have been damaged during the process of extraction. If the mitochondria are intact and function, the graph will run at a slight decline in this section.
10. Once the 8-10 minute run is complete, press STOP and save the file (go to respiration and save under appropriate folder).
11. Stop the electrode by pressing the button, this will turn off the stir bar. Take out the stopper and then remove the stir bar with the metal rod. Wipe both the stopper and stir bar dry. Then suction out the VO₂ Buffer/Mitochondria out and rinse with ddH₂O 3 times with suction.

12. At the end of the entire analysis, put away the stopper, stir bar, metal rod, and glass syringe. Turn off the electrode and the computer system. Fill up the electrode with ddH₂O and then place parafilm laboratory film (Bemis, PM-996) over the lid to cover.
 - a. File → Exit from Program → USB → Release
13. **Repeat from step 4 for the next mitochondrial subfraction. This is completed for both SS and IMF curves. Below is an example of the curve you will likely observe:**



Analysis:

1. On the computer that is used for respiration with the clark electrode, open the Windows XP mode. Instead of clicking experiment this time, click ANALYZE. This will then take you to your previous respiration folder (click on the specific graph to analyze).
2. A window will open where you will need to adjust the “edit experiment values”. Temperature = 30°C; Oxygen Consumption at Saturation = 28.5; Water Volume = 300 (for both text sections). Press Okay and your graph will automatically adjust.
3. Open the excel spreadsheet and input the appropriate values into the red boxes below. Each animal should have both their SS and IMF analyzed. To input the values you are required to move the two sectional lines on the graph on the computer within the drift, glutamate, ADP and NADH sections to find a section that is 1 min in length and representative of that section. Input the time for the first line and the second line and the total time length. Each of these lines will have an associated %saturation value that you will then input for the start (first line) and end (second line).
 - a. The difference in saturation is calculated by: Start % saturation – Final % saturation
 - b. % saturation/min is calculated by: Saturation difference/time of line analysis
 - c. Corrected %saturation/min is calculated by: (%saturation/min of glutamate OR ADP OR NADH)/ (%saturation/min of drift)

- d. Protein is calculated by: (Protein concentration from Bradford/5)*50
- e. Respiration Glutamate is calculated by: (Corrected %saturation/min for glutamate*1112.5)/Protein
- f. Respiration ADP is calculated by: (Corrected %saturation/min for ADP*1112.5)/Protein
- g. RCR is calculated by: Respiration ADP/Respiration glutamate
 - i. RCR values need to be above 3

		136 SS										Respiration		RCR
		Start	End	Start	End	Saturation	Corrected	Protein	Respiration		Respiration			
		(hh:mm:ss)	(hh:mm:ss)	min	(%satn)	(%satn)	Difference (%)	(%satn/min)	(%satn/min)	Respiration		Respiration		
										Respiration		Respiration		
										Respiration		Respiration		
	DRIFT	0:01:17	0:02:17	0:01:00	1.00	90.6	85.6	5	5					
state 4	Glutamate	0:02:41	0:03:41	0:01:00	1.00	83.5	78.1	5.4	5.4	0.4	326.09	1.36	4.25	
state 3	ADP	0:05:02	0:06:02	0:01:00	1.00	70.8	64.1	6.7	6.7	1.7	326.09	5.80		
	NADH	0:06:51	0:07:51	0:01:00	1.00	58.9	50.8	8.1	8.1	3.1				
		136 IMF										Respiration		RCR
		Start	End	Start	End	Saturation	Corrected	Protein	Respiration		Respiration			
		(hh:mm:ss)	(hh:mm:ss)	min	(%satn)	(%satn)	Difference (%)	(%satn/min)	(%satn/min)	Respiration		Respiration		
										Respiration		Respiration		
	DRIFT	0:01:21	0:02:21	0:01:00	1.00	89.3	84.8	4.5	4.5					
state 4	Glutamate	0:03:06	0:04:06	0:01:00	1.00	79.2	72.1	7.1	7.1	2.6	332.23	8.71	11.98	
state 3	ADP	0:04:20	0:05:10	0:00:50	0.83	70.6	40.9	29.7	35.64	31.14	332.23	104.27		
	NADH	0:06:35	0:07:35	0:01:00	1.00	24	15.3	8.7	8.7	4.2				

The units for respiration is expressed in units of natoms. Thus State 3 or 4/mg protein x 968 natoms O₂ = x natoms O₂/mg protein/min.

Mitochondrial Reactive Oxygen Species (ROS) Emission

Background: Mitochondria are the primary source of reactive oxygen species (ROS) to the cell. It is estimated that about 2% of total cellular oxygen is converted ROS by the inappropriate reduction of molecular oxygen by intermediate members of the electron transport chain (ETC). ROS are damaging molecules that are capable of compromising the integrity of macromolecules within the mitochondria and may lead to overall organelle dysfunction. In particular, mtDNA may be prone to attack by ROS because 1) mtDNA is located in close proximity to the ETC, 2) mtDNA lacks the protective sheath of histones compared to nuclear DNA and, 3) mitochondria have an insufficient repair system for mtDNA mutations. ROS can exist in a variety of molecular permutations such as superoxide (O_2^-), hydroxyl radical (OH^-) and hydrogen peroxide (H_2O_2).

DCF (2,7-dichloro-fluorescein; Fig.1) is a reagent that is non-fluorescent until the acetate groups are removed by intracellular esterases and oxidation occurs within the mitochondria (Fig.1). DCF is oxidized by all of the different forms of ROS and this can be detected by monitoring the increase in fluorescence with a fluorometric plate reader. The appropriate plate reader filter settings for fluorescein are the following: **Excitation 485/20 and Emission 528/20** (Fig.2).

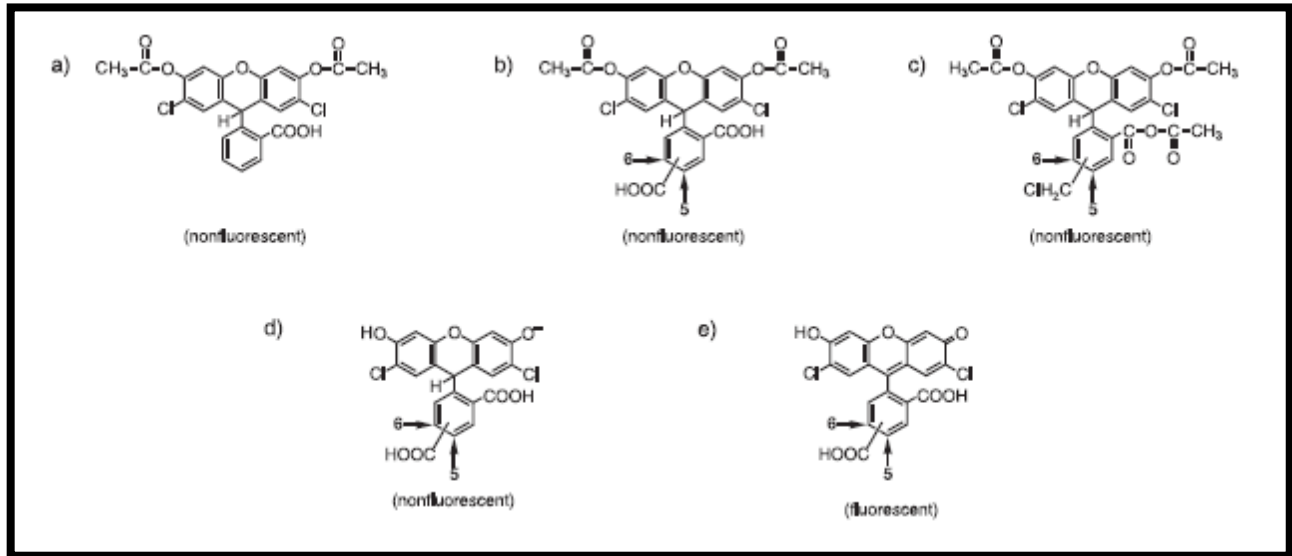


Fig.1-DCF molecule and oxidation of DCF resulting in fluorescence

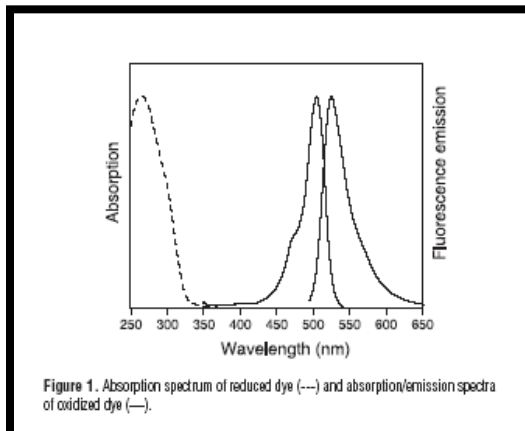


Figure 1. Absorption spectrum of reduced dye (---) and absorption/emission spectra of oxidized dye (—).

Fig.2-Absorption and Emission Spectra of oxidized dye

Reagents:

1. **DCF** (2,7-dichlorodihydrofluorescein diacetate – H2DCFDA) reagent MW=487.29 (Life Technologies, cat#: 1871963, store at -20°) * *very light sensitive when added to liquid*
 - a. *Stock solution* is made by measuring 24 mg into a 1.5 mL eppendorf (MCT Graduated Natural Eppendorfs; cat# 05-408-129; Fischer Brand). Then add 1 mL of 100% anhydrous ethanol (ethyl alcohol anhydrous, Commercial Alcohols, lot#: 022933). Wrap the eppendorf in aluminum foil and vortex (Mini Vortex, cat#: 02215365, Fischer Scientific) until no chunks are visible in the solution. This is to be stored at -20°C for multiple uses.
 - b. *Working solution* (used for experiment and must be made fresh) is made by adding 990 µl of 100% anhydrous ethanol to a 1.5 mL eppendorf and then adding 10 µl of the H2DCFDA stock solution. The eppendorf is immediately covered in aluminum foil and vortexed.
2. **VO₂ Buffer:** Refer to the mitochondrial isolation protocol for making this buffer. It should be left out for 20-30 minutes to stabilize to room temperature.
3. **Glutamate:** measure 51.4 mg of Glutamate (L-glutamic acid potassium salt monohydrate, Sigma-Aldrich, cat#: G1501-100G, Store at room temperature) into a 1.5 mL eppendorf. Add 1 mL of ddH₂O. Vortex to ensure adequate mixing.
4. **ADP:** measure 4.69 mg of ADP (Adenosine 5'-diphosphate sodium salt, Sigma-Aldrich, cat#: A2754-500 mg, store at -20°C) into a 1.5 mL eppendorf. Add 1 mL of ddH₂O. Vortex to ensure adequate mixing.

Procedure:

1. Prior to setting up the plate, the KC4 plate reader (Program KC4 V3.1 Rev 15, License#: 5YNM-66P96) set up to the Synergy HT (BioTek) Plate Reader, must be prepared. The following are the parameters that need to be changed in order to utilize the DCF and measure time-dependent ROS production from isolated mitochondria:
 - a. Open WIZARD to access the Reading Parameters Settings
 - b. Reading Type: Options “End Point, Kinetic, Spectrum” - choose Kinetic
 - i. Click on larger box labeled Kinetic to set parameters- **Run Time 0:30:00, Interval time – for minimal interval time, measure every 3 minutes,** click on box labeled **Individual Well Auto Scaling-** The Auto scaling allows for monitoring each individual well during the experiment and scales it appropriately. For the scales – click Auto for both options.
 - c. Synergy HT-I On: Options “Absorbance, Fluorescence, Luminescence” – choose Fluorescence
 - d. Then adjust the following options:
 - i. Filter Set = choose #1 and set the excitation to 485/20
 - ii. Emission = 528/20

- iii. Optics Position= The optics position should be set to the **TOP** (i.e. readings are taken from the top of the well)
- iv. Sensitivity = set at **50** (depending upon the amount and/or nature of the sample).
- e. Plate-Type-choose **96-well plate (8 x 12)**, choose which wells are to be read i.e. **C1-D9**
- f. Shaking-**Intensity** set at **1**, **Duration** set at **15s** and then click the box that is labeled **before every reading** (it shakes the samples for 15 s before every reading).
- g. Temperature Control- Click on the box indicating **YES**, also click on box labeled pre-heating, and put 37°C into the temperature box. Once the heating is reached, and your plate is loaded with the mitochondrial sample and VO₂ buffer, press start as the heating lamp will require an additional 2 minutes to reach temperature. During this time, rapidly add the glutamate, ADP and DCF.

Procedure:

Below is a typical pipette plan for layout. All mitochondrial concentrations obtained through a Bradford Assay must be divided by 5 first and then placed into the pipette plan in the [mito] column.

STATE III											
WELLS	C1	C2	C3	C4	C5	C6	C7	C8	C9		
Mito	CON	126 SS	127 SS	142 SS	160 SS	126 IMF	127 IMF	142 IMF	160 IMF		
µg mito	0	75	75	75	75	75	75	75	75		
conc		41.661	32.02	31.109	40.079	37.44	36.517	36.121	32.692		
[mito]	0	8.3322	6.404	6.2218	8.0158	7.488	7.3034	7.2242	6.5384		
µL mito	0	9.00	11.71	12.05	9.36	10.02	10.27	10.38	11.47	2	
µL V02 buffer	225	196.00	193.29	192.95	195.64	194.98	194.73	194.62	193.53	1	
µL DCF(24 mg/mL)	25	25	25	25	25	25	25	25	25	5	very quick
µL Glutamate (51.4 mg/mL)	0	10	10	10	10	10	10	10	10	4	very quick
µL ADP (4.69 mg/mL)	0	10	10	10	10	10	10	10	10	3	very quick
µL Total volume	250	250	250	250	250	250	250	250	250		
STATE IV											
WELLS	D1	D2	D3	D4	D5	D6	D7	D8	D9		
Mito	CON	126 SS	127 SS	142 SS	160 SS	126 IMF	127 IMF	142 IMF	160 IMF		
µg mito	0	75	75	75	75	75	75	75	75		
conc		41.661	32.02	31.109	40.079	37.44	36.517	36.121	32.692		
[mito]	0	8.3322	6.404	6.2218	8.0158	7.488	7.3034	7.2242	6.5384		
µL mito	0	9.00	11.71	12.05	9.36	10.02	10.27	10.38	11.47	2	
µL V02 buffer	225	206.00	203.29	202.95	205.64	204.98	204.73	204.62	203.53	1	
µL DCF(24 mg/mL)	25	25	25	25	25	25	25	25	25	4	very quick
µL Glutamate (51.4 mg/mL)	0	10	10	10	10	10	10	10	10	3	very quick
µL ADP (4.69 mg/mL)	0	0	0	0	0	0	0	0	0		
µL Total volume	250	250	250	250	250	250	250	250	250		

1. SS and IMF mitochondria are isolated as described in the mitochondrial isolation protocol. Only fresh mitochondria may be used for this functional assessment.

2. Prepare a solid white 96-well plate (96-nontreated white microwell SI, Thermo Scientific, cat#: 236105). In the specified rows add the appropriate level of VO₂ Buffer to each well. Then add the mitochondria (SS and IMF) according to the volume as seen in the pipette plan. Remember to include a *control* with only VO₂ buffer and DCF reagent as in Well #1 *at this point, begin the count-down timer for 2 min for heating the KC4 reader lamp.
3. Next add 10 µl of the glutamate solution rapidly to all wells (both State 4 and 3 ROS). Do not change tips in between adding glutamate to each well.
4. Next add 10 µl of the ADP solution rapidly to only State 3 ROS wells. Do not change tips in between adding ADP to each well.
5. As the final concentration of DCF is 50 µM and the total volume of the reaction mixture is 250 µl, 25 µl of DCF is used in the reaction mixture since this represents a 10-fold dilution. Add the DCF rapidly to the reaction mixture. Once added, immediately place the plate into the KC4 reader and press READ.
6. Once completed, go to REPORT to print. Under Availab Data/Select add KINETIC CURVES and M485/528. Then click add to move to selected data, then print. Documents can be visualized below:

Kinetic Curve



Analysis of ROS:

1. ROS is analyzed by inputting the following values in the pipette plan below. The initial reading on the chart (time 0) and the final reading on the chart (time 28:49) are put into the initial and final sections of the table and the difference is calculated. Example of the M458/528 is below:

Time	A1	A2	A3	A4	A5	A6	A7	A8	A9
00:00:00	13350	13735	16023	16478	15090	13554	13457	14232	13372
00:01:15	13343	13854	16159	16606	15214	13512	13552	14361	13427
00:02:30	13314	14001	16272	16743	15353	13599	13649	14505	13483
00:03:45	13301	14167	16411	16866	15481	13795	13779	14711	13553
00:05:00	13311	14361	16555	19039	15619	13975	13929	14945	13657
00:06:15	13295	14574	16735	19236	15786	14209	14119	15234	13757
00:07:30	13325	14651	16919	19441	15973	14500	14326	15565	13899
00:08:45	13363	15151	17143	19698	16182	14776	14574	15958	14073
00:10:00	13375	15500	17382	19954	16412	15138	14860	16302	14286
00:11:15	13415	15865	17637	20273	16666	15541	15190	16668	14492
00:12:30	13470	16318	17912	20601	16973	15987	15543	17416	14736
00:13:45	13531	16778	18234	20956	17280	16430	15906	17987	15043
00:15:00	13612	17320	18557	21336	17608	16951	16334	18622	15325
00:16:15	13683	17866	18923	21777	17968	17482	16779	19279	15675
00:17:30	13774	18495	19307	22216	18353	18041	17230	19966	16010
00:18:45	13864	19122	19706	22691	18790	18564	17751	20753	16388
00:20:00	13968	19823	20146	23200	19209	19299	18292	21539	16770
00:21:15	14097	20585	20598	23732	19699	19921	18792	22332	17185
00:22:30	14210	21346	21101	24302	20169	20605	19377	23172	17627
00:23:45	14341	22174	21588	24894	20678	21295	19976	23966	18066
00:25:00	14487	23013	22115	25514	21195	21978	20594	24800	18518
00:26:15	14636	23937	22694	26121	21709	22747	21230	25609	19033
00:27:30	14782	24855	23250	26715	22210	23483	21886	26712	19525
00:28:45	14959	25827	23861	27381	22756	24258	22546	27681	20063
00:30:00	15157	26902	24631	28123	23360	25111	23274	28697	20626

0 min time point

30 min time point

STATE III ROS									
	CON	132 SS	133 SS	163 SS	164 SS	132 IMF	133 IMF	163 IMF	164 IMF
Initial Value	2472	2828	2936	2941	3086	3419	3298	3235	3265
Final Value	2930	13040	8616	9152	8875	9320	7351	7872	7990
Difference	458	10212	5680	6211	5789	5901	4053	4637	4725
STATE IV ROS									
	CON	132 SS	133 SS	163 SS	164 SS	132 IMF	133 IMF	163 IMF	164 IMF
Initial Value	2583	3084	3046	3061	3166	3553	3459	3336	3380
Final Value	2906	8228	8142	10861	12888	9276	8019	8011	8667
Difference	323	5144	5096	7800	9722	5723	4560	4675	5287

2. Then values are corrected for respiration in the following pre-existing excel spreadsheet. The final values in the highlighted section are what is analyzed in graphpad.

	132 (WT UT)				133 (WT UT)				163 (KO UT)				164 (KO UT)		
	Control	IMF	SS		Control	IMF	SS		Control	IMF	SS		Control	IMF	SS
State 4	323	5723	5144	State 4	323	4560	5096	State 4	323	4675	7800	State 4	323	4725	9722
State 3	458	5901	10212	State 3	458	4053	5680	State 3	458	4637	6211	State 3	458	5287	5789
Corrected 4	5400.00	4821.00		Corrected 4	4237.00	4773.00		Corrected 4	4352.00	7477.00		Corrected 4	4402.00	9399.00	
Corrected 3	5443.00	9754.00		Corrected 3	3595.00	5222.00		Corrected 3	4179.00	5753.00		Corrected 3	4829.00	5331.00	
Corrected 4/ug	72.00	64.28		Corrected 4/ug	56.49	63.64		Corrected 4/ug	58.03	99.69		Corrected 4/ug	58.69	125.32	
Corrected 3/ug	72.57	130.05		Corrected 3/ug	47.93	69.63		Corrected 3/ug	55.72	76.71		Corrected 3/ug	64.39	71.08	
state 4 resp	4.12	1.28		state 4 resp	5.61	3.06		state 4 resp	15.1	3.05		state 4 resp	10.36	7.49	
state 3 resp	110.43	10.89		state 3 resp	120.03	17.8		state 3 resp	87.14	13.2		state 3 resp	128.04	55.09	
State 4 ROS	17.48	50.22		State 4 ROS	10.07	20.80		State 4 ROS	3.84	32.69		State 4 ROS	5.67	16.73	
State 3 ROS	0.66	11.94		State 3 ROS	0.40	3.91		State 3 ROS	0.64	5.81		State 3 ROS	0.50	1.29	

Equations:

- State 4 & 3 Control, IMF and SS are the difference values inputted from the above chart.
- Corrected 4 SS = State 4 SS – State 4 Control
- Corrected 3 SS = State 3 SS – State 3 Control
- Corrected 4 IMF = State 4 IMF – State 4 Control
- Corrected 3 IMF = State 3 IMF – State 3 Control
- State 4 & 3 SS resp and State 4 & 3 IMF resp values are the respiration values from the mitochondrial respiration procedure once quantified.
- SS Corrected 4/ug = corrected 4 SS/75 (*repeat for IMF)
- Corrected 3/ug = corrected 3 SS/75 (* repeat for IMF)
- SS State 4 ROS = Corrected SS 4/ug / SS state 4 resp
- SS State 3 ROS = Corrected SS 3/ug / SS state 3 resp

Western Blotting

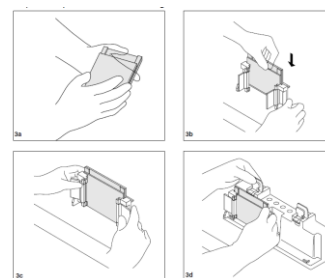
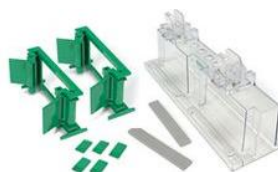
Reagents:

1. **Acrylamide/Bis-Acrylamide**, 30% Solution 37.5:1 (BioShop, ACR010.500, store at 4°C).
2. **Under Tris Buffer:** Measure out 1 M of Tris-HCL (Tris (Hydroxymethyl) aminomethane, Bioshop, cat#: 77-86-1, stored at room temperature) which is 60.5 g into 400 mL of ddH₂O. Then, with acid, pH to 8.8. Volume up with ddH₂O to a total of 500 mL. Store at 4°C.
 - a. **5N HCl Acid:** Combine 82 mL of HCl (Caledon, 6025-1-29) with 118 mL ddH₂O. Pour the acid over the water.
3. **Over Tris Buffer:** Measure out 1 M of Tris-HCL (Tris (Hydroxymethyl) aminomethane, Bioshop, cat#: 77-86-1) which is 12.1 g into 80 mL of ddH₂O. Then pH to 6.8. Add Bromophenol Blue (Electrophoresis Purity Reagent, Bio-Rad, cat# 161-0404, stores at room temperature) after pH is done for colour. Volume up with ddH₂O to a total of 100 mL. Store at 4°C.
4. **Ammonium Persulfate (APS) Buffer:** Add 10% (w/v) APS (Sigma-Aldrich, cat# A3678-25G, stored at room temperature) in ddH₂O (1g/10mL ratio). Store at 4°C.
5. **Sodium Dodecyl Sulfate (SDS) Buffer:** Add 10% (w/v) SDS (Bioshop, cat#: 151-21-3, stored at room temperature) in ddH₂O (1g/10mL ratio). Store at room temperature (solidifies at 4°C).
6. **TEMED (N,N,N',N'-tetramethyl-ethylenediamine)** (Sigma-Aldrich, T-9281-50ml, stored at 4°C).
7. **Electrophoresis Buffer:** Add 25mM Tris (30.34g), 192mM Glycine (144g) (Bioshop, 56-40-6, stored at room temperature), 0.1% SDS (10g) into a large nalgene bucket. Add 4 L of ddH₂O and stir. Using the pH meter, pH to 8.3. Add acid very slowly, the buffer takes time to adjust to the pH. Then pour into the large jug containing 6 L of ddH₂O for a total volume of 10L. Store at room temperature.
8. **Blocking Solution:** 5% Skim Milk Powder, 10% Skim Milk Powder, stored at 4°C.
 - a. 5% (w/v) skim milk powder (pasteurized instant skim milk powder, Loblaws/No Frills, stored at room temperature) in wash buffer (more common) OR
 - i. For example, for 400 mL of blocking solution, measure out 20 mg. Calculate this by $400 \times 0.05 = 20$ mg skim milk powder to add.
 - b. 5% (w/v) Bovine Serum Albumin (Sigma-Aldrich, cat#: A2153-50G, stored at 4°C) in wash buffer
9. **Transfer Buffer:** Measure out 0.025M TRIS (12.14g), 0.15M Glycine (45.05g), 20% methanol (800 mL) (CH₃OH, Caledon, cat#: 6700-1-42, stored at room temperature). Add 4 L of ddH₂O and leave it on the stirring plate to mix. Store at 4°C.
10. **Wash Buffer:** Measure out TRIS (12 g), NaCl (58.5g) (Sodium Chloride, Bioshop, cat#: 7647-14-5, stored at room temperature), and 0.1% TWEEN 20 (10 mL) (Sigma-Aldrich, cat#: P1379-500ml, stored at room temperature) into a large nalgene bucket. Add 4 L of ddH₂O and stir. Using the pH meter, pH to 7.5. Add acid very slowly, the buffer takes

time to adjust to the pH. Then pour into the large jug containing 6 L of ddH₂O for a total volume of 10L. Store at room temperature

11. **Sample Dye:** Make up 40% of sucrose (C₂H₂₂O₁₁) (Caledon Laboratories Inc., cat# 8270-1) in electrophoresis buffer (4g / 10 mL buffer). Add a spatula tip-full of Bromophenol Blue (Electrophoresis Purity Reagent, Bio-Rad, cat# 161-0404, stores at room temperature) to obtain the colour required. Store in 1 mL aliquots at -20°C.
12. **Beta-mercaptoethanol** (Sigma-Aldrich, M6250, stored at room temperature)
13. **2X Lysis Buffer:** Measure out 100% glycerol (heated) (50 mL) (Caledon, 5650-14-40), SDS (11.5 g), and 1M TRIS (weigh out 12.1 g TRIS/ 100 mL ddH₂O, pH to 6.8, then add 31.25 mL of this solution) and add 400 mL of ddH₂O. Then pH to 6.8. Volume up with ddH₂O to a total of 500 mL. Store at 4°C.
14. **6X SDS (not used frequently):** Warm 100% glycerol in water bath at 65°C for 30 minutes. Measure out SDS (1.2 g), Bromophenol Blue (0.06 g), 1M Tris (weigh out 12.1 g TRIS/ 100 mL ddH₂O, pH to 6.8, then add 3 mL of this stock solution to the SDS and Bromophenol Blue) and ddH₂O (1 mL) in a beaker. Then stir at 4°C for 5 minutes. Add the glycerol (6 mL) to the beaker, stir and aliquot the mixture. Store at -20°C. Add 5% (v/v) β-mercaptoethanol to the 6X SDS just prior to use
15. **Ponceau Stain (Red):** Measure out 0.1% (w/v) Ponceau S (200 mg) (Sigma-Aldrich, cat#: P3504-10G, stored at room temperature), 0.5% (v/v) Acetic Acid (10 mL) (Glacial, cat#64-19-7, stored at room temperature) and 94% ddH₂O (190 mL). Store at room temperature.
16. **Butanol** (2-methyl-2-butanol, Sigma-Aldrich, cat#:152463-1L, stored at room temperature)
17. **Enhanced Chemiluminescence Fluid (ECL)** (Santa Cruz, cat#:sc-2048, stored at room temperature)
18. **Protein Ladder** (Precision Plus Protein Kaleidoscope, Bio-Rad, cat#: 161-0375, stored at -20°C)
19. **Nitrocellulose Membrane** (0.45µm, Bio-Rad, cat#:10484060, stored at room temperature)
20. **1 X TBS:** Dilute 10X TBS in a 1:10 ratio. For example, add 100 mL 10X TBS: 900 mL ddH₂O.
 - a. **10X TBS:** Measure out NaCl (80 g) (Sodium Chloride, Bioshop, cat#: 7647-14-5, stored at room temperature), KCl (2 g) (Sigma-Aldrich, cat#: P3911-1kg, stored at room temperature), TRIS (30 g) in 900 mL of ddH₂O. Then pH to 7.4. Volume up for a total of 1000 mL or 1 L. Store at -4°C,
21. **Stripping Buffer:** Measure TRIS (7.6 g), SDS (20 g), β-mercaptoethanol (7 mL) in 700 mL of ddH₂O. pH to 6.8. Volume up for a total of 1000 mL or 1 L. Store at room temperature.

* All Western Blot experimental equipment is from Bio-Rad



Procedure:

1. Prepare electrophoresis separating gels:

- a. Clean 1.5 mm spacer plates (Glass Plates, Bio-Rad, cat# 1653312) and short glass plates (Short Plates, Bio-Rad, cat# 1653308) thoroughly with soap followed by a rinse with 95% wash ethanol. Let them dry naturally.
- b. Then assemble glass plates by attaching together the spacer plate and short plate and fit them into the green holder. In the gel holding rack, place sponges along the bottom grooves and then clip the green holder.
- c. Next, check the seal by adding ddH₂O until the top, then pour off and dry the plates using air suction.
- d. Then prepare to make the separating gel according to the percentage and volume requirements listed below. These volumes are listed per one gel, multiply volumes by however many gels are being made.

	8%	10%	12%	15%	18%
Acrylamide	2.7 ml	3.3 ml	4.0 ml	5.0 ml	6.0 ml
ddH₂O	4.1 ml	3.5 ml	2.8 ml	1.8 ml	0.8 ml
Under Tris	3.0 ml	3.0 ml	3.0 ml	3.0 ml	3.0 ml
SDS	100µl	100µl	100µl	100µl	100µl
APS	100µl	100µl	100µl	100µl	100µl
TEMED	10µl	10µl	10µl	10µl	10µl

Benefits of making different percentage gels allows for greater separation of bands at certain molecular weights. For example, an 8 or 10% gel will cutoff around the 37 kDa mark and upwards, thus providing large separation for higher molecular weight proteins. On the other hand the 12 and 15% gels will allow for a full analysis of all of the molecular weight markers with greater separation occurring at the lower molecular weights.

- e. To a 200 mL beaker, add the solution volumes of the gel in order, adding first acrylamide, ddH₂O, Under Tris, SDS, and APS. Place on the stir plate with a stir bar and allow to mix. When ready to pour into the plate, add TEMED and let stir for 10 sec.
- f. Slowly pour the solution into the space between the two plates while keeping plates tilted to prevent bubble formation. Pour just above the first green line of the green holder.
- g. Then add 1000 µl of butanol to coat top surface of gel solution and prevent evaporation.
- h. Allow 30-40 minutes for gel polymerization. Keep the beaker with the remaining solution to observe when solidified.

- i. Remove the butanol by pouring it off and remove any remainder with a small piece of whatman paper.
- j. Next, prepare the stacking gel by adding the following solutions below in order to a 50 mL beaker. Place on a stir plate with a stir bar until ready to use.

	Large Volume (4-5 gels)	Small Volume (2-3 gels)
Acrylamide	1000 μ l	500 μ l
Over Tris	1.25 mL	625 μ l
ddH₂O	7.5 mL	3.75 mL
SDS	100 μ l	50 μ l
APS	100 μ l	50 μ l
TEMED	15 μ l	7.5 μ l

- k. When ready to pour into the plate, add TEMED and let stir for 10 sec. Then slowly pour until it overflows the space between the glass plates.
- l. Add 10 well or 15 well comb (Bio-Rad, 1.5 mm wells) for the desired number of wells.
- m. Allow ~40 minutes for gel polymerization.
- n. Once solidified, wrap each gel in wet paper towel and cover with plastic wrap to prevent gel dehydration. Store at 4°C. Good for 2-3 days stored.


2. Preparation of samples:

- a. Taking the concentration of the sample from the Bradford assay, place into the “protein for 5 ul” row in the pipette plan observed below. Adjust the total protein used. The more total protein, the greater the concentration and thus increased density of the bands.
 - i. Protein ug/ul = Protein for 5 ul / 5
 - ii. Total protein = Protein Concentration (40) / Protein ug/ul
 - iii. 2X lysis buffer = total protein

Lanes	1	2	3	4	5	6	7	8	9	10
		Muscle Specific				Whole Body				
Sample Name		WT		KO		WT		KO		
	Marker	UT	T	UT	T	UT	T	UT	T	
Sample Description		106	108	103	102	83	33	24	31	
Protein for 5 ul		49.409	65.26	60.289	67	60.835	59.858	66.676	18.333	
Protein ug/ul		9.88	13.05	12.06	13.40	12.17	11.97	13.34	3.67	0.00
Total Protein (ug)	40	4.05	3.06	3.32	2.99	3.29	3.34	3.00	10.91	#DIV/0!
2X lysis buffer		4.05	3.06	3.32	2.99	3.29	3.34	3.00	10.91	#DIV/0!
sample dye		5.0	5.0	5.0	5.0	5.0	5.0	5.0	5.0	5.0
Total	10	13.1	11.1	11.6	11.0	11.6	11.7	11.0	26.8	#DIV/0!

- b. Prepare 1.5 mL eppendorfs (MCT Graduated Natural Eppendorfs; cat# 05-408-129; Fischer Brand) labelled with the appropriate sample ID.
- c. Prepare the lysis buffer solution. Add a ratio of 475 μ l 2x lysis buffer with 25 μ l of beta mercaptoethanol. A larger ratio can be used of 950:50 μ l if required. Vortex (Mini Vortex, cat#: 02215365, Fischer Scientific) to mix.
- d. Add the appropriate volume of lysis buffer solution to each labelled eppendorf. The volume of lysis buffer to sample is a 1:1 ratio.
- e. Next add the sample to the labelled eppendorfs.
- f. Lastly add 5 μ l of sample dye to each tube.
- g. Briefly centrifuge each sample using the eppendorf centrifuge 54150 (Brinkmann Instruments, 5425-41150) machine to bring volume to the bottom of the eppendorf and to mix.
- h. Turn on the block heater to 95°C and incubate each sample at 95 °C for 5 minutes in the heating block to denature the proteins.
- i. Briefly spin again to return volume to the bottom of the eppendorf and store in the -20°C freezer until ready to use or use immediately.

3. Assemble Mini-PROTEAN gel caster system:

- a. If one gel is only being run, a plastic rectangular pseudo plate (Buffer Dam, Bio-Rad) must be clamped on the other side of the gasket to still create the well. Place the correct way so that the ridges of the pseudo plate are facing towards the inside (or towards the gasket). If using two gels, fit appropriately so that the short place on either side is facing towards the inside of the gasket. 
- b. Place the gasket apparatus with the gels into a plastic castor (2 gels = Mini-Protean 3 Cell, Bio-Rad, cat#: 525BR-049940; 4 gels = Mini-Trans-Blot Cell, Bio-Rad, cat#: 153BR81099). The square castor is sufficient to hold two gels. However the rounded castor is sufficient to hold 4 gels. Two gaskets (one with pointed prong conductors and one with flat conductors) will be used, each able to hold two gels.
- c. Fill the castor with electrophoresis buffer by first filling in the well created between the plates, allowing the buffer to overflow and fill the rest of the castor. Fill to the top. *** very important that the well space between the plates is always filled to the top, otherwise the proteins may run down the gel on an angle.*
- d. Slowly remove the comb using both hands (one on each side) by pulling the comb straight upwards.
- e. Rinse out each well with a small and gentle flush of electrophoresis buffer using a B-D (10 mL) syringe. Fix any wells that are deformed using the syringe.
- f. Place 13 μ l of protein ladder into the first well. This allows you to visualize the molecular weights along the gel.
- g. Withdraw the entire volume of the sample using a 25 μ l Hamilton syringe. Inject volume slowly into the bottom of the well, being careful of losing solution with bubbles that form. Then pick up 5-8 μ l of the electrophoresis buffer and place

back into the empty eppendorf. Swirl around, then pick it up to obtain any leftover sample and place back into the same well.

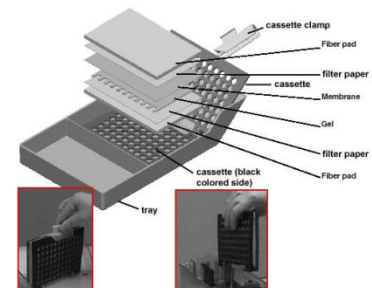
- h. Once all the samples are loaded into the wells, refill the center well between the plates with more electrophoresis buffer so that it is overflowing.

4. Gel electrophoresis

- a. Immediately after all samples are loaded place the lid on the gel chamber.
- b. Place positive (red) and negative (black) plugs into the power supply and turn on power supply. Ensure colour coding is correct.
- c. Set power supply to 120V. Gel will run for ~1.5- 2 hours depending on percent gel made.
- d. When the bromophenol blue sample dye has run off the bottom of the gel (or when gel has separated the desired amount) turn off the power supply to the electrophoresis machine. Remove plugs from power supply and remove lid.
- e. Prepare for electrotransfer of proteins from the gel to nitrocellulose membrane.

5. Western Blotting Transfer

- a. Prior to shutting off the electrophoresis machine, prepare the following set-up
 - i. Small rectangular glass dish with a test tube;
 - ii. Paper towel with green wedge (Bio-Rad) and water bottle with a thin pipette tip attached;
 - iii. Square dish containing Whatman paper (GE Healthcare-Life Sciences, cat#: 3030-917) sliced 8 ½ cm by 6 cm. You will need 6 pieces per gel, they must be placed in groups of 3 pieces;
 - iv. Another square dish containing nitrocellulose membrane sliced 8 ½ cm by 6 cm. You will need one membrane per gel;
 - v. One plastic sandwich Cassette per gel containing one thicker green sponge placed on the black side of the cassette and two thin black sponges placed on the clear side of the cassette;
 - vi. Transfer buffer that has been refrigerated at 4°C;
 - vii. Black and Red Transfer chamber with prongs, placed inside a 2-gel square castor. Place a stir bar at the bottom of the castor underneath the transfer chamber. Place the entire apparatus into a glass dish placed on a stir plate.
- b. Once set-up, shut off the electrophoresis machine and remove the electrophoresis glass plates from chamber.
- c. Lay the glass plate down on the paper towel and use the green wedge to lift between the plates, thus lifting away the short plate. With the wedge, cut away the stacking gel wells.
- d. Next, in the glass dish, place the cassette with the sponges so that the black side is facing down in the glass dish. Pour a small amount of transfer buffer over top and use the test tube (Corex 15 mL, cat#: 8441) to roll out the thick green sponge with the



liquid. Then place a set of 3 Whatman paper onto the green sponge. Roll out to make flat.

- e. Then using the water bottle with the thin tip, gently slide under the gel and spray the water to lift the gel up off the 1.5 mm glass spacer plate. Go around all edges of the gel. Using the green wedge/spatula, lift under the ladder section of the gel and lift off the 1.5 mm spacer plate and lie flat along the Whatman paper on the cassette. The ladder on the gel **MUST** be on the right side. Roll out with the test tube gently to ensure the gel is flattened.
- f. Then, removing the protective blue sheets around the white nitrocellulose membrane, place the membrane directly over the gel. Roll out repeatedly with the test tube to ensure there are no bubbles trapped between the membrane and the gel.
- g. Then place another stack of 3 Whatman papers on top of the nitrocellulose membrane as a protective layer. Roll out with the test tube.
- h. Clamp together the cassette and place in the transfer chamber with the black side of the cassette facing the black side of the chamber.
- i. Place an ice pack in the chamber to prevent over-heating of the membrane/gel. Place ice around the base of the castor as well.
- j. Fill up the castor with transfer buffer until it reaches the top of the castor.
- k. Place lid on the chamber and connect the leads to the power supply.
- l. Turn on the power supply and run at 120V for 1 hour and 45 minutes.

6. Removal of transfer membrane:

- a. After the 1 hour and 45 minutes, turn off the power supply and disconnect leads from the power supply, then remove the lid from the chamber.
- b. Remove each cassette from the chamber one at a time by pulling upwards.
- c. Open the cassette, remove the Whatman paper and gel and place the nitrocellulose membrane in a plastic dish so that it is upright, with the ladder now on the left side of the square plastic dish.
- d. Add Ponceau S stain on the membrane, enough so that it is submerged, and gently swirl.
- e. Drain off the remaining Ponceau S and save for reuse. Repeat for all blots simultaneously.
- f. Rinse the membrane with ddH₂O and swirl to reduce the red background; rinse approximately 3-4 times. Lay the blot face up on top of plastic wrap and label with a sticker to keep track of the membranes. Then wrap with the plastic wrap and use a kim wipe to smooth out any creases. Either take a picture or scan the image (*allows you to keep your ponceau for use as a loading control later on, if required*).
- g. Next, prepare a faux gel plan of the proteins to be analyzed, their molecular weight and where to cut along the membrane. Refer to this prior to cutting the membrane. Once satisfied, use a scalpel and a ruler to precisely cut at the planned sections. Cut while the blot is still in the plastic wrap. Use a pen to label at the end (where no protein is) the ID of the gel as well as the protein being analyzed.

Using forceps, take the membrane strip and place in a square plastic dish. Repeat for all other proteins, placing similar proteins in similar plastic dishes.

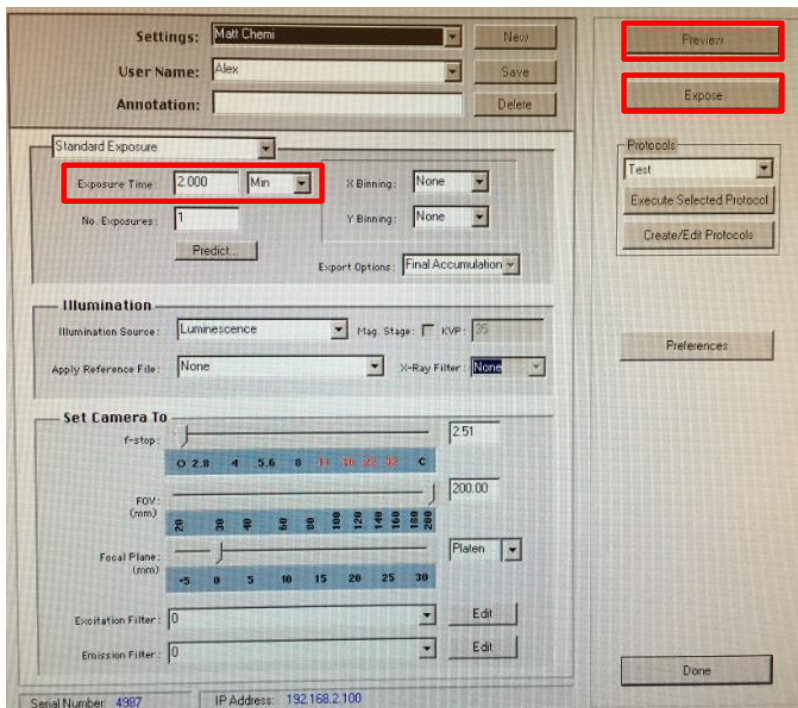
- h. Then add enough wash buffer to submerge the blots. Swirl on a mixing plate (GFL (3017) Man-Tech Associates Inc Mixing Plate, Sarstedt, ref#: 62-151.006, lot#: 6092911) at room temperature until the remaining red Ponceau S has been removed. Remove the plastic wrap bits with forceps while stirring.
- i. Next, incubate the blots for 1 hour with 5% skim milk blocking solution while on rotation at room temperature.
 - i. During this hour, prepare the primary antibodies. Depending on the primary volume, use either 1.5 mL eppendorfs, 2 mL eppendorfs or 13 mL Rhoer tubes (Sarstedt, ref#: 62-515.006, lot# 6092911). Add first the 5 or 10% skim milk blocking solution and then add the specific antibody (stored at either 4°C, -20°C or -80°C) ordered from the company.
 - ii. Prepare the dish to place the blots in overnight. Using a large glass dish, set up a small plastic square dish upside down as a support. Then take a glass plate and wrap it in parafilm to prevent creases. Place four kimwipe balls (2 kimwipes wrapped together, sprayed with water, and rolled into a ball) into each corner of the -glass dish. Place plastic wrap overtop the glass dish to prevent evaporation.
- j. Once the blocking is complete, lift each blot and place it face up onto the parafilm dish. Spread each blot as far apart as possible to prevent accidental mixtures of primary antibody. Then place the glass dish into the 4°C fridge. Vortex primary antibody and place 1000 µl of primary antibody over each specific blot to cover. Once all is added, cover the plastic wrap and close the fridge door.

7. Immunodetection

- a. The next day, take the glass dish out of the 4°C fridge and place on the bench. Remove the blots and place them into a square plastic dish. Wash the blots in wash buffer with gentle rotation for 5 minutes, repeat this wash 3 times. Pour out wash buffer and add new wash buffer in between each rinse.
 - i. During these washes, wipe off the excess primary antibody from the parafilm glass plate. Re-soak the kimwipe balls with ddH₂O.
 - ii. Prepare the secondary antibodies using rabbit, mouse or goat (stored at -20°C) added to 5% blocking skim milk. Again, prepare this in a 1.5 mL, 2.0 mL eppendorf or a 13 mL Rhoer tube.
- b. Once the 3 by 5 min washes are complete, lay the blots face up onto the parafilm plate. Incubate the blots for 1 hour in room temperature with 1000 µl of the appropriate secondary antibody diluted in blocking solution. Vortex before adding.
- c. Once the one hour is up, then lightly dab the blot to remove excess secondary onto a kimwipe, transfer to a plastic square dish, and then repeat the 3 by 5 min washes with wash buffer. Pour out wash buffer and add new wash buffer in between each rinse.

8. Enhanced Chemiluminescence Detection

- Mix ECL fluids “A” and “B” in a 1:1 ratio in a disposable Rohr tube. For each blot, 1000 µl of solution is required (i.e. 500 µl of A and 500 µl of B). The ECL in the brown bottle is extremely light sensitive – only add when immediately ready to use. When ready mix the two solutions vigorously.
- Place blots on plastic wrap face up and apply ECL solution for 5 minutes.
- Dab off excess ECL on a kimwipe and place blots face down on a fresh piece of plastic folder and seal tightly.
- Place the blot face down onto the imager and latch close the machine.
- Open the Carestream Molecular Imaging Software connected to the Carestream Imaging Apparatus (K4589-0020). Make sure the machine is turned on. Go to Capture In Vivo FX. Settings should be already pre-set at Matt Chemi. Settings will look like below:

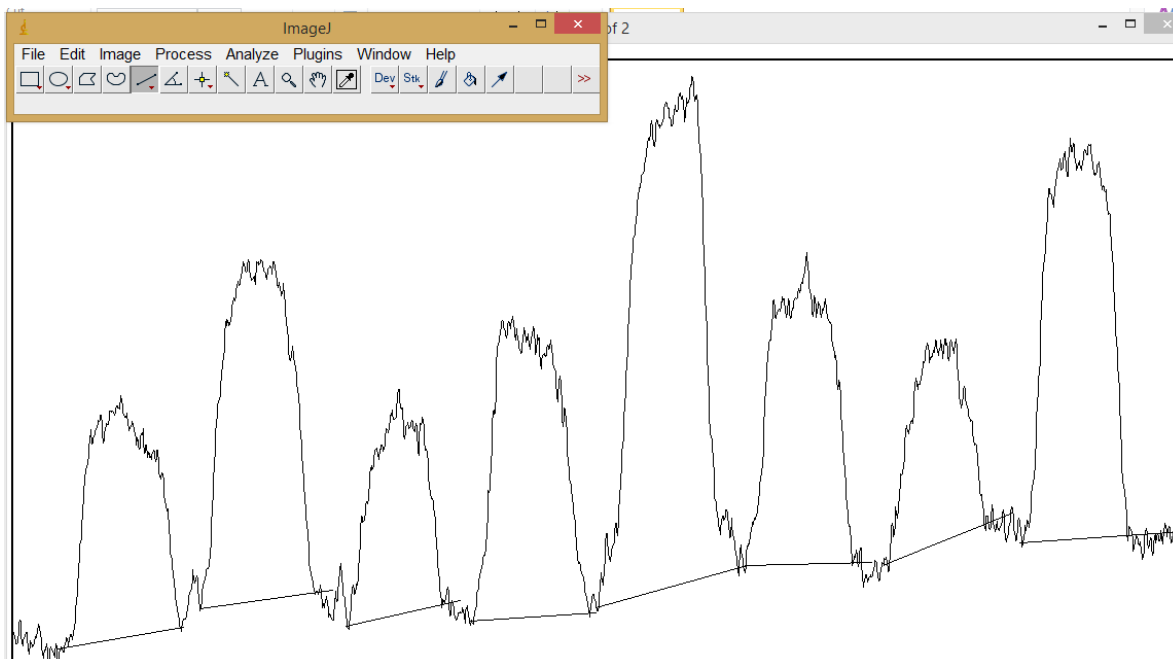



- Click “Preview” to detect how long the first exposure must be. The preview will run for 10 sec. If distinct blots can be viewed through the preview, then expose for less time (around 2 min). If not blots can be visualized from the preview, expose for longer (around 10 min and up). Adjust the exposure time value and click “Expose”.
- Expose blot to film (time will vary depending on protein and antibody).
- Once the exposure is completed, play with the contrast and background using the blue and red lines respectively on the righthand Image Display panel. Move them along the scale to create the perfect image.
 - Click “Auto” to go back to the initial exposure contrast.


- i. Save the Carestream image. Then go to Export Data → Image → File type → JPEG. This is so that later analysis can be performed.
- j. Repeated exposures can then be made for the same blot. There is an approximate 20 min ECL lifetime.
- k. Once completed, discard blot and shut down the program. Retrieve images off the program using a USB to then analyze with the Image J software.

9. Western Blot Analysis

- a. Open the image J software. Within the software click OPEN → select blot to analyze.
- b. Click the button to highlight the blot. If multiple bands, highlight the specific band interested in analyzing.
 - i. You can crop and adjust the rotation as well during this time to ensure only the bands interested in highlighting are highlighted. Click Image → Crop. Then click Image → Transform → Rotate → Input Angle (degrees) → negative number turns the image counter clockwise and a positive number turns the image clockwise. Start with a small number.
- c. Then click the number“1” to confirm the highlighted region and that the line is horizontal, then click the number“3” to analyze. A new window will open containing peaks for each specific band shown:



- d. Select the  function and then connect the base of the peak by drawing a line from one point to the next. Do this for all of the peaks.

- e. Click on the  button. Then click on the inside of each of the peaks. The peaks will be highlighted and a new window will open containing the volume under each peak. These are the final quantified values of the contrast of each blot.
- f. Place these values into an excel spreadsheet. Perform steps 2-5 for the control protein. Then divide the values of the protein of interest by the control proteins to obtain the final protein value which can then be grouped and graphed using the Graphpad Prism 6.0 software.

10. Stripping & Re-probing

This process is required to analyze more than one protein at a similar molecular weight to another, without having to re-do the entire western blot process. Another method is the Arturo stripping method, however that is only recommended for stripping the blot for the same protein, rather than a different one which is what this method is beneficial for.

- a. Once the original protein has been developed using the Carestream imager software, do not throw out the blot; instead, place the blot in a square plastic dish. Then wash the blot in wash buffer 3 times for 5 min intervals.
- b. After the final wash, remove the excess wash buffer and add 1 x TBS. Then seal the plastic container and leave in the fridge until ready to use.
 - i. If stripping right after developing, ignore the 3 by 5 min washes and the 1X TBS and proceed directly to step C.
- c. Empty the wash buffer or TBS that the blot is submerged in. Add in fresh wash buffer into the plastic dish and wash on the mixing plate for 15 min. Repeat this for a total of two times.
- d. Then turn on the rotating heating oven (NIO/CAN Scientific TEK STAR Hybridization Oven) and set it to 56°C. Prepare two long glass cylinder containers.
- e. Once the blots are washed, take the blot and lie it face up, flat along the inside of the glass container. The blot should be placed near the lid of the container, with the ladder facing towards the bottom of the cylinder. If multiple blots, place the blots across from each other and not directly beside.
- f. Then, add 4 mL of stripping buffer to the bottom of each container. The stripping buffer is light sensitive, only add when the blots are placed. Close the lid of the glass container.
- g. Place the glass containers into the rotating oven making sure that they are equally balanced. Then begin the rotation, close the door and time for 30 minutes.
- h. Once completed, remove the blots and place them back into the square dish and repeat the 2 times 15 minute washes with wash buffer on the mixing plate.
- i. Next, empty out the wash buffer and add the 5% skim milk blocking solution to the plastic dish. Leave on the mixing plate for 1 hour.

- i. In the meantime, prepare similarly to how you prepare for step I and J in the **Removal of transfer membrane** section.
 - i. Prepare primer antibodies and prepare glass dish for incubation.
- j. Continue with the method dictated in Step 7 (Immunodetection) and proceed onwards.

COX Enzyme Activity Assay

The COX Enzyme activity assay is an indirect measure of mitochondrial content. This assay is based on observation of the decrease in absorbance of ferrocytochrome c measured at 550 nm, which is caused by its oxidation to ferricytochrome c by cytochrome c oxidase. This kit is suitable for the detection of mitochondrial outer membrane integrity/mitochondrial stress and for the detection of mitochondria in subcellular fractions.

Reagents

1. **Muscle Enzyme Extraction Buffer:** Measure out 20 mM Hepes (2.383 g/500 mL ddH₂O) (Sigma-Aldrich, cat#H3375-500G) and pH to 7.4. Then in a separate beaker, measure out 2 mM EGTA (0.3804 g/500 mL) (Sigma-Aldrich, E4378-100C, store at room temperature), 1% Triton-X-100 (5 mL/500 mL), 50% glycerol (10 mL/500 mL) (Caledon, 5350-1-40), and 50 mM β -glycerophosphate (5.4 g/500 mL) into 400 mL of ddH₂O and pH to 7.4. Then volume up to 500 mL total and store at 4°C.
2. **Cytochrome c from equine heart** (Sigma-Aldrich, cat#: C2506-1G, store at -20°C)
3. **Sodium Dithionite** (Sodium hydrosulfite, Sigma-Aldrich, cat#: 157953-5G, store at room temperature)
4. **10 mM KPO₄:** Dilute 0.1 M KPO₄ buffer prepared below with ddH₂O in a 1:10 ratio (exp. 10 mL buffer + 90 mL ddH₂O). Store at 4°C.
5. **100 mM KPO₄:** Measure 0.1 M KH₂PO₄ (13.6 g/1000 mL ddH₂O) (Potassium Phosphate Monobasic, Fischer Scientific, cat#: P285-500) and pH to about 5. Then prepare the 0.1 M K₂HPO₄·3H₂O (17.4 g/ 1000 mL ddH₂O) (Potassium Phosphate, Fischer Scientific, P288B-500) and pH this solution to 8. Then mix these two solutions in equal proportions and pH to 7.0. Store at 4°C.

Procedure:

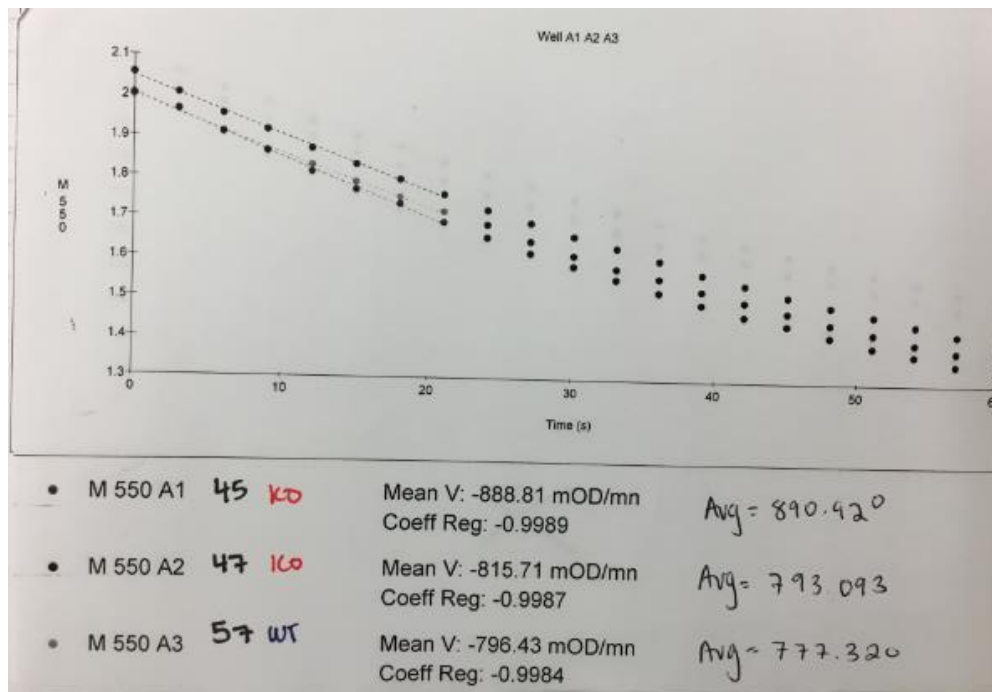
1. Prepare the appropriate set-up:
 - a. Beige two-section dish;
 - b. Metal tool with a small scoop at one end and a metal clamp for samples;
 - c. Prepare a small liquid nitrogen tank containing the powdered samples in cryotubes (2 mL micro tube, Sarstedt, ref# 72.694.003, lot#: 3084701).
 - d. Prepare two sets of 1.5 mL eppendorfs (MCT Graduated Natural Eppendorfs; cat# 05-408-129; Fischer Brand) with the ID of the powdered samples. Label one tube with a 20 (for the 20-fold dilution) and label the other set of tubes with an 80 (for the 80-fold dilution).
2. Add 50 μ l of muscle enzyme extraction buffer to the 20-fold dilution labelled 1.5 mL eppendorfs.

3. Next, pour liquid nitrogen into the beige dish. Place the metal clamp and metal tool into the liquid nitrogen. Remove a powdered sample (in a cryotube) from the liquid nitrogen. Tap 3-4 times on the table and slightly twist the top open to let out extra gas from the cryotube. Then remove the lid and place the cryotube in the clamp in the liquid nitrogen. ***The sample must always be stored in liquid nitrogen.*
4. Then, place the 20-fold dilution eppendorf with the 50 μ l of muscle enzyme extraction buffer onto the scale and zero it.
5. Next, using the metal tool, scoop out 5-7.5 mg of powdered tissue and place it in the 20-fold eppendorf. Record the final measurement.
6. Once correctly measured, remove the cryotube from the metal clamp and close the lid. Tap and open and close the lid multiple times until there is no more sound of gas escaping.
7. Then volume up for the sample according to the following calculation. For example, if 6.2 mg was measured $\rightarrow 6.2 \times 19 - 50 = 67.8$ μ l of muscle enzyme extraction to volume up.
8. Complete steps 2-7 for all samples.
9. Next, place the samples on an aluminum eppendorf block on ice in a small plastic container. Ensure ice is surrounding the block. Place all samples inside the block, open the lids and place inside each one a mini stirring rod.
10. Place the plastic container onto a mixing plate and turn on. Ensure that all of the stirring rods are moving in a circular motion. Start a timer for 15 min.
11. While mixing, the cytochrome c test solution can be prepared.
 - a. Turn on the large 30°C oven and allow to heat up.
 - b. In a small glass scintillation vial, weigh out 20 mg of horse heart cytochrome c (stored normally at -20°C).
 - c. Add 1 mL of 10 mM KPO₄ buffer to the scintillation vial and swirl around with the cytochrome c to mix. This should be a dark red colour.
 - d. In a 1.5 mL eppendorf, weight out between 7-10 mg of sodium dithionite. Add the equivalent of 10 mM KPO₄ buffer. For example, if 8.3 mg was measured, then add 830 μ l of 10 mM KPO₄ buffer. Vortex vigorously to mix.
 - e. Next, prepare three items: two pieces of aluminum foil (large enough to cover the scintillation vial), 8 mL of ddH₂O, and 1 mL of 100 mM KPO₄ buffer.
 - f. Add 40 μ l of the sodium dithionite solution to the cytochrome c solution and swirl to mix. There should be an immediate colour change to a light red/orange. As soon as this colour change occurs, quickly add the 8 mL of ddH₂O and the 1 mL of 100 mM KPO₄ buffer and cover in aluminum foil.
 - g. Place in the 30°C oven for ~30 minutes.
12. Once the eppendorfs with the 20-fold dilution are finished mixing, remove the stir bars with a magnet and rinse with ethanol to clean. Leave the eppendorfs in the aluminum block.

13. Sonicate with the Microson Ultrasonic Cell Disruptor machine (model MS-50) at 30% power three times for three rounds. One round consists of sonicating all the samples three times consecutively. Repeat this for an additional two rounds. Clean the probe with a kimwipe in between each sample. Move slowly during sonication.
14. Once sonication is complete, in the 80-fold labelled eppendorfs, add 150 μ l of the muscle extraction buffer.
15. To these eppendorfs, then add 50 μ l of the 20-fold solution. When picking up the 20-fold solution, pipette from the bottom rather than near the top where bubbles may be located. Leave the new 80-fold dilution samples on ice. The leftover 20-fold solution can be thrown out.
16. In a clear 96 well-plate, quickly add 280 μ l of the cytochrome c test solution to Row A for trial 1. Add into the wells depending on how many samples being analyzed. If 6 samples, only add from A1-A6. Once added cover the plate immediately with aluminum foil, wrap up the test solution with aluminum foil, and place the 96-well plate into the oven for 10 min.
17. In another 96-well plate, add the 80-fold samples into Row A. Add 30 μ l of each sample into its own well. For example, if 6 samples, add from A1-A6 consecutively. Cover with a kim wipe until ready to use.
18. Then prepare the KC4 plate reader while the test solution is heating up. Open Wizard to access the Reading Parameters Settings.
 - a. Reading Type: Options “End Point, Kinetic, Spectrum” - choose Kinetic
 - i. Click on larger box labeled Kinetic to set parameters- **Run Time 0:01:00, Interval time – for minimal interval time, select minimum (under these conditions, it should measure the plate every 3 seconds)**, click on box labeled **Allow Well Zoom**- This allows to see the data in real time. Do not select individual well auto scaling (takes too long to occur). For the scales – click Auto for both options.
 - b. Synergy HT-I On: Options “Absorbance, Fluorescence, Luminescence” – choose Absorbance and set the wavelength to 550 nm.
 - c. Select Sweep for Read Mode
 - d. Plate-Type-choose **96-well plate (8 x 12)**, choose which wells are to be read i.e. **A1-A6**
 - i. 4 trials will be completed for the 6 samples. The plate will read therefore: A1-A6, C1-C6, E1-E6, G1-G6
 - e. Shaking-**Intensity** set at **0**, **Duration** set at **0s**. Shaking is not necessary as it will delay the first reading.
 - f. Select yes for temperature control and check pre-heating. Enter 30 for temperature control.
19. Once the test solution is ready, remove it from the oven. With a multi-pipette, pick up 250 μ l of the test solution from the wells at the same time and quickly add it to the

samples in the other 96-well plate. Immediately, place the sample plate into KC4 reader and press start.

20. During the reading time, add the test solution to the next set of wells on the clear 96-well plate— row C this time, filling one well for each of the number of required samples. Place the plate into the oven for 10 minutes.
21. Once finished reading, save the first trial and remove the 96-well plate with the samples. To prevent analysis of the entire curve (all 21 points) which can increase variability between trials, only take the average of the first 8 points. On the chart table, press shift and then click of the graphs. Once all are highlighted, like the finger off the shift button and a chart will open. Click options and the adjust the final point number from 21 to 8. Then to print, go to Report → Add Well Zoom (for wells A1-A6→ overlay wells) and Add the Kinetic Curve. Print and record the sample ID.
22. Then in this same plate that was just read, add in the samples for the next trial – this time row C.
23. Alter the settings for the KC4 reader this time, making sure that the wells being read are the C row between C1 to C4 for example.
24. Then repeat steps 19-22 for trial 2 (row C).
25. Repeat steps 19-23 for trial 3 (row E)
26. Repeat steps 19-23 for trial 4 (row G)
27. Below is an example of the graph and values. The graph should be starting around or above 2 on the y-axis.



To analyze the results, take the average Mean V value across all four trials. Exclude any values that are outliers from the average calculation. Do this for all of the samples. Then, divide the Mean V by 1000 and enter the Mean V values into the below calculation. Values to enter include the volume of the sample ($30\mu\text{l}/1000=0.030$), total well volume ($30\mu\text{l sample} + 250\mu\text{l test solution} = 280\mu\text{l}/1000=0.280$), and the fold dilution (80):

$$COX Activity = \frac{(Mean V)(Total Well Volume)(Fold Dilution)}{(18.5)(Volume of Sample)}$$

Therefore, an example calculation for a mean V of -284.2 would be:

$$COX Activity = \frac{(0.284)(0.280)(80)}{(18.5)(0.030)} = 11.462 \mu\text{mol}/\text{min}/\text{g tissue OR U}/\text{g tissue}$$

Muscle Extraction Procedure – Protein Extracts

Reagents:

1. **Sakamoto Buffer:** For a volume of 10 mL, add muscle extraction buffer (9.8 mL), 1 mM DTT (10 μ l), 1 mM PMSF (100 μ l), 1 mM Sodium Orthovanadate (50 μ l), 2 μ l/ml leupeptin (20 μ l), 1 μ l/ml pepstatin A (10 μ l), and 1 μ l/ml aprotinin (10 μ l). Store at 4°C.
2. **Protease Inhibitor Buffer** (Protease Inhibitor Cocktail Tablets, Roche, cat#: 11697498001, store at 4°C): Measure out 1 tablet with 1000 μ l ddH₂O. Vortex until tablet is dissolved. Store at -20°C.
3. **Phosphatase Inhibitor Cocktail 2** (Sigma-Aldrich, cat#: P726-5ml, store at 4°C)
4. **Phosphatase Inhibitor Cocktail 3** (Sigma-Aldrich, cat#: P0044-5ml, store at 4°C)

Procedure:

1. Label two sets of 1.5 mL eppendorfs (MCT Graduated Natural Eppendorfs; cat# 05-408-129; Fischer Brand) with the sample ID. The second set, label more extensively with the date, animal ID, animal conditions, and personal initials.
2. Prepare the muscle extraction buffer in a 15 mL Falcon polystyrene conical tubes (Falcon, cat#: 352095).
 - a. For however many samples you have, multiple this number by 200 μ l and this is how much Sakamoto Buffer you will add to the Falcon tube.
 - b. Then add 10 μ l of the phosphate buffers and the protease buffers per 1 mL of Sakamoto buffer.
 - i. For example, if you have 9 samples, $9 \times 200 = 1800$ μ l OR 1.8 mL of Sakamoto Buffer. Then you would add 18 μ l of the phosphate and protease buffers.
 - c. Vortex to ensure adequate mixing.
2. Add 50 μ l of this muscle extraction buffer to the first ID labelled 1.5 mL eppendorfs. Place these tubes on ice in a Styrofoam cooler.
3. Prepare the appropriate set-up:
 - a. Beige two-section dish filled with liquid nitrogen;
 - b. Metal tool with a small scoop at one end and a metal clamp for samples; placed inside the liquid nitrogen of the beige dish;
 - c. Take a medium sized cooler and fill it up with liquid nitrogen. A small pee cup will be required;
 - d. Small liquid nitrogen canister with the cryotubes to make protein extract samples from.

4. Remove one of the cryotubes and open and close to remove excess gas. Once opened, place it inside the beige dish into the liquid nitrogen using the clamp to hold it upright.
5. Place the corresponding 1.5 mL eppendorf with the 50 μ l Muscle extraction buffer on the scale. Zero the scale.
6. Measure out 15-20 mg of the powdered sample. Record the value.
7. Then volume up for the sample according to the following calculation. For example, if 16.3 mg was measured $\rightarrow 16.3 \times 10 - 50 = 113$ μ l of muscle extraction buffer to volume up.
8. Complete steps 5-8 for other samples.
9. Rotate all homogenates end over end using the Barnstead Thermolyne "LabQuake" Shaker (model 415110) in a 4°C fridge.
10. Then place the 1.5 mL eppendorfs in an aluminum block on ice.
11. Sonicate with the Microson Ultrasonic Cell Disruptor machine (model MS-50) machine at 30% power three times for three rounds. One round consists of sonicating all the samples three times consecutively. Repeat this for an additional two rounds. Clean the probe with a kimwipe in between each sample. Move slowly during sonication.
12. Centrifuge samples using the eppendorf centrifuge 54150 (Brinkmann Instruments, 5425-41150) machine at 14, 000 ref for 10 min at 4°C.
13. Then extract the supernate from the 1.5 mL eppendorfs and place the supernate into the second set of extensively labelled eppendorf tubes. Dispose of the pellet. Repeat for all samples.
14. Store protein extracts at -80°C until use for Bradford assay to determine protein concentration, OR until required to make protein samples for Western blotting.

Mitochondrial Protein Release Assay for Cytochrome C and AIF

Reagents:

- Hydrogen Peroxide:** Prepare a 15 mL Falcon polystyrene conical tubes (cat#: 352095, Falcon) tube with 10 mL of ddH₂O. Add 10 µl of 30% H₂O₂ (Hydrogen Peroxide Solution (30%) w/w in H₂O, contains stabilizer, Sigma-Aldrich, cat#: H1009-100ml, store at 4°C) to the falcon tube and vortex prior to using. Leave on ice until ready to use.
- Ferrous Sulfate:** Measure 278 mg of FeSO₄ (Ferrous Sulfate, BDH Chemicals, cat#ACS354, store at room temperature) into a 15 mL falcon tube. Add 10 mL of ddH₂O to the falcon tube and vortex until completely mixed. Leave on ice until ready to use.
- Mitochondrial Isolation Resuspension Buffer** (see recipe above)

Procedure:

- Prepare mitochondrial SS and IMF subfractions. Refer to the mitochondrial isolation procedure. Prepare a Bradford on these subfractions and enter the concentrations into the pipette plan as observed below:

Lanes	1	2	3	4	5	6	7	8	9	10	11	12	13	14	15	14	15			
Sample Name	LADDER	71 (KO SED)				76 (KO T)					83 (WT SED)				98 (WT T)					
Mito Subfraction		SS		IMF		SS		IMF			SS		IMF		SS		IMF			
Sample Description		CON	TREATED	CON	TREATED	CON	TREATED	CON	TREATED		CON	TREATED	CON	TREATED	CON	TREATED	CON	TREATED		
Protein for 5 ul		42.72	42.72	31.76	31.76	49.94	49.94	37.11	37.11		44.46	44.46	33.36	33.36	39.78	39.78	37.91	37.91		
Protein ug/ul		8.54	8.54	6.35	6.35	9.99	9.99	7.42	7.42		8.89	8.89	6.67	6.67	7.96	7.96	7.58	7.58	For TREATED	For CON
Total Protein (ug)	150	17.56	17.56	23.62	23.62	15.02	15.02	20.21	20.21		16.87	16.87	22.48	22.48	18.85	18.85	19.78	19.78	Add 1st	Add 1st
Resusp. Buffer		70.44	70.44	64.38	64.38	72.98	72.98	67.79	67.79		71.13	71.13	65.52	65.52	69.15	69.15	68.22	68.22	Add 4th	Add 3rd
H2O2		0.00	10.00	0.00	10.00	0.00	10.00	0.00	10.00		0.00	10.00	0.00	10.00	0.00	10.00	0.00	10.00	Add 2nd	
FeSO4		0.00	2.00	0.00	2.00	0.00	2.00	0.00	2.00		0.00	2.00	0.00	2.00	0.00	2.00	0.00	2.00	Add 3rd	
ddH2O		12.00	0.00	12.00	0.00	12.00	0.00	12.00	0.00		12.00	0.00	12.00	0.00	12.00	0.00	12.00	0.00		Add 2nd
Total		100.0	100.0	100.0	100.0	100.0	100.0	100.0	100.0		100.0	100.0	100.0	100.0	100.0	100.0	100.0	100.0	then vortex	then vortex

Equations:

- Protein ug/ul = Protein for 5 ul / 5
 - Total Protein = 150 / Protein ug/ul
 - Resuspension Buffer = Total – (Total Protein + H₂O₂ + FeSO₄ + ddH₂O)
 - H₂O₂ (constant- 10), FeSO₄ (constant -2), ddH₂O (constant -12)
- Prepare two sets of 1.5 mL eppendorfs (MCT Graduated Natural Eppendorfs; cat# 05-408-129; Fischer Brand) for each sample. The second set of tubes should be more distinctly labelled including the animals conditions, experimental information, date and personal initials.
 - Next, prepare the hydrogen peroxide and ferrous sulfate and leave on ice.
 - Then add the mitochondrial subfractions to all of the tubes first. Prepare the control tubes first. Add the ddH₂O and then add the resuspension buffer last. Next prepare the treated tubes. Add the H₂O₂ first, then add the FeSO₄, last add the resuspension buffer. Tap all the tubes to mix.

5. Incubate the eppendorfs in the water bath (model 1122S, cat#: 13271-138, VWR) for 90 min at 30°C. Take out the eppendorfs and flick every 30 min to mix, place back in the water bath.
6. Once completed, centrifuge in the eppendorf centrifuge 54150 (Brinkmann Instruments, 5425-41150) machine at 9000 g for 5 min at 4°C.
7. Carefully extract the supernate (without touching the pellet) and transfer to the second labelled tubes. Discard the pellet. The supernate will contain the final released products from the mitochondria.
8. Better to prepare samples fresh and utilize immediately in a western blot or can store the samples at -80°C until ready for western blot analysis.

Sample Preparation:

1. To prepare samples, add 30 µl of the mitochondrial supernate, 10 µl of 2x Lysis Buffer, and 5 µl of sample dye. Add the lysis buffer first, then the mitochondrial supernate and lastly the sample dye. Tap to mix the solution together.
2. Heat on the hot plate(VWR Block Heater, cat#: 12621-104) for 3-5 min.
3. Utilize samples immediately, or store at -20 °C for later use.
4. Run on a 15 % gel and follow the Western protocol. Probe for cytochrome c (15 kDa) and AIF (67 kDa). No control protein is required as analysis is performed by dividing the treated sample by the control sample for each mitochondrial subfraction.

Nuclear and Cytosolic Fractionation

Reagents:

1. **D-PBS** (Dulbecco's Phosphate Buffered Saline 1X (DPBS), Wisent Inc, cat# 311-425-CL, store at 4°C).
2. **Protease Inhibitor Buffer** (Protease Inhibitor Cocktail Tablets, Roche, cat#: 11697498001, store at 4°C): Measure out 1 tablet with 1000 μ l ddH₂O. Vortex (Mini Vortex, cat#: 02215365, Fischer Scientific) tablet is dissolved. Store at -20°C.
3. **Phosphatase Inhibitor Cocktail 2** (Sigma-Aldrich, cat#: P726-5ml, store at 4°C)
4. **Phosphatase Inhibitor Cocktail 3** (Sigma-Aldrich, cat#: P0044-5ml, store at 4°C)
5. **NE-PER Nuclear and Cytoplasmic Extraction Reagent kit** (Thermo Scientific, cat#: 78835)
 - a. Cytoplasmic Extraction Reagent I (CER I), cat#: 78835A
 - b. Cytoplasmic Extraction Reagent II (CER II), cat#: 78835B
 - c. Nuclear Extraction Reagent (NER), cat#: 78835C

Procedure:

1. Prior to tissue extraction, prepare a 1.5 mL eppendorf (MCT Graduated Natural Eppendorfs; cat# 05-408-129; Fischer Brand) for the number of animal tissues to extract.
 - a. Each eppendorf will require the addition of 500 μ l of PBS, 5 μ l of the protease inhibitor solution, and 5 μ l of the phosphatase inhibitors 2 and 3. Leave eppendorfs on ice during tissue collection.
 - b. If more than one tissue, prepare a stock solution in 15 mL Falcon polystyrene conical tubes (cat#: 352095, Falcon), following the above ratio of 500 μ l PBS: 5 μ l of inhibitors for each sample (multiple values) and then aliquot to the number of 1.5 mL eppendorfs.
2. Place the extracted tissue (one TA) into the prepared eppendorf.
3. Next, prepare the reagent volume by adding the appropriate volume of CER I reagent which is equal to 400 μ l x the number of samples. Prepare this in a 10 mL falcon tube. Then add the protease inhibitor and the phosphatase 2 & 3 inhibitors for a volume of 10 μ l for each 1 mL of CER I buffer.
4. Next, place the tissue onto a curved watch glass dish on ice. Dab away extra solution. Trim away any fat and connective tissue. Then using tweezers and scissors, proceed mince the muscle with forceps and scissors until it resembles the consistency of jam and no large pieces remain.
5. Once minced, place the tissue on the inside of the small glass test tube specific for the Fischer Scientific homogenizer machine (Eberbach Corporation). Place it near the top of

- the inside. Next with a p-1000, add 400 μ l of the CER I buffer solution into the test tube, washing down the minced tissue to the bottom of the test tube.
6. Fit the mini pestle into the homogenizer. Then turning the machine on, place the pestle tightly into the test tube and move up and down until the tissue is broken down (10-30 sec).
 7. Once the homogenization is complete, pour the tissue solution into a new labelled 1.5 mL eppendorf making sure to obtain the majority of the tissue chunks. Place on ice. Wipe down the test tube and the pestle and prepare for the next sample.
 8. Then add 20 μ l of the CERII reagent to each eppendorf and vortex vigorously for 10-15 sec. Shake 3 times to mix. Leave the tube on ice to sit for 1 min. Then vortex again for 15 seconds vigorously and shake up and down once more to mix.
 9. Centrifuge at maximum speed (16 000 g) in the eppendorf centrifuge 54150 (Brinkmann Instruments, 5425-41150) in the 4°C fridge. If the tubes are still very murky after the spin and not clearly separated, centrifuge for another 5 minutes.
 10. Using a p-200, take up the supernate and place in a new 1.5 mL labelled eppendorf. This is the cytoplasm. Store on ice.
 11. The leftover pellet then needs to be washed. Slowly, with a p-1000, pour 1 mL of PBS into the eppendorf, being careful not to touch the pellet. Then centrifuge the sample in the centrifuge located in the 4 °C fridge for 30 sec. Then slowly pick up the supernate and discard it (be careful to not pick up the pellet). Repeat this wash step another two more times for a total of 3 washes.
 12. After the last wash, add between 150 – 200 μ l of the NER reagent. The amount added depends on the size of the pellet. The larger the pellet, the more NER reagent you will add.
 13. Next place the eppendorfs on an aluminum block on ice. Sonicate each eppendorf using the Microson Ultrasonic Cell Disruptor machine (model MS-50) machine set to 30% power output. Sonicate 3 by 3 (sonicate in order). Wipe the tip with a kim wipe between the sonication of each sample.
 14. After sonication, place the samples on ice for 40 min. Every 10 min, vortex each sample vigorously for 15 sec.
 15. Then place the samples in the 4°C centrifuge for 10 min at maximum speed (16 000 g). Take up the supernate and transfer it to a new labelled 1.5 mL eppendorf. This is the nuclear fraction. The pellet is discarded.
 - a. If after the centrifugation, there are two phases, take up the clear supernate. However, if there are three phases, take up the clear and murky sections, but not the bottom pellet.
 16. Once completed, store the cytoplasm and nuclear subfractions in the -80°C freezer. Utilize samples for the Bradford assay to determine protein concentration for later western blot analyses.

RNA Isolation

*****RNA isolation is a sterile procedure. Use sterile pipette tips, sterile eppendorfs and tubes, and continually wash hands and items being handled with ethanol to prevent any contamination of the sample. TriZol is a dangerous solution to work with, work with care.*****

Reagents:

1. **TriZol Reagent** (Life Technologies, Ref#: 15596018, lot# 111701)
2. **0.1 M NaOH** (Sodium Hydroxide, Caledon, 7860-1)
3. **Chloroform** (Caledon, 3000-1)
4. **Isopropanol** (2-propanol, Caledon, 8600-1)
5. **75% ethanol:** Combine 100% anhydrous ethanol (ethyl alcohol anhydrous, Commercial Alcohols, lot#: 022933) to ddH₂O, in a ratio of 75 mL: 25 mL respectively.

Procedure:

Day 1

1. The homogenizer tip for the IKA T25 Digital Ultra-Turrax polytron machine (model# T25DS1) must be sterilized in 0.1M NaOH and rinsed in sterile water prior to use. Rinse homogenizer in sterile water between samples.
2. On ice, prepare one 13 mL Rhorh (Sarstedt, ref#: 62-515.006, lot# 6092911) tube per sample. In each Rhorh tube, under the fumehood, carefully add 1 mL of TRIZol reagent.
3. Prepare two sets of 1.5 mL sterile eppendorfs (MCT Graduated Natural Eppendorfs; cat# 05-408-129; Fischer Brand) and label accordingly.
4. Prepare the appropriate set-up:
 - a. Beige two-section dish filled with liquid nitrogen;
 - b. Metal tool with a small scoop at one end and a metal clamp for samples, placed in the beige dish in liquid nitrogen;
 - c. Prepare a small liquid nitrogen tank containing the powdered samples in cryotubes (2 mL micro tube, Sarstedt, ref# 72.694.003, lot#: 3084701).
5. Remove a powdered sample (in a cryotube) from the liquid nitrogen. Tap 3-4 times on the table and slightly twist the top open to let out extra gas from the cryotube. Then remove the lid and place the cryotube in the clamp in the liquid nitrogen. *****The sample must always be stored in liquid nitrogen.***
6. Place the rhorh tube on the measuring scale and zero the scale. Then measure out 70-80 mg of powdered tissue. Tap the rhorh tube to mix. Record the measured value.
7. Remove the homogenizer tip from the NAOH solution and attach to the IKA T25 Digital Ultra-Turrax polytron homogenizer machine (model# T25DS1) set at 40% power output (9.8 Hz). Homogenize each tube at 9000 g for 10 sec. During the 10 seconds vigorously move around the bottom of the rhorh tube. Do this for each tube 2-3 times if required.

There should be no visible chunks present at the bottom of the rhorh tube. Work through each sample once and then repeat if required.

- a. Have a cup of ddH₂O to rinse the homogenizer tip between each sample. Use tweezers to remove any large pink chunks stuck within the homogenizer tip. Wipe with a kim wipe.
 - b. The homogenizer tip must be taken apart and cleaned intensely, removing remaining clumps of pink solidified Trizol and sample solution. Do not re-add to NAOH to sterilize in between each 2-3 samples.
8. Once completed, transfer homogenized solution to a sterile 1.5mL labelled eppendorf, and let stand for 5 min at room temperature.
 9. Add 200µl of chloroform and shake vigorously for 15 sec, let stand for 2-3 min at room temperature. Solution should turn a bubblegum pink once shaking is complete.
 10. Spin at maximum speed (16 000 g) for 15 min in the eppendorf centrifuge 54150 (Brinkmann Instruments, 5425-41150) in the 4°C fridge.
 11. Following centrifugation, carefully transfer the clear aqueous phase to a new sterile 1.5 mL eppendorf, making sure not to pick up any of the remaining pink solution.
 - a. If the pink solution is picked up, place the remaining supernate picked up and centrifuge for 1 min to allow for separation.
 - b. Discard of the remaining pink solution properly in the phenol waste bag.
 12. Add 500 µl of the isopropanol solution. Shake vigorously for 15 seconds until bubbles are visible. Place in the -20°C freezer over night to allow for RNA precipitation overnight so as to continue the experimentation the next day, OR place in the -80°C freezer for one hour and then continue. The -20°C option is preferred.

Day 2

1. Remove the RNA samples from the freezer and let it sit at room temperature for 10 min to allow for thawing.
2. Next, spin the samples at maximum speed (16 000 g) for 10 min, in the centrifuge located in the 4°C fridge.
3. Remove the supernate by pouring it into an empty beaker and discarding the contents.
4. Add 700 µl of the 75% ethanol. During this addition process, slowly and carefully wash the white pellet at the bottom of the eppendorf, off of the wall so that it is floating in the tube.
5. Spin the samples at maximum speed (16 000 g) for 10 min, in the centrifuge located in the 4°C fridge
6. Discard the supernate by pouring it into the beaker. Use the p-20 to suck up any additional left at the bottom of the eppendorf, while carefully avoiding the pellet.
7. Next, the pellet must air-dry for about 1 hour.
8. Dissolve the pellet in 20 µl of sterile water. Pipette up and down to mix for 1 min. Repeat for all samples.
9. Next, the RNA concentration is measured using the Nanodrop 2000 Spectrophotometer (Thermo Scientific, Serial# M757) at an absorbance at 260 nm and 280 nm to determine RNA purity and concentration.
 - a. Open the Nanodrop 2000 Program

- b. Click Nucleic Acid option. Remove the kim wipe placed between the lid and base of the nanodrop machine.
- c. Change the Type to RNA and alter the concentration to read $\mu\text{g}/\mu\text{l}$
- d. With a sterile p-10, pick up 1 μl of sterile grade water and place it gently on the top of the nanodrop machine on the centre of the metal tip. Do not touch the surface. Close the lid of the nanodrop machine.
- e. Click Blank in the top left corner and write Blank into the sample ID space in the top right of the program. Then press measure. The value located under the Nucleic Acid Concentration column should be as close to 0 as possible. Take multiple readings of the same drop if required to obtain a concentration close to 0. If unattainable, open the nanodrop lid, lightly wipe off the drop of water with a kim wipe, and then redo steps d-e with another fresh drop of sterile water.
- f. Once a water drop concentration of 0 has been read, wipe away the water drop with a kim wipe. Then pipette 1 μl of the RNA sample from step 8. Place it on the centre of the metal tip of the nanodrop reader and close the lid. Type in the sample ID and click measure for a total of 3 trials. This will ensure a more accurate reading when obtaining the average of the 3 trials for the concentration of the RNA.
 - i. To ensure the measurement is accurate, the 260/280 column ratio should have a value around 2, with an appropriate deviation of 0.03. If it is not around 2, it may mean the sample is contaminated (often less than 2 if you measure powdered tissue <50 mg). Therefore, repeated measures may sometimes be required (remove the current RNA drop, clean the tip and place a new drop).
- g. Repeat steps d-f for each sample, always place a fresh drop of sterile water on the nanodrop machine prior to adding the RNA. Need to zero before every RNA trial.
- h. To print the document with all of the RNA values, go to Reports → Print tab (landscape) → Print (top left). Below is an example of the RNA report.

Sample ID	User name	Date and Time	Nucleic Acid Conc.	Unit	A260	A280	260/280	260/230	Sample Type	Factor
	dhoodlab	10/18/2017 11:11:41 AM	0.0008	$\mu\text{g}/\mu\text{l}$	0.019	0.007	2.74	0.85	RNA	40.00
935	dhoodlab	10/18/2017 11:12:18 AM	1.3608	$\mu\text{g}/\mu\text{l}$	34.021	16.857	2.02 x	1.93	RNA	40.00
935	dhoodlab	10/18/2017 11:12:23 AM	1.3623	$\mu\text{g}/\mu\text{l}$	34.057	17.002	2.00 ✓	1.94	RNA	40.00
935	dhoodlab	10/18/2017 11:12:28 AM	1.3665	$\mu\text{g}/\mu\text{l}$	34.162	16.981	2.01 ✓	1.95	RNA	40.00
935	dhoodlab	10/18/2017 11:12:32 AM	1.3690	$\mu\text{g}/\mu\text{l}$	34.224	17.030	2.01 ✓	1.93	RNA	40.00
	dhoodlab	10/18/2017 11:13:09 AM	0.0011	$\mu\text{g}/\mu\text{l}$	0.027	0.006	4.16	1.02	RNA	40.00
	dhoodlab	10/18/2017 11:13:44 AM	-0.0001	$\mu\text{g}/\mu\text{l}$	-0.002	-0.007	0.30	0.78	RNA	40.00
940	dhoodlab	10/18/2017 11:14:19 AM	1.2143	$\mu\text{g}/\mu\text{l}$	30.358	15.371	1.98 ✓	1.44	RNA	40.00
940	dhoodlab	10/18/2017 11:14:25 AM	1.2116	$\mu\text{g}/\mu\text{l}$	30.290	15.408	1.97 ✓	1.43	RNA	40.00
940	dhoodlab	10/18/2017 11:14:29 AM	1.2135	$\mu\text{g}/\mu\text{l}$	30.337	15.452	1.96 ✓	1.42	RNA	40.00
940	dhoodlab	10/18/2017 11:14:34 AM	1.2243	$\mu\text{g}/\mu\text{l}$	30.608	15.623	1.96 x	1.42	RNA	40.00
	dhoodlab	10/18/2017 11:15:14 AM	0.0011	$\mu\text{g}/\mu\text{l}$	0.027	0.007	3.71	0.18	RNA	40.00
	dhoodlab	10/18/2017 11:15:21 AM	0.0020	$\mu\text{g}/\mu\text{l}$	0.050	0.023	2.18	0.26	RNA	40.00

- i. Once printed, shut down the program and place a kim wipe between the nanodrop base and lid for protection.

Reverse Transcription

First-strand cDNA synthesis is performed following the manufacturer's recommendations that are outlined below. Performed on the same day as “Day 2” of RNA isolations.

Reagents:

1. **Total RNA** (isolated as described above)
2. **Oligo(dT)₂₀** (Invitrogen, cat#: 18418020)
3. **10 Mm dNTP** (each dATP, dTTP, dCTP, dGTP is diluted in sterile DEPC treated water)
4. **Sterile DEPC treated ddH₂O** (Sterile Molecular Grade Water, Wisent Inc., cat#: 809-115-66, Store at room temperature)
5. **RNase OUT** (Ribonucleotide Inhibitor [recombinant], Invitrogen, cat#: 10777-019)], store at -20°C)
6. **0.1M Dithiothreitol (DTT)** (Invitrogen, P/N Y00147, cat#: 1305696, store at -20°C)
7. **5X First-strand Buffer** (Invitrogen, P/N Y02321, cat# 1788535, store at -20°C)
8. **SuperScript III Reverse Transcriptase** (Life Technologies, cat#: 18080-044, store at -20°C)
9. **PerfeCTA SYBR Green Supermix ROX** (Quanta Biosciences, P/N 84018, lot# 015507, store in aluminum foil at -20°C).

Procedure:

1. Prepare the pipette plan below. Add in the RNA concentrations into the highlighted regions at the bottom and the rest of the reagent concentrations will adjust accordingly:

order to add	Sample	106	109	181	107	171	172	165	170
<i>MM1</i>									
1	DEPC st. H2O (ul)	10.03	9.92	9.88	9.89	10.10	10.16	10.03	10.11
3	Oligo(dT) ₂₀ (ul)	1	1	1	1	1	1	1	1
3	10mM dNTP (ul)	1	1	1	1	1	1	1	1
2	RNA (ul)	0.97	1.08	1.12	1.11	0.90	0.84	0.97	0.89
Thermocycler FILE#24: at 65 C for 5min, let stand for 1min on ice									
<i>MM2</i>	1	5x First-strand buff.	4	4	4	4	4	4	4
	1	0.1m DTT	1	1	1	1	1	1	1
(sensitive)	2	RNase OUT	1	1	1	1	1	1	1
(sensitive)	2	SuperScript III RT	1	1	1	1	1	1	1
FILE #57: 50 C for 50 min, 72 C for 20 min									
		Total Volume	20	20	20	20	20	20	20
		[RNA] (ug/ul)	1.5541	1.3871	1.3386	1.3474	1.6705	1.7755	1.5402
		[RNA] (1.5 ug)	0.97	1.08	1.12	1.11	0.90	0.84	0.97
		Insert [RNA] from RNA isolation procedure							

Equations:

- $\text{RNA (1.5 ug)} = 1.5 / \text{RNA ug/ul}$
 - $\text{RNA (ul)} = \text{RNA (1.5 ug)}$
 - $\text{DEPC st. H}_2\text{O} = 20 - (\text{oligo}20 + 10 \text{ mM dNTP} + \text{RNA (ul)} + 5\text{x First Strand} + 0.1\text{m DTT} + \text{RNase OUT} + \text{SuperScript III RT})$
2. Next, prepare in a 1.5 mL sterile eppendorf mastermix 1 which contains an equal volume of oligo(dT)20 and the 10 mM dNTP. 1 μl of each is added to each sample. Prepare a volume +2 (room for error) into the eppendorf. Pipette up and down to mix. Leave on ice until ready to use.
 3. Label 0.5 mL Flat-Cap PCR “mini” eppendorf tubes (cat#: 87-C500-F, Ultident Scientific) according to the number of samples. Then follow the first section of the pipette plan above. First add the sterile water to each of the mini eppendorfs. Then add the RNA to the appropriate tubes. Lastly add 2 μl of the mastermix 1 solution to each tube. Pipette repeatedly to ensure adequate mixing.
 4. Employ the DNA Thermal Cycler (Perkin Elmer, model TC480) to heat mixture to 65°C for 5 minutes. Do not let the thermal cycler cool down and immediately once the 5 minutes is done, leave the mini eppendorfs on ice for 1 min. Remove from ice and leave at room temperature while performing the next steps.
 5. In a second 1.5 mL sterile eppendorf, prepare mastermix 2. This contains 4 μl of the 5x first strand buffer and 1 μl of the 0.1 m DTT. Once again, prepare a volume +2 (room for error) in the eppendorf. Pipette up and down to mix. Leave on ice until ready to use.
 6. Then add 5 μl of mastermix 2 to each of the mini eppendorfs with the RNA.
 7. Once added, remove superscript III RT from the -20°C freezer. This solution is light sensitive and should not be left out for long. Only remove from the freezer immediately prior to using. Add 1 μl to each mini eppendorf.
 8. Next, remove RNase OUT from the -20°C freezer. This solution is light sensitive and should not be left out for long. Only remove from the freezer immediately prior to using. Add 1 μl to each mini eppendorf. Pipette up and down to fully mix mini eppendorf.
 9. Using a thermal cycler, incubate at 50°C for 50 minutes, and then inactivate the reaction by heating at 72°C for 20 minutes. In the meantime, keep the original 1.5 mL RNA eppendorfs on ice.
 10. During the cycling process, prepare and label another set of sterile mini eppendorfs. These eppendorfs will be used to dilute the cDNA (currently in the thermal cycler) to a more manageable concentration to utilize for experimentation.
 11. Once the thermal cycler is completed, add 29 μl of sterile water to the newly labelled (empty) mini eppendorfs. Then add 1 μl of the cDNA. Mix up and down repeatedly to mix. This is a 1:30 ratio. As this volume is low and will be used up rapidly, make a large ratio; for example, prepare 4 μl cDNA: 116 μl sterile water.
 12. The diluted cDNA is now ready for use in PCR amplification. Both the diluted cDNA and the original amplified cDNA can be stored at -20°C until further use.

Oligonucleotide Primer Design

Websites required:

- Pubmed Nucleotide Search
- Primer3 Primer Design Program → <http://Frodo.wi.mit.edu/primer3>
- BLAST – <http://www.ncbi.nlm.nih.gov/tools/primer-blast/>
- IDT website – <http://www.idtdna.com/calc/analyzer>

Process:

1. Know the gene of interest. Search up the protein/gene ahead of time to determine relevant associated information. Determine if there are alternative names the genes is called in the same species or different species.
 - a. Useful website is “Gene Card” under google.
2. Go to the Pubmed.com cite; click on the nucleotide option in the drop down menu. Type in the gene and then the species.
 - a. For example: p53 mus
 - b. Mus= mus muscularis (mouse)
 - c. Pick the option that best fits the gene description (i.e. in the above example, the best option that fits p53 mRNA in mouse). There may be many options available, therefore choose the best fit for specific experimental protocol. Investigate the different contenders by viewing the publications/sources available in the description of the option clicked.
3. Once the best option has been chosen, click the “Fasta” hyperlink under the blue title (underlined) on the option page. This will give the entire sequence of the gene at interest.
4. Copy and paste the sequence and into a word document and save it.
5. Open the Primer3program. If the program is not bookmarked, it can be found at the weblink above. Click on “go to new version.” Copy the entire sequence from the word document and paste into the large text space at the bottom of the web page. Remove numbers from the copied sequence because the program will treat them as nucleotides. Then make the following changes to the options on the web page.
 - a. Product Size Ranges: 100-150 (nucleotides)
 - b. Number to Return: 10
 - c. Primer Size: 18 Opt: 20 Max:22
 - d. Primer TM: 58 Opt: 60 Max: 62
 - e. Max TM Difference: 2
 - f. Primer GC%: Min: 40 Opt: 50 Max: 60
 - g. Max Self Complementary: 6

- h. Max 3' Self Complementary: 2
 - i. Max Poly-X: 3
 - j. End Stability: 9
 - k. Click on the "Pick Primers" button.
6. Open the IDT website (oligo analyzer website). The webpage is listed above. After clicking pick primers, a list of primers at the bottom of the web page will be generated. This list will contain primary and secondary sequences. You will have to test both of the primary and secondary sequences for each primer to determine if the primer fits or fails with your conditions. To do this, follow the steps below:
 - a. For copying the primary or secondary sequence (found at the bottom of the web page under additional oligos), make sure that the row doesn't end in a G or C (if it does, do not highlight the G or C when copying).
 - b. Copy the primary sequence for the first primer set and past it into the top text box on the EDT web page. Click analyze.
 - c. Next click "Hairpin." This determines if the primer folds back on itself. Scroll down the page and if the ΔG is >-9 , then it passes this test.
 - d. Next click "Self-Dimer." This determined if the primer binds to itself. Scroll down the page and if the ΔG is >-9 , then it passes this test
 7. Then go back to the additional oligo page and take the secondary sequence of the primer set (do not highlight G or C again when copying). Copy the secondary and place it into the secondary sequence box on the IDT web page. Click calculate and the value should be greater than -9.
 8. Click NCBI Blact first. Then to check specificity using BLAST (big blue button). Which will open a new tab with information mentioning if any other genes bind to the gene of interest. Go through the list. You only want to see your gene of interest in your species (i.e. mus. Muscularis).
 9. Return to the IDT webpage and repeat steps 10b-d for the secondary sequence. If the values are < -9 , then it fails the test. Will then need to try the second primer set and if both the primary and secondary of the second set fail, then move onto the third set, so on and so forth until you obtain a primer set that passes all the tests. When you find the one that does, this will be the primer sequence to be ordered.

Polymerase Chain Reaction (qPCR)

1. Primers must first be optimized prior to analyzing the cDNA with the primer of interest. Primers are either designed as indicated by the instructions above or are borrowed from previous studies in the laboratory (no expiration date on the primers). All primers can be orders from customdna@sial.com.

a. Once Forward and Reverse primers for each mRNA are received, they must be diluted to 300 μmol . On the primer, there is a nmol concentration. Enter that into the shaded pipette plan below. Automatically the sterile H_2O volume will adjust according to the equation ($=X/1000/300*1000*1000$) where X is the nmol concentration and that μl sterile H_2O volume is how much is required to be added to the primer bottle. Constant pipetting up and down for 1 min is required for adequate mixing.

To get 20 μM stock:			
Add = 186.67μl st H_2O			
and 13.3μl of each 300μM stock primer			
* multiple by 2 to get larger stock			
GENE	Primer	nmol	add st. H_2O (μl)
PGC-1a	F'	55.8	186.0
	R'	51.4	171.3

b. Once diluted appropriately, prepare separate sterile 1.5 mL eppendorfs for the Forward and Reverse primers. To create a 20 μM stock, add 186.67 μl of sterile water to the eppendorf. Then add 13.3 μl of the 300 μM stock primer. As these are low volumes and are utilized quickly, you can make a larger volume by multiplying this ratio. For example, if multiplied by 4, add 746.68 μl of sterile water first and then add 53.2 μl of the appropriate stock primer. You should always have a forward and reverse tube (2 tubes) for each RNA. Leave on ice to thaw until ready to use.

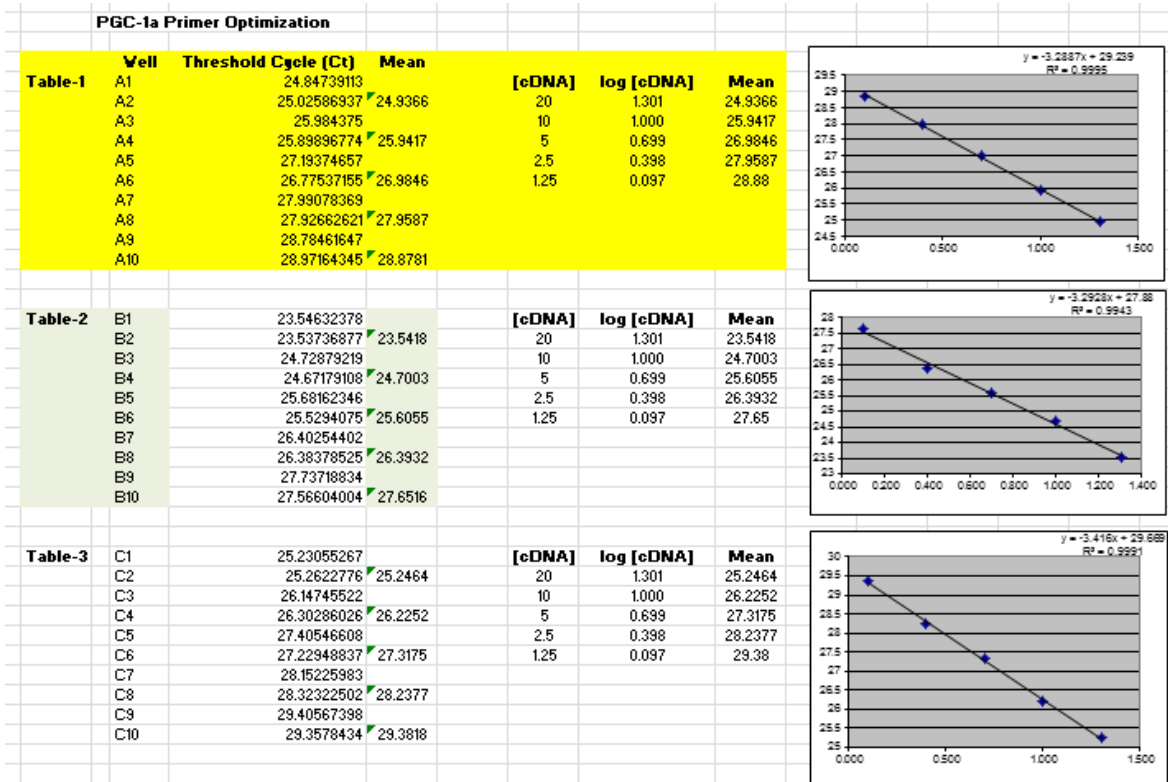
2. Next, prepare 5 mini sterile eppendorfs. Label 1:1, 1:2, 1:4, 1:8, and 1:16 ratios on the 5 tubes respectively. As you want to find the appropriate primer concentrations to use for your conditions, you will need 2-3 representative samples for each condition for each primer. For example, if using the conditions Whole Body (WB) mouse WT UT, WB WT T, WB KO UT, WB KO T and Muscle Specific (MS) mouse WT UT, MS WT T, MS KO UT, MS KO T, that involves a total of 8 conditions and therefore 8 required samples. It is a better representation however if you obtain 2 samples for each condition, for a total of 16 samples.

a. In the 1:1 tube, you will add 4 μl from each condition (any samples you decide), obtaining a volume of 64 μl total of RNA (two samples from each condition). These samples are all being mixed into the same tube. Then you will add the corresponding 64 μl of sterile water to satisfy the 1:1 ratio.

6. Add first 2 μ l of the serial dilution cDNA to the appropriate wells of the plate. Check the bottom of the plate to ensure a small visible drop of the cDNA in each well (often wells can be skipped – must check prior to adding the mastermix). Then quickly add 23 μ l the appropriate table 1, table 2 and table 3 mastermixes to the associated wells. Do not need to change pipette tips between each well – only change between each table mastermix.
 - a. Total reaction volumes are always 25 μ l
 - b. Use negative wells to monitor contamination, using 2 μ l sterile ddH₂O in place of cDNA.
7. Once all is added, place an adhesive cover over the plate and smooth down. Cover then with aluminum foil to prevent excessive light exposure as the SYBR green is light sensitive.
8. Remove the aluminum foil and spin the plate in the Sorval ST16R centrifuge (Thermo Scientific, cat#: 75004381) for 2 min at 4000 g to mix the cDNA with the mastermix and to bring solution to the bottom of the wells. Re-cover with the aluminum foil to minimize light exposure.
 - a. If making multiple plates at once and one plate is currently reading in the Applied Biosystems StepONE^{PLUS} Real-Time PCR System (serial#: 272002347), store the ready-made plate at 4°C for later use. One plate may be stored overnight if required and put through the reader early the next morning.
9. Set-up the PCR machine.
 - a. Allow time for the PCR machine to connect with the computer program – may take a couple minutes if just turned on. Place the plate into the machine by fitting it within the well template.
 - b. Once on and connected, open the StepOne Software program.
 - c. Use Guest → click OK
 - d. Ignore calibration and continue
 - e. Click Run/Quickstart option.
 - i. Enter the experiment title and browse through documents for where the results will be saved
 - ii. Quantitation, SYBR Green + Melt Curve, 2 hours, cDNA options.
 - iii. On the next tab labelled “Run”, enter 25 μ l to be read.
 - iv. Then click Start at the bottom
 - v. Ignore the calibration settings and continue
 - vi. The machine lid will move upwards once it has start running – confirm this movement.
 - vii. Next, set-up the plate reader to mimick the template of the plate with the template on the program. Go to Set-up → Plate Set-up
 1. Under Assign Targets, write **gene name** and **Table #**, for example PGC-1a Table 1. Add a new target to continue adding until you have all of the targets listed (should be 6 targets for the plate above

- for example: PGC-1a Plate 1, PGC-1a Plate 2, PGC-1a Plate 3, Tfam Plate 1, Tfam Plate 2, Tfam Plate 3).
 - 2. Next under Assign samples, in this case, adding the serial dilution ID. For example, 1:1, 1:2, 1:4, 1:8, and 1:16.
 - 3. Click the tab “Assign Target and Sample” and you will mimic the plate set-up. Highlight the appropriate wells in the example plate on the program and assign the targets. Then highlight the specific wells associated with the appropriate serial dilutions. Once everything is assigned, you do not need to save (automatically saves the layout). **Wait for the 2 hour run to be completed.**
- f. Save the file once completed. Save on the computer and then save on the USB to bring over to another computer (not hooked up to the machine) to then analyze the curves.
- i. Open the StepOne Software on the KC4 reader. Continue the program without the connection the PCR machine.
 - ii. Click Analyze Experiment (top right corner). Open the file from the USB.
 - iii. The file will open to the curve graph with the layout beside. If there is a 1 or 2 in the layout wells, it means that the duplicates of the same serial dilution is not identical (some variation is present). Highlight each duplicate to see how different the curves are from each other. Want the curves to overlay perfectly. Make a note of the tables/samples that may not have a perfect overlap.
 - iv. Then go to Plate Set-Up → Assign Targets & Samples → At the bottom, select dye and change from ROX to None (must turn ROX off to analyze the melt curve stage).
 - v. Then go to Analysis → Melt Curve
 - 1. Multiple curves in the lines means that two separate products are melting and the primer only binds to one, OR the primer is binding to multiple sites OR it binds to itself if there is too much primer volume in the mastermix.
 - 2. Therefore, highlight each table, 1, 2 and 3, and see if there are bumps in the curves (do not highlight the negative). Record the best looking curves for each primer.
 - a. Curves of different heights are normal because of the serial dilutions
 - 3. Then highlight the whole table by clicking the small white square in the top left corner of the plate. Click Export Data. Select Results, then save the appropriate folder, and export. This will export all the data in an excel spreadsheet.

4. In the Excel exported file, only look at the C_T values. This is the cycle threshold values. These are the values that will be inputted into the Threshold cycle column in the excel spreadsheet below. Everything else will be pre-calculated. The mean is just the average of the two duplicates for each serial dilution; the $\log[cDNA]$ column = $\text{LOG}[cDNA]$; the graph is a combination of the $\log[cDNA]$ and mean.
 - a. In terms of selection for the best table – require an $R^2 > 0.99$ and an m value of around – 3.32 (this is the more important requirement). Therefore, pick the graph with the best values and also take into account any variabilities that were seen in the melt curves.
5. Save the file, take note of the appropriate table selection. Repeat for all primers including the control primers.



10. Now that the primers have been optimized, prepare the pipette plans for analyzing the diluted cDNA samples. A maximum of 16 diluted cDNA samples can be analyzed per plate as each plate is required to also analyze two control primers. Example plates can be seen below. For PGC-1a for example, all three primers (PGC-1a, GAPDH and B2M) have all been optimized for table 1. On the other hand however, GAPDH and B2M are

optimized for Table 1 and Tfam is optimized for Table 3. Other controls can be used, GAPDH and B2M are just examples.

2017-11-01 - PGC-1a with samples - Plate 1																	
	1	2	3	4	5	6	7	8	9	10	11	12			Table 1		
A	MS- 107 WT UT	MS- 130 WT UT	MS- 132 WT UT	MS- 133 WT UT	MS- 150 WT UT	MS- 152 WT UT							Table 1	PGC-1a	SYBR	175 x 3	525
B	MS- 108 WT T	MS- 109 WT T	MS- 121 WT T	MS- 131 WT T	MS- 138 WT T	MS- 140 WT T									F Primer	35 x 3	105
C	MS- 149 WT T	MS- 151 WT T	MS- 219 WT T	MS- 220 WT T	MS- 107 WT UT	MS- 130 WT UT									R Primer	35x3	105
D	MS- 132 WT UT	MS- 133 WT UT	MS- 150 WT UT	MS- 152 WT UT	MS- 108 WT T	MS- 109 WT T									ddH2O	77 x 3	231
E	MS- 121 WT T	MS- 131 WT T	MS- 138 WT T	MS- 140 WT T	MS- 149 WT T	MS- 151 WT T							Table 1	GAPDH			
F	MS- 219 WT T	MS- 220 WT T	MS- 107 WT UT	MS- 130 WT UT	MS- 132 WT UT	MS- 133 WT UT											
G	MS- 150 WT UT	MS- 152 WT UT	MS- 108 WT T	MS- 109 WT T	MS- 121 WT T	MS- 131 WT T											
H	MS- 138 WT T	MS- 140 WT T	MS- 149 WT T	MS- 151 WT T	MS- 219 WT T	MS- 220 WT T							Table 1	B2M			

2017-11-02 - Tfam with samples - Plate 1																	
	1	2	3	4	5	6	7	8	9	10	11	12			Table 1		
A	MS- 107 WT UT	MS- 130 WT UT	MS- 132 WT UT	MS- 133 WT UT	MS- 150 WT UT	MS- 152 WT UT							Table 3	Tfam	SYBR	175 x 3	525
B	MS- 108 WT T	MS- 109 WT T	MS- 121 WT T	MS- 131 WT T	MS- 138 WT T	MS- 140 WT T									F Primer	35 x 3	105
C	MS- 149 WT T	MS- 151 WT T	MS- 219 WT T	MS- 220 WT T	MS- 107 WT UT	MS- 130 WT UT									R Primer	35x3	105
D	MS- 132 WT UT	MS- 133 WT UT	MS- 150 WT UT	MS- 152 WT UT	MS- 108 WT T	MS- 109 WT T									ddH2O	77 x 3	231
E	MS- 121 WT T	MS- 131 WT T	MS- 138 WT T	MS- 140 WT T	MS- 149 WT T	MS- 151 WT T							Table 1	GAPDH			
F	MS- 219 WT T	MS- 220 WT T	MS- 107 WT UT	MS- 130 WT UT	MS- 132 WT UT	MS- 133 WT UT									SYBR	175 x 3	525
G	MS- 150 WT UT	MS- 152 WT UT	MS- 108 WT T	MS- 109 WT T	MS- 121 WT T	MS- 131 WT T									F Primer	8.75 x 3	26.25
H	MS- 138 WT T	MS- 140 WT T	MS- 149 WT T	MS- 151 WT T	MS- 219 WT T	MS- 220 WT T							Table 1	B2M	R Primer	8.75 x 3	26.25
															ddH2O	129.5x 3	388.5

11. Before loading the plate, prepare 1.5 mL sterile eppendorfs, one for each primer. Multiple the values by the number of rows being utilized for each primer. Prepare extra. For example, if 2.5 rows are being used, then prepare the mastermix for 3 rows, i.e. multiple the values by 3 (as shown below). Add the ddH₂O first, then add the already prepared forward and reverse primers for the specified mRNA being analyzed. DO NOT ADD THE SYBR GREEN YET (add only immediately prior to use). Leave these samples on ice.

12. In the 96 well mRNA plate, add the 2 µl of the diluted cDNA as shown in the layout plate example above. Add in duplicates. Check the bottom to ensure that the diluted cDNA has been added to the appropriate wells.

13. Once the diluted cDNA has been

added to all of the appropriate wells add the SYBR green to the three mastermixes prepared (i.e. PGC-1a, GAPDH and B2M). Mix up and down to mix as the SYBR green is viscous and required multiple pipetting (10 times) to mix fully. When everything is added to the eppendorf, place in the black sterile lidded box as well until ready to use.

Table 1	14X	(14x) x 3
Quanta PerfeCta SYBR Green Master Mix	175	525
20 uM Forward Primer	35	105
20 uM Reverse Primer	35	105
ddH2O	77	231

Table 2	14X	(14x) x 3
Quanta PerfeCta SYBR Green Master Mix	175	525
20 uM Forward Primer	17.5	52.5
20 uM Reverse Primer	17.5	52.5
ddH2O	112	336

Table 3	14X	(14x) x 3
Quanta PerfeCta SYBR Green Master Mix	175	525
20 uM Forward Primer	8.75	26.25
20 uM Reverse Primer	8.75	26.25
ddH2O	129.5	388.5

14. Add 23 μ l of the PGC-1a to each of the wells listed on the pipette plan containing the diluted cDNA. Do not change tips when adding. Add quickly as the mastermix is now light sensitive with the SYBR green. Next add the GAPDH mastermix solution to the appropriate wells. Lastly add the B2M mastermix solution to the appropriate wells. Once all is added, place an adhesive cover over the plate and smooth down. Cover then with aluminum foil to prevent excessive light exposure as the SYBR green is light sensitive.
15. Remove the aluminum foil and spin the plate in the Sorval ST16R centrifuge (Thermo Scientific, cat#: 75004381) for 2 min at 4000 g to mix the cDNA with the mastermix and to bring solution to the bottom of the wells. Re-cover with the aluminum foil to minimize light exposure.
 - a. If making multiple plates at once and one plate is currently reading in the Applied Biosystems StepONE^{PLUS} Real-Time PCR System (serial#: 272002347), store the ready-made plate at 4°C for later use. One plate may be stored overnight if required and put through the reader early the next morning.
16. Then set-up the plate reader the exact same way as indicated in step 10 and onwards. Run the plate for two hours and save the file onto the computer and onto a USB.
17. To analyze the plates, continue on from step 10f.
 - a. The only alteration to the analysis process is that there is no need to make note of any differences in the curves and melt curves as they have already been adjusted for. Export data the same way.
 - b. Then taking the values from the excel spreadsheet, place the CT values into the spreadsheet below. Enter the CT values from the exported excel spreadsheet into the highlighted column on the left (should be two values for each sample). The mean will be taken for these sampled and the STD will be calculated. From the sample exported file, you will also have the control values – enter those into the GAPDH and B2M column. The value you require is 2^{*-X} which is then multiplied by 100 to create a whole number. This is the value that is then analyzed in Graphpad.

z	PGC-1a				Ct				*					
	Ct	Mean	SD	% CV	GAPDH	B2M	Mean	SD	% CV	Delta Ct (Ct PGC-1a - Ct HOUSE)	delta delta Ct (kd-con	Fold-increase	2 ^{-X}	*100
107	23.18556				16.1856937	22.48012								
	23.04927	23.11741	0.096374	0.416889179	16.1353683	22.12973	19.23273	3.550409						
130	23.94487				16.5724621	22.81421			18.46025	3.884685993	0.000	1.000	0.067700674	6.77007
	23.69113	23.818	0.17942	0.753296413	16.5789852	22.83478	19.70011	3.607741						
132	24.00316				16.8625107	22.93995			18.3133	4.117891312	0.233	0.851	0.057598851	5.75959
	23.87506	23.93911	0.090584	0.378393447	16.6981487	22.58496	19.77139	3.45747						
133	24.19187				16.8168736	22.41477			17.48724	4.167721272	0.283	0.822	0.055640482	5.56405
	24.0136	24.10273	0.126062	0.523017671	16.884346	22.34518	19.61529	3.192626						
150	23.84468				16.6932047	22.21658			16.27621	4.48744154			0.044580557	4.45806
	23.53419	23.68943	0.219544	0.926758929	16.5780849	22.08148	19.38984	3.186805						
152	23.81859				16.8017902	22.51724			16.43544	4.299598694			0.050779898	5.07799
	23.92911	23.87385	0.078152	0.327352795	16.6593304	22.45546	19.60846	3.323712						
108	23.59362				16.2498016	21.98937			16.9504	4.265396118			0.051998142	5.19981
	23.67387	23.63375	0.056741	0.240088518	16.0643635	21.82602	19.03239	3.321651						
109	23.56711				16.5353527	22.66357			17.45262	4.601356983			0.041195856	4.11959
	23.58515	23.57613	0.012756	0.054105562	16.5057354	22.63368	19.58458	3.538091						
121	24.35633				16.9138203	22.92673			18.06569	3.99154377			0.062867414	6.28674
	24.24117	24.29875	0.081437	0.335149555	16.8309765	22.5431	19.80366	3.388516						

OTHER CONTRIBUTIONS TO LITERATURE

PEER-REVIEWED PUBLICATIONS

1. **Beyfuss K** & Hood DA. A systematic review of p53 regulation of oxidative stress in skeletal muscle. *Redox Report* 23(1):100-117, 2018.
2. Erlich AT, Brownlee DM, **Beyfuss K**, Hood DA. Exercise induces TFEB expression and activity in skeletal muscle in a PGC-1 α dependent manner. *Am J Physiol Cell Physiol* 314(1):C62-C72, 2017.
3. Erlich AT, Tryon LD, Crilly MJ, Memme JM, Moosavi ZSM, Oliveira AN, **Beyfuss K** & Hood DA. Function of specialized regulatory proteins and signaling pathways in exercise-induced muscle mitochondrial biogenesis. *Integrative Medicine Research* 5(3):187-197, 2016.

PUBLISHED ABSTRACTS AND CONFERENCE PROCEEDINGS

1. Erlich AT, **Beyfuss K**, Hood DA. Regulation of TFEB transcriptional activity and translocation during exercise by PGC-1 α . 7th Annual Muscle Health Awareness Day (MHAD). Toronto, ON. May 2016 – Poster presentation.
2. Erlich AT, Brownlee D, **Beyfuss K** & Hood DA. PGC-1 α -dependent TFEB expression and activation with exercise. Ontario Exercise Physiology (OEP) Conference. Barrie, ON. January 2017 – Poster Presentation.
3. Erlich AT, Brownlee D, **Beyfuss K** & Hood DA. PGC-1 α -dependent TFEB expression and activation with exercise. Experimental Biology (EB) Conference. Chicago, IL. April, 2017 – Poster Presentation.
 - a. Proceedings published in The FASEB Journal, April 2017; 31:707.10
4. **Beyfuss K**, Erlich AE, Hood DA. Subcellular localization of p53 identifies its role in mitochondrial biogenesis, autophagy and antioxidant signaling pathways with chronic training. Experimental Biology (EB) Conference. Chicago, IL. April, 2017 – Poster Presentation.
 - a. Proceedings published in The FASEB Journal, April 2017; 31:839.16
5. **Beyfuss K**, Erlich AE, Hood DA. Is p53 required for mitochondrial biogenesis with exercise? 8th Annual Muscle Health Awareness Day (MHAD). Toronto, ON. May 2017 – Poster presentation.
6. Hood DA, **Beyfuss K**, Oliveira A, Erlich AE. Mitochondrial turnover during exercise and chronic disuse. IMPACT II Symposium. Korea, 2016.

ORAL PRESENTATIONS

1. **Beyfuss, K**. Role of p53 in exercise training-induced mitochondrial adaptations: a comparison of two mouse models. Ontario Exercise Physiology (OEP) Conference. Barrie, ON. January 2018 – Oral Presentation.

2. **Beyfuss, K.** p53 regulation of cellular homeostasis in skeletal muscle with training: An evaluation of two mouse models. Ontario Exercise Physiology (OEP) Conference. Barrie, ON. January 2017 – Oral Presentation.
3. **Beyfuss, K.** The role of p53 in determining skeletal muscle phenotype and mitochondrial adaptations to training. *KAHS Graduate Seminar 2017*. York University, Toronto, ON. March 2017 – Oral presentation.